

Particles, Cosmology and Applications: Scale-Symmetric Theory (SST)

Sylwester Kornowski

2022

Poland, Western Pomerania, Szczecin

First publication:

The first version of the book was entitled “*General Theory of Singularities*”,
Szczecin: Tajgeta, ISBN 83-901005-1-7 (1997);

Available in Polish National Library: Signature: NR_BBN: PB 9041/2000
or in Jagiellonian Library: Signature: B 250180.

The first publication contains the foundations of the Scale-Symmetric Theory i.e. the phase transitions of the inflation field and the atom-like structure of baryons.

The first version of the atom-like structure of baryons appeared in 1996 (Polish edition).

Technical Notes: The book is divided into chapters (e.g. 2 or 2.) and sections (e.g. 2.1.). The figures and tables are numbered with consecutive natural numbers. The numbering of the formulas is as follows: (chapter.section.current-number) (e.g. (2.7.13)). Literature is provided at the end of each of the first three chapters and at the end of each application in the fourth chapter. Formulas, figures and tables in applications are preceded by a letter name and a number given to each application (e.g. B.3....). The Index leads to page(s) containing the main information about the search term.

Copyright © 2022 by Sylwester Kornowski
All rights reserved

Cite this book

Sylwester Kornowski (7 October 2022). “Particles, Cosmology and Applications”
viXra:2110.0171v2

About the author

I am a physicist.

I graduated in physics at the Poznań University (UAM) 1971, Poland.

E-mail: sylwester.kornowski@gmail.com

Preface

This book is an attempt to organize the main ideas and to unify the descriptions that were included in my letters, papers and books written in 1976-2022 on particle physics, cosmology, astrophysics, atomic nucleus physics, atomic physics, brain-mind interactions, chaos theory, or quantum physics. It is a book about the missing part of the theory of everything (ToE). The Scale-Symmetric Theory (SST) is based on two pillars. The first pillar describes the four successive phase transitions of the initial inflation field composed of tachyons/pieces-of-space and it is the basis of the ToE. The second pillar is the atom-like structure of baryons, which is due to the electroweak and nuclear strong interactions. This second edition of my book is the result of the revision of the International System of Units, the SI, which entered into force on 20 May 2019. In this version, I have introduced significant simplifications. Moreover, the obtained results are more accurate.

Contents

1. Introduction	6
1.1. Need for new methods	6
1.2. Nomenclature used in SST	7
1.3. Initial conditions used in SST	11
1.4. Derivation of the very frequently applied formulas and laws	17
1.5. Electron and the matter-antimatter asymmetry	21
1.6. Uncertainty of experimental results	23
References	23
2. Particle Physics	24
2.1. Classical thermodynamics and phase transitions of inflation field, physical constants, and dark-matter (DM) particles	24
2.2. Dynamics of the core of baryons	28
2.3. Structure of the bare electron and the electromagnetic interactions	29
2.4. The other coupling constants and masses of pions	31
2.5. Energy frozen inside the SST-absolute-spacetime components	37
2.6. Magnetic moment of electron	37
2.7. The atom-like structure of baryons at low energy	39
2.8. Masses and magnetic moments of nucleons	42
2.9. The origin of the SST Higgs potentials (volumetric and circular) for the SST-absolute-spacetime components	43
2.10. Muon	45
2.11. Tauon and fine-structure constant at high energies	47
2.12. Photons, gluons and selected properties of fundamental particles	48
2.13. The mass of W^\pm and Z^0 bosons	49
2.14. Degrees of freedom	49
2.15. The seven types of interactions	50
2.16. Higgs boson and a prediction of new particle	52
2.17. Lamb-Retherford shift	52
2.18. Lifetimes	53
2.19. Radius of proton	56
2.20. Selected mesons	58
2.21. Hyperons	60
2.22. $\Delta(1232)$ resonance	61
2.23. Masses of quarks	62

2.24. The PMNS neutrino-mixing matrix	63
2.25. The CKM quark-mixing matrix	65
2.26. Larger structures	67
2.27. The ultimate equation	68
2.28. Turning points in the formulation of the Scale-Symmetric Theory	68
2.29. Summary	69
2.30. Tables	70
References	74
3. Cosmology	75
3.1. Introduction to the SST cosmology and abundances of baryonic matter (BM), dark matter (DM) and dark energy (DE)	75
3.2. Inflation, universes and radius of the inner Cosmos (i.e. of the SST absolute spacetime)	77
3.3. Neutron black holes (NBHs)	78
3.4. The large-scale structure of the very early Universe	80
3.5. The correct age of the Universe, Hubble constants and CMB	81
3.6. The origin of CMB power spectrum	84
3.7. Initial evolution of the expanding Universe	88
3.8. The standard ruler in cosmology	88
3.9. Black body spectrum	89
3.10. The hydrogen-to-helium-4 ratio in the expanding Universe	90
3.11. Summary	90
3.12. Tables	91
References	92
4. Applications	93
A. Atomic physics	93
A1. Derivation of the Pauli Exclusion Principle	93
A2. Meaning simplification of the Dirac theory of the hydrogen atom	96
A3. Frequency of the hydrogen spin-flip transition and the Bohr radius	99
B. Superconductivity	102
B1. The three phonon fields in superconductors	102
B2. Cooper-pair breaking	109
C. Nuclear physics	114
C1. The four-shell model of atomic nucleus	114
C2. Coupling constants and binding energy	115
C3. Model of dynamic supersymmetry for nuclei	117
D. Brain-mind interactions	119
D1. The brain-mind interactions	119
E. Chaos theory	120
E1. Feigenbaum constants	120
F. Quantum physics	121
F1. Quantum physics in SST	121
G. Extraterrestrial communication	124
G1. Wow! signal	124
H. Cosmology and astrophysics	129
H1. Rotation curves of disc galaxies outside their bulges	129
H2. Age of the Universe from the degree of curvature of the major arms of the massive spiral galaxies	132
H3. Conditions for intensive evaporation of black holes	134
H4. The main equation in theory of gamma-ray bursts (GRB)	135
H5. New theory of the Solar System	136
H6. Magnetars versus pulsars	141

H7. Space roar and the second mass of the bottom quark	144
H8. Absorption profile from the primordial cold hydrogen field	147
H9. The SST large numbers law, Gravity versus the Standard Model, and the gravitational black holes	148
H10. Creation of dark energy (DE) and dark matter (DM)	148
I. Particle physics	150
I1. The origin of the transverse radii of hyperons at the LHC	150
I2. Masses of the Upsilon and χ_b mesons	151
I3. The neutron mean square charge radius and the origin of the Standard Model	152
I4. Lepton universality	155
I5. The structure of Type-X particles	156
I6. Internal structure of all particles	162
I7. Harbingers of a revolution in physics	181
J. A very short recapitulation	185
Index	188

Chapter 1

Introduction

1.1. Need for new methods

For decades we are still not able to solve dozens of basic problems in physics and cosmology. Why?

The most common error in theories is not separating the definitions from the laws of Nature. The definitions can be freely chosen and do not require justification. On the other hand, the laws of Nature, i.e. mathematical formulas that describe the internal structures of objects or their dynamics, must always be justified on the basis of possible physical phenomena resulting from the initial conditions.

If, for example, differential equations appear in theory as some hocus-pocus, and then we add a large enough number of free parameters to fit the theoretical results with the experimental data, this is quackery that has nothing with real physics.

The laws of conservation of some physical quantities (or symmetries) are laws of Nature, so they must be derived from the initial conditions. For example, in mainstream physics there is no justification why an electric charge is invariant. The claim that this is due to the symmetry of a gauge transformation is not an explanation because such a transformation is a mathematical operation and not a physical phenomenon.

So gauge transformations are not the right way to formulate the missing part of the theory of everything (ToE).

Physics needs new methods and here we present them.

Here, due to the viscosity that results from smoothness of surfaces of the inertial masses, due to the possible quantum entanglement and/or confinement of the components of the Scale-Symmetric-Theory (SST) absolute spacetime (SST-As), instead of solving differential equations of motion or looking for symmetries resulting from the gauge transformations, we are looking for stable or metastable dynamical distributions of the components of such spacetime. The distributions lead to the coupling constants which are the core of the dynamical description. Most of such distributions cannot result from solutions of the equations of motion because the observed particles have too rich internal structure which requires the use of various methods for single particles.

The General Theory of Relativity (GR) starts from the assumptions that the inertial mass and gravitational mass, M_{inertial} and $M_{\text{gravitational}}$ respectively, have the same value

$$M_{\text{inertial}} = M_{\text{gravitational}} \quad (1.1.1)$$

and that there is an upper speed limit $v_{\text{upper}} = c = 299,792,458 \text{ m/s}$. Such a theory leads to the relativistic masses which are consistent with experimental results – for the upper speed limit, there appears a relativistic-mass singularity so within GR we cannot describe phenomena concerning such a singularity and tachyons i.e. objects that are moving with superluminal speeds.

In this book, we show that the four fundamental phase transitions of the inflation field lead to the five levels of Nature: to the tachyons the SST Higgs field (SST-Hf) consists of, to the superluminal quantum-entanglement objects (entanglons), neutrino-antineutrino pairs the SST absolute spacetime (SST-As) consists of, to the core of baryons, and to the core of the cosmological Protoworld – dynamics of the last three objects is similar. The strength of SST comes from the fact that it contains only 11 parameters and leads to physical constants and all the basic physical quantities used in particle physics and cosmology, and many used in other areas of physics. SST is the classical non-perturbative theory.

In the last section we show that the SST is the seven-parameter theory but then the math of such a theory is much more complicated because we have to solve systems of equations with a large number of unknowns.

Here we will show that the Quantum Mechanics (QM) is the result of neglecting the exchanges of the spin-1 superluminal objects (the entanglons) the general-relativity and quantum-mechanics matter consists of (i.e. matter with the upper speed limit equal to c). In SST, there appear the entanglons so we do not apply the QM formalism. The quantum behaviour of a particle (i.e. the disappearance in one place of a field and appearance in another one, and so on) has a classical but superluminal origin.

Generally, the matter and energy behave classically so the SST is the pure classical theory with physical quantities quantized classically.

Each spinning object immersed in a granular field curves the field, i.e. creates a gradient with non-spherical symmetry. Gravitational mass have objects that at distances a few times bigger than such objects can create in the Higgs field a gravitational gradient with spherical symmetry – such gradient is defined by the known gravitational constant G . Neutrinos are the smallest objects that create such gradients. **We assume that objects with invariant inertial mass (i.e. such mass does not depend on velocity) can be tachyonic.** There are two such objects: the tachyons the SST Higgs field consists of and the entanglons the neutrinos consist of. Let us emphasize that the SST neutrinos have specific properties because their mass is invariant even though their inertial mass is equal to the gravitational mass. This does not apply to their inertial and gravitational energies, as they are made of superluminal entanglons, and the neutrinos themselves travel at the speed of light in “vacuum” c relative to the object with which they are entangled. Neutrinos cannot change their mass because the SST spacetime does not contain free entanglons from which neutrinos are built of. SST shows that neutrinos are boundary objects of the GR that do not obey the laws described in it.

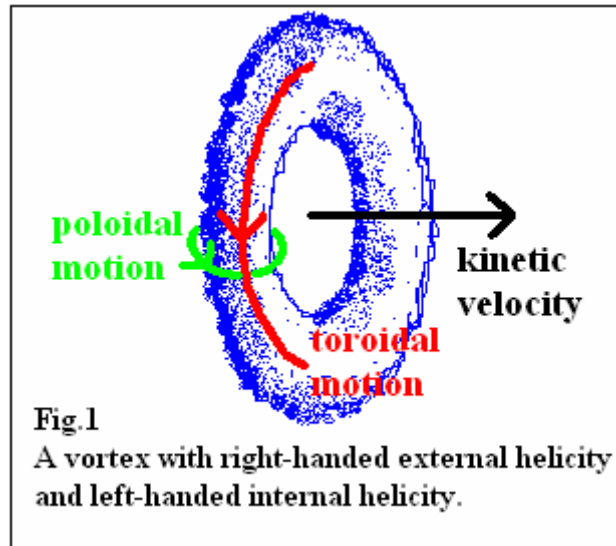
Without understanding the properties of neutrinos (i.e. the Planck scale), we cannot formulate the theory of everything.

Tachyonic objects (i.e. the tachyons and entanglons) we can call the imaginary objects because we can detect them only indirectly as a gravitational field and quantum entanglement, respectively. But we can precisely define their properties because when we apply the minimum number of initial conditions, only the unique set of initial physical quantities leads to the experimental data.

1.2. Nomenclature used in SST

The definitions of structures, physical quantities and their units are not laws of Nature, but the language of description. Using the same definitions allows you to compare the theoretical results obtained in different theories with experimental data. Let us emphasize, however, that new and extended definitions must emerge in the broader theories. SST is the missing core of ToE, so new and extended definitions are needed. Redundant definitions appear in incomplete and at least partially erroneous theories.

External helicity and internal helicity: external helicity is defined by toroidal motion and kinetic velocity while internal helicity is defined by poloidal motion and toroidal motion (Fig.1). Thin torus (loop) and other tori with central hole are the simplest objects that can have internal helicity. We will show that the poloidal motions lead to the low violation of the CP symmetry, where C denotes the charge conjugation, and P is the parity transformation.



Tachyon: a spinning internally structureless inertial mass (a piece of space) with a size about 29 orders of magnitude lower than the Planck length. It is a physical volume with the same inertial-mass density at all points inside it. Spinning inertial masses create some non-spherical gradients in fields composed of inertial masses but they do not cause a relativistic mass of the inertial mass to appear.

Closed string: a circle-like superluminal spin-1/2 loop made of tachyons being in direct contact, with a radius about 10 orders of magnitude and thickness about 29 orders of magnitude lower than the Planck length.

SST Higgs field (SST-Hf): a field composed of tachyons.

Entanglon: a superluminal spin-1 binary system of the closed strings responsible for quantum entanglement. It is very stable because it is immersed in the SST Higgs field.

Initial inflation field: the field with left-handed external helicity composed of tachyons packed to maximum.

SST absolute spacetime (SST-As): a field composed of the non-entangled (entanglement is directional) and non-confined (confinement is volumetric or circular) and non-rotating spin-1 neutrino-antineutrino pairs moving with their natural speed c in relation to such absolute spacetime. The SST-As behaves as superfluid.

SST spacetime (SST-S): the two-component spacetime composed of the SST Higgs field and the SST absolute spacetime (SST-Hf and SST-As).

Quantum entanglement: the entanglement of the components of the SST absolute spacetime caused by exchanges of the superluminal entanglons. Distance between entangled components can change. But there are the two very stable states for the two shortest-distance quantum entanglement.

Confinement: it is the confinement of the spin-1 components of the SST absolute spacetime (or neutrinos) caused by the SST Higgs potential created by them. Distance of such confinement is invariant. Ranges of the SST Higgs potential are different for spacetime condensate and electron loop.

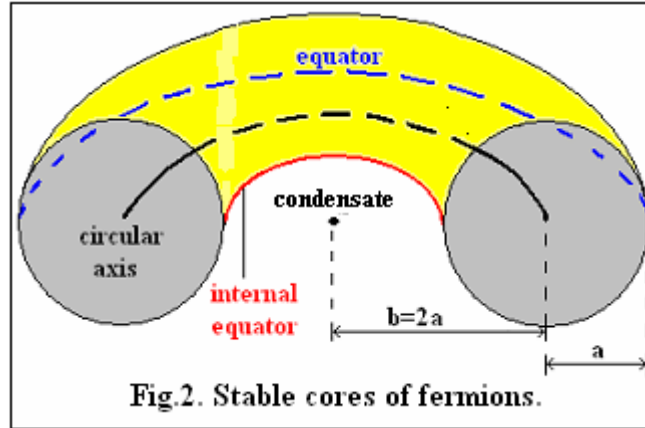
Photons and gluons: photons and gluons are the rotational energies of single component or entangled components of the SST absolute spacetime. In fields that have internal helicity (the nuclear strong fields have such helicity), because of the three helicities of the components of the SST absolute spacetime, the photons behave as gluons so instead of the one type of photons we have the 8 types of gluons. In SST, the gluons are not confined in the nuclear strong fields.

Baryons and electrically charged leptons: cores of such fermions consist of a spin-1/2 torus/electric-charge and a spin-0 central ball/condensate both composed of the components of the SST absolute spacetime (Fig.2). We know that following equation defines a torus:

$$(x^2 + y^2 + z^2 - a^2 - b^2)^2 = 4 b^2 (a^2 - z^2) . \quad (1.2.1)$$

The spin-1/2 tori are most stable when $b = 2a$ because then the distance between points in the same state on the torus in the plane of the equator is $4a = \lambda$, where λ is the classical radius of a fermion (it is the $4/3$ of the quantum radius). Then the maximal changes in amplitude of the standing wave coincide with the centre of the condensate and a point on the circular axis of the torus, while its three nodes are placed on the torus. The spin speed on the equator is c so the mean spin speed of the torus is $2c/3$ – it forces the radial and poloidal motions of the SST-As components so there appears the spin-0 condensate in the centre of the torus. Mean radius of the tori is the $2/3$ of their equatorial radius.

Outside the core of baryons is obligatory the Titius-Bode law for the nuclear strong interactions.



Instead the torus/electric-charge of the electron, there can be a spin-1/2 loop (it has the poloidal and toroidal speeds) with radius equal to the equatorial radius of the torus.

Neutrinos: there are three species of neutrinos, i.e. the 6 different neutrinos. The tau-neutrino consists of 3 different smallest neutrinos so we have 4 different smallest neutrinos, i.e. 2 species of smallest neutrinos (the electron-neutrino and muon-neutrino). Cores of smallest neutrinos look as both the core of baryons and cores of electrically charged leptons but instead the SST-As components there are the superluminal spin-1 entanglons. It means that the smallest neutrinos carry the weak charge. The smallest neutrinos differ by orientation of the spins of entanglons on their torus and by the internal helicity. Their radius is close to the Planck length. The neutrino-antineutrino pairs are moving with the speed c despite the fact that they have the gravitational

masses – it follows from the fact that they cannot attach entanglons because there are not free entanglons in the SST spacetime. On the other hand, for example, a moving proton can attach SST-As components so there appears the relativistic mass – it follows from the conservation of the spin of the torus/electric-charge of the proton and from the fact that the natural speed of the SST-As components in the SST absolute spacetime is c . Due to the tremendous non-gravitating energy frozen in each neutrino, neutrinos are the very stable particles. Oscillations of neutrinos are an illusion resulting from the switching round of neutrinos in collisions of free neutrinos with free or bound neutrinos.

Zero-energy field: the zero-energy field is associated with the excited states of the SST absolute spacetime. Rotational motions of photons and gluons and other ordered motions decrease dynamic pressure in the local SST-As so local density of it must increase. Mass of the additional spacetime components is equivalent to the carried energy – it leads to the origin of the Einstein formula $E = mc^2$. We see that momentum density and momentum flux both increase the local energy density, i.e. they increase density of the zero-energy field. The same concerns the shear stress because it forces creation of the particle-antiparticle pairs. Such is the origin of replacement of the Newtonian mass density with the Einsteinian stress-energy-momentum tensor. We can say that such a tensor leads to the *granular* SST absolute spacetime and vice versa. But emphasize that contrary to the Einstein's spacetime, the SST-As is not elastic but granular and it does not concern the gravitational fields.

Unification of GR and QM: In SST, gravitating masses create gradients in the SST Higgs field, i.e. create the gravitational fields. Such gradients cause that the GR time is not absolute. On the other hand, gradients are not produced in the SST absolute spacetime – there are created the virtual pairs. It means that time in QM, which is associated with the SST absolute spacetime, is absolute. It is impossible to merge the not absolute time with absolute time within the same methods so unification of GR and QM is impossible – we can “unify” such theories only via the phase transitions of the initial inflation field.

Dark matter (DM) loops: they are a circle-like loops composed of the SST-As components with spins tangent to the loop (in the electron loop, the spins are perpendicular to the loop so they can rotate, i.e. they can interact electromagnetically). Such loops cannot interact electromagnetically because the spins of the SST-As components cannot rotate. We show in this book that mass of the DM-loop is $\sim 2.08 \cdot 10^{-47}$ kg. Such DM-loop with shortest-distance quantum entanglement has radius $\sim 0.23 \cdot 10^{-15}$ m (~ 0.23 fm). A DM-torus built of such DM-loops has mass ~ 727.4392 MeV.

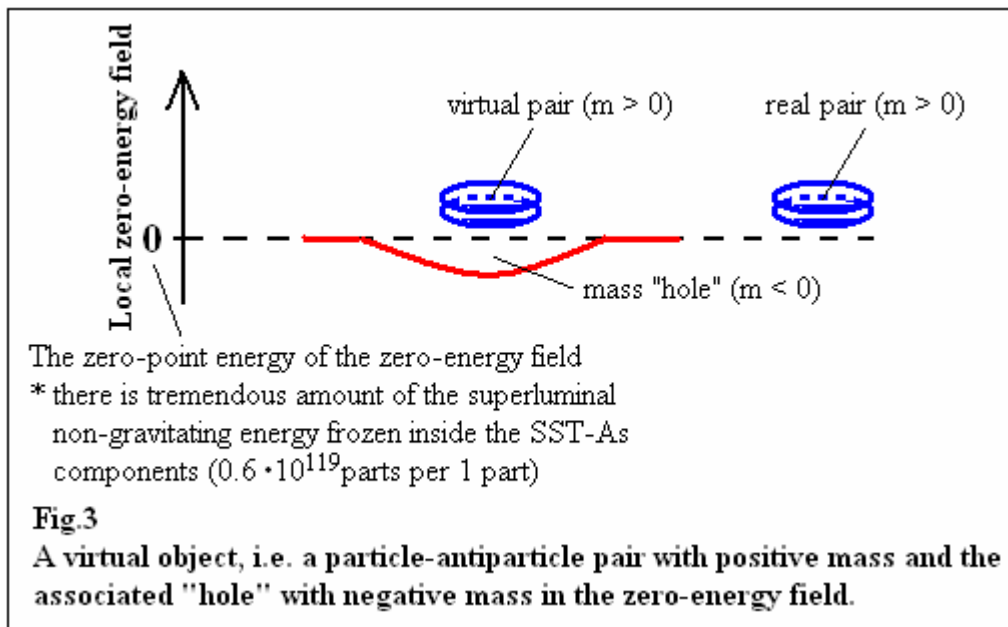
Dark energy (DE): the field composed of the DM strings, i.e. of the open DM-loops. Such DE components/segments move with the speed c so they increase dynamic pressure of the ground state (i.e. of the not excited state) of the SST-As. At sufficiently high mass/energy density, there can be the transitions of the DE-segments into the DM-loops and DM-tori, and vice versa. For example, the DM-tori were produced at the end of the SST inflation.

Our Cosmos: from the succeeding phase transitions of the inflation field follows that radius of our Cosmos is about $2.3 \cdot 10^{30}$ m. Our Universe is a part of our Cosmos.

Virtual particles: They are the objects created spontaneously in the SST absolute spacetime – there appear the bare (i.e. without the radiation masses) particle-antiparticle pairs with positive mass and the associated with them “holes” in the SST-As with negative mass in such a way that the total mass is equal to zero (Fig.3).

Speed c : It is the natural speed of the non-entangled SST-As components in relation to the SST absolute spacetime, and it is the speed of photons and gluons in relation to the object with which they interacted for the last time. In the Michelson-Morley experiment,

the interferometer is the last-interaction object so it always will measure the speed c . Photons and gluons are entangled with the last-interaction object, i.e. there are exchanged the superluminal entanglons between the photons or gluons and the last-interaction object. The Special Theory of Relativity (SR) is valid only for particles that are entangled with the frame of reference we are considering. Here we calculated the speed c from our initial conditions. Generally, we cannot define speed of a photon which is entangled with two or more inertial frames. The protogalaxies were surrounded by the photons entangled with them so because the SST-As behaves as a superfluid, some protogalaxies in the initial protuberances in the early Universe have reached radial velocities many times higher than the c . Some similar phenomena appear in other superfluids. For example, we know that a wire rod moving through a helium-3 superfluid does not break apart the Cooper pairs above the critical Landau velocity [1]. It is because particles in the superfluid stick to the rod. Of course, the superluminal cosmological protuberances were damped – galaxies whose relative speed in relation to the Earth has fallen below the speed c can be observed by us but due to the quantum entanglement, we measure the initial redshift, i.e. the redshift higher than 1.



SST quarks: they are the loops or condensates built of the SST-As components with the masses equal to the masses of quarks in the Standard Model (SM). Other properties of the SM quarks are not important. Here, the masses of the SST quarks are derived from our initial conditions.

Neutron black holes (NBHs): they are the neutron stars with the spin speed equal to c on their equator.

1.3. Initial conditions used in SST

Due to a collision of the externally left-handed initial inflation field with a much bigger cosmological inertial mass, there appeared the inflation inside the much bigger object. As a result there was created the SST spacetime with a stable boundary.

SST inflation was partly random (for example, at the end of the SST inflation there was an undercooling of expanding spacetime) and this caused the number of parameters (11) to be greater than for the initial inflation field.

The Theory of Everything (ToE) should start from 11 parameters/physical-quantities that should relate to the excited state of the SST two-component spacetime, so to virtual processes as well. Here we show that in such theory, we do not have to use the results that appear in the later stages of the theory – this is the natural behaviour of Nature. In the last section of this book we show that, in reality, **the SST is the 7-parameter theory**.

The SST Higgs field has 6 degrees of freedom while the excited state of the SST absolute spacetime has 26 degrees of freedom, i.e. the SST two-component spacetime has 32 degrees of freedom (see Section 2.13) – emphasize that its ground state has $6+24=30$ degrees of freedom.

Let us note one fact that may be a coincidence but may have a deep meaning. Namely, among the first 32 natural numbers there are 11 prime numbers (2, 3, 5, 7, 11, 13, 17, 19, 23, 29 and 31) which resonates with the number of degrees of freedom of our excited spacetime (32) and the number of parameters (11).

***The 11 SST parameters**

The 11 parameters applied in SST are as follows.

*Mean radius of the tachyons

$$r_t = 4.757105905231615 \cdot 10^{-65} \text{ m.}$$

*Mean linear speed of tachyons

$$v_t = 2.38634397 \cdot 10^{97} \text{ m/s.}$$

*Mean spin speed on equator of tachyons

$$v_{st} = 1.725740638 \cdot 10^{70} \text{ m/s.}$$

*Mean inertial mass of tachyons

$$m_t = 3.7526736431501 \cdot 10^{-107} \text{ kg.}$$

*Dynamic viscosity resulting from smoothness of surfaces of tachyons

$$\eta_t = 1.87516465 \cdot 10^{138} \text{ kg m}^{-1} \text{ s}^{-1}.$$

*The present-day mean inertial mass density of the SST Higgs field

$$\rho_{Hf} = 2.645954 \cdot 10^{-15} \text{ kg m}^{-3}.$$

*Mean gravitational mass density of the SST absolute spacetime

$$\rho_{As} = 1.1022013011 \cdot 10^{28} \text{ kg m}^{-3}.$$

*Mass of the lightest non-rotating-spin neutrino

$$m_{\text{Neutrino}} = 3.3349269504 \cdot 10^{-67} \text{ kg.}$$

Mass of the local zero-energy field around a neutrino depends on frequency of its spin rotation so measured masses of neutrinos can be even tens of orders of magnitude higher than of the non-rotating-spin neutrinos.

*Elementary electric charge (it is defined in the SI; in the SST, it depends on the invariant number of lines of electric forces produced by the SST-As components the different tori/electric-charges or loops/electric-charges are built of)

$$e^{\pm} = 1.602176634 \cdot 10^{-19} \text{ C.}$$

*Mass density of the absolute-spacetime condensates (we will show that it is due to the range of the SST Higgs potential for neutrinos and the SST-As components)

$$\rho_Y = 2.7306383581 \cdot 10^{23} \text{ kg m}^{-3}.$$

*Mass of the electron. We will show that mass of the electron follows from its bare mass (it consists of the electron-loop and central spacetime condensate) and from the electroweak interactions of the bare electron with only one virtual electron-positron pair, so the renormalization does not appear:

$$m_e = 0.510998946 \text{ MeV.} \quad (1.3.1)$$

***The 5 new symmetries and one new asymmetry**

4-closed-string symmetry (generally, the 4-object/particle/fermion symmetry): it follows from the fact that internal helicity and spin of the inflation field was conserved. The tachyons rotate so the created closed strings have internal helicity and spin. To create an object with zero internal helicity and zero spin, the closed strings must be created as binary systems of binary systems. The constituents of the single binary systems have parallel spins and opposite internal helicities whereas the binary systems in a binary system have opposite spins. Such four-object symmetry can be adopted by other objects on higher levels of Nature.

Saturation symmetry: it follows from collisions of the free and bound tachyons. Consider an object composed of four parts each composed of four elements. Then three elements of each part are exchanged between a part and the three other parts while the fourth element represents the part. We see that if a smaller object contains N elements then the next bigger one contains N^2 elements.

Invariant surface-density symmetry: surface density of different tori created due to the phase transitions of the expanding inflation field is invariant so Nature can immediately repair damages to the tori.

Adoption symmetry: on the higher levels of Nature, the half-integral spin of the closed strings and the unitary spin of the binary closed strings (entanglon) are adopted by other particles/objects. Tori and loops are the simplest surfaces which can adopt the internal helicity and spin of the closed strings.

Decay symmetry: there are the symmetrical decays of bosons in fields surrounding objects in which on their equator the spin speed is equal to the c . Such processes lead to the SST Titius-Bode law which is valid in the plane of the equator.

Half-jet asymmetry: the poloidal motion in fermions (there is torus/charge or loop/charge) creates in the SST spacetime a half-jet that is the cause of the CP (Charge conjugation and Parity) and T (Time reversal) violations. Poloidal motions follow from the spin speed of tachyons which is very low in comparison with its linear velocity – it causes that the violation of symmetries is also very low.

The tachyons have infinitesimal spin so all fermions have internal helicity (helicities) which distinguishes fermion from antifermion. On surface of the tori/electric-charges, all spins of the SST-As components point towards the circular axis of the torus (see Fig.2) or all point in the opposite direction which distinguishes electric charge from opposite one (Fig.4).

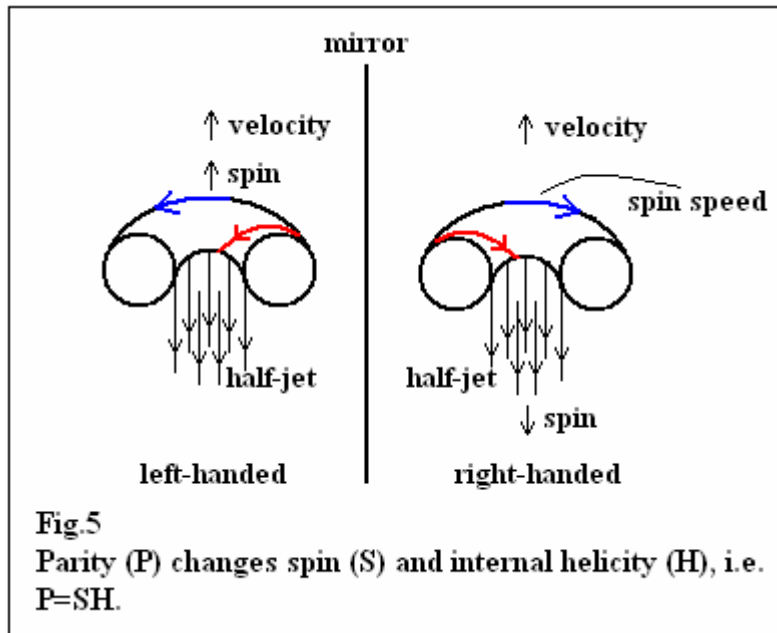
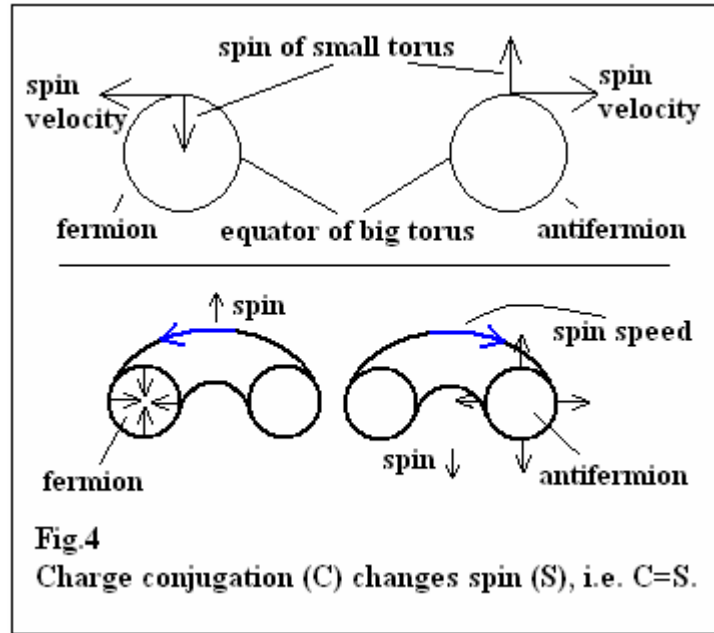
Due to the half-jets, there appears an asymmetry between parallel and antiparallel orientations of spin of fermions in relation to their velocity.

From Figures 4, 5 and 6 follows that the CPT symmetry is always valid

$$CPT = S SH H = S^2 H^2 = 1^2 1^2 = (-1)^2 (-1)^2 = 1 \text{ (always)}. \quad (1.3.2)$$

This means that symmetry-breaking of a system composed of fermion-antifermion pairs is impossible.

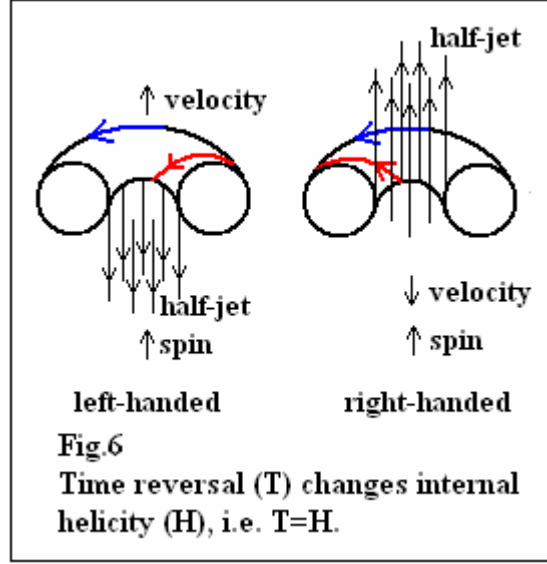
The observed in our Universe the baryon-antibaryon asymmetry does not follow from a *CPT*-symmetry violation. Asymmetry follows from the fact that the initial inflation field had the left-handed external helicity.



The nuclear strong interactions are *CP*-invariant. It results from the fact that single neutral pion, which is responsible for the nuclear strong interactions of

baryons, is composed of two loops that simultaneously create antiparallel half-jets so asymmetry does not appear.

The origin of the symmetries used in mainstream physics will be reported on an ongoing basis during the calculations performed.



*The three fundamental equations

Assume that the closed string is composed of K^2 adjoining tachyons (the square of the K means that calculations are far simpler). The saturation symmetry causes that the tori created during the succeeding phase transitions of the Higgs field should contain K^2 , K^4 , K^8 , K^{16} tachyons (the K^{16} tachyons is the upper limit that follows from the size of our Cosmos). The mass of the tori are directly proportional to the number of closed strings. This means that the stable objects contain the following number of closed strings: K^0 , K^2 , K^6 , K^{14} , and means that the mass of the stable objects are directly proportional to $K^{2(d-1)}$, where $d = 1$ for closed strings, $d = 2$ for the torus of the lightest neutrinos (it consists of the entanglons), $d = 4$ for the torus inside the core of baryons (it consists of the neutrino-antineutrino pairs), and $d = 8$ for a cosmological torus (in the core of the Protoworld) which consisted of the DM particles – their masses were the same as the core of baryons. The early Universe (its baryonic part) arose inside the Protoworld as the double cosmic loop composed of the neutron black holes (NBHs) grouped in protogalaxies. The evolution of the Protoworld leads to the dark matter, dark energy, and to the expanding Universe.

The radii of the tori are

$$r_d = r_1 K^{d-1}, \quad (1.3.3)$$

whereas the rest masses of the tori are

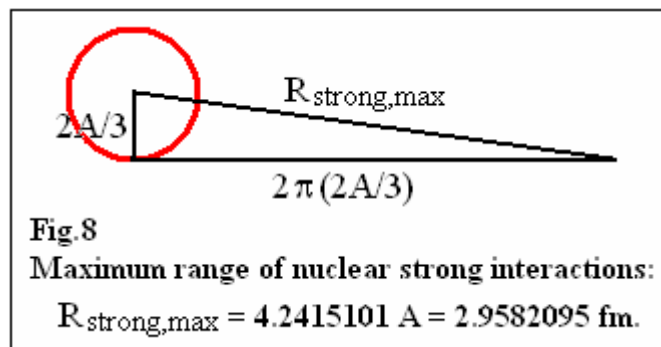
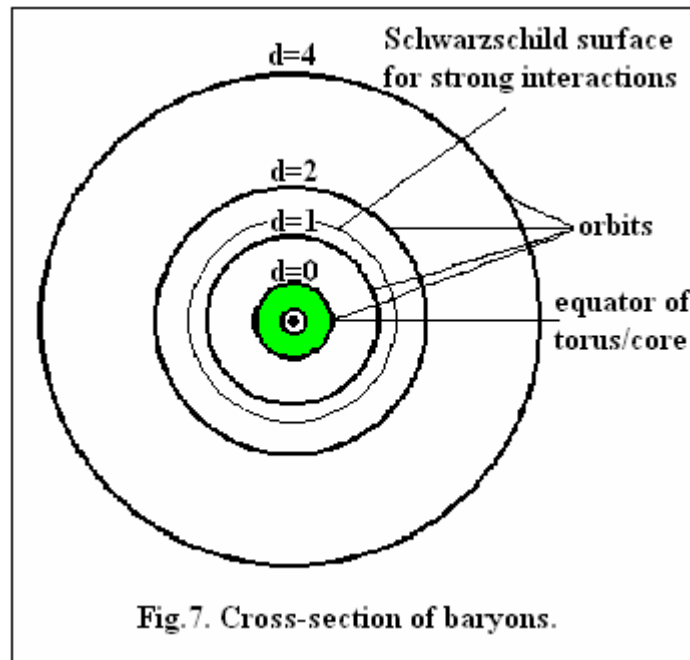
$$m_d = m_1 K^{2(d-1)}, \quad (1.3.4)$$

where r_1 and m_1 are for the closed string.

On equator of the core of baryons, there appear virtual bosons that to equalize their number density in spacetime are emitted. Assume that the radius of the equator of the core of baryons is A , and that the range of a virtual boson is B . At distance $A + B$ there is symmetrical decay of the virtual boson to two identical parts. One part is moving towards the equator whereas the second one is moving in the opposite direction. It means that in the place of decay, in the field surrounding the core, there is produced a “hole”. When the first part reaches the equator then the second one stops and decays to two identical parts – it takes place in distance $A + 2B$. In the place of decay is created “hole” in the zero-energy field. The next decay takes place in distance $A + 4B$. A statistical distribution of the “holes” in the field (of the circular tunnels in the field) in the plane of the equator is defined by following formula

$$R_d = A + d B, \quad (1.3.5)$$

where R_d denotes the radii of the circular tunnels, the A denotes the external/equatorial radius of the torus/core, $d = 0, 1, 2, 4$; the B denotes the distance between the second tunnel ($d = 1$) and the first tunnel ($d = 0$). The first tunnel is in contact with the equator of the torus. Formula (1.3.5) is the Titius-Bode (TB) law for the nuclear strong interactions (Fig.7).



The gluon loop which overlaps with the circular axis of the torus (Fig.2) in the core of baryons, we will call the fundamental gluon loop (FGL) – from Fig.2 we have that its radius is $R_{\text{FGL}} = 2A/3$.

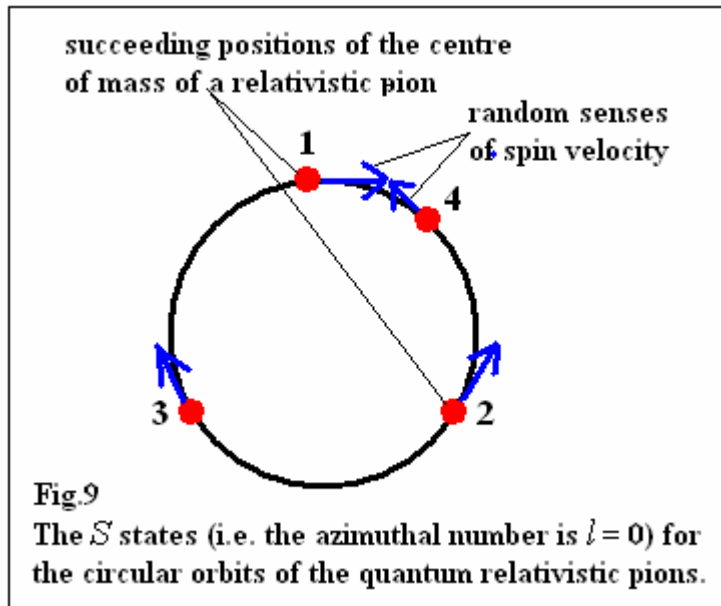
Circumference and radius of FGL determine the maximum range of the nuclear strong interactions in baryons (Fig.8) – it is

$$R_{\text{strong,max}} = 4.24151008771155A . \quad (1.3.6)$$

Our calculations will show that $A = 0.697442532080863 \text{ fm}$ so $R_{\text{strong,max}} = 2.95820953542007 \text{ fm}$.

Our calculations also will show that value of the B and the maximum range of the strong interactions in baryons cause that the $d = 4$ in formula (1.3.5) defines the radius of the last TB orbit (i.e. the radius of the last tunnel in the zero-energy field) for the strong interactions.

Why all the d states of the relativistic pions in baryons are the S states i.e. why all the azimuthal/secondary quantum numbers of the relativistic pions are $l = 0$? It results from the fact that a pion in defined d state behaves as follows. Centre of mass of a relativistic pion disappears in one point of defined circular orbit/tunnel and appears in another one, and so on, but senses of the spin velocities of the pion change randomly – it causes that resultant angular momentum on the circular orbit is equal to zero (Fig.9).



1.4. Derivation of the very frequently applied formulas and laws

In this book, we apply some laws used in mainstream physics. But SST is the supreme theory so we have to show that they can also be derived from the SST initial conditions.

Formula for relativistic mass

It is not true that pure energy, i.e. rotational energy of something or kinetic energy of something can directly transform into inertial or gravitational mass. The Einstein's formula $E = mc^2$ is valid because with each pure energy (it does not gravitate), E , is associated a local concentration of the SST absolute spacetime. The gravitational mass of it, m , (we must subtract the density of the absolute spacetime from the density of the local concentration and

then multiply the result by volume of the concentration) is equivalent to the energy and such gravitational mass is a part of the zero-energy field.

Consider a rigid loop composed of the entangled SST-As components. Assume that linear/relativistic velocity of it is parallel to its spin – then the spin is conserved. The resultant speed of the SST-As components must be equal to c . Their spin speed we denote by v_{spin} while their linear/relativistic speed by v . Then for the rigid loop is

$$v_{\text{spin}}^2 + v^2 = c^2 . \quad (1.4.1)$$

We can multiply it by $N_{\text{Rel}}^2 m^2$, where N_{Rel} denotes the number of the SST-As components, and m denotes the mass of single component in relativistic loop

$$N_{\text{Rel}}^2 m^2 v_{\text{spin}}^2 + N_{\text{Rel}}^2 m^2 v^2 = N_{\text{Rel}}^2 m^2 c^2 . \quad (1.4.2)$$

Spin of the rigid loop is

$$\mathbf{spin} = N_i m v_{\text{spin}} \mathbf{r} , \quad (1.4.3)$$

where N_i denotes number of the SST-As components.

Since spin and radius of the rigid loop and the mass of the SST-As components, m , are invariant, we have

$$N_0 c = N_{\text{Rel}} v_{\text{spin}} , \quad (1.4.4)$$

$$m_{\text{Rel}} = N_{\text{Rel}} m , \quad (1.4.5)$$

$$m_0 = N_0 m , \quad (1.4.6)$$

where N_0 denotes number of the SST-As components in the resting rigid loop, m_{Rel} is the relativistic mass of the loop, and m_0 is the rest mass of the loop.

From formulae (1.4.1)-(1.4.6) we obtain

$$m_{\text{Rel}} = m_0 / (1 - v^2 / c^2)^{1/2} . \quad (1.4.7)$$

We can see that when we accelerate such a rigid loop, it attaches more and more the SST-As components, i.e. the relativistic mass is real.

Emphasize that in a particle, there is the non-gravitating energy, E , and the particle has the bare mass M_{Bare} equal to the E (it is when units of E and M are the same) so the sum of absolute values of energies of virtual particles created outside the bare particle cannot be greater than $E + M_{\text{Bare}} = 2M_{\text{Bare}} = 2E$.

The Stefan-Boltzmann law and the Wien's displacement law

In SST, we very frequently apply the Stefan-Boltzmann law and the Wien's displacement law so we must derive them from our initial conditions.

The Stefan-Boltzmann law states that the radiated total energy (per unit surface area), denoted by $-\Delta E^*$, is directly proportional to the fourth power of the black body's thermodynamic temperature T

$$-\Delta E^* \sim T^4 . \quad (1.4.8)$$

Wien's displacement law states that the black-body-radiation curve, for different temperatures, T , peaks at different wavelengths, λ_{Peak} , and λ_{Peak} is inversely proportional to T

$$\lambda_{\text{Peak}} \sim 1 / T . \quad (1.4.9)$$

We can define the temperature T as inversely proportional to the radius R of a circle-like loop composed of the entangled SST-As components, so the T , because there is $\lambda = 2\pi R$, is also inversely proportional to the wavelength of the loop λ

$$T \sim 1 / R \sim 1 / (2 \pi R) \sim 1 / \lambda . \quad (1.4.10)$$

For a vortex composed of such loops with a peak radius, R_{Peak} , we have

$$T \sim 1 / (2 \pi R_{\text{Peak}}) \sim 1 / \lambda_{\text{Peak}} . \quad (1.4.11)$$

By comparing (1.4.9) and (1.4.11), we see that the Wien's displacement law that follows from experimental data suggests that black bodies consist of vortices composed of loops built of the entangled SST-As components. We will show that it is true. For example, in the baryons can be produced such loops with different radii – in higher temperatures, number density of created loops with smaller radii is higher. The atom-like structure of baryons and the creations of such loops in them lead to the black body spectrum and to the temperature fluctuations in CMB. The structure of baryons suggests that for sufficiently high temperature of a black body, the smallest wavelengths should be two times smaller than λ_{Peak} and we should see a threshold for density of the longest wavelengths for $\lambda = 2\pi\lambda_{\text{Peak}}$ (see Chapter "Cosmology").

In reality, formula (1.4.11) and our considerations suggest that the Wien's displacement formula is a definition of thermodynamic temperature of a black body.

Consider a spinning circle-like loop, composed of the SST-As components, that collapses to a spin-0 condensate/ball with a loop on its equator that is emitted. Assume that the final condensate has radius r . Then for the initial loop is

$$\mathbf{spin} = M v_{\text{spin}} R . \quad (1.4.12)$$

For the final loop is

$$\mathbf{spin} = \Delta M v_{\text{spin}}^* r . \quad (1.4.13)$$

For the condensate/ball we have

$$M - \Delta M \sim r^3 . \quad (1.4.14)$$

From (1.4.12)-(1.4.14) is

$$1 / (v_{\text{spin}} R) - 1 / (v_{\text{spin}}^* r) \sim r^3 \quad (1.4.15)$$

or

$$r / (v_{\text{spin}} R) - 1 / v_{\text{spin}}^* \sim r^4 . \quad (1.4.16)$$

For $r \ll R$ and from (1.4.10) is

$$- v_{\text{spin}}^* \sim T^4 . \quad (1.4.17)$$

Energy of the final loop is

$$\Delta E^* = \Delta M v_{\text{spin}}^{*2} . \quad (1.4.18)$$

From (1.4.13) and (1.4.18) we have

$$\Delta E^* \sim v_{\text{spin}}^* \quad (1.4.19)$$

so from (1.4.17) and (1.4.19) we obtain the Stefan-Boltzmann law

$$-\Delta E^* \sim T^4 . \quad (1.4.20)$$

Lifetimes of particles and stars

Dynamic pressure of a field, p_{Dyn} , is defined as directly proportional to its energy density ρ_{Energy}

$$p_{\text{Dyn}} = \rho_{\text{Energy}} c^2 / 2 . \quad (1.4.21)$$

Since photons and gluons raise the zero-point of the zero-energy field, so the radiation pressure, p_{Rad} , is directly in proportion to the four powers of absolute temperature T

$$p_{\text{Rad}} \sim T^4 . \quad (1.4.22)$$

We see that the theory of stars follows from the dynamics of loops created in baryons.

Since absolute temperature of a loop is inversely proportional to its radius (so to radius of the final condensate as well) so for mass inversely proportional to radius of a loop we have that absolute temperature is directly proportional to mass m

$$T \sim m . \quad (1.4.23)$$

Spin of a virtual loop we can define as the product of its energy ($-E^*$) and period of spinning which is the lifetime, τ_{Lifetime} , of the virtual loop

$$\tau_{\text{Lifetime}} \sim 1 / -E^* . \quad (1.4.24)$$

From formulae (1.4.20), (1.4.23) and (1.4.24) we have

$$\tau_{\text{Lifetime}} \sim 1 / m^4 , \quad (1.4.25)$$

where m is the mass of a condensate or loop composed of the SST-As components or m is the mass of a star.

In SST, coupling constants, α_i , are defined as follows

$$\alpha_i = G_i M m / (c \hbar) , \quad (1.4.26)$$

where G_i are the constants of interactions (such as, for example, the gravitational constant G), M is mass of source of interactions, m is mass of carrier of interactions, and \hbar is the reduced Planck constant.

The following formula defines the energy of an interaction

$$\Delta E_i = G_i M m / r . \quad (1.4.27)$$

Then from (1.4.26) and (1.4.27) we obtain

$$\Delta E_i = \alpha_i c \hbar / r = m_i c^2 . \quad (1.4.28)$$

From (1.4.24) and (1.4.28) we obtain

$$\tau_{\text{Lifetime}} \sim 1 / \alpha_i . \quad (1.4.29)$$

Emphasize that we derived all formulae in this Section from our initial conditions.

Applications of the Stefan-Boltzmann law

Let us consider a transition from circular motions (or circular motions on a virtual “hole” in the SST absolute spacetime (it can be a binding energy; $\lambda = 2\pi r$)) to diagonal oscillations ($\lambda^* = 2r$). Then from (1.4.10) and (1.4.20) results that there is emitted following energy

$$- \Delta E^* = E_o / \pi^4 , \quad (1.4.30)$$

where E_o is the initial energy (real or virtual).

By some analogy, for a transition from circular motions to radial oscillations ($\lambda^{**} = r$) we have

$$- \Delta E^{**} = E_o / (2 \pi)^4 . \quad (1.4.31)$$

1.5. Electron and the matter-antimatter asymmetry

The electron plays an important role in our theory so we described its internal structure (which follows from properties of the SST-As) in this separated Section. In our book, we show that the very simple structure of the electron leads to the correct value for the anomalous magnetic moment.

Due to the SST adoption symmetry, in collisions of photons and gluons can be created the spin-1 photon loop or gluon loop that shape is similar to the entanglement, i.e. a loop consists of two spin-1/2 loops with opposite internal helicities which represent the charge and anticharge of a fermion-antifermion pair (electron-positron pair or quark-antiquark pair, respectively).

Consider the behaviour of a spin-1/2 photon loop in such a system created in the SST absolute spacetime. The electron, due to the SST circular Higgs potential (see Section 2.9), is created as the electron loop composed of the SST-As components – its density is a little

higher than the SST-As so such a loop represents the mass of the electron elementary charge. It is very difficult to detect such a mass because it only insignificantly differs from the SST-As. Such a loop represents also the half-integral spin of the electron. Due to the adoption symmetry, the electron loop must consist of K^2 of the SST-As components and distance between them are defined by the SST Higgs potential. It leads to conclusion that radius of the loop is strictly determined – it is the reduced Compton wavelength of the bare electron, $\lambda_{e,bare}$. The same concerns its spin, $\hbar/2$, and spin speed of the spin-1/2 electron loop, c , so we can calculate mass of the bare elementary electric charge, $m_{e,bare}/2$

$$(m_{e,bare} / 2) c \lambda_{e,bare} = \hbar / 2 . \quad (1.5.1)$$

We obtain

$$m_{e,bare}/2 = 0.25520352567528 \text{ MeV} . \quad (1.5.2)$$

This value is derived from our initial conditions (see Section 2.3).

Such electron loop, due to the superluminal quantum entanglement, immediately transforms into the torus/electric-charge because the torus is more stable than the loop – it follows from the fact that in the torus there appear the radial motions/waves of the SST-As components that lead to creation of the spin-0 central condensate with a mass equal to mass of the elementary electric charge. The central condensate is created due to the SST volumetric Higgs potential (see Section 2.9). It is very difficult to detect such a condensate because it only insignificantly differs from the SST-As. The torus/electric-charge is only the polarized part of the SST absolute spacetime so its apparent mass is zero. Due to the adoption symmetry, it has the right-handed internal helicity. We see that the total mass of the bare electron is $m_{e,bare}$. Emphasize that the electric lines of forces converge on the circular axis of the electron torus (see Fig.2) which has radius equal to $2\lambda_{e,bare}/3$ – notice that the equatorial radius of the electron torus is $\lambda_{e,bare}$, i.e. it is the radius of the electron loop. We can see that the resultant mass of the electric charge is on the equator while the mean radius of the torus/electric-charge, e^\pm , is $2\lambda_{e,bare}/3$. All spins of the SST-As components on surface of the torus point towards the circular axis of the torus or all point in the opposite direction – it distinguishes the positive electric charge from negative one. The SST-As components swap places, which causes them to rotate on the circular axis of the torus, i.e. there is raised the local zero-point of the zero-energy field. But emphasize that such processes do not change mass and the half-integral spin of the electron loop.

Number of the electric lines of force produced by the tori/electric-charges of the electrically charged leptons and proton is the same so their electric charges are the same as well. In SST, the electron and the electrically charged core of antiproton are similar, i.e. there is torus/electric-charge and central condensate, but distribution of mass is different. For example, emphasize that in the core of baryons, because there is much higher mass density, masses of the real torus and central condensate are not the same.

In similar way behave the spin-1 gluon loops that transform into the pairs of the spin-1/2 quark loops.

Outside the electron torus, there is created only one the virtual bare electron-positron pair (the virtual dipole) which behaves in a quantum way i.e., it disappears in one place and, due to the superluminal entanglons, appears in another one, and so on. The virtual dipole is polarised along the electric lines of forces that converge on the circular axis of the electron torus (Fig.2). When we take into account the radiation mass of the electron, then we obtain

$$m_e / m_{e,\text{bare}} = 1 + a_e \approx 1 + 0.0011596522, \quad (1.5.3)$$

where the number a_e represents the anomalous magnetic moment of the electron (see Section 2.6).

In this book we have:

e^\pm denotes electric charge of the electron or positron,

m_e is the mass of electron or positron, and

$m_{e,\text{bare}}$ is the bare mass of electron or positron.

Electron as a whole behaves in a quantum way (i.e. it disappears in one place and appears in another one, and so on) so in QM is introduced the wavelength of electron.

It is not true that the bare electron is a point-like particle.

Electric charge: We define the elementary electric charge (EEC) as the type-Fig.2 torus composed of the $8.50713316753319 \cdot 10^{38}$ SST-As components – we will show that this number follows from properties of the core of baryons.

The matter-antimatter asymmetry

The above description shows how are created the virtual or real electrons in the electron-positron pairs – the electron, the same as the antiproton, has the right-handed internal helicity while the positron, the same as the proton, is left-handed.

At the end of the SST inflation, there were very energetic collisions of the photons. On the other hand, because mass of the torus/electric-charge of the left-handed proton is much higher than mass of the electric charge of the right-handed electron so the left-handed internal helicity of the proton dominates. Since the SST initial inflation field had the left-handed external helicity (it transformed into the left-handed internal helicity) so at the end of the SST inflation, there appeared more the proton-electron pairs than the antiproton-positron pairs – it is the origin of the observed matter-antimatter asymmetry. We can see that the key to understanding matter-antimatter asymmetry is the internal helicity of the tori/electric-charges and the initial left-handedness of the initial inflation field.

One may ask why the matter-antimatter asymmetry did not manifest itself during inflation at the level of neutrino-antineutrino pairs. It follows from the fact that masses of all the tori/weak-charges in all the three species of neutrinos are the same. Moreover, the mean gravitational-mass density in the neutrinos is about 10 orders of magnitude higher than in protons, so breaking the matter-antimatter symmetry at the neutrino level is incomparably more difficult.

1.6. Uncertainty of experimental results

The interactions are associated with the virtual and real processes that can change local density of the zero-energy field – such changes cause that there appears a broadening of experimental results. Higher value of coupling constant causes that broadening of obtained result is bigger.

References

- [1] D. I. Bradley, *et al.* (18 July 2016). “Breaking the superfluid speed limit in a fermionic condensate”
Nature Physics **12**, 1017-1021 (2016)

Chapter 2

Particle Physics**2.1. Classical thermodynamics and phase transitions of inflation field, physical constants, and dark-matter (DM) particles**

In this Section, we apply the formulae (1.3.3) and (1.3.4).

The definition of the Reynolds number N_R for the SST Higgs field with tachyons packed to maximum looks as follows

$$N_R = \rho_t v_t (2 r_t) / \eta_t = 1.00760468827334 \cdot 10^{-19} . \quad (2.1.1)$$

where ρ_t is the inertial-mass density of single tachyon

$$\rho_t = m_t / (4 \pi r_t^3 / 3) = 8.32192366156326 \cdot 10^{85} \text{ kg m}^{-3} . \quad (2.1.2)$$

The radius of closed string which can be produced due to the value of the Reynolds number is (it consists of tachyons which are in direct contact)

$$r_1 = (2r_t) / N_R = 0.944240526189592 \cdot 10^{-45} \text{ m} . \quad (2.1.3)$$

We can calculate the number of tachyons, K^2 , a closed string consists of

$$K^2 = 2 \pi r_1 / (2 r_t) = (0.78966855476252 \cdot 10^{10})^2 . \quad (2.1.4)$$

The spin of each closed string is half-integral while of the entanglons is unitary

$$\hbar = 2 K^2 m_t v_t r_1 = 1.05457181764623 \cdot 10^{-34} \text{ Js} . \quad (2.1.5)$$

The Planck constant, \hbar , is

$$\hbar = 2 \pi \hbar = 4 \pi K^2 m_t v_t r_1 = 6.6260701500004 \cdot 10^{-34} \text{ Js} .$$

Due to the International System of Units (SI), since 2019, the Planck constant is not measured (it is defined as follows: $\hbar = 6.62607015 \cdot 10^{-34} \text{ Js}$). We can see that our calculated value of the \hbar is consistent with the SI definition for the first 13 digits. Such high accuracy is enough to compare the SST results with experimental results.

We can express the \hbar by only the initial parameters

$$\hbar = (64 \pi^4 / 9) \eta_t^2 r_t^5 / (v_t m_t) = 6.6260701500004 \cdot 10^{-34} \text{ Js} .$$

We see that the Planck constant depends on four initial parameters: $\hbar = f(\eta_t, r_t, v_t, m_t)$. Why the spins of particles are the same in all inertial frames? It follows from the fact that the invariant viscosity of the tachyons, η_t , fixes their speed v_t in relation to an inertial frame with which a particle composed of tachyons interacts – there must be the quantum entanglement between the particle and the inertial frame.

Spins of all objects defined by formulae (1.3.3) and (1.3.4) are half-integral so from definition of spin

$$\mathbf{Spin} = M \mathbf{v} R \quad (2.1.6)$$

we can calculate the speed of light in “vacuum” c

$$c = 3 \hbar / (4 m_4 r_4) = 3 \hbar / (4 m_t r_1 K^{11}) = 299792458.00004 \text{ m/s} . \quad (2.1.7)$$

Such high accuracy of the c is enough to compare the SST results with experimental results as well.

We can express the c by only the initial parameters

$$c = (3 v_t / 2) [3 v_t m_t / (4 \pi^2 \eta_t r_t^2)]^{9/2} = 299792458.00004 \text{ m/s} .$$

We see that the speed of light in “vacuum” also depends on four initial parameters: $c = f(\eta_t, r_t, v_t, m_t)$. Why the c is the same in all inertial frames? It follows from the fact that the invariant viscosity of the tachyons, η_t , fixes their speed v_t in relation to an inertial frame with which a particle composed of tachyons interacts – there must be the quantum entanglement between a neutrino or photon or gluon and the inertial frame.

Mass of the superluminal closed string is

$$m_1 = m_t K^2 = 2.34007881976868 \cdot 10^{-87} \text{ kg} . \quad (2.1.8)$$

Speed of the closed string is

$$v_1 = 3 \hbar / (4 m_t r_1 K^5) = 0.726925274854337 \cdot 10^{68} \text{ m/s} . \quad (2.1.9)$$

We can calculate the factor which changes kg into MeV

$$F = 10^6 e / c^2 = 1.78266192162742 \cdot 10^{-30} \text{ kg/MeV} . \quad (2.1.10)$$

Mass of the torus/electric-charge in the core of baryons is

$$X^\pm = m_4 / F = m_1 K^6 / F = 318.295548099756 \text{ MeV} . \quad (2.1.11)$$

The ratio of the masses of the lightest neutrino, m_{neutrino} , and its torus, m_2 , and the ratio of the masses of the electrically charged core of baryons, H^\pm , and its torus, X^\pm , and the ratio of the masses of the core of the Protoworld, $M_{\text{Pw,core}}$, and its torus, $M_{\text{Pw,torus}}$, are the same so we have

$$H^\pm = X^\pm m_{\text{Neutrino}} / m_2 = 727.439224547912 \text{ MeV}, \quad (2.1.12)$$

where

$$m_2 = m_1 K^2 = 1.45921798788058 \cdot 10^{-67} \text{ kg}. \quad (2.1.13)$$

The equatorial radius of the lightest neutrinos is

$$r_{\text{neutrino}} = 3 r_1 K / 2 = A / K^2 = 1.1184555774965 \cdot 10^{-35} \text{ m}, \quad (2.1.14)$$

where A is the equatorial radius of the torus/electric-charge in the core of baryons

$$A = 3 r_4 / 2 = 3 r_1 K^3 / 2 = 0.697442532080863 \text{ fm}. \quad (2.1.15)$$

By an analogy, the core of the cosmological Protoworld, i.e. the cosmological torus and its central condensate, should be built of the cores of baryons. But the cores of baryons are the SST black holes in respect of the nuclear strong interactions, so they capture relativistic pion which is in the $d = 1$ state (see formula (1.3.5)) – it is because such TB orbit is below the Schwarzschild surface for the nuclear strong interactions. Masses of nucleons do not satisfy the formulae (1.3.3) and (1.3.4). We need a stable particle with a mass equal to H^\pm . Consider a torus composed of K^2 entangled loops each composed of K^2 entangled lightest neutrinos with spins tangent to the loops – we will call such a torus and such a loop the dark-matter (DM) objects because due to the orientations of the spins of neutrinos, they cannot interact electromagnetically. Then the shortest-distance quantum entanglement causes that two nearest neutrinos in a loop are in distance equal to

$$L_{\text{Neutrinos}} = 2 \pi r_{\text{neutrino}} / 3. \quad (2.1.16)$$

Such distance results from the geometry of the torus of lightest neutrino.

We assume that the distance between neutrinos in the nearest loops on the equator of the DM torus is also defined by the geometry of the torus of lightest neutrinos, so it is

$$L_{\text{Neutrinos,loops}} = 2 \pi r_{\text{neutrino}}. \quad (2.1.17)$$

The above remarks lead to a conclusion that the radius of a single DM loop is

$$R_{\text{DM-loop}} = K^2 L_{\text{Neutrinos}} / (2 \pi) = K^2 r_{\text{neutrino}} / 3 = r_1 K^3 / 2 = A / 3. \quad (2.1.18)$$

On the other hand, the equatorial radius of the DM torus is

$$R_{\text{DM-torus}} = K^2 L_{\text{Neutrinos,loops}} / (2 \pi) = K^2 r_{\text{neutrino}} = 3 r_1 K^3 / 2 = A. \quad (2.1.19)$$

We see that sizes of the DM torus are the same as of the torus/electric-charge in the core of baryons.

Mass of the DM loop is

$$M_{\text{DM-loop}} = K^2 m_{\text{Neutrino}} = 2.07958182997121 \cdot 10^{-47} \text{ kg}. \quad (2.1.20)$$

$$M_{\text{DM-loop}} = 10^6 K^2 m_{\text{Neutrino}} / F = 1.16655985340885 \cdot 10^{-11} \text{ eV} . \quad (2.1.21)$$

Mass of the DM torus is

$$M_{\text{DM-torus}} = K^4 m_{\text{Neutrino}} / F = H^\pm = 727.439224547912 \text{ MeV} . \quad (2.1.22)$$

Emphasize that the masses of the charged core of baryons and the DM torus are the same, both tori have the same sizes, but in centre of the DM torus is no spacetime condensate, and contrary to the core of baryons, the DM torus does not interact electromagnetically.

Ratio of masses of the charged core of baryons, H^\pm , and the charged torus/electric-charge, X^\pm , is

$$F_{\text{H/X}} = H^\pm / X^\pm = 2.28542066922006 . \quad (2.1.23)$$

The Protoworld was the stable cosmological object because its core, i.e. the cosmological torus and the central condensate both were built of the binary systems of the DM tori.

Mass of the core of the Protoworld was

$$H^+_{\text{Protoworld}} = F_{\text{H/X}} m_1 K^{14} = 1.96076008846624 \cdot 10^{52} \text{ kg} . \quad (2.1.24)$$

The equatorial radius of the core of the Protoworld was

$$\begin{aligned} A_{\text{Protoworld}} &= 3 r_8 / 2 = 3 r_1 K^7 / 2 = 2.71198826517478 \cdot 10^{24} \text{ m} = \\ &= 286.66350758233 \text{ million light-years [Mly]} . \end{aligned} \quad (2.1.25)$$

The internal helicity of the closed string resulting from the infinitesimal spin of the tachyons and their viscosity means that the entanglons a neutrino consists of, outside the neutrino transform the chaotic motions of tachyons into divergently moving tachyons. The direct collisions of divergently moving tachyons with tachyons the SST Higgs field consists of produce a gradient in this field. The gravitational constant, G , results from behaviour of all closed strings a neutrino consists of. Constants of interactions are directly proportional to the mass densities of fields carrying the interactions then the G we can calculate from following formula

$$G = g \rho_{\text{Hf}} = 6.67429778367877 \cdot 10^{-11} \text{ m}^3/(\text{kg s}^2) , \quad (2.1.26)$$

where the g has the same value for all interactions and is equal to (it depends on the tachyon spin speed and the viscosity of tachyon – both quantities are the invariants)

$$g = v_{\text{st}}^4 / \eta_t^2 = 25,224.5420127439 \text{ m}^6/(\text{kg}^2 \text{ s}^2) . \quad (2.1.27)$$

Notice that curvature of the SST Higgs field produced by the entanglons is residual and has not spherical symmetry so such curvature does not relate to the G .

Emphasize that the Planck scale, i.e. the Planck length, Planck time, Planck mass and Planck energy density, are defined by the basic physical constants \hbar , c and G that are calculated in SST with perfect accuracy. But the Planck quantities are defined for an *abstract cube* so to obtain the real values for the Planck quantities we must take into account the shape and size of the lightest neutrino because the $\hbar/2$, c and G concern such object – it is the lightest object for which the gravitational and inertial masses are the same.

2.2. Dynamics of the core of baryons

The virtual or real fundamental gluon loop (FGL) is created on the circular axis (Fig.2) of the torus/electric-charge in the core of baryons (they initially overlap) from the SST-As components. Masses of spinning virtual objects can be calculated from the definition

$$E T_{\text{Period}} = \hbar, \quad (2.2.1)$$

where $E = mc^2$.

Mass of the resting FGL is

$$m_{\text{FGL}} = 3 \hbar / (4 \pi A c F) = 67.5444131256272 \text{ MeV}. \quad (2.2.2)$$

The central condensate, Y , is created due to the transition of the FGL from its circumference to its radius so the mass increases 2π times. In such a process is emitted energy/mass defined by formula (1.4.31), i.e. by the Stefan-Boltzmann law. From the Wien's displacement law follows that temperature is inversely proportional to radius so the emitted energy is directly proportional to $1/(2\pi)^4$, so we have

$$Y = 2 \pi m_{\text{FGL}} \{1 - 1 / (2\pi)^4\} = 424.121762762297 \text{ MeV}. \quad (2.2.3)$$

The condensate Y is the SST black hole for the nuclear weak interactions so the spin speed on its surface is c .

The number of the neutrino-antineutrino pairs, N_{NA} , on the torus in the core of a baryon is

$$N_{\text{NA}} = X^\pm F / (2 m_{\text{Neutrino}}) = 8.50713316753319 \cdot 10^{38}. \quad (2.2.4)$$

Mean distance, L_{NA} , of the neutrino-antineutrino pairs on the torus in the core of a baryon is

$$L_{\text{NA}} = (8 \pi^2 A^2 / (9 N_{\text{NA}}))^{1/2} = 7.08256264113404 \cdot 10^{-35} \text{ m}. \quad (2.2.5)$$

Notice that surface density of the torus in the core of baryons is about 300,000 times higher than in SST-As – it is very important in the theory of the neutron black holes.

Mean distance, L_{As} , of the neutrino-antineutrino pairs in the SST-As is

$$\begin{aligned} L_{\text{As}} &= (2 m_{\text{Neutrino}} / \rho_{\text{As}})^{1/3} = 3.92601360788938 \cdot 10^{-32} \text{ m} = \\ &= 3510.20969172255 r_{\text{neutrino}}. \end{aligned} \quad (2.2.6)$$

2.3. Structure of the bare electron and the electromagnetic interactions

The ratio, N^* , of the mean distances is

$$N^* = L_{As} / L_{NA} = 554.321056772292 . \quad (2.3.1)$$

It characterizes the projection of the proton electric charge on the SST absolute spacetime. We can say that it relates the effective distances between the As components on the torus/electric-charge of proton with distances between the As components in the SST absolute spacetime. But the real distances between the As components on the proton torus are $2\pi r_{\text{neutrino}}$. Effective distances are bigger because some of the As components change places to keep the torus stable. It leads to conclusion that the As components in the electron loop that represents the mass of the electric charge of the bare electron are in distances equal to $L_{e,\text{bare}} = 2\pi r_{\text{neutrino}} N^*$

$$L_{e,\text{bare}} = 2 \pi r_{\text{neutrino}} N^* = 3482.90191937193 r_{\text{neutrino}} . \quad (2.3.2)$$

Due to the adaption symmetry, the bare-electron loop consists of K^2 of the SST-absolute-spacetime components. Then radius of such loop, $\lambda_{e,\text{bare}}$, is

$$\lambda_{e,\text{bare}} = K^2 L_{e,\text{bare}} / (2 \pi) = 3.86607081421007 \cdot 10^{-13} \text{ m} . \quad (2.3.3)$$

It is the Compton length, $\lambda_{e,\text{bare}}$, of the bare electron and we can calculate it also from following formula

$$\lambda_{e,\text{bare}} = A N^* = 3.86607081421007 \cdot 10^{-13} \text{ m} . \quad (2.3.4)$$

It is very difficult to detect the bare-electron loop because distances of the As components in it are close to the distances in the absolute spacetime. Moreover, it is the quantum object so there is a distribution of it in whole spacetime.

The bare mass of electron is

$$m_{e,\text{bare}} = \hbar / (c \lambda_{e,\text{bare}}) = 9.09883214972773 \cdot 10^{-31} \text{ kg} , \quad (2.3.5)$$

$$m_{e,\text{bare}} = \hbar / (c \lambda_{e,\text{bare}} F) = 0.51040705135056 \text{ MeV} . \quad (2.3.6)$$

Spin of the bare-electron loop should be half-integral and it is (in our model of the electron, mass of the bare-electron loop is equal to mass of the central spacetime condensate)

$$(m_{e,\text{bare}} F / 2) c \lambda_{e,\text{bare}} = \hbar / 2 . \quad (2.3.7)$$

On comparing the two definitions of the fine-structure constant for low energies, α_{em} , we arrive at the relation

$$k e^2 / (\hbar c) = G_{\text{em}} m_e^2 / (\hbar c) , \quad (2.3.8)$$

where $k = c^2 \mu_0 / (4\pi)$ whereas the electromagnetic constant at low energy, G_{em} , is

$$G_{em} = G \rho_{As} / \rho_{Hf} = 2.78025230260979 \cdot 10^{32} \text{ m}^3/(\text{kg s}^2) . \quad (2.3.9)$$

Emphasize that since 2019 the magnetic constant (permeability in vacuum), μ_0 , is the measured quantity.

From formulae (2.3.8) and (2.3.9), we can calculate the magnetic constant

$$\begin{aligned} \mu_0 &= 4 \pi G_{em} m_e^2 F^2 / (c^2 e^2) = 1.25663706211168 \cdot 10^{-6} \text{ H/m} = \\ &= 4 \pi (1.00000000053775) \cdot 10^{-7} \text{ H/m} . \end{aligned} \quad (2.3.10)$$

The electric constant (vacuum permittivity) is

$$\epsilon_0 = 1 / (c^2 \mu_0) = 8.85418781285662 \cdot 10^{-12} \text{ F/m} . \quad (2.3.11)$$

The fine-structure constant at low energy

The fine-structure constant, α_{em} , is

$$\alpha_{em}^{-1} = 2 h / (e^2 c \mu_0) = 137.035999085012 . \quad (2.3.12)$$

Notice that the ratio of masses of the electron and bare electron is

$$F_{1+a} = m_e / m_{e,bare} = 1.00115965217932 \approx 1.00115965218 . \quad (2.3.13)$$

We later will calculate the anomalous magnetic moment from our model of electron (i.e. there is only one virtual electron-positron pair outside the bare electron (it is the bare-electron loop, torus/electric-charge and the central spacetime condensate).

We can assume that the ratio $L_{NA}/(2\pi r_{neutrino}) = 1.0078405229268$ defines the electromagnetic coupling constant at high energy

$$L_{NA} / (2 \pi r_{neutrino}) = 1 + \alpha_{em,high} \quad (2.3.14)$$

so we have

$$\alpha_{em,high} = 1 / 127.542513342079 . \quad (2.3.15)$$

This value corresponds to the minimum distance between the As components on the proton torus/electric-charge, i.e. to distance equal to $2\pi r_{neutrino}$.

Notice that there is satisfied following relation

$$(L_{As} / L_{e,bare})^2 = X_{2\pi}^{\pm} / X^{\pm} = 1.01574251965336 , \quad (2.3.16)$$

where $X_{2\pi}^{\pm}$ is an abstract mass of the torus/electric charge in which the As components occupy squares with the side equal to $2\pi r_{neutrino}$. For the torus $X_{2\pi}^{\pm}$ we have

$$X_{2\pi}^{\pm} = (2 / 9) (A / r_{neutrino})^2 2 m_{neutrino} = 323.306322021294 \text{ MeV} . \quad (2.3.17)$$

We see that because $\text{mass} \sim 1/L^2$ so when L_{As} leads to X^{\pm} then $L_{e,bare}$ leads to $X_{2\pi}^{\pm}$.

2.4. The other coupling constants and masses of pions

The ratio of the binding energy of two FGLs, ΔE_{FGL} (it results from creations of the virtual electron-positron pairs), to the mass of FGL, m_{FGL} , is (energy is inversely proportional to a length, and m_{FGL} is associated with A while ΔE_{FGL} with $\lambda_{e,\text{bare}}$)

$$\Delta E_{\text{FGL}} / m_{\text{FGL}} = A / \lambda_{e,\text{bare}} . \quad (2.4.1)$$

From this formula we obtain $\Delta E_{\text{FGL}} = 0.121850707817101 \text{ MeV}$.

During creation of the bound neutral pion from two fundamental gluon loops, due to the electromagnetic interactions, there is released additional energy equal to $\alpha_{\text{em}} \Delta E_{\text{FGL}}$. The total binding energy of the bound neutral pion is

$$\Delta E_{\text{pion(o),bound}} = \Delta E_{\text{FGL}} (1 + \alpha_{\text{em}}) = 0.122739895392852 \text{ MeV} . \quad (2.4.2)$$

The mass of bound neutral pion

This means that the mass of bound neutral pion (i.e. placed in nuclear strong field) is

$$\pi_{\text{bound}}^0 = 2 m_{\text{FGL}} - \Delta E_{\text{pion(o),bound}} = 134.966086355861 \text{ MeV} . \quad (2.4.3)$$

Assume that the virtual Y spacetime condensates appear on the equator of the core of baryons in such a way that they are tangent to the equator. The spin speed on the equator is c so spin speed for the effective radius of the $d = 0$ state (the effective radius is $A + r_{\text{C(p)}}$, where $r_{\text{C(p)}}$ is the radius of the central spacetime condensate) is (radius is inversely proportional to squared spin speed)

$$(A + r_{\text{C(p)}}) / A = (c / v_{d=0})^2 , \quad (2.4.4)$$

The $r_{\text{C(p)}}$ we can calculate from following formula

$$4 \pi r_{\text{C(p)}}^3 / 3 = Y F / \rho_Y \quad (2.4.5)$$

so we have

$$r_{\text{C(p)}} = 0.871101810916649 \cdot 10^{-17} \text{ m} . \quad (2.4.6)$$

From (2.4.4) we obtain

$$v_{d=0} = 0.99381292525557 c . \quad (2.4.7)$$

From the Einstein formula for relativistic mass we obtain that in the $d = 0$ state, the ratio of the relativistic mass and rest mass is

$$M_{\text{Rel}} / M_o = 1 / \{(1 - A / (A + r_{\text{C(p)}}))\}^{1/2} = 9.00357766478564 . \quad (2.4.8)$$

The mass of charged pion

Assume that the charged pion, π^\pm , is created due to emission of the two bare electrons and two bare positrons (the 4-particle symmetry) by Y or by the precursor of Y , i.e. by $2\pi m_{\text{FGL}}$. Then one of the electrons appears in the $d^* = 0$ state (its radius is smaller than $r_{\text{C(p)}}$ because of the emission of the quadrupole) and is absorbed by the bound neutral pion. Mean mass of the spacetime condensate is

$$Y_{\text{Mean}} = [(Y - 4 m_{\text{e,bare}}) + (2 \pi m_{\text{FGL}} - 4 m_{\text{e,bare}})] / 2 . \quad (2.4.9)$$

From (2.4.5) we calculate the new radius of the spacetime condensate $r_{\text{C(p)}}^*$ and then from (2.4.8) we calculate the relativistic mass of the electron

$$m_{\text{e,rel}} = 9.01025390829349 m_{\text{e}} . \quad (2.4.10)$$

The mass of charged pion π^\pm is

$$\pi^\pm = \pi_{\text{bound}}^0 + m_{\text{e,rel}} = 139.570316606192 \text{ MeV} . \quad (2.4.11)$$

Masses of bound and free charged pions are the same.

We very frequently will use the mass distance between the charged pion and the bound neutral pion

$$\Delta\pi = \pi^\pm - \pi_{\text{bound}}^0 = 4.60423025033035 \text{ MeV} . \quad (2.4.12)$$

The Y is responsible for the nuclear weak interactions and it is the weak SST black hole so we have

$$r_{\text{C(p)}} = G_{\text{w}} Y F / c^2 . \quad (2.4.13)$$

From (2.4.13) we obtain value of the constant of the weak interactions, G_{w} , for baryons

$$G_{\text{w}} = r_{\text{C(p)}} c^2 / (Y F) = 1.03550247948936 \cdot 10^{27} \text{ m}^3/(\text{kg s}^2) . \quad (2.4.14)$$

The invariant coupling constant for the nuclear weak interactions

The characteristic feature of the nuclear weak interactions is that Y is both the source and the carrier of interactions so from the definition of the coupling constants is

$$\alpha_{\text{w(p)}} = G_{\text{w}} (Y F)^2 / (c \hbar) = 0.0187228951018952 , \quad (2.4.15)$$

where $\alpha_{\text{w(p)}}$ is the coupling constant for the nuclear weak interactions.

The invariant coupling constant for the weak interactions of electrons in absence of dark matter

Mass of the condensate in the centre of electron is a half of its bare mass so it is $N_{Y/m(\text{e})\text{-bare}}$ times lower than Y

$$N_{Y/m(\text{e})\text{-bare}} = Y / (m_{\text{e,bare}} / 2) = 1661.89617341709 . \quad (2.4.16)$$

The ratio, $N_{p/e}$, of the radii of the Y and the condensate in electron is

$$N_{p/e} = r_{C(p)} / r_{C(e)} = \{Y / (m_{e,bare} / 2)\}^{1/3} = 11.8449881145892 . \quad (2.4.17)$$

Then

$$r_{C(e)} = 0.735418054023824 \cdot 10^{-18} \text{ m} . \quad (2.4.18)$$

From formulae (2.4.14) and (2.4.15) results that the ratio of the coupling constants is directly proportional to both the ratio of masses of the condensates and the ratio of their radii, so the coupling constant of the weak interactions of the charged leptons is

$$\alpha_{w(e)} = \alpha_{w(p)} / (N_{Y/m(e)-bare} N_{p/e}) = 0.951118188679747 \cdot 10^{-6} . \quad (2.4.19)$$

The invariant coupling constant for the weak interactions of electrons in presence of dark matter

Electron is a pure quantum particle because its torus/electric-charge and the bare-electron loop behave as a virtual particle. We cannot say it about the torus/electric-charge inside the core of baryons because its surface density is about 300,000 times higher than in the SST absolute spacetime. Such scenario causes that an electron disappears in one place and appears in another one, and so on. It causes that outside hadrons we must take into account the dark matter. From observational data we know that density of dark matter is about 5.4 times higher than the baryonic matter. On the other hand, in SST is assumed that the baryonic matter of our Universe appeared similarly to the two fundamental gluon loops (it leads to the bound neutral pion) in the core of baryons – there were two cosmological loops overlapping with the circular axis of the core of the Protoworld. Each loop was composed of the protogalaxies built of the neutron black holes (NBHs). These remarks lead to the ratio, ξ^* , of the total mass of dark matter, $M_{Pw,core}$, to the baryonic mass of the Universe, $M_{Baryonic}$

$$\xi^* = M_{Pw,core} / M_{Baryonic} = H^\pm / (2 m_{FGL}) = 5.38489558858802 . \quad (2.4.20)$$

The formula (2.4.20) concerns a binary system such as, for example, two gluon loops or the electron-positron pair. For a single electron is

$$\xi = 2 \xi^* = H^\pm / m_{FGL} = 10.769791177176 . \quad (2.4.21)$$

Coupling constants, α_i , are directly proportional to constants of interaction, G_i , and from (2.1.26) we have that G_i are directly proportional to densities of fields, so for an electron in presence of dark matter we have

$$\alpha'_{w(e),DM} = \alpha_{w(e)} (1 + \xi) = 1.11944624655745 \cdot 10^{-5} . \quad (2.4.22)$$

Constants of interactions, G_i , are directly proportional to the inertial mass densities of fields carrying the interactions. The following formula defines the coupling constants of all interactions

$$\alpha_i = G_i M_i m_i / (c \hbar) = v_{spin}^2 r m_i / (c \hbar) = v_{spin} / c , \quad (2.4.23)$$

where M_i defines the sum of the masses of the sources of interaction being in touch via a field plus the mass of the component of the field, whereas m_i defines the mass of the carrier of interactions.

The coupling constant for the nuclear strong interactions inside hadrons at low energy

The FGL is responsible for the nuclear strong interactions in hadrons. At low energy, the spin speed of the FGL is $v_{\text{spin}} = c$ so at low energy, the coupling constant for the nuclear strong interactions inside hadrons is

$$\alpha_S = 1 . \quad (2.4.24)$$

The mass of neutral pion (free)

The ratio of the densities of the absolute spacetime and the spacetime condensates is

$$f = \rho_{A_S} / \rho_Y = 40,364.2356312214 . \quad (2.4.25)$$

Calculate mass, m_C , that relates to ρ_Y when ρ_{A_S} relates to the strong-electroweak mass of FGL transiting to its radius

$$m_C = 2 \pi m_{\text{FGL}} (\alpha_S + \alpha_{w(p)} + \alpha_{em}) / f = 0.0107876910334727 \text{ MeV} . \quad (2.4.26)$$

Mass of the neutral pion is the sum of masses of the bound neutral pion and the m_C

$$\pi^0 = \pi^0_{\text{bound}} + m_C = 134.976874046895 \text{ MeV} . \quad (2.4.27)$$

$$\Delta\pi^* = \pi^\pm - \pi^0 = 4.59344255929688 \text{ MeV} . \quad (2.4.28)$$

The ratio of the coupling constant for the nuclear weak interactions to the coupling constant for the weak interactions of electrons is

$$X_{w(p/e)} = \alpha_{w(p)} / \alpha_{w(e)} = 19685.1404218066 . \quad (2.4.29)$$

The coupling constant for the nuclear strong interactions outside baryons at low energy

We know that the bound neutral pion is a binary system of FGLs composed of the rotating-spin-1 neutrino-antineutrino pairs (the SST-As components). This means that inside the bound neutral pion, the SST-As components are exchanged whereas between the bound neutral pions the FGLs are exchanged. We can neglect the mass of the SST-As components in comparison to the mass of the neutral pion. On the other hand, from (2.4.23) it follows that coupling constant for the FGL is unitary because its spin speed, v_{spin} , is equal to the c . For strongly interacting bound neutral pion is

$$\alpha_S^{\pi\pi, \text{FGL}} = \alpha_S = G_S (2 \pi^0_{\text{bound}}) m_{\text{FGL}} F^2 / (c \hbar) = v_{\text{spin}} / c = 1 . \quad (2.4.30)$$

Then the constant of the strong interactions is $G_S = 5.45650811315259 \cdot 10^{29} \text{ m}^3 \text{ s}^{-2} \text{ kg}^{-1}$. Coupling constant for strongly interacting proton at low energies is

$$\alpha_S^{pp,\pi} = G_S (2 p + m_{FGL}) \pi^0_{\text{bound}} F^2 / (c \hbar) = 14.3911871270098 . \quad (2.4.31)$$

In a relativistic version, the G_S is invariant. When we accelerate a baryon, then there decreases the spin speed of FGL so its energy decreases as well

$$E_{\text{Loop}} 2 \pi r_{\text{loop}} / v_{\text{spin}} = \hbar . \quad (2.4.32)$$

This condition leads to the conclusion that the value of the strong coupling decreases when energy increases, i.e. it is the running coupling constant for the nuclear strong interactions.

The running coupling constant for the nuclear strong interactions

For colliding nucleons, we cannot separate the nuclear weak and strong interactions of the cores of baryons. The nuclear weak interactions are realized by exchanges of the virtual or real Y condensates so there appears the factor 2. This means that the running coupling constant for the strong-weak interactions, α_{sw} , is defined by following formula

$$\alpha_{sw} = 2 \alpha_{w(p)} \alpha_{s,\text{running}} , \quad (2.4.33)$$

where $\alpha_{s,\text{running}}$ is the running coupling constant for the nuclear strong interactions.

For virtual FGL which is responsible for the nuclear strong interactions we have

$$E_{\text{FGL,running}} T_{\text{Period,FGL}} = \hbar , \quad (2.4.34)$$

where $E_{\text{FGL,running}}$ is the running energy of FGL. When we accelerate nucleons then the period of spinning, $T_{\text{Period,FGL}}$, increases (i.e. the spin speed decreases) so energy $E_{\text{FGL,running}}$ decreases. From (2.4.34) follows that the both changes decrease the coupling constant.

We can calculate the mass of the carrier of interactions, m_{running} , using the following formula

$$m_{\text{running}} = F \pi^0_{\text{bound}} \beta , \quad (2.4.35)$$

where

$$\beta = (1 - v^2 / c^2)^{1/2} , \quad (2.4.36)$$

where v denotes the relativistic speed of the nucleon.

Define energy of collision as $Q = Np$ then

$$\beta = 1 / N = p / Q . \quad (2.4.37)$$

When the energy of colliding protons increases, more sources interacting strongly appear. The sources are in contact because there is a liquid-like substance composed of the cores of baryons. There is the destruction of the atom-like structure of baryons so instead a collision of two protons we have a collision of two cores of baryons. This means that a colliding nucleon and the new sources behave as one source. Strong interactions are associated with the torus

X^\pm whereas the mass of the core is H^\pm . The mass of the source, M_{sw} , for colliding proton is (formula (2.4.31) can be useful)

$$M_{sw} = F \{ 2 H^\pm + \pi_{\text{bound}}^0 \beta / 2 + X^\pm (p / H^\pm) / \beta \} . \quad (2.4.38)$$

The torus-antitorus pairs are produced from the energy Q but number of the tori is not proportional to number of protons but to the ratio p/H^\pm .

The formula

$$\alpha_{sw} = F^2 2 \alpha_{w(p)} G_S M_{sw} m_{\text{running}} / (c \hbar) \quad (2.4.39)$$

leads to

$$\alpha_{sw} = a_u \beta^2 + b_u \beta + c_u , \quad (2.4.40)$$

where $a_u = 0.0187059$, $b_u = 0.403283$, $c_u = 0.113801$.

Within the Standard Model the parton shower (PS) is not good understood so the phenomena associated with the PS can change the experimental data concerning the running coupling for the strong interactions.

In SST, PS is produced due to the weak decays of condensates composed of the carriers of gluons and photons, i.e. of the SST-As components.

Table 1 *Running strong coupling constant*

Q [GeV]	$\alpha_{SST}(Q)$
2,000	0.08030
$Z^0 = 91.180$	0.11795
50	0.12477
20	0.14019
10	0.16157
p	0.55044

In the collisions of nucleons there are produced the Z^0 bosons. For energies lower than Z^0 there are produced the SST-As condensates that increase the density of the zero-energy field so they increase value of the running coupling. For energy equal to Z^0 , the α_{sw} should be defined by formula (2.4.40) while for higher energies the created additional Z^0 bosons decrease the density of the zero-energy field so α_{sw} is lowered. From formula (2.4.30) we have that coupling constants are directly proportional to spin speeds so from the conservation of spin we have that α is inversely proportional to radius of a loop. The above remarks lead to

$$\alpha_{SST} = \alpha_{sw} + \alpha_{w(p)} \{ 1 - (Q / Z^0)^{1/3} \} . \quad (2.4.41)$$

We calculated a few results that follow from formula (2.4.41) – they are collected in Table 1.

A generalization of the weak interactions

Notice that there is satisfied following relation

$$\alpha_{w(p)} = 3 r_{C(p)} [1 - 1 / (2 \pi)^4] / (2 A) . \quad (2.4.42)$$

The expression $[-1/(2\pi)^4]$ suggests that the nuclear weak interactions follow from the transitions of the circular motions to the radial oscillations.

For a cascade of some interactions, the resultant coupling is a product of coupling constants, while for a set of simultaneous interactions the resultant coupling is a sum of coupling constants.

The virtual $2(e^+e^-)_{\text{virtual}}$ quadrupoles produced by the Y spacetime condensates in the cores of the baryons decay to the virtual $(e^+e^-)_{\text{virtual}}$ pairs and locally interact weakly with the galactic dark-matter loops, so the resultant coupling constant is (there are the simultaneous interactions so the resultant coupling is a sum of coupling constants)

$$\alpha_{w2,\text{core}} = 2 \alpha_{w(e)} . \quad (2.4.43)$$

Consider the weak interactions of dark matter with proton in the hydrogen atom via the external electron (it is the global interaction and a cascade of two interactions). The resultant coupling is

$$\alpha_{w,\text{DM-e-p}} = \alpha'_{w(e),\text{DM}}{}^2 . \quad (2.4.44)$$

2.5. Energy frozen inside the SST-absolute-spacetime components

The SST-As consists of the non-rotating-spin-1 neutrino-antineutrino pairs. Gravitational energy of a single lightest neutrino is

$$E_G = m_{\text{Neutrino}} c^2 . \quad (2.5.1)$$

On the other hand, the not observed non-gravitating superluminal energy of the entanglons the lightest neutrino consists of is (see formula (2.1.9))

$$E_S = m_{\text{Neutrino}} v_1^2 . \quad (2.5.2)$$

The ratio of these energies is

$$E_S / E_G = v_1^2 / c^2 \approx 0.6 \cdot 10^{119} . \quad (2.5.3)$$

We see that inside the SST-As is frozen tremendous amount of unobserved energy about $0.6 \cdot 10^{119}$ parts per 1 part of the observed gravitating energy.

2.6. Magnetic moment of electron (it is an extension of Section 1.5)

We can introduce the symbol

$$\gamma = \alpha_{\text{em}} / (\alpha'_{w(e),\text{DM}} + \alpha_{\text{em}}) = 0.998468305339348 , \quad (2.6.1)$$

where γ denotes the mass fraction in the bare mass of the electron that can interact electromagnetically, whereas $1-\gamma$ denotes the mass fraction in the bare mass of the electron

that can interact weakly. Whereas the electromagnetic mass of a bare electron is equal to its weak mass.

For photon loops, mass is inversely proportional to radius, and αM denotes a mass which is responsible for an interaction. Since the distance between the constituents of a virtual electron-positron pair (virtual dipole) is equal to the length of the equator of the electron torus (because such is the length of the virtual photons) so the ratio of the radiation mass (created by the virtual pair), $\Delta m_{\text{rad}}^{**}$, to the bare mass of electron is (it concerns only the virtual dipole)

$$\begin{aligned} \delta &= \Delta m_{\text{rad}}^{**} / m_{e,\text{bare}} = \gamma \alpha_{\text{em}} / 2\pi + (1 - \gamma) \alpha'_{w(e),\text{DM}} / 2\pi = \\ &= 0.00115963353674058 . \end{aligned} \quad (2.6.2)$$

The virtual dipole is polarized in such a way that its electric line converges on the circular axis of the electron torus so the distance of such axis to the electron condensate is equal to $2/3$ of the equatorial radius of the electron torus – such a factor must appear for the weak interactions of the virtual dipole with the real bare electron. The ratio of the total mass of an electron to its bare mass, which is equal to the ratio of the magnetic moment of the electron to the Bohr magneton for the electron, without the virtual-field correction described below, is (it concerns the virtual dipole and its weak interactions with the real bare electron (the $\Delta m_{\text{rad}}^{**}$ is a part of the total radiation mass Δm_{rad}^*))

$$\begin{aligned} \varepsilon &= (\Delta m_{\text{rad}}^* + m_{e,\text{bare}}) / m_{e,\text{bare}} = m_e^* / m_{e,\text{bare}} = 1 + \delta + \delta \alpha'_{w(e),\text{DM}} / (2 / 3) = \\ &= 1.00115965300895 . \end{aligned} \quad (2.6.3)$$

Each real electron is entangled with proton and it is the virtual proton field that increases the density of the zero-energy field, so measured mass of electron is a little lower than it would be for a free electron (i.e. for electron not entangled with proton). There are the weak interactions of the Y with the two condensates in the virtual electron-positron pair (its total mass is equal to the bare mass of electron). It causes that we must subtract from ε following value

$$\Delta \varepsilon_{\text{electron}} = (\varepsilon - 1) (\alpha'_{w(e),\text{DM}} m_{e,\text{bare}}) / (\alpha_{w(p)} Y) = 8.34419428182199 \cdot 10^{-10} . \quad (2.6.4)$$

The final ratio of the magnetic moment of the electron to the Bohr magneton for the electron, describes the formula

$$\varepsilon' = 1 + a_e = m_e / m_{e,\text{bare}} = \varepsilon - \Delta \varepsilon_{\text{electron}} = 1.00115965217453 . \quad (2.6.5)$$

This result is very close to (2.3.13) so we showed the origin of the radiation mass of electron.

Our model of the electron leads to following mass of it

$$m_{e,\text{SST}} = \varepsilon' m_{e,\text{bare}} = 0.510998945997556 \text{ MeV} . \quad (2.6.6)$$

2.7. The atom-like structure of baryons at low energy

Hyperons arise very quickly because of the nuclear strong interactions. Due to the electroweak interactions, they decay slowly on the TB orbits (in the “tunnels” in the SST-As).

The relativistic pions in the tunnels “circulate” the torus (they are the S states i.e. $l = 0$). Such pions we refer to as $W_{(+o),d}$ pions because they are associated with the strong-electroWeak interactions.

The distance B we can calculate on the condition that the relativistic charged pion in the $d = 1$ state, which is responsible for the properties of nucleons, should have unitary angular momentum (this state is the ground state for the $W_{(+o),d}$ pions)

$$W_{(+o),d=1} (A + B) v_{d=1} = \hbar, \quad (2.7.1)$$

where $v_{d=1}$ denotes the orbital speed of the $W_{(+o),d=1}$ pion in the $d = 1$ state.

We can calculate the relativistic mass of the $W_{(+o),d}$ pions using Einstein’s formula (see our derivation in Section 1.4.)

$$W_{(+o),d} = \pi^{\pm o}_{\text{bound}} / (1 - v_d^2 / c^2)^{1/2}. \quad (2.7.2)$$

For the SST black holes, the square of the orbital speed is inversely proportional to the radius R_d and for A we have c^2 so we have

$$v_{d=1}^2 / c^2 = A / (A + B). \quad (2.7.3)$$

From (2.7.2) and (2.7.3) is

$$W_{(+o),d} = \pi^{\pm o}_{\text{bound}} (1 + A / (d B))^{1/2}. \quad (2.7.4)$$

The formulae (2.7.1)–(2.7.4) give two solutions for the B . The first solution is

$$B = 0.501835443499653 \text{ fm}. \quad (2.7.5)$$

Then

$$A / B = 1.3897833266162. \quad (2.7.6)$$

The second solution is $B^* = 0.969294002358965 \text{ fm}$ but this solution is not realized by Nature. It follows from the fact that after creation of a baryon, inside the core dominates the nuclear weak interaction defined by $\alpha_{w(p)}$ while outside it there dominates the electroweak interaction defined by $(\alpha_{em} + \alpha_{w(p)})$. There can be also the electroweak interactions of the virtual quark-antiquark pairs and of the virtual electron-positron pairs defined by $2\alpha_{w(e)}$. We know that coupling constant is directly proportional to exchanged mass while the mass is inversely proportional to its range so we have

$$(A / B)_\alpha = (\alpha_{em} + \alpha_{w(p)}) / \alpha_{w(p)} \approx 1.38976. \quad (2.7.7)$$

This value is very close to (2.7.6).

The A/B^* differs very much from (2.7.7) so the value B^* is not realized in baryons.

Creation of a resonance is possible when gluon loops overlap with the tunnels. Such bosons we call $S_{(+o),d}$ bosons because they are associated with the nuclear Strong interactions. The spin speeds of the $S_{(+o),d}$ bosons (they are equal to the c) differ from the speeds calculated on the basis of the Titius-Bode law for the strong interactions.

The masses of the charged and neutral core of resting baryons are denoted by $H^{\pm 0}$. The maximum mass of a virtual $S_{(+o),d}$ boson cannot be greater than the mass of the core so we assume that the mass of the $S_{(+o),d}$ boson, created in the $d = 0$ tunnel, is equal to the mass of the core. As we know, the ranges of virtual particles are inversely proportional to their mass. As a result, we obtain

$$H^{\pm 0} A = S_{(+o),d} (A + d B) . \quad (2.7.8)$$

There is some probability that a virtual $S_{(+o),d}$ boson arising in the $d = 0$ tunnel decays to two parts. One part covers the distance A whereas the remainder covers the distance $4B$.

Notice that there is

$$4 \pi^{\circ}_{\text{bound}} / (H^{\pm} - 4 \pi^{\circ}_{\text{bound}}) = 4 B / A \approx 2.8781 , \quad (2.7.9)$$

so for the remainder we have

$$S_{(+o),d=4} = H^{\pm} - 4 \pi^{\circ}_{\text{bound}} . \quad (2.7.10)$$

The nucleons and pions are respectively the lightest baryons and mesons interacting strongly, so there should be some analogy between the carrier of the electric charge interacting with the core of baryons (it is the mass distance between the charged and neutral core) and the carrier of an electric charge interacting with the charged pion (this is the electron). It leads to following formula

$$(H^{\pm} - H^0) / H^{\pm} = m_e / \pi^{\pm} . \quad (2.7.11)$$

From (2.7.11) we obtain

$$H^0 = 724.775902675025 \text{ MeV} . \quad (2.7.12)$$

The mass distance $\Delta H = H^{\pm} - H^0$ is

$$\Delta H = H^{\pm} - H^0 = 2.66332187288708 \text{ MeV} . \quad (2.7.13)$$

For electron (plus electron antineutrino) placed on the circular axis of the core (i.e. the centre of the electron condensate is placed on this axis) we obtain that the electromagnetic binding energy is

$$\Delta E_{\text{em}} = 3 k e^2 / (2 A c^2 F) = 3.09695311426693 \text{ MeV} . \quad (2.7.14)$$

The results are collected in Table 2 (the masses are provided in **MeV**).

The binding energy of the core of baryons is

$$\Delta E_{\text{core}} = X^{\pm} + Y - H^{\pm} = 14.9780863141413 \text{ MeV} . \quad (2.7.15)$$

Table 2 *Relativistic mass on the TB orbits*

d	S_{(+−),d}	S_{(o),d}	W_{(+−),d}	W_{(o),d}
0	$H^{\pm} = 727.439225$	$H^0 = 724.775903$		
1	423.04375	421.49489	215.76069	208.64305
2	298.24411	297.15217	181.70381	175.70966
4	187.57394	186.88719	162.01257	156.66800

There is the four-object symmetry so the symmetrical decays of a virtual boson with a mass four times higher than the remainder

$$M_{\text{TB}} = M_4 = 4 S_{(+−),d=4} = 750.295768225635 \text{ MeV} \quad (2.7.16)$$

lead to the Titius-Bode law for the strong interactions. The group of four virtual remainders reaches the $d = 1$ state. There, it decays to two identical bosons. One of these components is moving towards the equator of the torus whereas the other one is moving in the opposite direction. When the first component reaches the equator of the torus, the other one is stopping and decays into two particles, and so on. In place of the decay, a “hole” appears in the SST absolute spacetime. A set of such holes is some “tunnel”.

The $d = 4$ orbit is the last orbit for the strong interactions.

The probability of the occurrence in the proton of the state $H^+W_{(o),d=1}$ is y while the probability of the occurrence of $H^0W_{(+),d=1}$ is $1-y$. The probabilities y and $1-y$, which are associated with the lifetimes of protons in the above-mentioned states, are inversely proportional to the relativistic masses of the $W_{(+−),d}$ pions so we have

$$y = \pi^{\pm} / (\pi^{\pm} + \pi^0_{\text{bound}}) = 0.508385464005236 , \quad (2.7.17)$$

$$1-y = \pi^0_{\text{bound}} / (\pi^{\pm} + \pi^0_{\text{bound}}) = 0.491614535994764 . \quad (2.7.18)$$

The probability of the occurrence in the neutron of the state $H^+W_{(-),d=1}$ is x while the probability of the occurrence of H^0 , π^0_{bound} and Z^0 is $1-x$, where $Z^0 = W_{(o),d=1} - \pi^0_{\text{bound}}$ (the pion $W_{(o),d=1}$ decays because in this state both particles, i.e. the torus and the $W_{(o),d=1}$ pion, are electrically neutral). Since the $W_{(o),d=1}$ pion only occurs in the $d = 1$ state and because the mass of the resting bound neutral pion is greater than the mass of Z^0 (so the neutral pion lives shorter) then

$$x = \pi^0_{\text{bound}} / W_{(-),d=1} = 0.625536027373375 , \quad (2.7.19)$$

$$1-x = 0.374463972626625 . \quad (2.7.20)$$

The mean square charge for the proton is

$$\langle Q_{\text{proton}}^2 \rangle = e^2 [y^2 + (1-y)^2] / 2 = 0.25e^2 \text{ (quark model gives } 0.33e^2 \text{)} . \quad (2.7.21)$$

The mean square charge for the neutron is

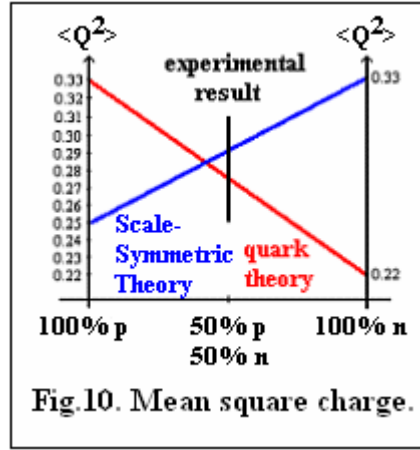
$$\begin{aligned} \langle Q_{\text{neutron}}^2 \rangle &= e^2 [x^2 + (-x)^2] / (2x + 3(1-x)) = \\ &= 0.33e^2 \text{ (quark model gives } 0.22e^2), \end{aligned} \quad (2.7.22)$$

where $(2x + 3(1-x))$ defines the mean number of particles in the neutron.

The mean square charge for a nucleon is

$$\langle Q^2 \rangle = [\langle Q_{\text{proton}}^2 \rangle + \langle Q_{\text{neutron}}^2 \rangle] / 2 = 0.29e^2 \text{ (quark model gives } 0.28e^2). \quad (2.7.23)$$

The results are collected in Fig.10.



2.8. Masses and magnetic moments of nucleons

The mass of a baryon is equal to the sum of the masses of the components because the binding energy associated with the strong interactions cannot abandon the strong field – it follows from the fact that the periods of changes in masses that result from the strong interactions are shorter than lifetimes of the baryons and from the fact that the $d = 0$ and $d = 1$ TB orbits are placed under the Schwarzschild surface for the strong interactions.

The mass of the proton is

$$p = (H^+ + W_{(o),d=1}) y + (H^0 + W_{(+),d=1}) (1-y) = 938.272082 \text{ MeV} . \quad (2.8.1)$$

The not final mass of the neutron is

$$n^* = (H^+ + W_{(-),d=1}) x + (H^0 + W_{(o),d=1})(1-x) = 939.5372973 \text{ MeV} . \quad (2.8.2)$$

In the case of a slight difference between the theoretical and experimental result, as (2.8.2) for the neutron, one should look for unique interactions of a given particle to obtain the correct value.

In nucleons, the state $H^+W_{(-),d=1}$ in the neutron is the only one state when both components are charged so we should add the electroweak mass of the charged torus and a quadrupole of fermions produced by the spacetime condensate Y . Assume that the Y produces the virtual bare electron-positron quadrupoles and that there is the circle-radius transition – then mass of the quadrupole is

$$m_{\text{four}} = 2 \pi (4 m_{e,\text{bare}}) = 8 \pi m_{e,\text{bare}} . \quad (2.8.3)$$

Mass of the electroweak correction for neutron is

$$\Delta n_{\text{correction}} = (X^{\pm} + m_{\text{four}}) \alpha_{\text{em}} \alpha_{w(p)} x = 0.0282996 \text{ MeV} . \quad (2.8.4)$$

We obtain

$$n^{**} = n^{*} + \Delta n_{\text{correction}} = 939.5655970 \text{ MeV} \approx 939.5656 \text{ MeV} . \quad (2.8.5)$$

Moreover, the free neutron as a whole does not interact electromagnetically so the electromagnetic mass off the correction should be emitted, i.e. there should appear the factor $(1 - \alpha_{\text{em}})$. Our final mass of the free neutron is

$$n = n^{*} + \Delta n_{\text{correction}} (1 - \alpha_{\text{em}}) = 939.565390 \text{ MeV} \approx 939.5654 \text{ MeV} . \quad (2.8.6)$$

Let us emphasize that earlier measurements of the neutron mass suggested that it is $\sim 939.5656 \text{ MeV}$ and recent measurements suggest that it is $\sim 939.5654 \text{ MeV}$. As we can see, both of these results appear in our theory (see formulae (2.8.5) and (2.8.6)) – this gives additional credibility to our model.

The SST mass distance between neutron and proton is

$$n - p = 1.293308 \text{ MeV} . \quad (2.8.7)$$

Magnetic moments of nucleons

When measuring the magnetic moment, we place a nucleon in the external magnetic field, which forces a stronger interaction of the relativistic charged pion $W_{(+,-),d=1}$ with the baryon core, i.e. it increases its mass (its orbit radius slightly decreases).

In proton, the relativistic pion $W_{(+),d=1}$ interacts with two neutral objects, i.e. with Y (weakly) and $X^{+} e^{-} \nu_{e,\text{anti}}$ (also weakly) so the correction to mass is $W_{(+),d=1} \alpha_{w(p)}^2$.

The proton magnetic moment in the nuclear magneton is

$$\mu_{\text{proton}} / \mu_{\text{N}} = p y / H^{+} + p (1 - y) / [W_{(+),d=1} (1 + \alpha_{w(p)}^2)] = +2.7928505 . \quad (2.8.8)$$

In neutron, the relativistic pion $W_{(-),d=1}$ interacts with one neutral object and one charged object, i.e. with Y (weakly) and X^{+} (electromagnetically) so the correction to mass is $W_{(+),d=1} \alpha_{\text{em}} \alpha_{w(p)}$.

The neutron magnetic moment in the nuclear magneton is

$$\mu_{\text{neutron}} / \mu_{\text{N}} = p x / H^{+} - p x / [W_{(-),d=1} (1 + \alpha_{\text{em}} \alpha_{w(p)})] = -1.9130438 . \quad (2.8.9)$$

2.9. The origin of the SST Higgs potentials (volumetric and circular) for the SST-absolute-spacetime components

To explain the origin of the SST Higgs potential we need quanta which ranges are equal to the ranges in formulae (2.3.2) and (2.9.1).

There are two types of the SST long-distance Higgs potential. There is the volumetric Higgs potential and circular one. Generally, the cores of neutrinos and baryons more likely

interact in the planes of their equators so involved energy in circular loops with spins of its components perpendicular to them is higher so range of the circular Higgs potential should be shorter.

Generally, the Higgs potential should be associated with the lowered density of the zero-energy field, i.e. should concern the binding energy of the core of baryons or neutrinos. But in the cores are produced the virtual objects (there is the negative mass and the positive one) so they also can decrease density of the zero-energy field.

Range of the volumetric confinement for neutrinos (the SST volumetric Higgs potential)

The side of a mean cube occupied by one SST-As component in the condensate Y is (we denote it by L_{Y+As} – it is the range of the volumetric confinement and it is the range of the volumetric Higgs potential)

$$L_{Y+As} = \{2 m_{\text{Neutrino}} / (\rho_Y + \rho_{As})\}^{1/3} = 3510.1807044135 r_{\text{neutrino}} . \quad (2.9.1)$$

Notice that our result does not explain the origin of the range of the volumetric Higgs potential/confinement.

The theories of the core of lightest neutrinos and core of baryons are similar so the ratios of similar quantities in both theories have the same values. Instead to consider neutrinos we are considering the core of baryons.

Calculate the binding energy of the X^\pm and Y (i.e. of the core of baryons)

$$\Delta E_{\text{core}} = X^\pm + Y - H^\pm = 14.9780863141413 \text{ MeV} . \quad (2.9.2)$$

This binding energy lowers the zero-point of the zero-energy field.

But there can appear also following virtual processes that increase the binding energy. Calculate energy, ΔE_1 , which relates to the energy emitted during the described earlier collapse of the FGL (see formula (2.2.3)) that transits from the effective radii of the central spacetime condensate (see formulae (2.4.5) and (2.4.9); the radius is $r_{C(p)}^* = 0.86979529168408 \cdot 10^{-17} \text{ m}$) to the equator of the core of baryons (the radius is A)

$$\Delta E_1 = [2 \pi m_{\text{FGL}} / (2\pi)^4] (r_{C(p)}^* / A) = 0.00339592782587082 \text{ MeV} . \quad (2.9.3)$$

Such energy increases the energy defined by (2.9.2). Next the circular oscillations on edge of the total binding energy transform into diagonal oscillations (see formula (1.4.30)). Then energy of emitted quanta is

$$\Delta E_{\text{volumetric}} = (\Delta E_{\text{core}} + \Delta E_1) / \pi^4 = 0.153799630844903 \text{ MeV} . \quad (2.9.4)$$

Internal structure of baryons shows that range of the quadrupole of the bound neutral pions is A so range of the $\Delta E_{\text{volumetric}}$ is

$$R_{\text{volumetric}} = 4 \pi_{\text{bound}}^0 A / \Delta E_{\text{volumetric}} = 3510.17972 A . \quad (2.9.5)$$

By an analogy, for the SST-As components is

$$R_{\text{Higgs,volumetric}} = 3510.17972 r_{\text{neutrino}} . \quad (2.9.6)$$

This result differs from the result in (2.9.1) only by 1 part in about 3.6 million parts so we can say that we showed the origin of the SST volumetric Higgs potential.

In formulae (2.3.2) – (2.3.7) we showed that range of the circular Higgs potential in the bare-electron loop is

$$L_{e,\text{bare}} = 3482.90191937193 r_{\text{neutrino}} . \quad (2.9.7)$$

But it does not show the origin of the circular Higgs potential.

Range of the circular confinement for neutrinos (the SST circular Higgs potential)

Assume that the FGL captures an energy $\Delta E_{\text{circular}}$ which is an analog to the energy $\Delta E_{\text{volumetric}}$ in (2.9.4). Instead the transition from $r_{\text{C(p)}}^*$ to A there is the transition from the nuclear weak interactions inside the core of baryons (the coupling constant is $\alpha_{\text{w(p)}}$) to the electroweak interactions outside it (the total coupling constant is $\alpha_{\text{em}} + \alpha_{\text{w(p)}}$). By an analogy to (2.9.3) we have

$$\Delta E_2 = [2 (m_{\text{FGL}} + \Delta E_{\text{circular}}) / (2\pi)^4] (\alpha_{\text{em}} + \alpha_{\text{w(p)}}) / \alpha_{\text{w(p)}} . \quad (2.9.8)$$

By an analogy to (2.9.4) we have

$$\Delta E_{\text{circular}} = (\Delta E_{\text{core}} + \Delta E_2) / \pi^4 . \quad (2.9.9)$$

From (2.9.8) and (2.9.9) we have

$$\Delta E_{\text{circular}} = 0.15500423364331 . \quad (2.9.10)$$

And by an analogy to (2.9.5) we have

$$R_{\text{circular}} = 4 \pi_{\text{bound}}^0 A / \Delta E_{\text{circular}} = 3482.90065 A . \quad (2.9.11)$$

By an analogy, for the SST-As components is

$$R_{\text{Higgs,circular}} = 3482.90065 r_{\text{neutrino}} . \quad (2.9.12)$$

This result differs from the result in (2.9.7) only by 1 part in about 2.7 million parts so we can say that we showed the origin of the SST circular Higgs potential.

2.10. Muon

Muon is the electrically charged fermion. Mass of muon is close to the mass distance between Y and X^\pm so such mass distance and some interaction should define the mass of muon. Notice also that mass of a spin-0 charge-0 quadrupole of muons ($4\mu^\pm \approx 422.64 \text{ MeV}$) is a little lower than Y so in the central condensate of baryons there can be realized the four-muon symmetry. Muons are produced also in the decays of the electrically charged pions.

Assume that between a muon in Y and the torus/electric-charge X^\pm is exchanged a virtual bare electron-positron pair (i.e. there are the radial motions) that during the emission of the muon undergoes the radius-orbit transition i.e. there is emitted the energy equal to $E^* = 2m_{e,bare}/(2\pi) = m_{e,bare}/\pi$. Moreover, the muon inside the core of baryon interacts weakly with the Y (it is defined by $\alpha_{w(p)}$) and weakly with other muons (it is defined by $\alpha_{w(e)}$). After emission, the muon interacts only with Y . It leads to following mass of the muon

$$\mu^\pm = (Y - X^\pm - E^*) [\alpha_{w(p)} / (\alpha_{w(p)} + \alpha_{w(e)})] = 105.6583796 \text{ MeV} . \quad (2.10.1)$$

Muon looks similar to electron, i.e. there is a torus/electric-charge and central condensate – outside such a system, there are created the virtual electron-positron pairs. The two energetic neutrinos that appear in decay of muon are inside the central condensate. Such complex muon condensate behaves as the SST black hole in respect of the weak interactions.

By using the formula

$$c^2 = G_w M F / r_{C(e)}, \quad (2.10.2)$$

we can calculate the virtual or real energy/mass E of two neutrinos which should be absorbed by the condensate of electron (the two neutrinos means that the structure is stable) to create the SST black hole in respect of the weak interactions

$$M = E + m_{e,bare} / 2 = 35.80600998999 \text{ MeV} . \quad (2.10.3)$$

$$E = 2 E_{\text{neutrino}} = 35.55080646432 \text{ MeV} . \quad (2.10.4)$$

$$E_{\text{neutrino}} = 17.77540323216 \text{ MeV} . \quad (2.10.5)$$

Emphasize that the total mass of the muon condensate is a half of its bare mass.

The anomalous relative magnetic moments of electron and muon are different because they are created in different ways.

We can assume that due to some interactions, the radiation mass of the muon is a little higher than it should be by an analogy to the electron. Denote the additional radiation mass of the muon by $\Delta\mu_{\text{rad}}^\pm$. Then our formula for the anomalous magnetic moment of the muon is

$$a_\mu = a_e (1 + \Delta\mu_{\text{rad}}^\pm / \mu_{\text{bare}}^\pm) , \quad (2.10.6)$$

where $a_e = 0.00115965217932$ is for the electron (see (2.3.13)).

Due to the collisions of nucleons and the four-particle symmetry, there appears a quadrupole of the spacetime condensates created in the circle-radius collapse of four the fundamental gluon loops plus the mass of the two bare electron-positron pairs (it is the quadrupole as well) that are exchanged – the total mass of such a system is $M^* = 4(Y^* + m_{e,bare}) = 4(2\pi m_{\text{FGL}} + m_{e,bare})$. From it can be created the bare muon-antimuon pairs.

We can assume that the additional radiation mass of the muon, $\Delta\mu_{\text{rad}}^\pm$, is directly proportional to the mass distance between the charged and neutral pions ($\Delta\pi^* = \pi^\pm - \pi^0 = 4.59344255929688 \text{ MeV}$ – see (2.4.28)) while the mass of the bare muon, μ_{bare}^\pm , is directly proportional to the mass $M^*/2$, so we have

$$\begin{aligned} \Delta\mu_{\text{rad}}^{\pm} / \mu_{\text{bare}}^{\pm} &= (\pi^{\pm} - \pi^0) / (2 Y^* + 2 m_{e,\text{bare}}) = \\ &= 0.00540526503109431 . \end{aligned} \quad (2.10.7)$$

From (2.10.6) and (2.10.7) we obtain

$$a_{\text{SST},\mu} = 11659204.0669424 \cdot 10^{-10} \approx 0.0011659204067 . \quad (2.10.8)$$

We can compare the SST result with experimental data.

The new experimental average presented by the “Muon $g - 2$ ” Collaboration, B. Abi, *et al.* (7 April 2021) is [2]

$$a_{\mu}(\text{Exp}) = 0.00116592061(41) . \quad (2.10.9)$$

But emphasize that the earlier FNAL result was [2]

$$a_{\mu}(\text{FNAL}) = 0.00116592040(54) . \quad (2.10.10)$$

This experimental central value is in perfect agreement with our theoretical result. It cannot be a chance that the SST simple model leads to an excellent theoretical result!

The theoretical Standard-Model (SM) result [3] is inconsistent with experimental data

$$a_{\text{SM},\mu} = 0.00116591810(43) . \quad (2.10.11)$$

2.11. Tauon and fine-structure constant at high energies

Assume that the tauon is a result of transition of the FGL onto the orbit with a radius equal to its circumference ($2\pi 2A/3 = 4\pi A/3$) and next to a circle with a radius 2π times smaller than the equatorial radius of the torus of baryons ($R_{\text{resultant}} = A/(2\pi)$). With the tauon, which is electrically charged, is created the bare electron-positron pair which is responsible for the electromagnetic interactions.

From the conservation of angular momentum we have

$$m_{\text{FGL}} (4 \pi A / 3) c = (m_{\text{tauon}} + 2 m_{e,\text{bare}}) \{A / (2 \pi)\} c . \quad (2.11.1)$$

It leads to the tauon mass

$$m_{\text{tauon}} = 8 \pi^2 m_{\text{FGL}} / 3 - 2 m_{e,\text{bare}} = 1776.67688470713 \text{ MeV} . \quad (2.11.2)$$

The second solution follows from the fact that the mean distance between the entangled SST-As components on surface of the torus in the core of baryons is a little higher than the circumference of the equatorial radius of the lightest neutrino (see formulae (2.3.14) and (2.3.15))

$$L_{\text{NA}} / (2 \pi r_{\text{neutrino}}) = L_o = 1.0078405229268 = 1 + \alpha_{\text{em,high}} , \quad (2.11.3)$$

where $\alpha_{\text{em,high}} = 1 / 127.542513342079$ is the fine-structure constant at high energies.

Let us calculate mass of the tauon on the assumption that the distances between the neutrino-antineutrino pairs in it is $L_o r_{\text{neutrino}}$ instead the $2\pi N^* L_o r_{\text{neutrino}}$ as it is in the bare electron. We obtain following relation

$$(m_{\text{tauon}} + 2 m_{e,\text{bare}}) / m_{e,\text{bare}} = 2 \pi N^* . \quad (2.11.4)$$

From (2.11.4) results that mass of the tauon lepton is

$$m_{\text{tauon}} = 2 (\pi N^* - 1) m_{e,\text{bare}} = 1776.67688470713 \text{ MeV} , \quad (2.11.5)$$

i.e. the same as in (2.11.2).

2.12. Photons, gluons and properties of fundamental particles

Table 3 *New symbols*

* Particle	Internal helicity	Electric charge	Weak charge	* New symbol
* $\nu_{e(\text{anti})}$	L (left)		+	* $\nu_{e(\text{anti})L+}$
* ν_e	R (right)		-	* ν_{eR-}
* $\nu_{\mu(\text{anti})}$	R		+	* $\nu_{\mu(\text{anti})R+}$
* ν_{μ}	L		-	* $\nu_{\mu L-}$
* e^-	R	-		* e^-_R
* e^+	L	+		* e^+_L
* p^+	L	+		* p^+_L
* p^-	R	-		* p^-_R
* n	L¹⁾		+	* n_L
* $n(\text{anti})$	R¹⁾		-	* $n(\text{anti})_R$
* μ^-	R¹⁾	-		* μ^-_R
* μ^+	L¹⁾	+		* μ^+_L
* π^-	R¹⁾	-	+	* π^-_R
* π^+	L¹⁾	+	-	* π^+_L

¹⁾The resultant internal helicity is the same as the internal helicity of the torus having highest mass.

The neutrinos interact with the condensates in centres of the fermions. Physical states of them should be different. Components of a fermion should differ by internal helicity and, if not by it, by the sign of the electric charge and/or the weak charge carried by neutrinos. The possible bound states are as follows (symbols as in Table 3)

$$\mu^-_R \equiv e^-_R \nu_{e(\text{anti})L+} \nu_{\mu L-} ,$$

$$\mu^+_L \equiv e^+_L \nu_{eR-} \nu_{\mu(\text{anti})R+} ,$$

$$\pi^-_R \equiv e^-_R \nu_{e(\text{anti})L} L_L L_{LA} \rightarrow \mu^-_R \nu_{\mu(\text{anti})R+} ,$$

where L_{LA} denotes the FGL with the left helicity and antiparallel spin.

$$\pi^+_L \equiv e^+_L \nu_{eR-} L_R L_{RA} .$$

There are in existence the following 8 states of the rotating-spin neutrino-antineutrino pairs

$$\begin{aligned}
\gamma_{L1} &\equiv (v_{eR-} - v_{e(anti)L+})_L, \\
\gamma_{L2} &\equiv (v_{\mu L-} - v_{\mu(anti)R+})_L, \\
\gamma_{L3} &\equiv (v_{eR-} - v_{\mu(anti)R+})_L, \\
\gamma_{L4} &\equiv (v_{\mu L-} - v_{e(anti)L+})_L, \\
\gamma_{R1} &\equiv (v_{eR-} - v_{e(anti)L+})_R, \\
\gamma_{R2} &\equiv (v_{\mu L-} - v_{\mu(anti)R+})_R, \\
\gamma_{R3} &\equiv (v_{eR-} - v_{\mu(anti)R+})_R, \\
\gamma_{R4} &\equiv (v_{\mu L-} - v_{e(anti)L+})_R.
\end{aligned}$$

In fields with internal helicity, they behave as gluons (8 different types) whereas in field without internal helicity, they behave as photons (1 type only).

2.13. The mass of W^\pm and Z^0 bosons

Assume that due to the four-fermion symmetry, a spin-0 charge-0 quadrupole of bare electron-positron pairs ($8m_{e,bare}$) transits from the weak interactions of electrons to the nuclear weak interactions ($X_{w(p/e)} = 19685.1404218066$ – see formula (2.4.29)) and then to such an object is added the spin-1 virtual pair composed of electron (positron) and electron-antineutrino (electron-neutrino). Mass and spin of such a particle is equal to the mass and spin of the W^\pm boson

$$W^\pm = 8 m_{e,bare} X_{w(p/e)} + \{m_{e,bare} + v_{e(anti)}\}_{virtual} = 80.37948 \text{ GeV}. \quad (2.13.1)$$

But when there is absorption of energy defined by the very frequently applied formula (1.4.31) then we obtain

$$W_o^\pm = W^\pm [1 + 1 / (2 \pi)^4] = 80.43105 \text{ GeV}. \quad (2.13.2)$$

By same analogy, assume that instead the $8 m_{e,bare}$ in (2.13.1) there is the mass distance between the charged pion and the bound or free neutral pion which attaches its electromagnetic mass. Then for the spin-1 Z^0 boson we have

$$\begin{aligned}
Z^0 &= [\pi^+ - (\pi^0_{bound} + \pi^0) / 2] (1 + \alpha_{em}) X_{w(p/e)} + \{m_{e,bare} + v_{e(anti)}\}_{virtual} = \\
&= 91.18936 \text{ GeV}. \quad (2.13.3)
\end{aligned}$$

2.14. Degrees of freedom

To describe position, shape and motions of a spinning loop without internal structure, but with poloidal motion, we need 10 degrees of freedom: the three coordinates of its centre, mean radius of the loop, its thickness, toroidal/spin speed, poloidal speed, linear speed (i.e. time), and two angles describing rotation of the spin of the loop. A non-rotating-spin loop has 8 degrees of freedom.

To describe in such a way our core composed of a torus with central condensate (both components without internal structure) we also need 10 degrees of freedom. It follows from the fact that thickness of the torus depends on its mean radius so instead two sizes we have one size. But there appears the radius of the central condensate. A non-rotating-spin core has 8 degrees of freedom.

Emphasize that we should not take into account sizes which depend on some other size.

Table 4 *Degrees of freedom of fundamental objects*

Stable object	Co-ordinates and quantities needed to describe position, shape and motions
Tachyon	6 (they always are spinning)
Closed string Entanglon	10 or 8
Neutrino Neutrino-antineutrino (NA) pair	26 or 24 : 8 for entanglons on torus 8 for entanglons in condensate 8 (or 10) for the core as a whole
Core of baryons Electron	58 or 56 : 24 for NA pairs on torus 24 for NA pairs in condensate 8 (or 10) for the core as a whole
An abstract core of Protoworld composed of the baryonic core-anticore (CA) pairs	122 or 120 : 56 for CA on torus 56 for CA in condensate 8 (or 10) for the core as a whole

If N denotes the degrees of freedom then for our non-rotating-spin fundamental objects is

$$N = 8 (2d - 1), \quad (2.14.1)$$

where $d = 1, 2, 4, 8$ are the TB numbers.

For our rotating-spin fundamental objects we have

$$N = | 8 (2d - 1) + 2 |. \quad (2.14.2)$$

2.15. The seven types of interactions

There are seven types of interactions.

Viscosity of tachyons and viscosity between the tachyons and entanglons follows from smoothness of surfaces of the tachyons – such viscosity causes that the entanglons are the stable objects and that neutrinos curve the SST Higgs field, i.e. they produce the elementary gravitational fields. We call such forces *the viscid interactions*.

The neutrinos and the SST-As components can be entangled due to the exchanges of the superluminal entanglons they consist of. We call such directional forces *the directional entanglement*.

The gravitational interactions follow from the gradients produced in the SST Higgs field. Around the neutrinos there is a region filled with the emitted and absorbed entanglons – binary systems of entanglons are the spin-2 objects. We can call them the SST gravitons but emphasize that they are the superluminal objects. We calculated the gravitational constant G .

The emissions and absorptions of some groups of the SST entanglons cause that around the neutrinos is created the SST Higgs potential which leads to *the volumetric confinement* or *the circular confinement* of neutrinos and of the SST-As components. We calculated the ranges and we showed their origin.

The creations and annihilations of the virtual bare electron-positron pairs and their polarization are responsible for *the electromagnetic interactions*. We already calculated the fine-structure constants at low and high energies.

The scalar condensates are responsible for *the weak interactions*. We already calculated the three fundamental coupling constants for the weak interactions.

The FGL and its binary systems (the pions) are responsible for *the nuclear strong interactions*.

Gravitational fields are the gradients produced in the superluminal Higgs field by neutrinos. The total cross section of all tachyons in volume of a rectangular prism $1\text{m}\cdot 1\text{m}\cdot 2\cdot 10^{36}\text{m}$ is 1m^2 so all divergently moving tachyons sooner or later are scattered. It leads to conclusion that range of the gravitational interactions is about $2\cdot 10^{36}\text{m}$.

Gravitational fields are the result of the viscid interactions of the SST Higgs field with the entanglons the neutrinos consist of. Inside the region of the SST Higgs potential, the spin-2 binary systems of entanglons (we call them the SST gravitons) are emitted and absorbed so such a region is described by the SST quantum gravity. The flows of the SST tachyons in a SST graviton we present in Fig.11.

The SST Higgs mechanism presented in this Paragraph (which leads to the volumetric confinement) leads to the SST scalar condensates composed of the SST gravitons and to the SST-As scalar condensates which in SST are responsible for the weak interactions.

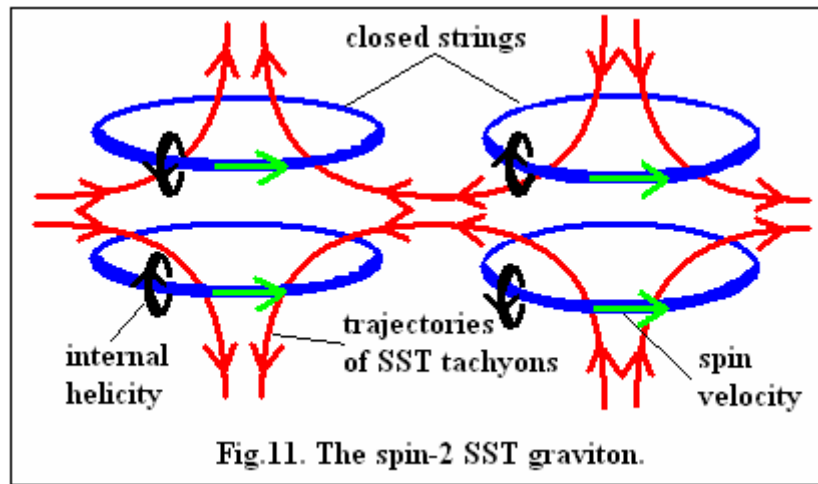


Fig.11. The spin-2 SST graviton.

We described four phenomena that cause that particles acquire their gravitational masses, i.e. the SST is the theory with mass gaps.

The first phenomenon shows how neutrinos acquire their masses – it is due to the viscid interactions between the SST Higgs field and the entanglons the neutrinos consist of. The second phenomenon shows how the SST-As condensates acquire their masses – it is due to the volumetric confinement (the SST volumetric Higgs potential) of the neutrinos and their pairs forced by the circle-diameter transitions of the virtual spin-1 loops created on the circular axes of the fundamental tori and by the initial radial transitions. The third phenomenon shows how the bare electron loops acquire their mass – it is due to the circular confinement (the SST circular Higgs potential) of the neutrinos and their pairs forced by the same circle-diameter transitions but instead the radial transitions there is the transition from the weak interactions to the electroweak interactions in the plane of the equators of the fundamental tori. The fourth phenomenon shows how the tori/charges and dark-matter particles acquire their masses – it is due to the two shortest-distance quantum entanglement, i.e. $2\pi R$ and $2\pi R/3$, where R is the equatorial radius of the tori, and due to the long-distance quantum entanglement.

2.16. Higgs boson and a prediction of new particle

Mass of the region of the SST absolute spacetime, H_{Higgs} , which overlaps with the electromagnetic binding energy of the bare electron on the circular axis of the torus in the core of baryons, $\Delta E_{\text{em}} = 3.09695311426693 \text{ MeV}$ (see formula (2.7.14)), is

$$H_{\text{Higgs}} = f \Delta E_{\text{em}} = 125.00615 \text{ GeV} . \quad (2.16.1)$$

where $f = 40,364.2356312214$ (see formula (2.4.25)). It is the Higgs boson – it is the composite scalar particle composed of the confined SST-As components.

There should be in existence a scalar (we call it the Higgs boson-high), $H_{\text{Higgs-high}}$, or/and spin-1 charged/neutral particle, H^* , H^{**} , with a mass equal to mass of the region of the SST-As, which overlaps with the condensate Y

$$H_{\text{Higgs-high}} = f Y \approx 17.1194 \text{ TeV} . \quad (2.16.2)$$

Notice that similar values we obtain applying three other formulae

$$H^* = f 2 \pi m_{\text{FGL}} \approx 17.1303 \text{ TeV} , \quad (2.16.3)$$

$$H^{**} = 4 W^{\pm} / \alpha_{\text{w(p)}} \approx 17.1724 \text{ TeV} . \quad (2.16.4)$$

$$H^{***} = H_{\text{Higgs}} / \alpha_{\text{em}} \approx 17.1303 \text{ TeV} . \quad (2.16.5)$$

We predict that mass of the new heavy Higgs boson will be about $17.12 \text{ TeV} - 17.17 \text{ TeV}$.

2.17. Lamb-Retherford shift

The Lamb shift is the difference in energy between the $^2S_{1/2}$ and $^2P_{1/2}$ energy levels. It was not predicted by the Dirac equation because from it follows that these two states should have the same energy. Now, in the mainstream physics, it is assumed that it is a result of interaction of the hydrogen electron with vacuum energy fluctuations.

We can calculate the Lamb shift using following formula

$$\Delta E_i = \alpha_i c \hbar / r = m_i c^2 . \quad (2.17.1)$$

The Lamb shift concerns the second orbit so we have $r = 4 R_B$. We can rewrite (2.17.1) as follows

$$v_{\text{L-R}} = \alpha_i c / (2 \pi \cdot 4 R_B) . \quad (2.17.2)$$

From the definition we have

$$\alpha_{\text{w(p)}} \sim Y^2 . \quad (2.17.3)$$

We claim that the Lamb shift is the result of the nuclear weak interactions of the energy which is equal to the energy distance between the relativistic mass of the charged pion in the $d = 1$ state and its rest mass with the radiation mass of the electron on the second shell in the hydrogen atom, so from the definition we have

$$\alpha_i \sim (W_{(+),d=1} - \pi^{\pm}) (m_e - m_{e,\text{bare}}) , \quad (2.17.4)$$

The last two formulae lead to

$$\alpha_i = \alpha_{w(p)} (W_{(+),d=1} - \pi^\pm) (m_e - m_{e,bare}) / Y^2, \quad (2.17.5)$$

so from (2.17.2) is

$$v_{L-R} = 1058.0742 \text{ MHz}. \quad (2.17.6)$$

The second solution is as follows.

From (2.4.23) results that for spherical symmetry is $\alpha \sim R$ so we have

$$\alpha_{w(p)} \sim A. \quad (2.17.7)$$

A change in the radius of the second orbit in the hydrogen atom, dr , should be because of the electromagnetic and weak interactions in presence of dark matter of the electron with proton so we have

$$dr / A = (\alpha'_{w(e),DM} + \alpha_{em}) / \alpha_{w(p)}. \quad (2.17.8)$$

From this $dr = 2.72248882025292 \cdot 10^{-16} \text{ m}$.

For the second shell of the hydrogen atom, the frequency associated with such a shift is

$$v_{L-R} = R_H c [1 / 4 - 1 / (4 + dr / R_B)] = 1057.8396 \text{ MHz}, \quad (2.17.9)$$

where the Rydberg constant calculated within SST is

$$R_H = F m_e e^4 / (8 \epsilon_0 h^3 c) = \alpha_{em}^2 F m_e c / (4 \pi \hbar) = 10973731.48210 \text{ m}^{-1}. \quad (2.17.10)$$

The two different phenomena lead to two different (but very close) frequencies. It suggests that the Lamb shift should be split unless the second mechanism dominates because it relates to the lower involved energy.

2.18. Lifetimes

Lifetimes we can calculate applying formulae (1.4.25) and (1.4.29)

$$\tau_{\text{Lifetime}} \sim 1 / m^4, \quad (2.18.1)$$

$$\tau_{\text{Lifetime}} \sim 1 / \alpha_i. \quad (2.18.2)$$

If the same mass can interact in different ways (i.e. the involved masses are $\alpha_1 m$ and $\alpha_2 m$) then from (2.18.1) we obtain

$$\tau_1 / \tau_2 = (\alpha_2 / \alpha_1)^4. \quad (2.18.3)$$

If one of the interactions is the nuclear strong interaction at low energy, say $\alpha_2 = \alpha_s = 1$, then from (2.18.2) we have

$$\tau_1 / \tau_2 = (1 / \alpha_i) , \quad (2.18.4)$$

or from (2.18.3) is

$$\tau_1 / \tau_2 = (1 / \alpha_i)^4 . \quad (2.18.5)$$

Contrary to appearances there is practically no ambiguity in the calculated lifetimes of particles.

Muons are created as quadrupoles from the Y condensates. It causes that they conserve the zero-electric-charge and the zero-spin of the condensate Y . Then the muon torus and the torus in the core of the baryon synchronize their spinning periods which are the initial lifetime of the muon

$$T_o = 2\pi A/c = 1.46173145895885 \cdot 10^{-23} \text{ s} . \quad (2.18.6)$$

The weak interactions of the muon increase its initial lifetime. There is the transition from the nuclear weak interactions (the involved mass is $m_{w,1} = \alpha_{w(p)} \mu^\pm$) to weak interaction of electron (the involved mass is $m_{w,2} = \alpha_{w(e)} \mu^\pm$). Such transition increases the muon lifetime. Since $X_{w(p/e)} = \alpha_{w(p)} / \alpha_{w(e)} = 19685.1404$ (see formula (2.4.29)) so from (2.18.3) the lifetime of muon is

$$\tau_{\text{muon}} = T_o X_{w(p/e)}^4 = 2.194935 \cdot 10^{-6} \text{ s} . \quad (2.18.7)$$

The weak interactions are responsible for the decay of the hyperons and because of these interactions they behave as a nucleon, whereas the muon behaves as an electron, so the lifetimes of the hyperons should be close to (there is a transition from weak interaction of electron to the nuclear weak interaction) – see (2.18.2)

$$\tau_{\text{hyperon}} = \tau_{\text{muon}} (1 / X_{w(p/e)}) = 1.115021 \cdot 10^{-10} \text{ s} . \quad (2.18.8)$$

The tauon decays because of the transition from the nuclear weak interaction to the nuclear strong interaction (see (2.18.3))

$$\tau_{\text{tauon}} = \tau_{\text{muon}} (\alpha_{w(p)} / \alpha_s)^4 = 2.697206 \cdot 10^{-13} \text{ s} . \quad (2.18.9)$$

The lifetime of the charm hyperon $\Lambda_c^+(2260)$ is (see (2.18.1))

$$\tau_{\Lambda(2260)} = \tau_{\text{hyperon}} (Y / Y_{\Lambda(2260)})^4 = 1.817 \cdot 10^{-13} \text{ s} , \quad (2.18.10)$$

where $Y_{\Lambda(2260)} = 2286 - 1115 + 940 = 2111 \text{ MeV}$.

The lifetime of the FGL created on the circular axis of the torus of the nucleon can be calculated using the formula $E_{\text{FGL}} \cdot \tau_{\text{FGL}} = \hbar$, where $m_{\text{FGL}} = 67.544413 \text{ MeV}$

$$\tau_{\text{FGL}} = 9.745 \cdot 10^{-24} \text{ s} . \quad (2.18.11)$$

The neutral pion (it consists of two the fundamental gluon loops) decays in respect of the transition from the strong interactions to the nuclear weak interaction. Consequently the lifetime of the neutral pion is (see (2.18.5))

$$\tau_{\text{pion}(0)} = \tau_{\text{FGL}} (1 / \alpha_{\text{w}(p)})^4 = 0.793 \cdot 10^{-16} \text{ s} . \quad (2.18.12)$$

The charged pion decays because of the transition from the nuclear strong interaction to the electromagnetic interaction, therefore (see (2.18.5))

$$\tau_{\text{pion}(+-)} = \tau_{\text{pion}(0)} (1 / \alpha_{\text{em}})^4 = 2.797 \cdot 10^{-8} \text{ s} . \quad (2.18.13)$$

The neutron and muon decay due to the weak interactions but in neutron, there is the transition from the FGL interacting with $\Delta\pi = \pi^\pm - \pi^0_{\text{bound}}$ to the bare electron. From (2.18.1) is

$$\tau_{\text{neutron}} = \tau_{\text{muon}} \{ (m_{\text{FGL}} + \Delta\pi) / m_{\text{e,bare}} \}^4 = 876.33 \text{ s} . \quad (2.18.14)$$

Ordered motions of neutrons at low energy decrease local density of field so neutrons absorb the smallest possible mass, i.e. the electron condensate, so we have

$$\tau^*_{\text{neutron}} = \tau_{\text{muon}} \{ (m_{\text{FGL}} + \Delta\pi + m_{\text{e,bare}} / 2) / m_{\text{e,bare}} \}^4 = 888.80 \text{ s} . \quad (2.18.15)$$

Lifetimes of the W^\pm and Z^0 bosons and of the H Higgs boson

The H, W^\pm and Z^0 bosons decay due to their weak mass, M_{weak} ,

$$M_{\text{weak}} = \alpha_{\text{w}(p)} M = \Gamma / c^2 , \quad (2.18.16)$$

where M is the mass of a condensate whereas the $M_{\text{weak}} c^2$ is the decay width Γ .

On the other hand, lifetime of a condensate is defined as follows

$$\tau = \hbar / \Gamma = \hbar / (M_{\text{weak}} c^2) = \hbar / (\alpha_{\text{w}(p)} M c^2) . \quad (2.18.17)$$

Applying formula (2.18.17) we obtain the rigorous theoretical lifetimes – they are the upper limits for experimental data. It follows from the fact that theoretical decay width always has higher accuracy than experimental ones (it is due to the systematic and statistical errors)

$$\Gamma_{\text{H,theory(SST)}} \approx 2.34 \text{ GeV} / c^2 \rightarrow \tau_{\text{H,theory}} = 2.82 \cdot 10^{-25} \text{ s} , \quad (2.18.18)$$

$$\Gamma_{\text{W,theory(SST)}} \approx 1.51 \text{ GeV} / c^2 \rightarrow \tau_{\text{W,theory}} = 4.38 \cdot 10^{-25} \text{ s} , \quad (2.18.19)$$

$$\Gamma_{\text{Z,theory(SST)}} \approx 1.71 \text{ GeV} / c^2 \rightarrow \tau_{\text{Z,theory}} = 3.86 \cdot 10^{-25} \text{ s} . \quad (2.18.20)$$

Applying formula (2.18.17) and knowing the decay widths, [4], we obtain the experimental lifetimes

$$\Gamma_{\text{H,exp.}} \approx 3.4 \text{ GeV} / c^2 \rightarrow \tau_{\text{H,exp.}} = 1.94 \cdot 10^{-25} \text{ s} , \quad (2.18.21)$$

$$\Gamma_{\text{W,exp.}} \approx 2.1 \text{ GeV} / c^2 \rightarrow \tau_{\text{W,exp.}} = 3.16 \cdot 10^{-25} \text{ s} , \quad (2.18.22)$$

$$\Gamma_{Z,\text{exp.}} \approx 2.5 \text{ GeV} / c^2 \rightarrow \tau_{Z,\text{exp.}} = 2.64 \cdot 10^{-25} \text{ s} . \quad (2.18.23)$$

Notice that

$$\tau_{\text{theory}} / \tau_{\text{exp.}} = \Gamma_{\text{exp.}} / \Gamma_{\text{theory}} = 2^{1/2} . \quad (2.18.24)$$

It suggests that the energy responsible for decay, Γ_{theory} , appears on the Schwarzschild surface for the weak or nuclear strong interactions. Then, its relativistic mass is $\Gamma_{\text{exp.}} = 2^{1/2} \Gamma_{\text{theory}}$ – it leads to the perfect consistency of the SST with experimental data concerning the lifetimes.

2.19. Radius of proton

Here we show that the charge radius of proton depends on kind of measurement.

We know that range/radius of interaction is inversely proportional to mass so an increase in mass due to some additional interactions causes that effective radius (for example, of proton), R_{eff} , decreases. It follows from the conservation of the angular momentum of a loop for an invariant spin speed of the loop – it can be a virtual photon loop or virtual gluon loop with energy equal to a characteristic mass that carries an interaction. It leads to following relationship

$$R_{\text{eff}} = R_o M_o / (M_o + \sum_i m_i) , \quad (2.19.1)$$

where R_o is the initial radius, M_o is the initial mass carrying an initial interaction, and $\sum_i m_i$ is the sum of masses of carriers of additional interactions.

On the other hand, coupling constants, α_i , are directly proportional to masses of carriers of interactions, m_i , (see (2.4.23))

$$\alpha_i \sim m_i . \quad (2.19.2)$$

From (2.19.1) and (2.19.2) we have

$$R_{\text{eff}} = R_o \alpha_o / (\alpha_o + \sum_i \alpha_i) , \quad (2.19.3)$$

where α_o is the initial coupling constant, and $\sum_i \alpha_i$ is the sum of coupling constants for additional interactions.

In the proton, there is occupied only the $d = 1$ state, i.e. $R_{d=1} = A + B = 1.199278 \text{ fm}$ – it is occupied by the positively charged relativistic pion, π^+ or relativistic bound neutral pion $\pi^{\circ}_{\text{bound}}$.

From the sizes of the torus/electric-charge follows that the charge radius of proton along the z-axis is

$$R_z = A / 3 . \quad (2.19.4)$$

The charged pion in the $d = 1$ state causes that the charged radius of proton along the x-axis and y-axis is

$$R_x = R_y = A + B . \quad (2.19.5)$$

The virtual gluons are emitted especially in directions parallel to the plane of the equator of the torus/electric-charge so the nuclear strong field has a shape of a cylinder.

The arithmetic mean of the orthogonal radii, which is the real mean charge radius of proton, $R_{o,p}$, is

$$R_{o,p} = (R_x + R_y + R_z) / 3 = [2 (A + B) + A / 3] / 3 = \mathbf{0.8770123 \text{ fm}} . \quad (2.19.6)$$

This value is consistent with the result obtained by Fleurbaey, *et al.* (2018) [5] – the result is $r_p = 0.877(13) \text{ fm}$. It is based on the 1S – 3S transition in hydrogen.

This value is consistent also with the result obtained by Sick (2018) [6] – the result is $r_p = 0.887(12) \text{ fm}$. It is based on the electron scattering.

The virtual nuclear strong field creates the virtual charged pion-antipion pairs (the $\pi^- \pi^+$ pairs). Decays of such pairs into muons cause that there appear the muon-antimuon pairs (the $\mu^- \mu^+$ pairs). On the other hand, the decays of the $\pi^- \pi^+$ pairs into the neutral pions cause that there appears a virtual cloud composed of the electron-electron antineutrino pairs and the positron-electron neutrino pairs with a mass of $\Delta\pi = \pi^\pm - \pi_{\text{bound}}^0$.

In measurements based on, for example, the muonic hydrogen Lamb shift, the virtual leptonic quadrupoles, $e^- \nu_{e,\text{anti}} e^+ \nu_e$, are forced to interact with the virtual $\mu^- \mu^+$ pairs. It causes that the effective charge radius of proton decreases. The mean muon charge radius, $R_{p(\mu)}$, of proton is

$$R_{p(\mu)} = R_{o,p} \mu^\pm / (\mu^\pm + \Delta\pi) = \mathbf{0.840391 \text{ fm}} . \quad (2.19.7)$$

This value is very close to the result obtained by Antognini, *et al.* (2013) [7] – the result is $r_p = 0.84087(39) \text{ fm}$. It is based on the $\mu^\pm p$ – atom Lamb shift.

Applying formula (2.19.3) we obtain

$$R_{p(\text{lower-limit})} = R_{o,p} \alpha_s / [\alpha_s + 2 (\alpha_{w(p)} + \alpha_{em})] = \mathbf{0.833630 \text{ fm}} , \quad (2.19.8)$$

where $\alpha_s = 1$ is the coupling constant for the nuclear strong interactions inside baryons at low energy. The factor 2 in formula (2.19.8) appears because the virtual leptonic field interacts with proton via the particle-antiparticle pairs, not via single particles.

This value is consistent with the result obtained by Bezginov, *et al.* (2019) [8] – the result is $r_p = 0.833(10) \text{ fm}$. It is based on the 2S-2P transition in hydrogen.

On the basis of the atom-like structure of baryons, we showed that the effective charge radii of proton strongly depend on the kinds of measurements.

We claim that the measurements based on the $nS - mS$ transitions in hydrogen, where n and m are the natural numbers, and based on the elastic electron-proton scattering in the low momentum transfer region, practically eliminate the electroweak interactions of the virtual leptonic field with proton. It causes that the nuclear strong interactions lead to the real charge radius of proton equal to 0.8770123 fm – it is the upper limit.

The electroweak interactions of proton with the virtual leptonic field composed of the muon-antimuon pairs ($\mu^- \mu^+$) and the lepton quadrupoles ($e^- \nu_{e,\text{anti}} e^+ \nu_e$) from the decays of the virtual

charged pion-antipion pairs ($\pi^- \pi^+$), cause that the effective charge radius of proton decreases to 0.840391 fm so we indeed can call such a radius the muon charge radius of proton.

The lower limit for the effective charge radius of proton we obtain using the coupling constants for the nuclear-strong, nuclear-weak and electromagnetic interactions – it is 0.833630 fm.

The calculated values should dominate but there can be also some mixtures of them.

2.20. Selected mesons

Mesons, meanwhile, are binary systems of gluon loops that are created inside and outside the torus of baryons. They can also be mesonic nuclei that are composed of the other mesons and the FGLs, or they can be binary systems of mesonic nuclei and/or other binary systems.

We can build three of the smallest unstable neutral objects containing the carriers of strong interactions i.e. the pions (134.96608 MeV (the bound state) and 139.57040 MeV) and the FGLs (67.54441 MeV). Each of those objects must contain the FGL because only then it can interact strongly.

The letter **a** denotes the mass of the object built of a bound neutral pion and one FGL

$$\mathbf{a} = 202.51 \text{ MeV.}$$

The parity of this object is equal to $P = +1$ because both the pion and the FGL have a negative parity so as a result the product has a positive value.

The letter **b** denotes the mass of the two bound neutral pions and one FGL

$$\mathbf{b} = 337.48 \text{ MeV.}$$

And **b'** denotes the mass of the two charged pions and one FGL

$$\mathbf{b}' = 346.69 \text{ MeV.}$$

The parity of these objects is equal to $P = -1$.

In particles built of objects **a**, **b**, and **b'**, the spins are oriented in accordance with the Hund law (the sign "+" denotes spin oriented up, the sign "-" denotes spin oriented down, and the word "and" separates succeeding shells), for example

+– and +– +++– – – and +– +++– – – +++++– – – – and etc.

Because electrically neutral mesonic nuclei may consist of the above three different types of objects whereas only one of them contains the charged pions, the charged pions should, therefore, be two times less than the neutral pions. It is also obvious that there should be some analogy for mesonic and atomic nuclei. I will demonstrate this for the Upsilon meson and the Gallion. The Gal is composed of 31 protons and has an atomic mass equal to 69.72. To try to build a meson having a mesonic mass equal to 69.5 we can use the following equation:

$${}^{69.5}\text{Upsilon} = Y(1S) = 8\mathbf{a} + 14\mathbf{b} + 9\mathbf{b}' = 9464.92 \text{ MeV (vector).}$$

Such a mesonic nucleus contains 18 charged pions, 36 bound neutral pions, 31 FGLs, and contains $31 = 8 + 14 + 9$ objects.

Lightest mesonic nuclei

The Eta meson is an analog to the Helion-4. Since the Eta meson contains three pions there are two possibilities. Such a mesonic nucleus should contain one charged pion but such objects are not electrically neutral. This means that the Eta meson should contain two charged pions or zero

$${}^4\text{Eta} = \eta = \mathbf{a} + \mathbf{b}' = 549.20 \text{ MeV (pseudoscalar),}$$

$${}^4\text{Eta}_{\text{minimum}} = \eta_{\text{minimum}} = \mathbf{a} + \mathbf{b} = 539.99 \text{ MeV (pseudoscalar).}$$

The Eta' meson is an analog to Lithion-7

$$\text{Eta}' = \eta'(958) = \mathbf{3a} + \mathbf{b}' = 954.22 \text{ MeV (pseudoscalar).}$$

We see that there are in existence the following mesonic nuclei ($\mathbf{a} + \mathbf{b}'$) and ($\mathbf{3a} + \mathbf{b}'$) – it suggests that there should also be ($\mathbf{2a} + \mathbf{b}'$). However, an atomic nucleus does not exist which has an atomic mass equal to 5.5. Such a mesonic nucleus can, however, exist in a bound state, for example inside a binary system of mesons

$$\text{X}' = \rho = \mathbf{2a} + \mathbf{b}' = 751.71 \text{ MeV (vector).}$$

The K kaons

The core of baryons is indestructible at high energies so particles that are created also at high energies must be created inside the baryonic core. Kaons, pions, or Higgs bosons all are produced inside the core. Therefore we do not have much choice – there is the X^\pm , Y , m_{FGL} , ΔE_{Core} , on the circular axis of the torus there can be the bare electron $\text{m}_{\text{e,bare}}$, and there is the four-fermion symmetry associated with Y ($4 \text{ m}_{\text{e,bare}}$ or $\text{Y} \approx 4 \mu^\pm$).

Assume that the spin-0 charged kaon K^\pm is a result of following interactions

$$\text{K}^\pm = [\text{Y} + \text{m}_{\text{FGL}} + (\text{e}^\pm \nu)_{\text{virtual}}] + 4 \text{ e}^\pm_{\text{bare}} = 493.708 \text{ MeV} . \quad (2.20.1)$$

In reality, one of the two FGLs in a charged pion (it is a pseudoscalar), due to the transition from its circumference to its radius, transforms into the spacetime condensate Y – it means that the $[\text{Y} + \text{m}_{\text{FGL}} + (\text{e}^\pm \nu)_{\text{virtual}}]$ is a pseudoscalar. The $4\text{m}_{\text{e,bare}}$ is a scalar, so K^\pm is a pseudoscalar $\text{J}^{\text{P}} = 0^-$. The $(\text{e}^\pm \nu)_{\text{virtual}}$ stabilizes the $[\text{Y} + \text{m}_{\text{FGL}}]$ pair.

The spin-0 neutral kaon K^0 is created because the neutral pion, after the transition described above, attaches the electromagnetic mass of the quadrupole of neutral pions ($\text{M}_{\text{em}} = 4\pi^0 \alpha_{\text{em}} = 3.940 \text{ MeV}$) to stabilize the $[\text{Y} + \text{m}_{\text{FGL}}]$ pair.

$$\text{K}^0 = [\text{Y} + \text{m}_{\text{FGL}} + \text{M}_{\text{em}}] + 4 \text{ e}^\pm_{\text{bare}} = 497.648 \text{ MeV} . \quad (2.20.2)$$

Due to the strong interactions, the neutral kaon decays into two pions (the coupling constant is equal to 1) or due to the weak interactions to three pions. The condensate of the proton is about π times greater than the rest mass of the neutral pion so the coupling constant of the weak interactions of two pions is π^2 times smaller than for the proton. This means that the K^0_{L} kaons should live approximately $\pi^2 / \alpha_{\text{w(p)}} = 527$ times longer than the K^0_{S} .

The K_0^* meson

The composition of $\text{K}_0^*(700)$ is as follows

$$\text{K}_0^*(700)_{\text{mass}} = 2 \text{ Y} = 848 \text{ MeV} . \quad (2.20.3)$$

But one of the two Y condensates can decay to two neutral pions so the mean mass is

$$K_0^*(700)_{\text{mean}} = Y + 2 \pi^0 = 694 \text{ MeV} \approx 700 \text{ MeV} . \quad (2.20.4)$$

2.21. Hyperons

The $d = 2$ state is the ground state outside the Schwarzschild surface for the strong interactions and is responsible for the structure of hyperons. During the transition of the W_d pion from the $d = 2$ state into $d = 4$, in the $d = 2$ state, some vector bosons occur as a result of decay of the W_d pions into two loops. Each loop has a mean energy equal to the E

$$E = (W_{(-),d=2} + W_{(o),d=2} - W_{(-),d=4} - W_{(o),d=4}) / 2 = 19.3664 \text{ MeV} . \quad (2.21.1)$$

The vector bosons interact with the W_d pions in the $d = 2$ state. The mean relativistic energy, E_W , of these bosons is

$$E_W = E / \{1 - A / (A + 2 B)\}^{1/2} = 25.2128 \text{ MeV} . \quad (2.21.2)$$

Groups of the vector bosons can contain d loops. Then in the $d = 2$ state there may occur particles that have mass which can be calculated using the following formula

$$M_{(+o),k,d=2} = W_{(+o),d=2} + \sum_{\substack{d < 2^k \\ d = 0,1,2,4}} d E_W , \quad (2.21.3)$$

where $k = 0, 1, 2, 3$, and the k and d determine the quantum state of the particle having a mass $M_{(+o),k,d}$.

The mass of a hyperon is equal to the sum of the mass of a nucleon and of the masses calculated from (2.21.3). We obtain good conformity with the experimental data assuming that hyperons contain the following particles (the values of the mass are in MeV)

$$\Lambda = n + M_{(o),k=0,d=2} = 1115.3, \quad (2.21.4)$$

$$\Sigma^+ = p + M_{(o),k=2,d=2} = 1189.6, \quad (2.21.5)$$

$$\Sigma^0 = n + M_{(o),k=2,d=2} = 1190.9, \quad (2.21.6)$$

$$\Sigma^- = n + M_{(-),k=2,d=2} = 1196.9, \quad (2.21.7)$$

$$\Xi^0 = \Lambda + M_{(o),k=1,d=2} = 1316.2, \quad (2.21.8)$$

$$\Xi^- = \Lambda + M_{(-),k=1,d=2} = 1322.2, \quad (2.21.9)$$

$$\Omega^- = \Xi^{-0} + M_{(o),k=3,d=2} = 1674.4. \quad (2.21.10)$$

Using the formulae (2.21.3)-(2.21.10) we can summarise that for the given hyperon the following selection rules are satisfied:

- each addend in the sum in (2.21.3) contains d vectorial bosons,
- for the $d = 2$ state the sum of the values of the k numbers is equal to one of the d numbers,
- the sum of the following three numbers i.e. of the sum of the values of the k numbers in the $d = 2$ state plus the number of particles denoted by $M_{(+o),k,d=2}$ plus one nucleon is equal to one of the d numbers,

- d) there can be only one object in the nucleon or hyperon having the mass $M_{(+o),k,d}$ for which the numbers k and d have the same values,
- e) there cannot be vector bosons in the $d = 1$ state because this state lies under the Schwarzschild surface and transitions from the $d = 1$ state to the $d = 2$ or $d = 4$ states are forbidden, so in the $d = 1$ state there can only be one W_d pion,
- f) the mean charge of the torus of the nucleon is positive so if the relativistic pions are not charged positively then electric repulsion does not take place – there is, however, one exception to this rule: in the $d = 1$ state there can be a positively charged pion because during that time the torus of the proton is uncharged,
- g) to eliminate electric repulsion between pions in the $d = 2$ state there cannot be two or more pions charged negatively,
- h) there cannot be a negatively charged W_d pion that does not interact with the vector boson in the $d = 2$ state in the proton because this particle and the W_d pion in the $d = 1$ state would annihilate,
- i) there cannot be a neutral pion in the $d = 2$ state in the proton because the exchange of the charged positively pion in the $d = 1$ state and of the neutral pion in the $d = 2$ state takes place. This means that the proton transforms itself into the neutron. Following such an exchange the positively charged pion in the $d = 2$ state is removed from the neutron because of the positively charged torus. Such a situation does not take place in the hyperon lambda $\Lambda = n W_{(o),d=2}$.

Using these rules we can conclude that the structure of hyperons strongly depends on the d numbers associated with the Titius-Bode law for strong interactions (i.e. with symmetrical decays) and on the interactions of electric charges.

The above selection rules lead to the conclusion that there are in existence only two nucleons and seven hyperons.

The spins of the vector bosons are oriented in accordance with the Hund law. The angular momentums and the spins of the objects having the mass $M_{(+o),k,d}$ are oriented in such a way that the total angular momentum of the hyperon has minimal value. All of the relativistic pions, which appear in the tunnels of nucleon, are in the S ($l = 0$) state. This means that hyperons Λ , Σ , and Ξ have half-integral spin, whereas Ω has a spin equal to $3/2$.

The strangeness of the hyperon is equal to the number of particles having the masses $M_{(+o),k,d=2}$ taken with the sign “–”.

Notice also that the percentages for the main channels of the decay of Λ and Σ^+ hyperons are close to the x , $1-x$, y , $1-y$ probabilities. This suggests that in a hyperon, before it decays, the $W_{(o),d=2}$ pion transits to the $d = 1$ state and during its decay the pion appears which was in the $d = 1$ state.

2.22. $\Delta(1232)$ resonance

The $\Delta(1232)$ resonance is the only one to behave in an unusual way that results from the dynamics of baryons. Decay of such resonance starts from $d = 2$ state as it is for all baryon resonances. But the relativistic radial speed of the charged pions, π^\pm , in the $d = 4$ state is

$$v_{\text{radial}} = (c^2 - v_{\text{spin},d=4}^2)^{1/2} = 0.8614783 c, \quad (2.22.1)$$

where $v_{\text{spin},d=4}^2 / c^2 = A / (A + 4B)$.

It causes that the relativistic mass of the charged pions in the $d = 4$ state is (it moves in radial direction)

$$\pi_{\text{rel},d=4}^{\pm} = 274.8560 \text{ MeV} \text{ and it is close to } \pi_{\text{rel}}^{\pm} = \pi^{\pm} + \pi^0 = 274.5472 \text{ MeV} , \quad (2.22.2)$$

so there is a resonance!

There is also the virtual part that leads to the mean mass of the vector boson (gluon) $E = 19.366444 \text{ MeV} \{J^P = 1^{-}\}$ (see (2.21.1)) that interacts with the relativistic charged pion – then the spin is equal to 1 as it is for the SST-absolute-spacetime components.

In SST, we have the four charge states of the $\Delta(1232)$ resonance:

$$\Delta(1232)^{++} \{3/2^{+}u\} = p + \pi_{\text{rel}}^{+} + E = 1232.186 \text{ MeV} , \quad (2.22.3)$$

$$\Delta(1232)^{+} \{3/2^{+}u\} = n + \pi_{\text{rel}}^{+} + E = 1233.479 \text{ MeV} , \quad (2.22.4)$$

$$\Delta(1232)^{0} \{3/2^{+}u\} = p + \pi_{\text{rel}}^{-} + E = 1232.186 \text{ MeV} , \quad (2.22.5)$$

$$\Delta(1232)^{-} \{3/2^{+}u\} = n + \pi_{\text{rel}}^{-} + E = 1233.479 \text{ MeV} . \quad (2.22.6)$$

The arithmetic mean of the four masses is

$$\Delta(1232) = N(938.92) + \pi_{\text{rel}}^{\pm} + E = 1232.83 \text{ MeV} \text{ and } J^P = 3/2^{+} . \quad (2.22.7)$$

The basic objects in $\Delta(1232)$ are created in the $d = 2$ state. Radius of the $d = 2$ state is $R_{d=2} = 1.7011 \text{ fm}$. It means that the FGL produced in the core of baryons reaches the $d = 2$ orbit after $\tau = R_{d=2} / c = 5.67 \cdot 10^{-24} \text{ s}$. From formula $\Gamma = \hbar / \tau$ we can calculate the full width that relates to τ : 116 MeV . On the other hand, the Breit-Wigner full width for mixed charges of the $\Delta(1232)$ is $114 < \Gamma < 120 \text{ MeV}$ so our result overlaps with the experimental data.

2.23. Masses of quarks

Within the 3-valence-quarks model of baryons we cannot calculate simultaneously the precise mass and spin of proton whereas it is possible within the SST. Here we showed that the quark theory is not important at low energy. But, of course, the masses of quarks should follow from presented here the atom-like structure of baryons. Most important are the masses of the quark-antiquark pairs.

Mass of the up quark ($M_{\text{Quark-u}} = 2.23 \text{ MeV}$) is equal to the half of the mass distance between the two states of proton.

Mass of the down quark ($M_{\text{Quark-d}} = 4.89 \text{ MeV}$) is equal to the half of the mass distance between the two states of neutron.

Mass of the strange quark ($M_{\text{Quark-s}} = 87.86 \text{ MeV}$) should be associated with the mass of the relativistic $W_{(o),d=2} = 175.710 \text{ MeV}$ pion – this state is responsible for the masses of strange hyperons so mass of the strange quark is equal to the half of this mass.

To calculate masses of the three heaviest quarks we must derive some formula.

Quark is a loop or a condensate of it. We showed that a loop has 10 degrees of freedom. A hypervolume of the phase space and its total mass (the mass is in proportion to the

hypervolume), i.e. the mass of the quark-antiquark pairs created in collisions, must be in proportion to the radius of a gluon loop to the power of 10.

On the equator of the torus, there arise the gluon condensates which masses are the same as the calculated within the atom-like structure of baryons. Range of a condensate is r_{range} . Then, there is created a loop with radius $r_{\text{loop}} = r_{\text{range}} + A$. Mass of such a loop we can calculate from following formula

$$M_{\text{Loop}} [\text{GeV}] = a_q (r_{\text{Loop}} [\text{fm}])^{10} = a_q (r_{\text{range}} [\text{fm}] + A [\text{fm}])^{10}, \quad (2.23.1)$$

where a_q is a factor whereas $A = 0.6974425 \text{ fm}$ is the radius of the equator of the torus in the core of baryons. For $H^\pm = 0.7274392 \text{ GeV}$ we should obtain $r_{\text{loop}} = A$ so then $a_q = 26.71238 \text{ GeV/fm}^{10}$.

Knowing that range of a mass equal to $S_{(+),d=4} = 187.5739 \text{ MeV}$ is $4B = 2.007342 \text{ fm}$, we can calculate range for a gluon condensate from formula

$$r_{\text{range}} [\text{fm}] = S_{(+),d=4} [\text{MeV}] 4B [\text{fm}] / m_{\text{condensate}} [\text{MeV}] = b_q / m_{\text{condensate}} [\text{MeV}], \quad (2.23.2)$$

where $m_{\text{condensate}}$ is the mass of a gluon condensate whereas $b_q = 376.5249 \text{ fm} \cdot \text{MeV}$.

We can rewrite formula (2.23.1) as follows

$$M_{\text{Loop}} [\text{GeV}] = a_q (b_q / m_{\text{condensate}} [\text{MeV}] + A [\text{fm}])^{10}. \quad (2.23.3)$$

Mass of gluon condensate equal to mass of the Upsilon $Y(1S, 9460 \text{ MeV})$ leads to the mass of the charm quark ($M_{\text{Quark-c}} = 1267 \text{ MeV}$).

Mass of a loop overlapping with the $d = 0$ orbit is 727.4392 MeV . Calculate mass of a condensate that is equal to mass of a loop overlapping with the last orbit, $d = 4$, on assumption that linear density is the same as for the loop overlapping with the $d = 0$ state. We obtain $m_{\text{condensate}} = 2821.116 \text{ MeV}$. Applying formula (2.23.3) we obtain mass of the bottom quark ($M_{\text{Quark-b}} = 4190.33 \text{ MeV}$).

Mass of gluon condensate equal to sum of masses of the torus inside the core of baryons ($X^\pm = 318.29555 \text{ MeV}$) and the condensate ($Y = 424.12176 \text{ MeV}$), i.e. $m_{\text{condensate}} = 742.4173 \text{ MeV}$, leads to the mass of the top quark ($M_{\text{Quark-t}} = 171.85 \text{ GeV}$).

2.24. The PMNS neutrino-mixing matrix

Since the SST parameters and the SM parameters concerning the PMNS neutrino-mixing matrix are the same so the SM mimics the properties and weak interactions of neutrinos described in SST.

The mixing angles are defined as follows.

A. The first fundamental phenomenon in the early nuclear plasma was the production of the charged pion-antipion pairs $F_{\pi\pi} = (\pi^- \pi^+) = 279.14 \text{ MeV}$ and next their decays to, first of all, electron-neutrinos and tau-neutrinos (see the explanation below) with the characteristic energy $E_{\text{o,neutrino}} = m_{\text{FGL}} / 2 = 33.77221 \text{ MeV}$. The ratio of these masses can define the

A_{13} angle which is a powerful discriminator of the neutrino theory because it appears in all three SST definitions of the mixing angles. We obtain

$$A_{13} [^\circ] = F_{\pi\pi} / E_{o,\text{neutrino}} = 8.2654 . \quad (2.24.1)$$

Notice that value of the first mixing angle is close to the ratio of the masses of the lightest hyperon (i.e. hyperon Λ that decays due to the nuclear weak interactions) and lightest meson (i.e. the bound neutral pion): $\Lambda / \pi_{\text{bound}}^0 = 8.264$.

B. The second fundamental phenomenon in the early Universe was and is the four-neutrino symmetry (there are the four stable neutrinos) that can lead to the transition of four protons into atomic nucleus of helium-4. We can call such mixing angle the solar angle because it is associated with the solar neutrinos – it is the mixing angle A_{12} . We can define the solar mixing angle using formula

$$A_{12} [^\circ] = 4 A_{13} = 33.0616 . \quad (2.24.2)$$

C. The third fundamental phenomenon in the early Universe was creation of objects composed of three entangled neutrinos with different flavours – such objects were composed of 5 stable neutrinos (see the explanation below) so the mixing angle A_{23} we can define using formula

$$A_{23} [^\circ] = 5 A_{13} = 41.3270 . \quad (2.24.3)$$

Such angles lead to the 9 SST PMNS-matrix elements.

In SST, the nuclear weak interactions are associated with the poloidal motions of the torus/electric-charge in the core of baryons – such motions change the direction of the particles' motion to the opposite, so the phase shift is 180 degrees, i.e. $\delta_{\text{weak}} [^\circ] = 180$ i.e. $\exp(i \delta_{\text{weak}}) = -1$.

According to SST, the tremendous non-gravitating energy inside the four stable neutrinos (i.e. the electron-neutrino, muon-neutrino and their antiparticles) causes that they are indestructible in the present-day inner Cosmos.

The charged pions can decay as follows

$$\pi^+ \rightarrow e^+ + \nu_e + \nu_{\mu,\text{anti}} + \nu_{\mu} , \quad (2.24.4)$$

$$\pi^- \rightarrow e^- + \nu_{e,\text{anti}} + \nu_{\mu} + \nu_{\mu,\text{anti}} . \quad (2.24.5)$$

There is a possibility that the three neutrinos that appear in the decays of charged pions will be entangled and will carry half-integral spin. We claim that such objects composed of three entangled stable neutrinos are the tau-neutrinos

$$\nu_{\tau} \equiv \nu_e (\nu_{\mu,\text{anti}} \nu_{\mu}) , \quad (2.24.6)$$

$$\nu_{\tau,\text{anti}} \equiv \nu_{e,\text{anti}} (\nu_{\mu} \nu_{\mu,\text{anti}}) . \quad (2.24.7)$$

The pair of neutrinos in the parentheses has the total weak charge and total internal helicity both equal to zero so the tau-neutrinos behave as the electron-neutrinos with shifted mass (mass is three times greater).

We can see that there are three flavours of neutrinos ν_n , where $n = e, \mu, \tau$.

Rotating neutrinos shift the zero-point of the local zero-energy field and such “mass” can be measured because of the very small size of the rotating neutrino.

Maximum “mass” of rotating electron- or muon-neutrino can be close to the Planck mass

$$M_{\text{Neutrino,max}} = h \nu / c^2 = \hbar / (r_{\text{neutrino}} c) = 3.1451 \cdot 10^{-8} \text{ kg} . \quad (2.24.8)$$

The CMB neutrinos should have the mean “mass” equal to the geometric mean of the mass of the non-rotating-spin neutrino and of $M_{\text{Neutrino,max}}$

$$M_{\text{Neutrino,CMB}} = (M_{\text{Neutrino,max}} m_{\text{Neutrino}})^{1/2} = 1.0241 \cdot 10^{-37} \text{ kg} = 0.05745 \text{ eV} . \quad (2.24.9)$$

The sum of the CMB masses of the three degenerate neutrinos with different flavours is

$$M_{3,\text{CMB}} = \sum_{n=e,\mu,\tau} M_N = 5 M_{\text{Neutrino,CMB}} = 0.2873 \text{ eV} . \quad (2.24.10)$$

This value is consistent with the observational facts [9]: $0.320 \pm 0.081 \text{ eV}$.

2.25. The CKM quark-mixing matrix

Contrary to the Standard Model (SM) of particle physics, we can test the Scale-Symmetric Theory (SST) via the experimental values of the elements of the CKM matrix. It follows from the fact that values of such elements result from the atom-like structure of baryons described in SST. In SM, such values are the free parameters.

Since the SST parameters and the SM parameters concerning the CKM quark-mixing matrix are the same so the SM mimics the true description of structure and interactions of hadrons described within SST.

The masses of quarks and mixings of quarks have the origin in the SST. In SST, the three mixing angles are defined by ratios of masses of the three characteristic masses for the atom-like structure of baryons to the mass of the torus/electric-charge in the core of baryons $X^\pm = 318.29555 \text{ MeV}$ that is the source of the Titius-Bode orbits for the nuclear strong interactions. The masses are as follows. The first virtual mass $M_{\text{TB}} = 750.2958 \text{ MeV}$ is created on the equator of the core of baryons (the $d = 0$ state) – its symmetrical decays are responsible for creation of the TB orbits for the nuclear strong interactions. The second virtual mass $m_{\text{FGL}} = 67.54441 \text{ MeV}$ is the mass of the fundamental gluon loop (FGL) created on the circular axis inside the core of baryons – it is responsible for the strong interactions inside hadrons. Above we showed that the third virtual mass $M_{\text{Quark-b}} = 4190.33 \text{ MeV}$ is the mass of the b quark which is associated with the last TB orbit for the strong interactions.

The mixing angles are defined as follows

$$A_{12} [^\circ] = M_{\text{Quark-b}} / X^\pm = 13.165 , \quad (2.25.1)$$

$$A_{13} [^\circ] = m_{\text{FGL}} / X^\pm = 0.212207 , \quad (2.25.2)$$

$$A_{23} [^\circ] = M_{TB} / X^\pm = 2.3572 . \quad (2.25.3)$$

Emphasize that in the SST CKM matrix, we need only mass of the **b** quark that is derived within the atom-like structure of baryons – other properties of quarks are useless.

Such angles lead to the 9 SST CKM-matrix elements.

In SST, the nuclear weak interactions are associated with the poloidal motions of the torus/electric-charge in the core of baryons – such motions change the direction of the particles' motion to the opposite, so the phase shift is 180 degrees, i.e. $\delta_{\text{weak}} [^\circ] = 180$ i.e. $\exp(i\delta_{\text{weak}}) = -1$. The SST nuclear strong interactions are associated with the radial motions of the gluons so the phase shift is equal to zero degrees, i.e. $\delta_{\text{strong}} [^\circ] = 0$ i.e. $\exp(i\delta_{\text{strong}}) = +1$. The SST electromagnetic interactions are associated with the toroidal motions of the torus/electric-charge.

Knowing that the phase shift for the nuclear strong interactions is zero degrees and applying the mainstream definitions of the CKM elements, we can calculate two of them needed here

$$|V_{ub}| = \sin A_{13} = 0.0037037 , \quad (2.25.4)$$

and

$$|V_{cb}| = \sin A_{23} \cos A_{13} = 0.041129 , \quad (2.25.5)$$

i.e. the ratio of them is

$$\hat{f}_{\text{high}} = [|V_{ub}| / |V_{cb}|]_{\text{high}} = 0.090051 . \quad (2.25.6)$$

This is the SST ratio for the high q^2 ranges because for such ranges, the nucleon-nucleon collisions cause the transitions of quanta from infinity, $R \rightarrow \infty$, onto the equator of the core of baryons with a radius of $A = 0.6974425 \text{ fm}$ (i.e. the $\infty \rightarrow A$ transition).

The SST theoretical result (2.25.6) is consistent with experimental data: 0.095(8) [10].

For lower-range transitions, the q^2 is lower so the ratio $|V_{ub}|/|V_{cb}|$ is lower too.

The radii of the TB orbits are defined by formula

$$R = A + d B , \quad (2.25.7)$$

where $B = 0.5018354 \text{ fm}$, and $d = 0, 1, 2$ and 4 .

Here we calculated the ratios \hat{f} for the low q^2 ranges (i.e. for $A + B \rightarrow A$) and for decays of the Λ_b^0 baryons (i.e. for $A + 4B \rightarrow A$).

The experimental results are as follows. For the low q^2 ranges we have 0.061(4) [10] and for the **b** hyperons is 0.079(6) [11].

The relativistic spin speeds on the TB orbits we can calculate from the boundary condition that on the equator of the core of baryons (the radius is A) the spin speed is c . From formula $v^2 = GM / R$ we obtain

$$v^2 / c^2 = A / (A + d B) . \quad (2.25.8)$$

On the other hand, the relativistic mass we can calculate from the Einstein formula (see our derivation in Section 1.4))

$$M_{\text{Rel}} / M_o = 1 / (1 - v^2 / c^2)^{1/2} . \quad (2.25.9)$$

In SST, the resultant ratio $f_{\text{Resultant}}$ is the product of $f_{\text{high}} = [|V_{ub}|/|V_{cb}|]_{\text{high}}$ and the ratio M_o/M_{Rel} so from (2.25.8) and (2.25.9) we have

$$f_{\text{Resultant}} = [|V_{ub}| / |V_{cb}|]_{\text{high}} [1 - A / (A + d B)]^{1/2} . \quad (2.25.10)$$

For the **high** q^2 ranges ($\infty \rightarrow A$) we have $d \rightarrow \infty$ so from (2.25.6) and (2.25.10) we have

$$f_{\text{Resultant,high}} = 0.090051 . \quad \text{exp. } 0.095(8) \quad (2.25.11)$$

For the **low** q^2 ranges ($A + B \rightarrow A$) we have $d = 1$ so from (2.25.10) we have

$$f_{\text{Resultant,low}} = 0.05825 . \quad \text{exp. } 0.061(4) \quad (2.25.12)$$

It is consistent with experimental data [10].

The mass of the **b** quark relates to the $d = 4$ state so for such **b-hyperon** q^2 ranges ($A + 4B \rightarrow A$) from (2.25.10) we have

$$f_{\text{Resultant,hyperon-b}} = 0.07758 . \quad \text{exp. } 0.079(6) \quad (2.25.13)$$

The LHCb measurement using the baryons decays of Λ_b^0 gives the ratio $|V_{ub}|/|V_{cb}| = 0.079 \pm 0.006$ [10], [11].

The CKM matrix is for the baryons, for example, we can use it to describe decays of the hyperons. Decays of kaons and pions can give values that differ from the values in the SST CKM-matrix.

2.26. Larger structures

The saturation of interactions via the SST Higgs field and the four-particle symmetry lead to the larger structures.

For the single objects such as, for example, fermions, and for the binary systems, as for example, the neutrino-antineutrino pairs or binary systems of massive galaxies, there are obligatory following formulae for number of constituents, N , in bigger composite structures

$$N = 4^d \text{ (for single objects) ,} \quad (2.26.1)$$

$$N = 2 \cdot 4^d \text{ (for binary systems) ,} \quad (2.26.2)$$

where $d = 1, 2, 4, 8, 16, 32$ are the Titius-Bode numbers. Such structures follow from the quantum entanglement, i.e. they result from the exchanges of the superluminal entanglons. We can see that simplest composite objects can contain 4 or 8 constituents.

It is easy to calculate that from energy equal to the rest mass of a nucleon can be produced at the very most six neutral pions. The simplest neutral pion consists of four rotating and

spinning in two loops neutrinos (two gluon loops). We showed as well that each nucleon has two different mass states. Moreover, the spin-1 gluon loops behave in the nuclear strong fields as the spin-1/2 electrons in atoms. These remarks lead to following formula for upper limit for number of neutrinos in a neutral pion

$$N_{\text{maximum}} = 2 \cdot 4^{32}. \quad (2.26.3)$$

2.27. The ultimate equation

We can write the ultimate equation which ties the properties of the pieces of space, i.e. tachyons, with the all masses/sources responsible for the all types of interactions.

The ultimate equation looks as follows

$$4 \pi m_t \rho_t / (3 \eta_t) = (2 m_l / \hbar)^2 (2 m_{\text{Neutrino}} / \rho_{\text{As}})^{1/3} (m_{\text{e,bare}} / 2) c (X^\pm / H^\pm)^{1/2}. \quad (2.27.1)$$

The $4\pi/3$ on the left side of the ultimate equation shows that the tachyons are the balls. The mean mass of tachyons is the mean mass of the source of the fundamental interaction that follows from the direct collisions of tachyons and their viscosity which results from smoothness of their surface. The ρ_t is the mass density of the pieces of space, i.e. of the tachyons (it is not the inertial mass density of the Higgs field). The η_t is the dynamic viscosity of the pieces of space, i.e. of the tachyons.

The two masses of the closed strings (i.e. the entanglon – its total spin is \hbar) on the right side of the ultimate equation are the carriers of the quantum entanglement. The two masses of neutrinos, i.e. the neutrino-antineutrino pair, are the source of the gravitational field, of the directional quantum entanglement and of the volumetric and circular confinement. The mass of single lightest neutrino is the smallest gravitational mass defined by the gravitational constant G . In the equation, the smallest gravitational mass is multiplied by 2 that points that the non-rotating-spin neutrino-antineutrino pairs are the components of the ground state of the SST absolute spacetime (the ρ_{As} in the denominator is the mass density of the SST-As). The half of the mass of the bare electron is the mass of the electric charge i.e. of the mass of the source of the electromagnetic interaction, but it is also mass of the central condensate of the electron, which is responsible for the weak interactions of the electrons. The c is the speed of photons and gluons. The X^\pm is the mass of the torus/electric-charge inside the core of baryons in which the FGLs arise – they are responsible for the nuclear strong interactions inside baryons. The H^\pm is the mass of the charged core of baryons which is equal to $H^\pm = X^\pm + Y - \Delta E_{\text{Core}}$, where the Y is the source of the nuclear weak interactions of the baryons.

The left and right side of the ultimate equation is $6.97611653279696 \cdot 10^{-159} \text{ kg s/m}^2$.

2.28. Turning points in the formulation of the Scale-Symmetric Theory

In 1976, I noticed that the following formula describes how to calculate the mass of a hyperon

$$m [\text{MeV}] = 939 + 176 n + 26 (d - 1), \quad (2.28.1)$$

where $n = 0, 1, 2, 3$, and $d = 1, 2, 4, 8$ are the Titius-Bode numbers.

For a nucleon it is $n = 0$ and $d = 1$ which gives 939 MeV . For hyperon Λ is $n = 1$ and $d = 1$ which gives 1115 MeV . For hyperons Σ is $n = 1$ and $d = 4$ which gives 1193 MeV .

For hyperons Ξ is $n = 2$ and $d = 2$ which gives **1317 MeV**. For hyperon Ω is $n = 3$ and $d = 8$ which gives **1649 MeV**.

I also noticed that the mass distances between the resonances and mass distances between the resonances and hyperons is approximately **200 MeV**, **300 MeV**, **400 MeV**, and **700 MeV**.

In 1985, I grasped that in order to obtain positive theoretical results for hadrons, we should assume that outside the core of a nucleon is in force the Titius-Bode law for nuclear strong interactions. On orbits are relativistic pions.

The year 1997 was the most productive for me because I described the phase transitions of the SST Higgs field. In this eventful year, I practically formulated new particle physics and new cosmology.

2.29. Summary

Both quantum mechanics and general relativity are highly incomplete theories due to the internal structure and interactions of fundamental particles and larger systems.

Moreover, these theories are partially based on incorrect initial conditions. Namely, the speed of light c is invariant only in relation to the object with which the photons are entangled, while the concept of many worlds is erroneous due to the superluminal quantum entanglement.

The SST absolute spacetime consists of the neutrino-antineutrino pairs. The electromagnetic, weak and strong interactions are directly associated with excitations of the SST-As. On the other hand, the neutrinos produce gradients/gravitational-fields in the superluminal SST Higgs field. From (2.1.26) follows that the constants of interactions G_i are directly proportional to densities of fields so the gravitational constant G is tens of orders of magnitude lower than the constants of interactions for electromagnetic, weak and strong interactions. Moreover, properties of the SST-As and SST-Hf are very different so unification of the four mentioned interactions within the same methods is impossible. We also emphasize that the waves wrongly called “gravitational waves” in mainstream physics are actually flows in the SST absolute spacetime.

The ratio of the superluminal energy of the entanglons frozen inside each neutrino in the SST-As spacetime to gravitational energy of the neutrino is $\sim 0.6 \cdot 10^{119}$ (see (2.5.3)). On the other hand, quantum mechanics predicts that the zero-point energy from virtual particles (the summation of energies of the virtual photons stops at the Planck length) is some 120 powers of ten more than the measured value of the zero-point energy (the dark energy). We can see that the considerations in quantum mechanics are not based on facts. SST shows that, generally, the zero-point energy is frozen in neutrinos – there is not a tremendous energy associated with virtual photons unless we will call the entanglons the dark photons. Just during interactions, due to the quantum entanglement and/or confinement, there are created virtual particles but their total energy is infinitesimal in comparison with the superluminal energy frozen inside the neutrinos. Practically the “zero-energy” field is very cold for an observer.

Within the Scale-Symmetric Theory we predict existence of new scalar boson and/or vector boson with a mass of **17.12 – 17.17 TeV** that results from structure of the core of baryons and density of the SST absolute spacetime (see Section **2.16**).

2.30. Tables

Table 5 *Theoretical results*

Physical quantity	Theoretical value*
Gravitational constant G	6.6742978 E-11 m ³ /(kg s ²)
Unitary spin	1.05457181764623 E-34 Js
Planck constant	6.62607015000 E-34 Js
Speed of light	2.99792458000 E+8 m/s
F (kg \leftrightarrow MeV)	1.78266192162742 E-30
Mass of electron (the SST model – Section 2.6)	0.510998945997556 MeV
Fine-structure constant for low energies	1/137.035999085012
Mass of bound neutral pion	134.966086355861 MeV
Mass of charged pion	139.570316606192 MeV
Mass of free neutral pion	134.976874046895 MeV
Mass distance $\pi^{\pm} - \pi^0$	4.5934426 MeV
Radius of closed string	0.9442405262 E-45 m
Linear speed of closed string	0.7269252749 E+68 m/s
Mass of closed string	2.3400788198 E-87 kg
External radius of neutrino	1.1184555774965 E-35 m
Mass of core of Protoworld and superluminal energy frozen inside lightest neutrino	1.9607600885 E+52 kg
External radius of core of Protoworld	286.66351 E+6 light-years
Baryonic mass of the Universe	3.6379137 E+51 kg
Radius of the early Universe loop	191.10901 E+6 light-years
External radius of torus of nucleon	0.6974425321 fm
Constant K	0.7896685548 E+10
Mass of FGL	67.544413 MeV
Mass of torus of core of baryons	318.295548 MeV
Mass of condensate of the nucleon	424.121763 MeV
Radius of the weak condensate of the proton	8.711018109 E-18 m
Binding energy of core of baryons	14.97808631 MeV
Mass of charged core of baryons	727.43922455 MeV
Ratio of mass of the core of baryons to mass of FGL	10.769791177176
Dark-matter/baryonic-matter ratio $\equiv H^{\pm} / \pi^0_{\text{bound}}$	5.389792682
Mass of muon	105.658379634 MeV
A/B in the Titius-Bode law for strong interactions	1.3897833266
Mass of proton	938.27208211 MeV
Mass of free neutron	939.565390 MeV
Proton magnetic moment in nuclear magneton	+2.7928505
Neutron magnetic moment in nuclear magneton	-1.9130438

*E-15=10⁻¹⁵

Table 6 *Theoretical results*

Physical quantity	Theoretical value
Radius of last tunnel for strong interactions	2.704784 fm
Mean square charge for nucleon	0.29
Mean square charge for proton	0.25
Mean square charge for neutron	0.33
Mass of the dark-matter loop	2.07958183 E-47 kg 1.16655995 E-11 eV
Mass of the dark-matter torus	727.43922455 MeV
External radius of torus of electron	386.60708142 fm
Radius of weak condensate of electron	0.7354180540238 E-18 m
Weak constant	1.0355016 E+27 m ³ /(kg s ²)
Electromagnetic constant for electrons	2.78025230261 E+32 m ³ /(kg s ²)
Magnetic constant μ_0	$4\pi (1.000000000538) E-7$
Electric constant ϵ_0	8.85418781285662 E-12
Coupling constant for weak interactions of the proton	0.018722895102
Coupling constant for electron-proton weak interaction	1.11944624655745 E-5
Coupling constant for electron-muon weak interaction	0.951118188679747 E-6
Coupling constant for strong-weak interactions inside the baryons	d=0: 0.993813 d=1: 0.762596 d=2: 0.640306 d=4: 0.507794
M _{TB} responsible for creation of the TB orbits	750.295768 MeV
Ratio of the hidden energy to mass of the neutrino	0.59 E+119
Range of volumetric confinement	3510.18070 r _{neutrino}
Range of circular confinement	3482.90192 r _{neutrino}
Electron radius of proton	0.8770123 fm
Muon radius of proton	0.840391 fm
Mass of tauon	1776.67688 MeV

Table 7 *Lifetimes*

Physical quantity	Theoretical value
* p	Stable
* n	876.33 s
* n (beam)	888.80 s
* μ^\pm	2.194935 E-6 s
* tauon	2.6972 E-13 s
* π^\pm	2.797 E-8 s
* π^0	0.793 E-16 s
* hyperons (mean)	1.115021 E-10 s
* H	1.99 E-25 s
* W^\pm	3.10 E-25 s
* Z^0	2.73 E-25 s

Table 8 *Values of the G_i*

Interaction	Relative value of the G_i
Strong	1 (for $G_S=5.45651 \cdot 10^{29} \text{ m}^3 \text{ s}^{-2} \text{ kg}^{-1}$)
Weak	$1.9 \cdot 10^{-3}$
Electromagnetic interaction of electrons	$5.1 \cdot 10^2$ (it is not a mistake)
Gravitational	$1.2 \cdot 10^{-40}$
XXXXXXXXXXXXXXXXXXXX	XXXXXXX
Coupling constant for strong interactions inside baryons and mesons at low energy	1
Coupling constant for strong interactions of nucleons at low energy	14.391187

Table 9 *New electroweak theory*

Physical quantity	Theoretical value
Electron magnetic moment in the Bohr magneton	1.0011596521793
Muon magnetic moment in the muon magneton	1.0011659204067
Lamb-Retherford Shift	1057.8396 MHz 1058.0742 MHz

Table 10 *Mesons*

Physical quantity	Theoretical value Mass
* H Higgs boson	125.006 GeV
* W^\pm	80.37948 GeV and 80.43105 MeV
* Z^0	91.18936 GeV
* K^\pm	493.708 MeV
* K^0	497.648 MeV
Ratio of lifetimes K_L^0 / K_S^0	527
* Y(1S)	9464.92 MeV
* η	549.20 MeV
* $\eta'(958)$	954.22 MeV
Predicted particle	17.12 – 17.17 TeV

Table 11 *Hyperons and Δ resonance*

Particle	Theoretical value Mass	Theoretical value		
		J	P	S
Hyperon Λ	1115.3 MeV	1/2	+1*	-1
Hyperon Σ^+	1189.6 MeV	1/2	+1	-1
Hyperon Σ^0	1190.9 MeV	1/2	+1	-1
Hyperon Σ^-	1196.9 MeV	1/2	+1	-1
Hyperon Ξ^0	1316.2 MeV	1/2	+1	-2
Hyperon Ξ^-	1322.2 MeV	1/2	+1	-2
Hyperon Ω^-	1674.4 MeV	3/2	+1	-3
Resonance $\Delta(1232)$	1232.8 MeV	3/2	+1	

*Assumed positive parity

Table 12 *Masses of quarks*

Physical quantity	Theoretical value
Up	2.23 MeV
Down	4.89 MeV
Strange	87.86 MeV
Charm	1267 MeV
Bottom	4190.33 MeV
Top	171.9 GeV

Table 13 *PMNS matrix and CKM matrix*

Physical quantity	Theoretical value
PMNS A_{12} [$^\circ$]	33.0616
PMNS A_{13} [$^\circ$]	8.2654
PMNS A_{23} [$^\circ$]	41.3270
PMNS phase shift δ [$^\circ$]	180
CKM A_{12} [$^\circ$]	13.165
CKM A_{13} [$^\circ$]	0.212207
CKM A_{23} [$^\circ$]	2.3572
CKM phase shift δ [$^\circ$]	0

There are many other important theoretical results.

References

- [1] Ramsey N. F. (1990).
Rev. Mod. Phys. **62** 541
- [2] “Muon $g - 2$ ” Collaboration
B. Abi, *et al.* (7 April 2021). “Measurement of the Positive Muon Anomalous Magnetic Moment to 0.46 ppm”
Phys. Rev. Lett. 126, 14, 141801 (2021)
arXiv:2104.03281
- [3] T. Aoyama, *et al.* (3 December 2020). “The anomalous magnetic moment of the muon in the Standard Model”
Physics Reports, Volume 887, 3 December 2020, Pages 1-166
- [4] P. A. Zyla, *et al.* (Particle Data Group)
Prog. Theor. Exp. Phys. **2020**, 083C01 (2020) and 2021 update
- [5] H el ene Fleurbaey, *et al.* (26 January 2018). “New Measurement of the 1S-3S Transition Frequency of Hydrogen: Contribution to the Proton Charge Radius Puzzle”
Phys. Rev. Lett. **120** (2018) 18, 183001
arXiv:1801.08816 [physics.atom-ph]
- [6] Ingo Sick (5 January 2018). “Proton charge radius from electron scattering”
arXiv:1801.01746 [nucl-ex]
- [7] Aldo Antognini, *et al.* (25 January 2013). “Proton Structure from the Measurement of 2S – 2P Transition Frequency of Muonic Hydrogen”
Science Vol. **339**, Issue 6118, pp. 417-420
- [8] N. Bezginov, *et al.* (7 September 2019). “A measurement of the atomic hydrogen Lamb shift and the proton charge radius”
Science Vol. **365** (2019) 6457, 1007-1012
- [9] Richard A. Battye and Adam Moss (6 February 2014). “Evidence for Massive Neutrinos from Cosmic Microwave Background and Lensing Observations”
Phys. Rev. Lett. **112**, 051303
- [10] LHCb Collaboration (9 December 2020). “First observation of the decay $B_s^0 \rightarrow K^- \mu^+ \nu_\mu$ and measurement of $|V_{ub}|/|V_{cb}|$ ”
arXiv:2012.05143 [hep-ex]
- [11] Heavy Flavor Averaging Group, Y. Amhis *et al.* (1 November 2019). “Averages of b-hadron, c-hadron, and τ -lepton properties as of 2018”
arXiv:1909.12524v2, updated results and plots available at <https://hflav.web.cern.ch>

Chapter 3

Cosmology

3.1. Introduction to the SST cosmology and abundances of baryonic matter (BM), dark matter (DM) and dark energy (DE)

In Chapter 2 we showed that the two-component spacetime (i.e. the SST Higgs field (SST-Hf) and the SST absolute spacetime (SST-As)) leads to a very simple and accurate description of particles. Properties of the two components are very different so unification of GR (gravitational fields are the gradients in the SST-Hf produced by neutrinos) and QM (we showed that the electrically charged leptons, the photons, gluons and hadrons are the excited states of the SST-As) within the same methods is impossible.

We showed also that the gravitational constant G is directly proportional to density of the SST-Hf. If both components of spacetime were free to expand, due to the enormous speed of the SST tachyons, the value of the G would change rapidly. The conclusion is simple, namely dark energy can expand while our two-component spacetime should be infinite or should have a solid boundary.

But endless and symmetrical spacetime does not lead to the observed matter-antimatter asymmetry. **So we assume that our inner Cosmos is the result of a collision of an asymmetric inflation field (i.e. with the left-handed external helicity) with a much larger cosmological object – this has led to the creation of the asymmetric inner Cosmos inside this larger cosmological object.** In the next Section, we calculated the radius of the inner Cosmos and we showed why it has a spherical symmetry.

Mainstream cosmology based on general relativity also has a big problem with the recession velocities v/c (more precisely we should call it the relative recession velocities) of galaxies in relation to their observed redshift z . When we neglect the peculiar velocity which is sensitive to the matter distribution, then the kinematic Doppler shift expression (KDSE) obtained within the Special Theory of Relativity (SR) for a motion in the line of sight looks as follows [1]

$$v / c = (z^2 + 2 z) / (z^2 + 2 z + 2) . \quad (3.1.1)$$

Intuition tells us that for the observed redshift of $z = 1$, the recession velocity should be 1 and this should be the maximum recession velocity in the Cosmos with a solid boundary. But in the distant Universe we see galaxies with $z > 1$. Why? Why from formula (3.1.1), for $z = 1$ is $v/c = 0.6$?

In SST there are galaxies with $v > c$ because at the beginning of the expansion of the Universe, the very high dynamic pressure and superfluidity of the SST absolute spacetime have contributed to the formation of superluminal protuberances in the SST-As, which accelerated the protogalaxies to superluminal speeds. We can observe today such protogalaxies because the superluminal protuberances were damped so their today recession velocities are below 1. The speed c is the speed of photons in relation to the object with which they are entangled so we can emphasize that we measure the redshift that directly

follows from the speed of photons they had in relation to the Earth when they were emitted, i.e. we measure $z > 1$. It is the reason that GR incorrectly describes the expansion of the Universe. A change in radial velocity of a galaxy in relation to the Earth (for example, due to the reduction in superluminal speed relative to the Earth) causes the same change in velocities of photons entangled with such galaxy but the measured redshift is invariant, i.e. it does not depend on the change. Moreover, we will show that when we neglect the initial protuberances in the expanding Universe then the recession velocity on the surface/front of the expanding baryonic matter is $v_{\text{front,BM}}/c = 0.6469$, i.e. it is close to the $v/c = 0.6$ we obtain from (3.1.1).

Presented here cosmology is based on the assumption that the cosmological inflation was separated in time from the expansion of our Universe which is immersed in the inner Cosmos. The gravitational interaction and phase transitions described in Chapter 2 make our Universe cyclical and in the stage of its highest average density it is similar to the neutron, so we can use the calculations that concern it. We showed that the core of the Protoworld (the cosmological torus with central condensate) was composed of the entangled dark-matter (DM) tori. The baryonic part of the Universe appeared on the circular axis of the cosmological torus as the two cosmological loops composed of protogalaxies each built of the neutron black holes (NBHs) – it was like creating the bound neutral pion in the core of baryons.

Initially, the Protoworld was the SST gravitational black hole, i.e. on the equator of the core of the Protoworld the spin speed was equal to c . The calculated mass of the DM-core of the Protoworld is (see (2.1.24))

$$H^+_{\text{Protoworld,DM}} = 1.96076 \cdot 10^{52} \text{ kg} . \quad (3.1.2)$$

Baryonic mass of the Universe relates to the mass of the bound neutral pion

$$M_{\text{BM}} = H^+_{\text{Protoworld,DM}} \pi^0_{\text{bound}} / H^+ = 0.363791 \cdot 10^{52} \text{ kg} . \quad (3.1.3)$$

The ratio of the dark matter to baryonic matter, $N_{\text{DM/BM}}$, is

$$N_{\text{DM/BM}} = H^+_{\text{Protoworld,DM}} / M_{\text{BM}} = 5.38979 . \quad (3.1.4)$$

In the $d = 1$ state of the Protoworld (i.e. $\mathbf{R} = \mathbf{A}_{\text{Protoworld}} + \mathbf{B}_{\text{Protoworld}}$, where $\mathbf{A}_{\text{Protoworld}} = 286.6635 \text{ Mly}$ – see (2.1.25), and $\mathbf{A}_{\text{Protoworld}} / \mathbf{B}_{\text{Protoworld}} = \mathbf{A} / \mathbf{B} = 1.38978$), there were the entangled photons and neutrinos with a total mass equal to

$$W_{(-),d=1,\text{Protoworld}} = H^+_{\text{Protoworld,DM}} W_{(-),d=1} / H^+ = 0.581567 \cdot 10^{52} \text{ kg} . \quad (3.1.5)$$

The total mass of the Protoworld was

$$M_{\text{Protoworld}} = H^+_{\text{Protoworld,DM}} + W_{(-),d=1,\text{Protoworld}} = 2.54233 \cdot 10^{52} \text{ kg} . \quad (3.1.6)$$

At the end of the SST inflation, some part of the dark-energy segments transformed into the DM-tori and DM-loops.

The Protoworld created virtual field, i.e. there was the positive mass of the virtual particle-antiparticle pairs which was two times higher than the mass of the Protoworld (see Section 1.4) and there was the negative mass of the virtual holes created in the SST-As. The virtual

particles were emitted – their collisions with the DE segments created a gradient in the DE field (the cross sections of the DE segments are much higher than the SST-As components so mainly number density of the DE segments decreased). We see that lowering the zero-point of the zero-energy field, due to such collisions, related to about two masses of the Protoworld and such a mass of dark energy initially has been pushed out of the Protoworld.

In Chapter 2, we showed that the superluminal energy frozen inside the lightest neutrino is equal to the mass of the core of the Protoworld so a new lightest neutrino created in the Protoworld stole entanglons exchanged among other entangled particles, so the Protoworld decayed and the inflows of dark-matter loops and dark energy (scattering of the DE segments was much lower than the SST-As components) into the baryonic part of the very early Universe forced the exit of the Universe from the black-hole state. From that moment on, we count the age of the Universe.

The decay of the Universe caused the dark energy with a mass twice that of the Protoworld to flow into its interior

$$M_{DE} = 2 M_{Protoworld} = 5.08466 \cdot 10^{52} \text{ kg} . \quad (3.1.7)$$

Now we can calculate the abundances of matter and energy just before the expansion of the Universe

$$\begin{aligned} & \text{BM} : \text{DM} : (\text{photons} + \text{neutrinos}) = \\ & = M_{BM} : H^+_{Protoworld,DM} : W_{(-),d=1,Protoworld} = \\ & = 12.52\% : 67.47\% : 20.01\% , \end{aligned} \quad (3.1.8)$$

and the abundance today

$$\begin{aligned} & \text{BM} : \text{DM} : \text{DE} = \\ & = M_{BM} : H^+_{Protoworld,DM} : M_{DE} = \\ & = 4.91\% : 26.46\% : 68.63\% . \end{aligned} \quad (3.1.9)$$

3.2. Inflation, universes and radius of the inner Cosmos (i.e. of the SST absolute spacetime)

During the SST inflation, due to the creations of entanglons (we described it by using the classical thermodynamics), due to the saturation symmetry, invariant surface-density symmetry, and the adoption symmetry, the inflation field transformed into the SST spacetime – such processes are described in Chapter 2. The inertia of the expanding in a superluminal way SST-As caused that after a very short period, on the surface of the expanding SST-As, the gravitational pressure inserted on a single neutrino had become higher than the dynamic pressure that was the cause of the expansion of the transforming inflation field. Compressive forces acting on the outer layer of the SST-As created a stable boundary of the inner-Cosmos/SST-As with spherical symmetry – it is placed inside the bigger cosmological object so there are two boundaries. Moreover, this compression produced a shockwave in which baryons and antibaryons, dark energy and dark matter were produced. The initial inflation field had a left-handed external helicity which was converted to the left-handed internal

helicity of the tori/electric-charges in the cores of baryons – notice that the tori/electric-charges in antibaryons have right-handed internal helicity. Left-handedness led to the matter-antimatter asymmetry. Why did this asymmetry not appear in the production of neutrinos during the inflation? The reason was the enormous energy frozen inside the neutrinos, which made it impossible to break the symmetry.

The baryonic shockwave, which was moving towards the centre of the inner Cosmos, produced universes with spin speed equal to c on their equators, so they are closed universes, but matter and energy can move within them.

We can calculate radius of the SST absolute spacetime from the condition that gravitational pressure inserted on a single neutrino on surface of the spacetime cannot be higher than the dynamic pressure inside it.

The effective radius of a single lightest neutrino is $L_{Y+As} = 3510.180704 r_{\text{neutrino}}$ (see (2.9.1)). The gravitational force acts on area that is the cross-section so the gravitational pressure, p_{gr} , is (we neglect the baryonic mass of the inner Cosmos in comparison with the mass of the SST-As)

$$\begin{aligned} p_{\text{gr}} &= F_{\text{gr}} / S_{\text{eff}} = (G M_{\text{Cosmos}} m_{\text{Neutrino}} / R_{\text{Cosmos}}^2) / (\pi L_{Y+As}^2) = \\ &= 4 G \pi \rho_{As} R_{\text{Cosmos}} m_{\text{Neutrino}} / (3 \pi L_{Y+As}^2). \end{aligned} \quad (3.2.1)$$

On the other hand, the dynamic pressure of the SST-As, $p_{\text{dyn-As}}$, is

$$p_{\text{dyn-As}} = \rho_{As} c^2 / 2. \quad (3.2.2)$$

From equality of the pressures we obtain

$$R_{\text{Cosmos}} = 3 L_{Y+As}^2 c^2 / (8 G m_{\text{Neutrino}}) = 2.334 \cdot 10^{30} \text{ m}. \quad (3.2.3)$$

Total mass of the SST-As in the inner Cosmos is

$$M_{\text{Cosmos}} = 4 \pi \rho_{As} R_{\text{Cosmos}}^3 / 3 = 5.870 \cdot 10^{119} \text{ kg}. \quad (3.2.4)$$

We can as well calculate the initial radius of the inflation field (i.e. of the field in which the tachyons were packed to maximum), R_{initial} , from which the SST spacetime was created (notice that in reality the radius was much bigger because there was created also the boundary)

$$R_{\text{initial}} = \{3 M_{\text{Cosmos}} / (4 \pi \rho_t)\}^{1/3} = 1.19 \cdot 10^{11} \text{ m}. \quad (3.2.5)$$

This radius is close to the radius of the orbit of the Venus.

3.3. Neutron black holes (NBHs)

We claim that the baryonic part of the Universe was created on the circular axis in the core of the Protoworld – there were two loops (it was an analog to the two gluon loops in neutral pion) composed of protogalaxies already grouped in bigger structures each composed of the NBHs – it causes that we need a theory of NBHs.

We claim that besides a very thin iron crust and very thin layer of nuclear plasma on surface of each neutron star (which we neglect in our calculations), the neutron lattice is composed of

cubes with neutrons in their vertices (see Fig.12). Such neutron lattice is the very stable object because of the strong interactions also between pairs of neutrons located at the ends of diagonals of the side walls of the cubes. The length of the diagonals is equal to the effective range, $R_{\text{eff,NS}}$, of the neutron matter which in SST is equal to the radius of the last TB orbit for the nuclear strong interactions

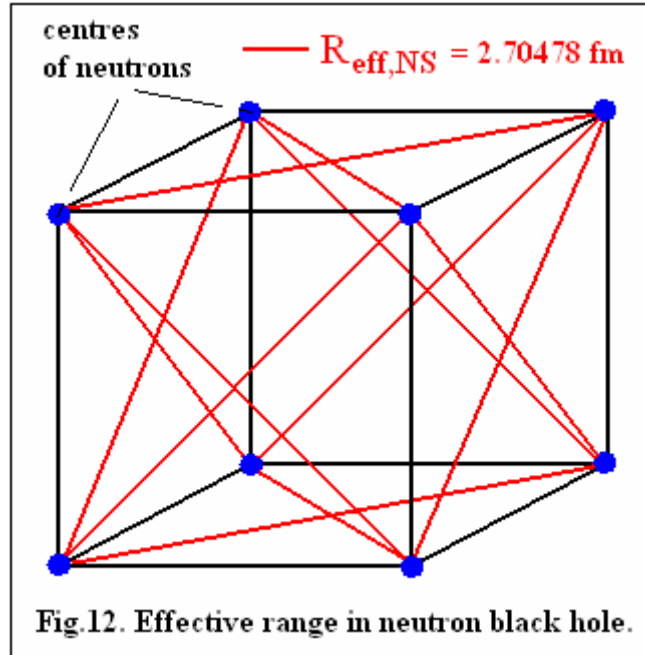
$$R_{\text{eff,NS}} = A + 4 B = 2.704784 \text{ fm} . \quad (3.3.1)$$

This value is consistent with the mainstream value (~ 2.7 fm) [2] but due to the distribution of the neutrons, we get a different density of neutron matter ρ_{NS} . Our value, contrary to the mainstream values, is invariant

$$\rho_{\text{NS}} = n F / (R_{\text{eff,NS}} / 2^{1/2})^3 = 2.39411 \cdot 10^{17} \text{ kg/m}^3 , \quad (3.3.2)$$

where $n = 939.5654 \text{ MeV}$ is the SST mass of neutron.

Why is the effective range $R_{\text{eff,NS}}$ equal to the length of the diagonal and not of the side of the cubes and why is it equal to the radius of the last orbit for the strong interactions of baryons? For diagonals smaller than $\sim 2.7 \text{ fm}$ (there can be ~ 1.7 fm, ~ 1.2 fm, or ~ 0.7 fm), the tori in the cores of baryons, which due to the very strong short-distance quantum entanglement cannot be destroyed (the half-integral spin and electric charge of such tori are conserved), partially overlap, which, because of the very high surface density of the tori, is forbidden. On the other hand, a cube with the side equal to $R_{\text{eff,NS}}$ is not in its ground state.



The upper limit for mass, $M_{\text{NS,upper}}$, and radius, $R_{\text{NS,upper}}$, of neutron stars (NSs) we obtain from the boundary condition that spin speed on equator of NS should be equal to c . We have two equations

$$R_{\text{NS,upper}} = G M_{\text{NS,upper}} / c^2 \quad (3.3.3)$$

$$M_{\text{NS,upper}} = \rho_{\text{NS}} 4 \pi R_{\text{NS,upper}}^3 / 3 , \quad (3.3.4)$$

which lead to following values

$$R_{\text{NS,upper}} = 36.64 \text{ km} , \quad (3.3.5)$$

$$M_{\text{NS,upper}} = 24.81 \text{ solar masses} . \quad (3.3.6)$$

Such a biggest neutron star we call “the neutron black hole (NBH)” because its equatorial spin speed is equal to c .

The binding energy of neutrons in neutron stars that follows from the nuclear strong interactions, due to the very short time of interactions ($\sim 10^{-23}$ s), is frozen inside the neutron star so there is no need to take it into account in calculations of NS mass.

But why can we also neglect the gravitational potential binding energy?

For example, let's calculate the gravitational potential binding energy of a neutron, ΔE_g , located at the surface of the neutron black hole

$$\Delta E_g = -G M_{\text{NS,upper}} n F / R_{\text{NS,upper}} = -F n c^2 = -939.5654 \text{ MeV} . \quad (3.3.7)$$

This value suggests that such neutron behaves as a virtual neutron because the sum of its mass and binding energy is equal to zero. So, do we really have to consider the change in mass due to gravitational interaction? Well, no, and this is due to phenomena occurring in the SST absolute spacetime.

When a star collapses into a neutron star or neutron stars collide, potential gravitational energy must be emitted, and this is due to the divergent flows in the SST-As, which the external observer observes as ripples in the SST-As. But due to the tremendous dynamic pressure in SST-As ($\sim 5 \cdot 10^{44}$ Pa), a reverse flow occurs that restores the initial state of local SST-As. Thus, it is the dynamic pressure in SST-As that means that we do not have to take into account the gravitational potential binding energy in the calculations of the mass of a neutron star.

We can say that neutrons in NBHs exchange virtual quanta composed of the SST-As components which are a part of the zero-energy field.

The colliding NSs with a total mass less or equal to 24.81 solar masses can merge into single neutron star, while NBHs cannot.

More massive black holes (BHs) consist of the NBHs and NSs.

The surface density of the torus in the core of baryons is about 300,000 times higher than in the SST-As – it causes that the moving cores try to drag the absolute spacetime. As a result the angular velocities of the NBH and of the SST-As inside NBH are the same so the NBH has always spherical symmetry and has not a relativistic mass resulting from its rotation.

3.4. The large-scale structure of the very early Universe

In Section 2.26, we showed that the four-object symmetry that follows from the superluminal quantum entanglement leads to following number of NBHs in groups of them or number of protogalaxies in larger structures: $N = 4^d$ for single objects, and $N = 2 \cdot 4^d$ for binary systems, where $d = 1, 2, 4, 8, 16, 32$ are the Titius-Bode numbers. We showed also that the upper limit for N is $N_{\text{maximum}} = 2 \cdot 4^{32}$.

Consider the binary systems of NBHs or protogalaxies. We have

$$N = 2 \cdot 4^d , \quad (3.4.1)$$

where $d = 0, 1, 2, 4, 8, 16$ is for a flattened spheroid-like structures, and $d = 3, 6, 12$ for a chain-like structures.

The cosmic structures composed of the binary systems of protogalaxies we will refer to as follows:

$$\begin{aligned}
 d = 0 & \text{ is for a binary system,} \\
 d = 1 & \text{ is for group,} \\
 d = 2 & \text{ is for supergroup,} \\
 d = 4 & \text{ is for cluster,} \\
 d = 8 & \text{ is for supercluster,} \\
 d = 16 & \text{ is for megacluster (the baryonic part of the Universe was the binary system} \\
 & \text{of megaclusters composed of the binary systems of protogalaxies),} \\
 d = 3 & \text{ is for chain,} \\
 d = 6 & \text{ is for superchain,} \\
 d = 12 & \text{ is for megachain.}
 \end{aligned} \tag{3.4.2}$$

We can use formulae (3.4.1) and (3.3.6) to test the SST cosmology. Maximum number of NBHs in one cosmological loop can be $2 \cdot 4^{32}$ but the baryonic part of the early Universe was composed of two such loops so the total number of NBHs was 4^{33} . We can calculate mass of the two loops

$$M_{\text{baryonic}} = 4^{33} M_{\text{NS,upper}} = 0.3640 \cdot 10^{52} \text{ kg}. \tag{3.4.3}$$

This result is consistent with (3.1.3).

3.5. The correct age of the Universe, Hubble constants and CMB

Initially, the baryonic matter consisted of the neutrons placed in the NBHs but due to the decay of the Protoworld and the inflows of the dark matter and dark energy, it transformed into nuclear plasma. The most abundant ions were the hydrogen and helium-4 ions. It is very reasonable to assume that initially there was the equivalence in number density of nucleons in the two different ions.

When mean distance between the nucleons in baryonic plasma increased to the size of bare electrons, i.e. to $2\lambda_{\text{C,bare}}$ (from the Wien's displacement law follows that then temperature of the plasma was $3.748 \cdot 10^9 \text{ K}$), there appeared gas containing 50% of ionized hydrogen and 50% of ionized helium-4 by number of nucleons, i.e. there was 75% of the protons and 25% of the neutrons. The mean binding energy of nucleon in helium-4 is 7.075 MeV [3]. On the other hand, from the 2018 CODATA central mass of the alpha particle and the PDG central masses of proton and neutron we obtain 7.0739 MeV. This value is also calculated within SST – our value is 7.0746 MeV (see Section C2). Here we assume that it is 7.075 MeV. The released energy per each initial neutron was

$$L_0 = 0.75 \cdot (n - p - m_e) + 0.5 \cdot 7.075 \text{ MeV} = 4.125 \text{ MeV}. \tag{3.5.1}$$

It leads to the CMB – the front of it was expanding with the radial speed equal to c . The energy of the CMB is

$$E_{\text{CMB}} = M_{\text{BM}} L_0 c^2 / n = 1.435 \cdot 10^{66} \text{ J} . \quad (3.5.2)$$

We know that today the density of the energy of the CMB is equal to $\rho_{\text{CMB}} = 4.175(4) \cdot 10^{-14} \text{ J/m}^3$ [4]. By applying the following formula

$$4 \pi R_{\text{CMB}}^3 / 3 = E_{\text{CMB}} / \rho_{\text{CMB}} \quad (3.5.3)$$

we can calculate the radius of the sphere filled with CMB

$$R_{\text{CMB}} = 2.017 \cdot 10^{26} \text{ m, i.e. } 21.32(1) \text{ Gly} . \quad (3.5.4)$$

The front of CMB has the recession velocity equal to 1 so the correct age of the Universe is 21.32 Gyr, not the 13.8 Gyr! This means that the today spatial distance to the CMB front is 21.32 Gyr.

In SST, due to the definition of the speed c , there are two different values of the Hubble constant, i.e. the spatial Hubble constant, $H_{\text{o,spatial}}$, and the time Hubble constant $H_{\text{o,time}}$ which depends on the time distance to the front of the baryonic matter.

The value from formula (3.5.4) leads to the spatial Hubble constant

$$H_{\text{o,spatial}} = c / R_{\text{CMB}} = 45.86 \text{ (km/s)/Mpc} . \quad (3.5.5)$$

To calculate the time Hubble constant notice that the Protoworld looked similar to the $H^+W_{(-),d=1}$ state of the neutron. The spin speed on the $d = 1$ TB orbit is $v_{\text{spin},d=1} = 0.7626c$ so the radial speeds, v_{rad} , of gluon/photon loops created on such orbit is

$$v_{\text{rad}} = (c^2 - v_{\text{spin},d=1}^2)^{1/2} = 0.6469c . \quad (3.5.6)$$

Such photon/gluon loops interacted with the baryonic matter so we can assume that the recession velocity of the front of the baryonic matter also is equal to 0.6469. This means that the time distance, $L_{\text{time,BM}}$, to the baryonic front is

$$L_{\text{time,BM}} = v_{\text{rad}} R_{\text{CMB}} / c = 13.79(1) \text{ Gyr} . \quad (3.5.7)$$

From it we obtain the mean value of the time Hubble constant

$$H_{\text{o,time,MEAN}} = c / L_{\text{time,BM}} = 70.90 \text{ (km/s)/Mpc} . \quad (3.5.8)$$

The redshifts higher than $z > 0.6469$ are from the protuberances which with time were damped.

After the collapse of the Protoworld and the inflow of dark energy, the Universe transformed into an expanding cosmological ball filled with dark energy, dark matter, baryonic matter, neutrinos, photons and photon loops. Total mass/energy, M_{Total} , of it was (see formulae (3.1.3), (3.1.6) and (3.1.7))

$$M_{\text{Total}} = M_{\text{BM}} + M_{\text{Protoworld}} + M_{\text{DE}} = 0.7991 \cdot 10^{53} \text{ kg} . \quad (3.5.9)$$

Volume of the CMB is

$$V_{\text{CMB}} = 4 \pi R_{\text{CMB}}^3 / 3 = 3.437 \cdot 10^{79} \text{ m}^3 . \quad (3.5.10)$$

Today practically whole M_{Total} is inside a sphere with a spatial radius of 13.79 Gly so its total volume is

$$V_{\text{Matter-Energy}} = V_{\text{CMB}} (v_{\text{rad}} / c)^3 = 0.9304 \cdot 10^{79} \text{ m}^3 . \quad (3.5.11)$$

It means that the today critical density, ρ_c , is

$$\rho_c = M_{\text{Total}} / V_{\text{Matter-Energy}} = 8.5888 \cdot 10^{-27} \text{ kg/m}^3 . \quad (3.5.12)$$

In the mainstream cosmology, the H_0 is Hubble's constant that corresponds to the Hubble parameter, H , which is time dependent. From Friedmann equations for $\Lambda = k = 0$ we have

$$\rho_c = 3 H^2 / (8 \pi G) = 1.879 \cdot 10^{-26} h^2 \text{ kg/m}^3 , \quad (3.5.13)$$

where $h = H_0 / [100 \text{ (km/s)/Mpc}]$.

From (3.5.12) and (3.5.13) is

$$H_0 = 67.6 \text{ (km/s)/Mpc} . \quad (3.5.14)$$

Why there is a difference between (3.5.8) (the mean value is 70.9) and (3.5.14) (there is 67.6)? Energy density of photons in the initial cosmological ball was higher in its central parts and lower close to surface of it, i.e. pressure exerted by photons was higher in central parts. There some radial protuberances of the clusters of protogalaxies appeared to equalize the pressure in the initial cosmological ball. It caused the number density of the clusters in the centre to be slightly lower than at the surface of the ball. According to the SST, the Milky Way Galaxy should be near the centre of the expanding Universe, so the lower number density of clusters of galaxies is for the local Universe and the higher number density for the distant (earlier) Universe. The inner protuberances have made the Hubble constant for the local Universe higher, but that does not mean that the expansion of the Universe is accelerating – the mean time Hubble constant is 70.9 (km/s)/Mpc.

We can roughly estimate the change of the Hubble parameter, ΔH , assuming that helium-4 (the binding energy per nucleon is $\Delta E_{\text{Binding/N}} \approx 7.07 \text{ MeV}$) was created mainly in the central parts of the initial cosmological ball and that the squared relative change of the Hubble parameter is directly proportional to the excess energy density of the photons ($H \sim v \sim E^{1/2}$)

$$\Delta H / H_0 = \{ \Delta E_{\text{Binding/N}} / 939 \text{ [MeV]} \}^{1/2} = 0.0868 . \quad (3.5.15)$$

From (3.5.8) and (3.5.15) we have (the observational data are in [12])

$$H = 70.9 \pm 3.1 \text{ (km/s)/Mpc} . \quad (3.5.16)$$

Emphasize that when we neglect the short period (in the cosmological scale) of the inner protuberances then in the SST cosmology, the Hubble's parameter H depends on position in the Universe but it practically does not depend on time.

Density of baryonic matter is

$$\rho_{\text{BM}} = M_{\text{BM}} / V_{\text{Matter-Energy}} = 0.391 \cdot 10^{-27} \text{ kg/m}^3 . \quad (3.5.17)$$

The time distance between the true age of the Universe and the time distance to the most distant visible Universe is the period of evolution of protogalaxies which we cannot see

$$T_{\text{unobservable}} = 21.32 \text{ Gyr} - 13.79 \text{ Gyr} = 7.53 \text{ Gyr} . \quad (3.5.18)$$

The most distant massive galaxies are already 7.53 Gyr old. We should not observe a “smooth field” of the dwarf galaxies as the first stage of the galaxies. Moreover, the Dark Ages are a scientific fiction.

We can see the CMB because the photons were scattered on the electron vortices with different recession velocities. Such vortices were produced in the very early Universe.

In paper [5] we can find a recapitulation concerning the ages of stars. There are cited the results obtained by Ludwig *et al.* (2009) [6]. Ludwig *et al.* derived solar ages from 1.7 to 22.3 Gyr.

Initially number of the entangled SST-As components in the gluon/photon loops created in protons was $2 \cdot 4^{32}$ (we call such objects the supergluons or superphotons). Similar as it was in the baryonic cosmological loops (in each of them there were $2 \cdot 4^{16}$ protogalaxies), the supergluons or superphotons are built of $2 \cdot 4^{16}$ photon “galaxies” (photons) so number of the photons is about $2 \cdot 4^{16} = 0.86 \cdot 10^{10}$ times higher. On the assumption that each proton produced one supergluon we obtain the number of the photon galaxies in CMB (initially the abundance of protons was 0.75)

$$N_{\text{CMB-photons}} = 2 \cdot 4^{16} \cdot 0.75 M_{\text{BM}} / (n F) = 1.3993 \cdot 10^{88} . \quad (3.5.19)$$

Number density of the photon galaxies in CMB from supergluons is

$$\rho_{\text{CMB-photons}} = N_{\text{CMB-photons}} / V_{\text{CMB}} = 407.1 \text{ per cubic centimetre} . \quad (3.5.20)$$

Outside the strong fields of baryons, the photon galaxies in the superphotons interacted electromagnetically not only with the bare electrons but also with their radiation masses so number of photon galaxies (photons) in CMB increased to

$$\begin{aligned} \rho^*_{\text{CMB-photons}} &= \rho_{\text{CMB-photons}} (1 + a_e)(\alpha_s + \alpha_{\text{em}}) / \alpha_s = \\ &= 410.6 \text{ per cubic centimetre} . \end{aligned} \quad (3.5.21)$$

3.6. The origin of CMB power spectrum

The temperature anisotropy in CMB follows from the atom-like structure of baryons which was excited by the inflows of the DM loops and by collisions of the NBHs.

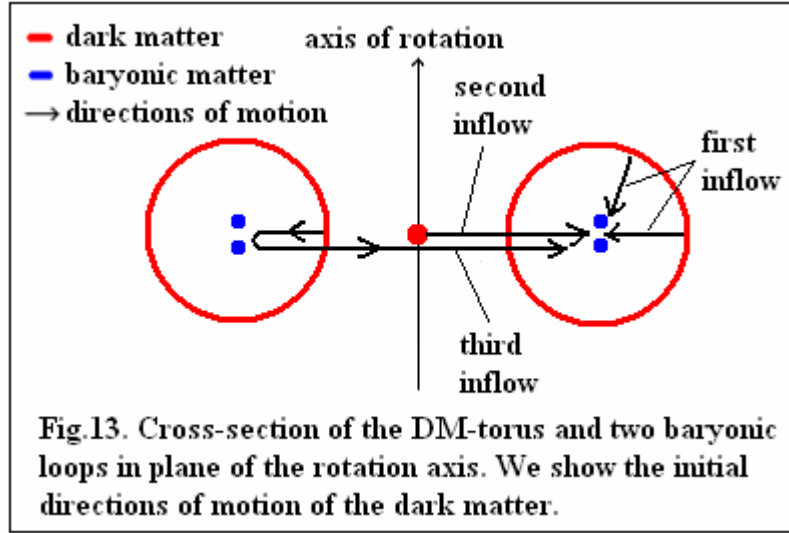
Due to the decay of the Protoworld, there were three succeeding inflows of DM into the baryonic matter (Fig.13).

The weak interactions of the virtual electron-positron pairs in presence of DM lead to the present-day mean anisotropy power, $T_{\text{a,mean}}^2$

$$T_{a,\text{mean}}^2 = (T_{\text{Universe}} \alpha'_{w(e),\text{DM}})^2 \approx (30.5 \mu\text{K})^2 \approx 931 \mu\text{K}^2, \quad (3.6.1)$$

where $T_{\text{Universe}} \approx 2.726 \text{ K}$ is the present-day temperature of the Universe [7], [11].

Initially, the baryonic matter consisted of the neutron black holes which are the cold objects, so there dominated the nuclear strong interactions at low energy. Initially, the inflow of DM was not intensive so the protons and neutrons interacted due to the exchanged fundamental gluon loops between pions in the $d = 1$ state. The coupling constant was $\alpha_s = \alpha_s^{\pi\pi,\text{FGL}} = 1$ (see formula (2.4.30)) and the created virtual gluon loops had the radius equal to $(A + B)$. Next there were the intensive inflows of the DM loops and creations of the alpha particles. Coupling constant for strongly interacting protons, at low energies (as it is in the atomic nuclei), is $\alpha_s^{\text{pp},\pi} = 14.391187$ (see formula (2.4.31)) whereas for strongly interacting neutrons is $\alpha_s^{\text{nn},\pi} = 14.410338$. To the alpha particle, we can apply the mean value $\alpha_s^{\text{NN},\pi} = 14.40076$.



Lifetimes are inversely proportional to coupling constants (see (1.4.29)) so we can divide the angular scale ($0^\circ - 90^\circ$) into two parts one related to the α_s (we denote it by $\Delta\phi_{\text{FGL}}$) and the second one related to the $\alpha_s^{\text{NN},\pi}$ (we denote it by $\Delta\phi_\pi$)

$$\Delta\phi_{\text{FGL}} = 90^\circ \alpha_s^{\text{NN},\pi} / (\alpha_s^{\text{NN},\pi} + \alpha_s) = 84.2^\circ \text{ i.e. } \phi \text{ from } 90^\circ \text{ to } 5.8^\circ. \quad (3.6.2)$$

The definition which ties angular scale with multipole momentum, l , looks as follows

$$l = 180^\circ / \phi, \quad (3.6.3)$$

so the SST plateau in CMB is from $l_{\text{pl,beginning}} = 2$ to

$$l_{\text{pl,end}} = 180^\circ / 5.8^\circ \approx 31. \quad (3.6.4)$$

We see that the SST plateau occupies almost whole angular scale so anisotropy power for the plateau should be only a little lower than the mean value. There is the largest triangle-like figure in Fig.14 so an excess in anisotropy temperature above the mean value is (see (3.6.8))

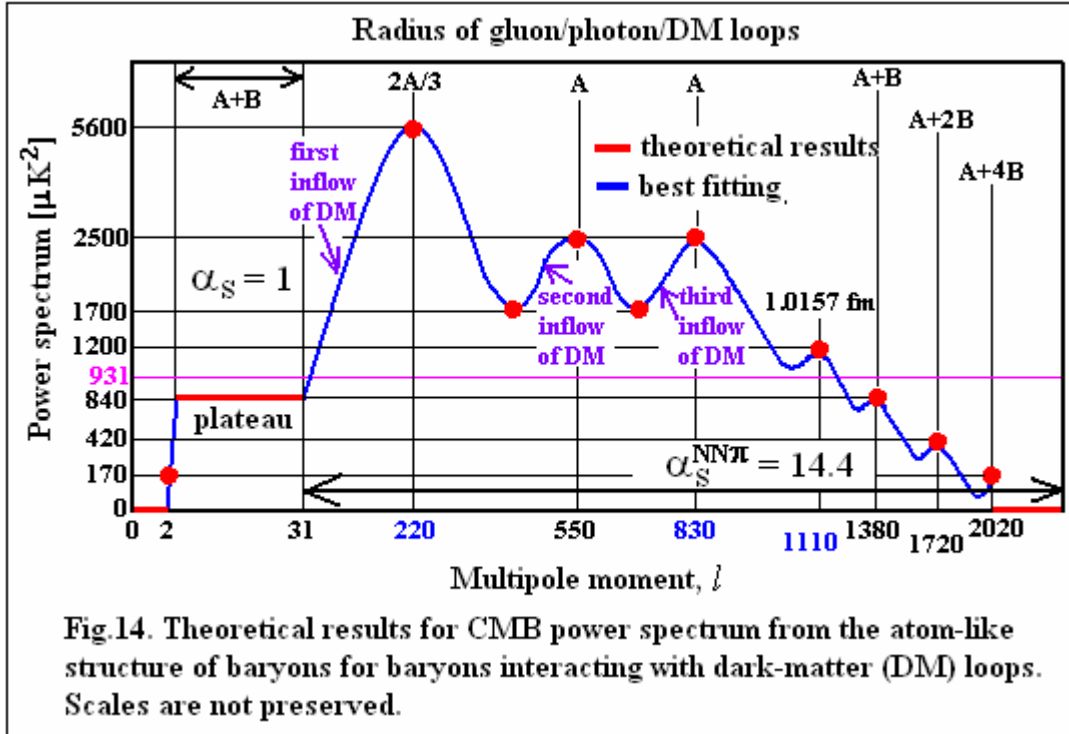
$$\Delta T \approx \{(5600^{1/2} - 931^{1/2}) / 2\} (5.8^\circ / 90^\circ) \approx 1.43 \mu\text{K}. \quad (3.6.5)$$

Such a value we must subtract from the mean anisotropy temperature so for the plateau we have

$$T_{\text{pl}}^2 = T_{\text{A+B}}^2 = (T_{\text{Universe}} \alpha'_{\text{w(e),DM}} - \Delta T)^2 \approx (29 \mu\text{K})^2 \approx 840 \mu\text{K}^2. \quad (3.6.6)$$

Emphasize that this value is for $R = A + B$.

Notice that similar results we obtain at high energies close to the rest mass of the Z^0 boson ($Q = Z^0$) for the electromagnetic interactions ($\alpha_{\text{em,high}} = 1 / 127.5425$ – see formula (2.3.15)) and the strong-weak interactions ($\alpha_{\text{sw,Q=Z}} = 0.11795$ – see Table 1). It follows from the fact that the ratio $\alpha_{\text{sw,Q=Z}} / \alpha_{\text{em,high}} = 15.0$ is close to the ratio $\alpha_s^{\text{NN},\pi} / \alpha_s = 14.4$. Value of the fine structure constant increases at high energies because of the increase in surface density of the torus/electric charge in the core of baryons forced by the nuclear weak interactions – in such processes, there locally increases the effective electric charge.



It is easy to calculate the anisotropy powers for the FGL and the TB orbits because from the Wien's displacement law (see (1.4.11)) results that temperature is inversely proportional to a peak radius R_{peak} which here is equal to one of the TB radii and to the radius of FGL. The curve should peak for following anisotropy powers

$$T^2 / T_{\text{pl}}^2 = \{(A + B) / R\}^2. \quad (3.6.7)$$

For the FGL is $R = 2A/3$ so we have

$$T_{\text{FGL}}^2 = T_{\text{pl}}^2 \{(A + B) / (2 A / 3)\}^2 \approx 5600 \mu\text{K}^2. \quad (3.6.8)$$

It is for the biggest peak that was created due to the first most intensive inflow of DM.
For $R = A$ is

$$T_{\text{FGL}}^2 = T_{\text{pl}}^2 \{(A + B) / A\}^2 \approx 2500 \mu\text{K}^2. \quad (3.6.9)$$

It is for the second and third peaks that were created due to the second and third less intensive inflows of DM. All the time the loops created in the distinguished states were scattered.

For $R = A + 2B$ is

$$T_{\text{A+2B}}^2 = T_{\text{pl}}^2 \{(A + B) / (A + 2B)\}^2 \approx 420 \mu\text{K}^2. \quad (3.6.10)$$

For $R = A + 4B$ is

$$T_{\text{A+4B}}^2 = T_{\text{pl}}^2 \{(A + B) / (A + 4B)\}^2 \approx 170 \mu\text{K}^2. \quad (3.6.11)$$

We can see that the fourth peak does not relate to any TB orbit. It follows from the fact that for such a peak the energy was distributed among several orbits. Consider the first four orbits

$$R_{\text{mean}} = \{2A/3 + A + (A + B) + (A + 2B)\} / 4 = 1.0157 \text{ fm}. \quad (3.6.12)$$

For $R = R_{\text{mean}}$ is

$$T_{\text{R-mean}}^2 = T_{\text{pl}}^2 \{(A + B) / R_{\text{mean}}\}^2 \approx 1200 \mu\text{K}^2. \quad (3.6.13)$$

During the scattering of loops from the $d = 0$ state (i.e. $R = A$) they first of all gather in distances equal to the muon radius of proton ($R_{\text{p}(\mu)} = 0.84039 \text{ fm}$ (see formula (2.19.7))). The anisotropy power for such distance is (it is a minimum)

$$T_{\text{R-p}(\mu)}^2 = T_{\text{pl}}^2 \{(A + B) / R_{\text{p}(\mu)}\}^2 \approx 1700 \mu\text{K}^2. \quad (3.6.14)$$

Calculate the increase in multipole moment per 1 MeV. Mass of the gluon loop in the $d = 0$ state (i.e. $R = A$) is $S_{(+0),d=0} \approx 727 \text{ MeV}$ – it relates to $l_A = 550$ while mass of the gluon loop in the $d = 4$ state (i.e. $R = A + 4B$) is $S_{(+0),d=4} \approx 187 \text{ MeV}$ – it relates to $l_{\text{A+4B}} = 2020$ so we have

$$F_{\Delta/\text{MeV}} = (2020 - 550) / (727 - 187) = 2.72 \Delta/\text{MeV}. \quad (3.6.15)$$

Mass of the gluon loop in $A + B$ is $S_{(+0),d=1} \approx 422 \text{ MeV}$ so we have

$$l_{\text{A+B}} = l_{\text{A+4B}} - (S_{(+0),d=1} - S_{(+0),d=4}) F_{\Delta/\text{MeV}} \approx 1380. \quad (3.6.16)$$

Mass of the gluon loop in $A + 2B$ is $S_{(+0),d=2} \approx 298 \text{ MeV}$ so we have

$$l_{\text{A+2B}} = l_{\text{A+4B}} - (S_{(+0),d=2} - S_{(+0),d=4}) F_{\Delta/\text{MeV}} \approx 1720. \quad (3.6.17)$$

Notice also that we should not observe anisotropy power for $l > l_{A+4B} = 2020$ because the **A+4B** is the last orbit – angular scale for the upper limit of l is

$$\varphi_{A+4B} = 180^\circ / l_{A+4B} = 0.0891^\circ . \quad (3.6.18)$$

The same is for following angular scales: $0 < \varphi < (90^\circ - \varphi_{A+4B})$, so we should have no anisotropy power for following multipole moments:

$$\text{for } 0 \leq l < \sim 2 \text{ is } T^2 = 0 . \quad (3.6.19)$$

Our results are in very good agreement with observational data [8].

3.7. Initial evolution of the expanding Universe

The initial state of the baryonic part of the Universe was the two cosmological loops with a radius $R_{\text{Cosmological}} = 0.191109 \text{ Gly}$ (the 2/3 of the equatorial radius of the core of the Protoworld (see (2.1.25))) both built of the NBHs which were the components of the protogalaxies. Collisions of the NBHs with DM and the mutual collisions of the NBHs caused that initially protogalaxies were embedded in a low-temperature baryonic-plasma ring (the NBHs are the cold objects). Such a ring, due to the nuclear strong interactions at low energy (the coupling constant for such interactions is $\alpha_S = 1$), had interacted with gluon loops that overlapped with the cosmological loops. It caused that the spin speed of the cosmological loops was close to c . So the period of rotation, $T_{\text{cosmological}}$, was

$$T_{\text{cosmological}} = 2 \pi R_{\text{Cosmological}} = 1.201 \text{ Gyr} . \quad (3.7.1)$$

The tidal locking (or a mutual spin-orbit resonance) of the Moon and the Earth caused that the rotation and revolution periods of the Moon are the same. Similar processes caused that the period of rotation of protogalaxies (so of the present-day massive galaxies as well) was (and still is) equal to the period of spinning of the two cosmological loops composed of the protogalaxies. Our exact result **1.201 Gyr** is close to the observational result $\sim 1 \text{ Gyr}$ [9].

Our Universe arose and developed as the double cosmic loop inside the torus of the core of the Protoworld. The magnetic axes of the neutrons in the cosmic structures were tangent to the double cosmic loop. Magnetic polarisation dominated because the neutrons are electrically neutral. The cosmic structures in the expanding Universe were mostly moving in radial directions. Due to the law of conservation of spin, the magnetic axes of the protogalaxies should be parallel or antiparallel to the direction of their acceleration. This means that there were the $\sim 90^\circ$ turns of the magnetic axes of the protogalaxies.

The dwarf galaxies appeared due to explosions of the protogalaxies.

The definition of the speed c leads to conclusion that we cannot see the initial period **7.53 Gyr** of the evolution of the protogalaxies. It causes that in the most distant visible Universe, we should not see a field composed only of dwarf galaxies.

3.8. The standard ruler in cosmology

The radius of the $d = 1$ state in the Protoworld is (there were produced photon loops and DM loops overlapping with this state)

$$R_{\text{ruler-in-cosmology}} = A_{\text{Protoworld}} + B_{\text{Protoworld}} = 151.13 \text{ Mpc} . \quad (3.8.1)$$

It causes that radius of baryonic loops interacting with such loops is the standard ruler in cosmology.

The analysis of the WMAP data (CMB) yielded $146.8 \pm 1.8 \text{ Mpc}$ for the sound horizon at the photon decoupling epoch and $153.3 \pm 2.0 \text{ Mpc}$ at the end of the baryon drag epoch [10].

3.9. Black body spectrum

Superphotons consist of $2 \cdot 4^{32}$ neutrino-antineutrino pairs and are produced as the gluon loops on the orbits in baryons. Their wavelengths depend on the internal temperature of the baryons/black-body. Via the Wien's law we can calculate the λ_T peak wavelength: $\lambda_T T = 2.897771955 \cdot 10^{-3} \text{ [m K]}$ – it is the 2018 CODATA value of the Wien's-wavelength-displacement-law constant numerically solved from Planck's law using Newton's method. Mostly such supergluons/superphotons transit from the $d = 0$ state (the equator) to the $d = 1$ state so the length of them increases to $2\pi(A + B)$ – emission is from the $d = 1$ state. From it we have

$$\lambda_T / \lambda_\nu = A / (A + B) = 0.5815520 , \quad (3.9.1)$$

where λ_T is a peak wavelength from the Wien's law, and λ_ν is a peak wavelength from the spectral radiance.

Using the central value of the today's temperature of the Universe from WMAP (2.7260(13) K [11]) we obtain $\lambda_T = 1.0630 \cdot 10^{-3} \text{ m}$, $\lambda_\nu = 1.8279 \cdot 10^{-3} \text{ m}$, and $\nu = 164.01 \text{ GHz}$.

We can calculate the λ_ν within the SST.

Outside the nuclear strong fields, the supergluons behave as superphotons and they decayed to the SST photon galaxies so length of them increased $N_1 = 2 \cdot 4^{16}$ times.

The superphotons were emitted, first of all, from surface of the initial ball which radius was equal to $A_{\text{Protoworld}} + B_{\text{Protoworld}} = 0.4929284 \text{ Gly}$. Radius of such surface increased to R_{CMB} , so length of the CMB photons increased additionally $N_2 = R_{\text{CMB}} / (A_{\text{Protoworld}} + B_{\text{Protoworld}}) = 43.252(20)$ times – accuracy of this value is limited by the measured energy density of CMB which is very low [4].

Assume that supergluons appear on the three orbits that lie below the Schwarzschild surface for the nuclear strong interactions, so the mean wavelength of the emitted supergluons was $\lambda_{\text{mean}} = 2 \pi \{2A/3 + A + (A + B)\} / 3 = 4.9462956 \text{ fm}$.

Notice also that first of all the superphotons produced the $\mu^+ \mu^-$ pairs that decayed to the electron-positron pairs. The ratio of anomalous magnetic moments a_μ/a_e is $N_3 = 1.0054062$, so energy of the superphotons increased a little so their wavelength decreased N_3 times.

For λ_ν we obtain

$$\lambda_\nu = \lambda_{\text{mean}} N_1 N_2 / N_3 = 1.8278(9) \cdot 10^{-3} \text{ m} . \quad (3.9.2)$$

Due to the different weak interactions of muons and electrons and the decays of the $\mu^+ \mu^-$ pairs into the electron-positron pairs, we should observe an excess in quanta with energy equal to

$$E_{\text{predicted}} = m_e (N_3 - 1) = 2.7626 \text{ keV} . \quad (3.9.3)$$

3.10. The hydrogen-to-helium-4 ratio in the expanding Universe

Due to evolution of the Universe, hydrogen transforms into helium whereas helium transforms into more massive atomic nuclei. It suggests that it can be that with time mass abundance of helium in relation to hydrogen can slowly decrease – it should not increase as it is assumed in the mainstream cosmology.

We use in this Section the Stefan-Boltzmann law which is derived within SST (see formula (1.4.20)). Assume that due to the big stars, a change in abundance of helium-4 (He-4), ΔP_{He} [%], is directly proportional to the temperature T (higher temperature means higher changes in abundance) whereas that total emitted energy is directly proportional to age of the Universe, τ_{Universe} [Gyr]. Then, we have

$$\Delta P_{\text{He}} [\%] = f (\tau_{\text{Universe}} [\text{Gyr}])^{1/4}. \quad (3.10.1)$$

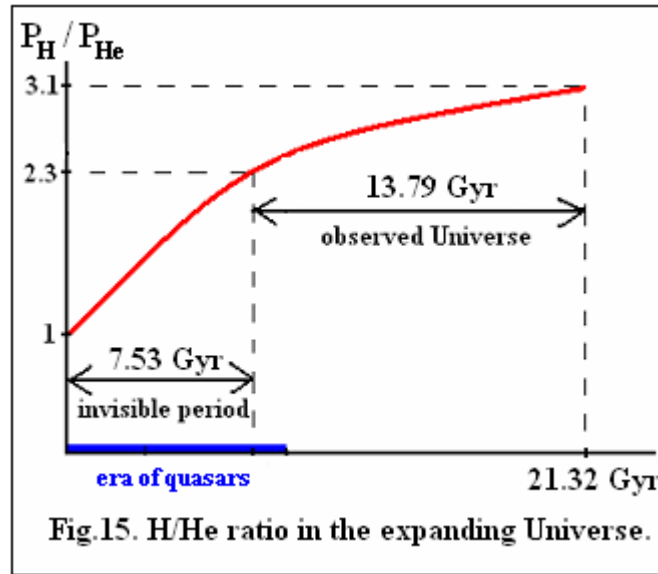


Fig.15. H/He ratio in the expanding Universe.

The resultant abundance of helium-4 is

$$P_{\text{He}} = P_{\text{initial,He}} - \Delta P_{\text{He}} [\%] = P_{\text{initial,He}} - f (\tau_{\text{Universe}} [\text{Gyr}])^{1/4}, \quad (3.10.2)$$

where $P_{\text{initial,He}} = 50\%$ is the primordial mass abundance of helium. On the assumption that the today abundances of helium-4 and hydrogen are respectively 24.5% and 75.5%, we obtain that the factor f is equal to $f = 11.87$.

From (3.10.2) we have that abundance of helium-4 in most distant observed Universe (i.e. $\tau_{\text{Universe-distant}} [\text{Gyr}] = 7.53$) should be 30.3% so abundance of hydrogen should be about $50\% + (50\% - 30.3\%) = 69.7\%$, so the ratio $P_{\text{H}}/P_{\text{He}} = 2.3$. The SST results are collected in Fig.15.

Above surfaces of the neutron stars and in the symmetrical decays of nuclei in the supernova explosions there appear protons so in such regions, with time, abundance of hydrogen increases.

3.11. Summary

The creation of the Protoworld and the expansion of the Universe were separated in time from the SST inflation that created the inner Cosmos.

The initial Universe was highly anisotropic because there were two baryonic loops and a rotating dark-matter torus. Protuberances inside and on the front of the early expanding Universe and the anisotropic inflows of the dark energy and dark matter into the baryonic part of the Universe caused that anisotropies of some regions of the Universe are higher. Only the creation of new neutrino (it took over most of the Protoworld rotational energy) and the damping of protuberances by a fairly symmetrical expansion of dark energy partially reduced the anisotropy.

The Universe is practically flat because the density of the isotropic SST absolute spacetime exceeds by many orders of magnitude the average density of matter and dark energy.

The Universe is 21.32(1) **Gyr** old, not 13.8 **Gyr**. We cannot see the initial period 7.53 **Gyr** of evolution of protogalaxies. We should observe the massive galaxies and quasars with supermassive black hole in their centre already in the most distant visible Universe.

Due to the different weak interactions of muons and electrons and the decays of the $\mu^+\mu^-$ pairs into the electron-positron pairs, we should observe an excess in quanta with energy equal to 2.76 **keV** (see Sections 3.9).

3.12. Tables

Table 14 *Inner Cosmos*

Cosmological quantity	Theoretical value*
Inertial-mass density of the initial inflation field	8.32192 E+85 kg/m ³
Radius of the inner Cosmos	2.3 E+30 m
Mass of the SST spacetime	5.9 E+119 kg

*2.3 E+30 = 2.3·10³⁰

Table 15 *Protoworld and early Universe*

Cosmological quantity	Theoretical value
Mass of the core of the Protoworld \approx \approx mass of the dark matter	1.96076 E+52 kg
Equatorial radius of the core of the Protoworld	0.2866635 Gly
Radius of the standard ruler in cosmology	151.13 Mpc
Mass of baryonic matter	0.36379 E+51 kg
Radius of the initial baryon-matter loops	0.191109 Gyr
Mass of protogalaxy	1.0656 E+11 solar masses
Mass of neutron black hole (NBH)	4.933 E+31 kg i.e. about 24.81 solar masses
Radius of NBH	3.664 E+4 m

Table 16 *Universe*

Cosmological quantity	Theoretical value
Present-day abundance of baryonic matter	4.91 %
Present-day abundance of dark matter	26.46 %
Present-day abundance of dark energy	68.63 %
λ_T / λ_v for black body	0.5815520
λ_v	1.8278(9) E-3
Radius of the CMB sphere	21.32(1) Gly
Age of the Universe	21.32(1) Gyr
Time distance to the observed front of the sphere filled with BM, DM and DE	13.79(1) Gyr
Time Hubble constant	$70.90 \pm 3.1 \text{ km}\cdot\text{s}^{-1}\cdot\text{Mps}^{-1}$
Spatial Hubble constant	$45.86 \text{ km}\cdot\text{s}^{-1}\cdot\text{Mps}^{-1}$
Mean anisotropy power	$931 \mu\text{K}^2$
Amplitude of the CMB temperature fluctuations	1.119446 E-5
Number of photon galaxies (photons) in cubic centimetre of CMB	410.6

References

- [1] H. S. Murdoch (14 October 1976). "Recession Velocities Greater than Light" *Q. Jl R. astr. Soc.* (1977) **18**, 242-247
- [2] James M. Lattimer (28 June 2019). "Neutron Star Mass and Radius Measurements" *Universe* **2019**, 5, 159
Doi:10.3390/universe5070159
- [3] sjsu.edu/faculty/Watkins/He4nuclide.htm
- [4] P. A. Zyla, *et al.* (Particle Data Group). "2. Astrophysical Constants and Parameters" *Prog. Theor. Exp. Phys.* **2020**, 083C01 (2020) 25th August, 2020
- [5] David R. Soderblom (31 March 2010). "The Ages of Stars" [arXiv:1003.6074v1](https://arxiv.org/abs/1003.6074v1) [astro-ph.SR]
- [6] Ludwig H-G, *et al.* (2009)
Astron. Astro-phys., in press
- [7] C. Patrignani *et al.* (Particle Data Group), *Chin. Phys. C*, **40**, 100001 (2016) and 2017 update, December 1, 2017
- [8] Planck Collaboration (15 September 2020). "Planck 2018 results. V. CMB power spectra and likelihoods" [arXiv:1907.12875v2](https://arxiv.org/abs/1907.12875v2) [astro-ph.CO]
- [9] Gerhardt R Meurer, *et al.* (9 March 2018). "Cosmic clocks: a tight radius-velocity relationship for HI-selected galaxies" *MNRAS*, Volume 476, Issue 2, May 2018, Pages 1624-1636
[arXiv:1803.04716](https://arxiv.org/abs/1803.04716) [astro-ph.GA]
- [10] E. Komatsu *et al.* (2009). "Five-Year Wilkinson Microwave Anisotropy Probe Observations: Cosmological Interpretation" *ApJS*, **180**, 330-376
- [11] D. J. Fixen (30 November 2009). "The Temperature of the Cosmic Microwave Background" *ApJ* **707** 916 (2009)
- [12] Wendy L. Freedman (29 June 2021). "Measurements of the Hubble Constant: Tensions in Perspective" [arXiv:2106.15656](https://arxiv.org/abs/2106.15656) [astro-ph.CO]; accepted to the *Astrophysical Journal*, 23 June 2021

Chapter 4

Applications**A. Atomic physics****A1. Derivation of the Pauli Exclusion Principle**

In general, the Pauli Exclusion Principle follows from the spectroscopy whereas its origin is not good understood. To understand fully this principle, most important is the origin of quantization of the azimuthal quantum number i.e. of the angular momentum quantum number. Here, applying the theory of ellipse and starting from very simple physical condition, we quantized the azimuthal quantum number. The presented model leads directly to the eigenvalue of the square of angular momentum and to the additional potential energy that appears in the equation for the modified wave function.

The Pauli Exclusion Principle says that no two identical half-integer-spin fermions may occupy the same quantum state simultaneously. For example, no two electrons in an atom can have the same four quantum numbers. They are the principal quantum number n that denotes the number of the de Broglie-wave lengths λ in a quantum state, the azimuthal quantum number l (i.e. the angular momentum quantum number), the magnetic quantum number m and the spin s .

On the base of the spectrums of atoms, placed in magnetic field as well, follows that the quantum numbers take the values:

$$n = 1, 2, 3, \dots$$

$$l = 0, 1, 2, \dots, n - 1$$

$$m = -l, \dots, +l$$

$$s = \pm 1 / 2.$$

The three first quantum numbers n , l , and m are the integer numbers and define a state in which can be maximum two electrons with opposite spins.

The magnetic quantum number m determines the projection of the azimuthal quantum number l on the arbitrary chosen axis. This axis can overlap with a diameter of the circle $l = 0$.

To understand fully the Pauli Exclusion Principle we must answer following questions concerning the azimuthal quantum number l :

1.
What is physical meaning of this quantum number?
2.
Why the l numbers are the natural numbers only?
3.
Why the zero is the lower limit?
4.
Why the $n - 1$ is the upper limit?

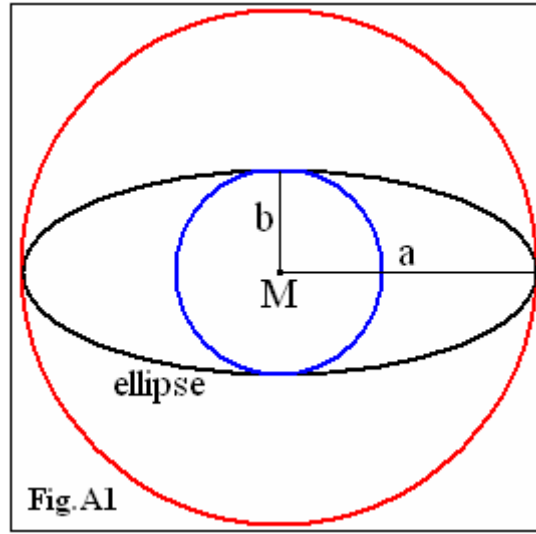
To answer these questions we must apply the theory of ellipse, especially the formula for its circumference C and eccentricity e . When we use the complete elliptic integral of the second kind and the Carlson symmetric form [1], we obtain for circumference C of an ellipse following formula

$$C = 2\pi a \left[1 - \frac{1}{2}e^2 + \frac{1}{8}(1-3e^2)^2e^4 - \frac{1}{16}(1-3e^2)(1-5e^2)^2e^6 + \dots \right], \quad (\text{A1.1})$$

where a is the major radius and e is the eccentricity defined as follows

$$e = (a^2 - b^2)^{1/2} / a, \quad (\text{A1.2})$$

where b is the minor radius.



In the Fig.A1, the circumference of the ellipse $C_{de-Broglie}$ is $C_{de-Broglie} = n \lambda = 2 \pi n \hat{\lambda}$, where the n is the principal quantum number whereas the $\hat{\lambda}$ is the reduced de Broglie-wavelength. Assume that there are allowed only ellipses that circumference is the arithmetic mean of the circumferences of two circles that radii are equal to the major and minor radii of the ellipse.

Similarly as for the circumference of the ellipse, the circumferences of the circles must be equal to a natural number multiplied by the de Broglie-wave length. This leads to following definitions

$$a = j \hat{\lambda} \text{ and } b = k \hat{\lambda}. \quad (\text{A1.3})$$

Notice that $j = k = 0$ has no sense.

Then, we can rewrite formula (A1.2) as follows

$$e = (j^2 - k^2)^{1/2} / j. \quad (\text{A1.4})$$

It is the natural assumption that the allowed circumferences of the ellipse should be the arithmetic mean of the sum of the circumferences of the two circles. It leads to following conclusion

$$(j + k) / 2 = n . \quad (\text{A1.5})$$

Define some number l as follows

$$(j - k) / 2 = l . \quad (\text{A1.6})$$

Formulae (A1.5) and (A1.6) lead to following relations

$$j = n + l , \quad (\text{A1.7})$$

$$k = n - l . \quad (\text{A1.8})$$

Since the j , k and n are the integers so the number l must be an integer as well. Applying formulae (A1.7) and (A1.8) we can rewrite formula (A1.4) as follows

$$e = 2 (n l)^{1/2} / (n + l) . \quad (\text{A1.9})$$

We can see that due to the square root, this formula has no real sense for $l < 0$. Since the l cannot be negative then from formulae (A1.5) and (A1.6) we have $l < n$.

Applying formulae (A1.3) and (A1.7), we can rewrite formula (A1.1) as follows

$$C_K = 2\pi(n + l)\lambda[1 - (1/2)^2 e^2/1 - (1 \cdot 3/(2 \cdot 4))^2 e^4/3 - (1 \cdot 3 \cdot 5/(2 \cdot 4 \cdot 6))^2 e^6/5 - \dots] . \quad (\text{A1.10})$$

Notice that for $n = l$ is $e = 1$ and then $C_{de-Broglie} > C_K$ i.e. l cannot be equal to n . For $l = 0$ is $C_{de-Broglie} = C_K$ and because l cannot be negative then the $l = 0$ is the lower limit for l .

Some recapitulation is as follows. We proved that the azimuthal quantum number l

- 1) is associated with transitions between the states j and k ,
- 2) is the integer,
- 3) cannot be negative and the lower limit is zero,
- 4) the $n - 1$ is the upper limit.

Some abbreviation of it is as follows

$$l = 0, 1, 2, \dots, n - 1.$$

The Quantum Physics is timeless because a quantum particle disappears in one region of a field or spacetime and appears in another one, and so on. There are no trajectories of individual quantum particles. Quantum Physics concerns the statistical shapes and their allowed orientations. Such procedure simplifies considerably the Quantum Physics.

An ellipse/electron-state we can resolve into two circles that radii are defined by the semi-axes of the ellipse. The two circles in a pair are entangled due to the exchanges of the binary systems of the closed strings (entanglons) the SST-As components (from which are built all the Principle-of-Equivalence particles) consist of. The spin-1 entanglons are responsible for the infinitesimal transformations that lead to the commutators. Calculate a change in the azimuthal quantum number l when the smaller circle or one of identical two circles emits one entanglon (since in this paper is $j \geq k$ so there is the transition $k \rightarrow k - 1$) whereas the second circle in the pair almost simultaneously absorbs the emitted entanglon (there is the transition $j \rightarrow j + 1$). Such transition causes that ratio of the major radius to the minor radius of the ellipse (or circle) increases. From formula (A1.5) follows that such emission-absorption does

not change the principal quantum number n whereas from formula (A1.6) follows that there is following transition for the azimuthal quantum number l : $l \rightarrow l + 1$. The geometric mean is $(l(l+1))^{1/2}$ and this expression multiplied by \hbar is the mean angular momentum L for the described transition. This leads to conclusion that eigenvalue of the square of angular momentum L^2 is $l(l+1)\hbar^2$.

The eigenvalue of the square of angular momentum leads to the additional potential energy E_A (it follows from the radial transitions i.e. from the changes in shape of the ellipses) equal to

$$E_A = L^2 / (2 m r^2) = l(l+1) \hbar^2 / (2 m r^2). \quad (\text{A1.11})$$

The energy E_A appears in the equation for the modified wave function.

The SST shows that inside the baryons are only the $l = 0$ states (i.e. there are only the circles) so the quantum mechanics describing baryons is much simpler than for atoms.

References

- [1] Carlson, B. C. (1995). "Computation of real or complex elliptic integrals"
Numerical Algorithms **10**: 13-26. arXiv:math/9409227

A2. Meaning simplification of the Dirac theory of the hydrogen atom

We showed that the Lamb shift follows from the fact that the charged relativistic pion in proton interacts due to the nuclear weak interactions while the electron interacts due to the electromagnetic and weak interactions in presence of dark matter (see Section 2.17).

We showed that the hyperfine splitting in the ground state of hydrogen (it leads to the ~21 cm line) follows from different binding energies of two vortices/spinning-tori (see Application A3). When spins are parallel but their directions does not overlap (it is in hydrogen atom) then the singlet state (spin = 0) has lower energy because binding energy is higher.

The Schrödinger equation with a Coulomb potential leads to the Bohr hydrogen atom. Here we show that the Dirac-Sommerfeld fine structure of hydrogen atom is a result of creations and exchanges of the virtual electron-positron pairs. Moreover, it is associated also with the fact that the atom-like structure of proton leads to an effective value of the base of the natural logarithm $e_{\text{eff}} = 2.66666\dots$

The fermions consist, at least for period of spinning, of the stable/classical structures/bare-fermions plus the quantum fields, so the semiclassical theories are simplest, most fruitful and contain least parameters. And such method is not a mathematical trick – just in such a way behaves Nature. We formulated a very simple semiclassical analog to the Dirac and Sommerfeld theories of the hydrogen atom.

Gravity is associated with the inverse square law. It is because gravitational fields are the gradients produced by masses in the superluminal SST Higgs field. There are the divergently moving classical tachyons so there appears the inverse square law

$$F \sim 1 / R^2. \quad (\text{A2.1})$$

Today, in the Higgs field cannot be created any virtual pairs as it is in the SST absolute spacetime. Polarisation and distribution of the virtual pairs in a field ψ composed of the SST-As components causes that such a field is defined by following function

$$\psi = \psi_0 \exp^{-R}, \quad (\text{A2.2})$$

where $\exp \approx 2.718\dots$ is close to the base of the natural logarithm. In reality, this formula is more complicated for $R \rightarrow 0$ because there appears a torus/charge/spin and central condensate.

We claim that the atom-like structure of baryons leads to an effective value, e_{eff} , of the base of the natural logarithm. We can define it as the sum of the inverses of the relative distances between the TB orbits in the baryons (it defines a slope of the field ψ in proton). There are the four TB orbits for the nuclear strong interactions – the relative distances between them are 1, 1 and 2. But there is also one photonic TB orbit outside the nuclear strong field. Outside such field, the virtual FGL behaves as virtual photon loop which can create one or two virtual electron-positron pairs – when spin of the pair is zero then there is created one pair while is equal to 1 then to conserve spin of the virtual photon loop there are created two virtual pairs with antiparallel spins. The range of the FGL due to its circumference is $2\pi(2A/3)$, but due to its energy, when we subtract energies of the created virtual pairs (their mean energy is $3m_{e,\text{bare}}$) is very close to $A + 10B$ (precisely, because the range of the M_{TB} is B , there instead the 10 is 9.889 for one pair and 10.065 for two pairs, so the mean is $9.977 \approx 10$). We see that the relative distance of the photonic orbit from the $d = 4$ TB orbit is very close to 6. So we have for baryons the series $1, 1, 2, 6 = 0!, 1!, 2!, 3!$ (there is $1, 1, 2, 5.977$) which leads to following effective value for the base of the natural logarithm for baryons (it is for a mixture of the strong and electromagnetic interactions)

$$e_{\text{eff}} = 1 / 0! + 1 / 1! + 1 / 2! + 1 / 5.977 = 2.667 \approx$$

$$\approx 8 / 3 = 1 / (1 - 1 / 2 - 1 / 8). \quad (\text{A2.3})$$

Define a following factor associated with the internal structure of proton

$$F_{\text{SST}} = 1 / e_{\text{eff}} \approx 0.375. \quad (\text{A2.4})$$

Can we quantize the value F_{SST} , i.e. can we write an expression that leads to F_{SST} ? Such expression is showed in (A2.3)

$$F_{\text{SST}} = (1 - 1 / 2 - 1 / 8) = 0.375. \quad (\text{A2.5})$$

Such expression quantizes the factors (1, 1/2, and 1/8) that can appear in formula for energy of the proton-electron system. Formula (A2.5) suggests as well that we should expand energy into a series because of the interactions via the exchanged virtual pairs. Such virtual pairs produce the holes in SST-As so their masses are negative – it leads to conclusion that the electromagnetic interactions via the virtual pairs must be associated with the second and third factor. With the second factor are associated two virtual electron-positron pairs (one from H^+ and one from electron). Radiation mass can create the second virtual pair so with the third factor are associated four virtual pairs (two from H^+ and two from electron).

In SST, the electromagnetic mass/energy of a mass/energy E is defined as

$$E_{\text{em}} = \alpha_{\text{em}} E, \quad (\text{A2.6})$$

where α_{em} is the fine structure constant.

The succeeding k interactions of virtual pairs (in a group of them) with some energy decrease the initial energy the α_{em}^k times.

Energy associated with a loop is inversely proportional to length of wave which is directly proportional to the principal quantum number n : $E \sim 1 / \lambda \sim 1 / n$. It leads to conclusion that each virtual electron-positron pair produced in state defined by n decreases energy (α_{em} / n) times.

The above remarks lead to following formula for hydrogen atom

$$E = m c^2 [1 - (\alpha_{em} / n)^2 / 2 - (\alpha_{em} / n)^4 / 8], \quad (A2.7)$$

where $m c^2 = 0.5109989 \text{ MeV}$ is the mass of electron.

Notice that for the transition from the electromagnetic interactions to the strong interactions at low energy ($\alpha_{em} \rightarrow \alpha_s = 1$) in the ground state ($n = 1$), the expression in parenthesis transforms into (A2.5).

The second component

$$E_{B,n} = -m c^2 (\alpha_{em} / n)^2 / 2 \quad (A2.8)$$

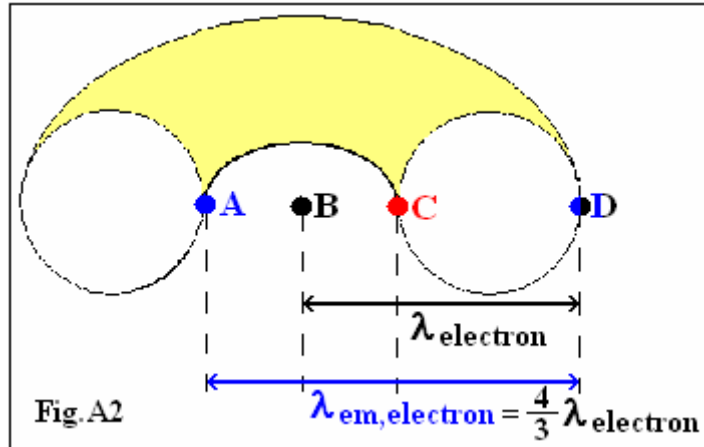
is equal to the energies of the Bohr orbits in the hydrogen atom and $E_{B,n=1} = -13.606 \text{ eV}$.

The third component is the fine structure energy

$$E_{FS,n} = -m c^2 (\alpha_{em} / n)^4 / 8. \quad (A2.9)$$

This component depends on classical and quantum structure of electron so we must write it in such a way to interpret it correctly. Write the factor $1/8$ as follows

$$1 / 8 = (1 - 3 / 4) / 2. \quad (A2.10)$$



The $3/4$ represents the classical mass of electron (see Fig.A2) which relates to the $\lambda_{em,electron}$ (the points A and D are in the same state) while the quantum mass of electron relates to $\lambda_{electron}$.

We know that maximum azimuthal quantum number l is $l_{max} = n - 1$ so $n / (l_{max} + 1) = 1$. This means that we can rewrite formula (A2.10) as follows

$$1 / 8 = [n / (l_{max} + 1) - 3 / 4] / 2 . \quad (\text{A2.11})$$

The n and $(l_{max} + 1)$ define the lengths of the de Broglie waves but the additional potential energy $E_A = l(l + 1) \hbar^2 / (2 m r^2)$ (see (A1.11)) suggests that for defined n there can appear spontaneously as well the other standing waves defined by $l + 1$. For smaller l , waves are shorter so corresponding absolute energy is greater. Since in formula (A2.9) is the sign “– “ so the levels defined by smaller and smaller l are closer and closer to the ground state $n = 1$. Finally, we can rewrite formula (A2.9) as follows

$$E_{FS,n} = -m c^2 (\alpha_{em} / n)^4 [n / (l + 1) - 3 / 4] / 2 . \quad (\text{A2.12})$$

The ground state is shifted by $E_{FS,n=1} = -m c^2 \alpha_{em}^4 [1 - 3 / 4] / 2 = -1.81 \cdot 10^{-4} \text{ eV}$.

Calculate the energy distance between the states $l = 0, 1$ for defined n

$$\Delta E_{FS,n} = -m c^2 (\alpha_{em} / n)^4 (n / 2) / 2 . \quad (\text{A2.13})$$

For $n = 2$ is $\Delta E_{FS,n=2} = -m c^2 (\alpha_{em} / 2)^4 (1) / 2 = -m c^2 \alpha_{em}^4 / 32 = -4.53 \cdot 10^{-5} \text{ eV}$.

Why we obtained results the same as in the Sommerfeld theory [1]? Why we obtained results the same as in the Dirac theory [2] neglecting the relativistic effects, the spin-orbit interactions, and so on?

It is due to the applied methods – just the standing waves defined by the quantum numbers cannot be changed by any phenomena. Just the quantum numbers define the total picture and must be conserved. The three theories are equivalent because the numbers n_θ in the Sommerfeld theory, $j + 1/2$ in the Dirac theory (the j is not the j in the last two Sections) and $l + 1$ in presented here theory, are the integers and change from 1 to n . But only presented here theory of hydrogen atom proves equivalence of the three theories and describes in all respects the physical origin of the final equation.

References

- [1] A. Sommerfeld (1916), *Ann. Physik*, **51**, 1
- [2] P. A. M. Dirac (1928), *Proc. Roy. Soc.*, **A117**, 610 (London)

A3. Frequency of the hydrogen spin-flip transition and the Bohr radius

Understanding the spin-flip mechanism in hydrogen was the most difficult, but it allowed us to better understand the electroweak interactions, especially the weak interactions of baryon matter with dark matter.

The parallel polarisation of two vortices on the same plane decreases the binding energy of a system

$$E_{\text{par}} = E - \Delta E_i , \quad (\text{A3.1})$$

whereas the antiparallel polarisation increases the binding energy

$$E_{\text{ant}} = E + \Delta E_i . \quad (\text{A3.2})$$

Since $\Delta E_i = \alpha_i c \hbar / r$ (it follows from the definition of the coupling constants – see (2.4.23), and there is $\Delta E_i = G_i M_i m_i / r$) so the change of the mutual orientation of spins causes that the emitted energy is

$$E_i = 2 \alpha_i c \hbar / r = h \nu , \quad (\text{A3.3})$$

and therefore

$$\nu = \alpha_i c / (\pi r) , \quad (\text{A3.4})$$

where ν denotes the frequency.

The mechanism is as follows. Assume that the virtual bare electron-positron pairs are created especially at distance $R_B/(2\pi)$ from the Bohr orbit, where $R_B = 5.29177210903(80) \cdot 10^{-11} \text{ m}$ is the Particle-Data-Group (PDG) experimental value of the Bohr radius [1] (i.e., there is a radius-circle transition what creates holes in the SST-As), and next they transit to the edge of the field composed of the virtual charged bosons produced in the nuclear strong field. Range is inversely proportional to mass of particle so we should take into account the lightest electrically charged boson – from Table 2 follows that it is the boson $W_{(+),d=4} \approx 162.01257 \text{ MeV}$. Such virtual bosons can be emitted from the $d = 0$ state (its radius is $R_{d=0} = A + r_{C(p)}$). Knowing that range of the $M_{TB} \approx 750.2977 \text{ MeV}$ is $B \approx 0.50183544 \text{ fm}$, we obtain

$$R_{W(+)} = R_{d=0} + B M_{TB} / W_{(+),d=4} = 3.03020162200159 \text{ fm} . \quad (\text{A3.5})$$

On the other hand, dark matter interacts weakly via the virtual bare electron-positron pairs with the real electron on the Bohr orbit and via the real electron with the proton, so we have (the two interactions occur one after the other, so we have the product of coupling constants)

$$\alpha_i = \alpha'_{w(e),DM}{}^2 . \quad (\text{A3.6})$$

Formula for frequency of emitted photon during the transition from the spin-1 state of the hydrogen atom to the spin-0 state is

$$\begin{aligned} \nu_{\text{flip}} &= \alpha'_{w(e),DM}{}^2 c / [\pi \{R_B/(2\pi) - R_{W(+)}\}] = \\ &= 1420.405476 \text{ MHz} . \end{aligned} \quad (\text{A3.7})$$

The SST value in (A3.7) is very close to the experimental result: 1420.4057517667(9) MHz [2].

The Bohr radius

The non-relativistic classical formula for the Bohr radius leads to

$$R_{B,\text{classical}} = \hbar / (F m_e c \alpha_{em}) = 5.29177215048007 \cdot 10^{-11} \text{ m} . \quad (\text{A3.8})$$

This value differs a little from the PDG value and in formula (A3.8) should appear the relativistic mass of the electron. It leads to a conclusion that there should be some corrections,

i.e. some additional phenomena. Corrections are needed to obtain the correct value for the frequency of the spin-flip.

Our definition of the Bohr radius looks as follows

$$R_{B,SST} = \hbar / (F m_{e,rel} c \alpha_i), \quad (A3.9)$$

where $Fm_{e,rel}$ is the relativistic mass of the electron in **kg** (i.e. $m_{e,rel} = m_e / (1 - \alpha_i^2)^{1/2}$), and $v_B = c\alpha_i$ is the orbital speed of the electron.

Notice that coupling is directly proportional to energy so the two first corrections are defined by formula (A2.7), i.e. they appear in the theory of hydrogen atom. But there should be also a third correction which is independent from the proton-electron interactions. Just the Y spacetime condensate produces the virtual $2(e^+e^-)_{virtual}$ quadrupoles. The components of each such quadrupole transit to the Bohr orbit. There appears a cascade of 4 electromagnetic interactions and the circular motions of the components transit into oscillations along the diameter of the Bohr orbit – it causes that the coupling increases π times, so we have $+\pi\alpha_{em}^4$. The resultant coupling is (see (A2.7) plus the third correction)

$$\alpha_i = \alpha_{em} [1 - \alpha_{em}^2 / 2 + (\pi - 1 / 8) \alpha_{em}^4] = 1 / 137.039646686156. \quad (A3.10)$$

The relativistic mass of the electron on the Bohr orbit is

$$m_{e,rel} = m_e / (1 - \alpha_i^2)^{1/2} = 0.511012551512095 \text{ MeV}, \quad (A3.11)$$

or

$$F m_{e,rel} = 9.10962617054279 \cdot 10^{-31} \text{ kg}. \quad (A3.12)$$

The relativistic speed on the Bohr orbit is

$$v_B = c \alpha_i = 2.1876330335747 \cdot 10^6 \text{ m/s}. \quad (A3.13)$$

From formulae (A3.9), (A3.12) and (A3.13) we have

$$R_{B,SST} = 5.29177211083714 \cdot 10^{-11} \text{ m}. \quad (A3.14)$$

From formulae (A3.7) and (A3.14) we have

$$\begin{aligned} v_{flip,SST} &= \alpha'_{w(e),DM}{}^2 c / [\pi \{R_{B,SST}/(2\pi) - R_{W(+)}\}] = \\ &= 1420.4054757 \text{ MHz}. \end{aligned} \quad (A3.15)$$

Notice that

$$F m_{e,rel} v_B R_{B,SST} = \hbar. \quad (A3.16)$$

But for the Bohr orbit is $l = 0$, i.e. the external electron very frequently changes direction of motion.

Most important is the fact that we calculated the spin-flip frequency by applying the theory of the hydrogen atom and the internal structure of the proton described in SST.

References

- [1] P. A. Zyla, *et al.* (Particle Data Group)
Prog. Theor. Exp. Phys. **2020**, 083C01 (2020) and 2021 update
- [2] B. Juhász, *et al.* (2011). “Measurement of the ground-state hyperfine splitting of antihydrogen”
Journal of Physics: Conference Series **335** (2011) 012059
doi:10.1088/1742-6596/335/1/012059

B. Superconductivity

B1. The three phonon fields in superconductors

The Scale-Symmetric Theory (SST) shows that the internal dynamics of the core of proton leads to superconductivity. The first, second and third phonon fields are created due to the electroweak interactions of the oscillation masses, radiation masses and masses of the electron-positron pairs, respectively. The composite phonons (they are the entangled spacetime condensates) are responsible for creation of both the spin-0 Cooper pairs and boson condensate composed of the Cooper pairs. We calculated that at atmospheric pressure, critical temperature of the Type II superconductors can be from 4.4 K up to 148 K. We calculated also that at extreme pressure, for relative volume equal to 0.67, critical temperature is 304 K. We show that it is impossible to make a material that is a superconductor at room-temperature and atmospheric pressure.

Superconductivity is a flow of a condensate of electron pairs (the Cooper pairs) without electrical resistance.

Our model of the superconductivity is as follows. In surroundings of the core of proton, the electroweak interactions of the oscillation masses, radiation masses and masses of the electron-positron pairs (and their associations due to the quantum entanglement) create the composite phonons which are the entangled condensates of the SST-As components. Such composite phonons are exchanged between the electrons in the spin-0 Cooper pair (it defines the binding energy) – such is the origin of the attractive interactions among electrons in the Cooper pairs. The composite phonons are exchanged also between the Cooper pairs so there is created a boson condensate composed of the Cooper pairs – it is the critical field responsible for superconductivity. In the Type I superconductors, there is the phonon field produced by both the oscillation masses and radiation masses, while in the Type II superconductors, there are the three phonon fields. Size of the Cooper pairs (here it is also the SST coherence length ξ_{SST}) is inversely proportional to the phonon energy. Different values for the coherence length result from different energies of the composite phonons. In superconductors, at higher intrinsic pressure (it depends on internal structures of the atomic nuclei and lattice of a superconductor as a whole), the composite phonons contain more the elementary phonons (more the entangled elementary condensates). Good superconductors are substances in which the number density of the created electron-positron pairs is relatively high – then the intrinsic pressure is higher so the boson condensate of the Cooper pairs is very stable. Moreover, in superconductor lattice, vibrational energies of the atomic nuclei increase with increasing intrinsic pressure – it validates the BCS theory.

Dependence of critical temperature on coherence length

From experimental data for the chemical elements at atmospheric pressure, we obtain our best fit dependence of critical temperature, $T_{c,SST}$ [K], on coherence length ξ_{SST} [nm]

$$T_{c,SST} = a / \xi_{SST}^b, \quad (B1.1)$$

where $a = 73.7$, and $b = 0.561$.

For Al is $\xi_{o,Al,Exp.} = 1600$ nm [1] so from (B1.1) we obtain $T_{c,SST,Al} = 1.175$ K – it is consistent with experimental data [2].

For Sn is $\xi_{o,Sn,Exp.} = 230$ nm [1] so from (B1.1) we obtain $T_{c,SST,Sn} = 3.49$ K – the experimental value is $T_{c,Sn,Exp.} = 3.72$ K [1].

For Nb is $\xi_{o,Nb,Exp.} = 40$ nm [1] so from (B1.1) we obtain $T_{c,SST,Nb} = 9.30$ K – the experimental value is $T_{c,Nb,Exp.} = 9.25$ K [1].

But notice that there are some theoretical values which differ significantly from experimental data. It suggests that sometimes untypical changes in intrinsic pressure in some materials change significantly the phonon-electron coupling.

We will apply formula (B1.1) to all types of superconductors to investigate a global behaviour of superconductors.

The relationship between the critical temperature and the coherence length (i.e. formula (B1.1)) is the most important and requires further research. We can rewrite formula (B1.1) as follows

$$T_{c,SST} = \text{Constant}_1 / \xi_{SST}^{0.561}. \quad (B1.2)$$

On the other hand, the Coulomb law looks as follows

$$F = \text{Constant}_2 / R^2. \quad (B1.3)$$

The R^2 says that the Coulomb field has spherical symmetry, i.e. the electromagnetic interactions of the elementary electric charge have spherical symmetry at distances much bigger than sizes of the tori/electric-charges. On the other hand, the $\xi_{SST}^{0.561}$ suggests that the phonon field between electrons in Cooper pairs has not spherical symmetry. For directional interactions (in an approximation, the nuclear weak interactions are directional/axial in direction of the spin), the acting force does not depend on distance so there should be the r^0 . We can calculate value of the b parameter for the nuclear electroweak interactions from following formula

$$b = 0 \cdot \alpha_{w(p)} / (\alpha_{w(p)} + \alpha_{em}) + 2 \cdot \alpha_{em} / (\alpha_{w(p)} + \alpha_{em}) = 0.561, \quad (B1.4)$$

i.e. the weak part ($\alpha_{w(p)} / (\alpha_{w(p)} + \alpha_{em})$) is directional (0) while the electromagnetic part ($\alpha_{em} / (\alpha_{w(p)} + \alpha_{em})$) is spherical (2).

It suggests that in protons dominate the axial weak interactions,

$$100\% \alpha_{w(p)} / (\alpha_{w(p)} + \alpha_{em}) = 72\%,$$

so electroweak interactions cannot have a spherical symmetry – it is consistent with the SST because in both protons and electrons there is the spin-1/2 torus/electric-charge with central condensate so it has also axial symmetry.

Now, from dynamics of the core of baryons, we can calculate value of the a parameter. By applying the Wien's displacement law

$$T_{\text{Peak}} \lambda = 2.898 \cdot 10^{-3} \text{ [K m]} \quad (\text{B1.5})$$

We can calculate temperature of the fundamental gluon loop T_{FGL}

$$T_{\text{FGL}} = 2.898 \cdot 10^{-3} \text{ [K m]} / (2 \pi R_{\text{FGL}}) = 0.99198 \cdot 10^{12} \text{ K}. \quad (\text{B1.6})$$

At temperature of the FGL, there is an increase of mass of the proton condensate from Y to mass of the charged core of protons H^+ (it is a virtual process). It forces similar transformation of the condensates in the electron-positron pairs created by protons. We know that at higher critical temperatures, the coherence length is smaller. Assume that at the T_{FGL} , the coherence length, ξ_e , is equal to the radius of the enlarged electron condensate (density of all spacetime condensates is invariant)

$$\xi_e = r_{C(e)} (H^+ / Y)^{1/3} = 0.88031 \cdot 10^{-18} \text{ m}. \quad (\text{B1.7})$$

It means that value of the a parameter is

$$a = T_{\text{FGL}} \xi_e^{0.561} = 73.7. \quad (\text{B1.8})$$

Energy of SST-As condensate from FGL and its range/coherence-length

SST shows that the transition (collapse) from the radial vibrations in the FGL to the circular motions in a spacetime condensate ($R \rightarrow R/(2\pi)$) increases energy 2π times. But the internal dynamics of the core of baryons shows that the final mass of the central spacetime condensate is Y . It leads to conclusion that there is emitted a spacetime condensate carrying following energy

$$M_{\text{Con}} = 2 \pi m_{\text{FGL}} - Y = 0.27230 \text{ MeV}. \quad (\text{B1.9})$$

Range/coherence-length of such condensate is equal to the radius of the FGL divided by 2π

$$\xi_{o,\text{Con}} = R_{\text{FGL}} / (2 \pi) = A/(3 \pi) = 7.4001 \cdot 10^{-17} \text{ m}. \quad (\text{B1.10})$$

In the next calculations, there will appear a product, F_{Con} , of M_{Con} and $\xi_{o,\text{Con}}$

$$F_{\text{Con}} = M_{\text{Con}} \xi_{o,\text{Con}} = 0.020151 \text{ [eV} \cdot \text{nm]}. \quad (\text{B1.11})$$

Superconductivity via the third phonon field at atmospheric pressure

In SST, when an interaction of a mass M is defined by a coupling constant α_i then an exchanged virtual energy, E , is $E = \alpha_i M$. A generalization for a few coupling constants looks as follows

$$E = \prod_i \alpha_i M = \alpha_{\text{Total}} M, \quad (\text{B1.12})$$

where \prod denotes a product.

Here, for the electroweak proton-electron interactions we have

$$\alpha_{\text{Total}} = \prod_i \alpha_i = \alpha_{\text{em}} \alpha_{\text{w(p)}} \alpha_{\text{w(e)}} = 1.2995 \cdot 10^{-10}. \quad (\text{B1.13})$$

The lower limit for phonon energy in the third phonon field (Phonon-III) produced by the electron-positron pairs is

$$E_{\text{Phonon-III,lower}} = \alpha_{\text{Total}} 2 m_e = 1.3281 \cdot 10^{-4} \text{ eV}. \quad (\text{B1.14})$$

Coherence length is inversely proportional to energy so by applying formula (B1.11) we obtain

$$\xi_{\text{0,Phonon-III,upper}} = F_{\text{Con}} / E_{\text{Phonon-III,lower}} = 151.73 \text{ nm}. \quad (\text{B1.15})$$

By applying formula (B1.1) we can calculate the lower limit for critical temperature for the Type II superconductors at atmospheric pressure

$$T_{\text{c,SST,Phonon-III,lower}} = a / \xi_{\text{0,Phonon-III,upper}}^b = 4.4 \text{ K}. \quad (\text{B1.16})$$

In the nuclear strong interactions, range of four bound neutral pions is equal to the equatorial radius A of the core of the baryons so such quanta should define the upper limit for critical temperature for the Type II superconductors at atmospheric pressure.

The upper energy for phonon is

$$E_{\text{Phonon-III,upper}} = 4 \alpha_{\text{Total}} \pi_{\text{bound}}^0 = 7.0155 \cdot 10^{-2} \text{ eV}. \quad (\text{B1.17})$$

The lower limit for coherence length of the Type II superconductors at atmospheric pressure is

$$\xi_{\text{0,Phonon-III,lower}} = F_{\text{Con}} / E_{\text{Phonon-III,upper}} = 0.28723 \text{ nm}. \quad (\text{B1.18})$$

By applying formula (B1.1) we can calculate the upper limit for critical temperature for the Type II superconductors at atmospheric pressure

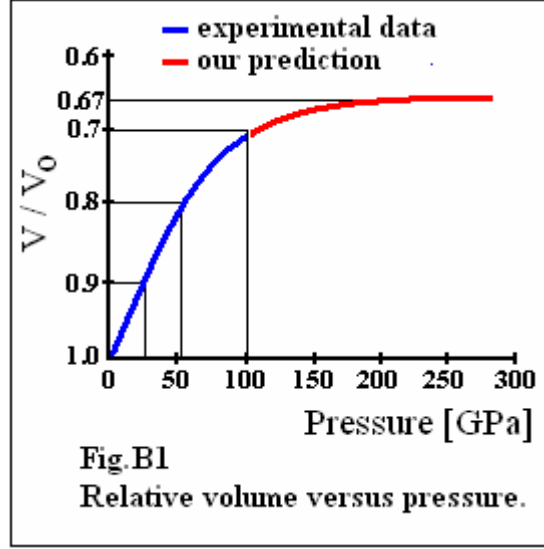
$$T_{\text{c,SST,Phonon-III,upper}} = a / \xi_{\text{0,Phonon-III,lower}}^b = 148 \text{ K}. \quad (\text{B1.19})$$

Our results are consistent with experimental data so we can assume that, generally, in the Type II superconductors dominates the third phonon field, i.e. phonons are created due to the electroweak interactions of the masses of the electron-positron pairs.

Type II superconductors at extreme pressure

Due to the four-particle symmetry, maximum energy of an object that can interact due to electroweak interactions is $4Y$. But emphasize that such energies can exist only at extreme pressure. The energy of phonon is

$$E_{\text{Phonon,pressure}} = 4 \alpha_{\text{Total}} Y = 0.22046 \text{ eV} . \quad (\text{B1.20})$$



It relates to following coherence length

$$\xi_{\text{o,Phonon,pressure}} = F_{\text{Con}} / E_{\text{Phonon,pressure}} = 0.091405 \text{ nm} . \quad (\text{B1.21})$$

We can calculate the critical temperature

$$T_{\text{c,SST,pressure}} = a / \xi_{\text{o,Phonon,pressure}}^b = 282 \text{ K} . \quad (\text{B1.22})$$

But extreme pressure changes volume of the superconductors. For relative volume equal to $V/V_0 = 0.67$, by applying formulae (B1.21) and (B1.22), we obtain that critical temperature is $T_{\text{c,SST,pressure}} = 304 \text{ K}$. For the carbonaceous sulphur hydride at $267 \pm 10 \text{ GPa}$, there is $T_{\text{c}} = 287.7 \pm 1.2 \text{ K}$ [3].

Available experimental data of volume versus pressure up to 100 GPa we can find in [4]. We predict that for pressures higher than about 200 GPa , for a function describing dependence of volume on pressure (Fig.B1), we should observe a plateau (or so).

Lower limits for critical temperature for Type I superconductors

The lowest energy of a phonon in the second phonon field (Phonon-II) is

$$E_{\text{Phonon-II,lower}} = \alpha_{\text{Total}} (m_{\text{e}} - m_{\text{e,bare}}) = 7.6917 \cdot 10^{-8} \text{ eV} . \quad (\text{B1.23})$$

Coherence length of such elementary phonon is

$$\xi_{\text{o,Phonon-elementary}} = F_{\text{Con}} / E_{\text{Phonon-II,lower}} = 2.6198 \cdot 10^5 \text{ nm} . \quad (\text{B1.24})$$

From (B1.1) we obtain the lowest critical temperature for critical field composed of such elementary phonons

$$T_{c,\text{Phonon-II,SST}} = a / \xi_{0,\text{Phonon-elementary}}^b = 0.067 \text{ K} . \quad (\text{B1.25})$$

Notice that at higher intrinsic pressure (it depends on structure of the lattice) or at higher intrinsic pressure plus external pressure, there are created the composite phonons composed of the elementary phonons so critical temperature increases.

In the Type I superconductors, there can be also phonons created by oscillations of the electron-positron pairs (Phonon-I) so the lower limit for critical temperature of the Type I superconductors is defined by

$$T_{c,\text{Phonon-I,SST}} > 0 \text{ K} . \quad (\text{B1.26})$$

There are only three Type I superconductors with critical temperatures defined by following interval

$$0 \text{ K} < T_c \leq 0.067 \text{ K} , \quad (\text{B1.27})$$

so, generally, in the Type I superconductors dominates the second phonon field produced in electroweak interactions of the radiation masses of the electron-positron pairs.

Here we have tried to capture the global features of superconductors and we believe that the effects are definitely better than the complexity and multiplicity of phenomena would imply.

The technological benefits of producing a good room-temperature superconductor operating at atmospheric pressure would be enormous, so in recent decades a huge amount of financial resources has been invested and many research teams worked to produce such a superconductor. So I don't think that the current thresholds for the different types of superconductors that result from experimental data, i.e. for the Type I chemical elements is

$$0 \text{ K} < T_c \leq 4.47 \text{ K} \text{ or } 7.193 \text{ K} , \quad (\text{B1.28})$$

for the Type II superconductors is

$$4.47 \text{ K} \text{ or } 7.193 \text{ K} \leq T_c \leq 139 \text{ K} \text{ or so} , \quad (\text{B1.29})$$

and the present-day upper limit for superconductor at extreme pressure (267 GPa) is

$$T_c = 288 \text{ K} , \quad (\text{B1.30})$$

will change radically in the future. On the other hand, our theoretical results are consistent with experimental data so it validates our very simple model for superconductivity.

For the Type II superconductors we obtained

$$4.4 \text{ K} \leq T_c \leq 148 \text{ K} . \quad (\text{B1.31})$$

For the Type I superconductors we obtained two thresholds

$$T_c > 0 \text{ K} \text{ and } T_c \geq 0.067 \text{ K} . \quad (\text{B1.32})$$

For the Type II superconductors at extreme pressure (~300 GPa), for relative volume 0.67, we obtained

$$T_c = 304 \text{ K} . \quad (\text{B1.33})$$

The global features for superconductivity are as follows.

*Here we showed that superconductivity follows from the dynamics of the core of baryons and concerns the electroweak interactions of the electron-positron pairs.

*There are three sources of the phonon fields: oscillations, radiation masses and masses of the electron-positron pairs. In the three phonon fields, masses/energies of the elementary phonons are different. When we neglect the phonons from the oscillations then mass-energy of elementary phonons in Type I is $7.6917 \cdot 10^{-8} \text{ eV}$ while in Type II is $1.3281 \cdot 10^{-4} \text{ eV}$. But emphasize that energy of the composite phonons can be much higher, for example, for the critical temperature 148 K we have $7.0155 \cdot 10^{-2} \text{ eV}$. A geometrical mean energy of upper and lower limits for phonons in Type II superconductors at atmospheric pressure is $\sim 3 \cdot 10^{-3} \text{ eV}$ (it is the mean binding energy of the Cooper pairs) – it relates to coherence length equal to $\sim 6.7 \text{ nm}$.

*We derived a global relationship between critical temperature and coherence length.

*We calculated the thresholds for critical temperatures for different types of superconductors.

*At critical temperature, there can be a resonance between the electroweak energy of the electron-positron pairs (produced in protons) and the vibrational energy of the ions in lattice of the superconductors – it validates the BCS theory.

*The electroweak structure of the Cooper pairs has both axial symmetry (from weak interactions) and spherical symmetry (from electromagnetic interactions).

*Intrinsic and external pressure decreases coherence length so increases critical temperature.

*A mixture of the three phonon fields and dependence of critical temperature on intrinsic pressure in superconductors (it depends on number density of the electron-positron pairs, on structure of the atomic nuclei, and on structure of the lattice as a whole) cause that sometimes formula (B1.1) gives results that differ from the experimental data.

*The Cooper pairs are some analogs to the spin-0 neutral pions which consist of two spin-1 fundamental gluon loops with the same internal helicity. In the nuclear strong interactions, the spin-1 loops behave as electrons in atoms, i.e. to both we can apply the Hund's rule. The neutral pions are created on the circular axis inside the core of baryons so to conserve the spin-1/2 of the torus/electric-charge, there are created the neutral pions with antiparallel spins of the FGLs – it looks as the s-states in atoms. But in the baryonic resonances (i.e. for very short time $\sim 10^{-23} \text{ s}$), outside their core, spins of the FGLs can be parallel. It suggests that in strong intrinsic magnetic fields, there can be a spin flip of one of the two FGLs – we can say that there is a fluctuation from spin-0 state to spin-2 state, and vice versa. Notice also that there is the spin flip in the cold hydrogen. Both electrons in the Cooper pairs are internally right-

handed so, similar to the neutral pions, the resultant spin of the Cooper pairs is zero. But in ferromagnetic superconductors, there are allowed the fluctuations from the spin-singlet state of the Cooper pairs to the spin-triplet state, and vice versa. It leads to conclusion that, because of the fluctuations, superconductivity and ferromagnetism can coexist.

*The composite phonons cause that there is created a boson condensate composed of the Cooper pairs.

*We showed that it is impossible to make a material that is a superconductor at room-temperature and atmospheric pressure.

References

- [1] Kevin A. Delin, Terry P. Orlando (28 October 2021). “Superconductivity”
web.mit.edu/6.763/www/FT03/PSfiles/CH-117_(KAD-TPO_revised)_corrected_1.pdf
- [2] Sandor Caplan and Gerald Chanin (31 May 1965). “Critical-Field Study of Superconducting Aluminum”
Phys. Rev. **139**, A1428
- [3] E. Snider, *et al.* (15 October 2020). “Room-temperature superconductivity in a carbonaceous sulphur hydride”
Nature **586** (7829): 373-377
- [4] K. Jasiewicz, *et al.* (2019). “Pressure effects on the electronic structure and superconductivity of (TaNb)_{0.67}(HfZrTi)_{0.33} high-entropy alloy”
Phys. Rev. B **100**, 184503 (2019)

B2. Cooper-pair breaking

Theoretical results obtained in this section are perfectly consistent with the experimental data presented by Mannila, et al. (2021) [2]. We described the origin of three new formulae for the normalized number density of quasiparticles, relaxation times of bursts, and statistical distribution of the broken Cooper pairs per burst. We show that the Cooper-pair breaking is due to the nuclear weak interactions of the spacetime condensates created in the core of nucleons.

Superconductors free from quasiparticles (QPs) that force decays of the Cooper pairs (CPs) into electrons, are very important in superconducting quantum computing. It is assumed that QPs corrupt the superposition. Just the Cooper-pair breaking decreases the coherence times of superconducting qubits.

Here we show that shielding against the ionizing radiation background (IRB) is not enough to eliminate QPs from superconductors built of chemical elements because the nuclear weak interactions, which are responsible for creations of QPs, are ubiquitous in all physical conditions.

The global features of superconductivity based on the SST we described in Section **B1**. There appear the three phonon fields.

We define the coupling constants as follows

$$\alpha_i = G_i M_i m_i / (c \hbar) , \quad (\text{B2.1})$$

where G_i , c and \hbar are the constant values, M_i is mass of a source, and m_i is mass of a carrier of interactions.

Assume that for the nuclear strong and weak interactions, there are equators for which is

$$G_i M_i = c^2 r_i , \quad (\text{B2.2})$$

so we have

$$\alpha_i \sim r_i m_i . \quad (\text{B2.3})$$

For a loop is $r_i = \text{const.}$ so we obtain

$$\alpha_i \sim m_i . \quad (\text{B2.4})$$

The nuclear weak interactions are responsible for the beta decay of neutrons so from (B2.4) we have that value of the coupling constant for such interactions is

$$\alpha_{w(p)} = \alpha_s (n - p) / m_{\text{FGL}} \approx 0.019 , \quad (\text{B2.5})$$

where $n = 939.565390 \text{ MeV}$ and $p = 938.272082 \text{ MeV}$.

For the spin-0 spacetime condensates we have $M_i = m_i$ so from (B2.1) is

$$\alpha_i \sim M_i^2 . \quad (\text{B2.6})$$

Assume that the weak mass of electron interacting with proton is

$$m_{w(e)} = \alpha_{w(p)} m_e . \quad (\text{B2.7})$$

From (B2.5), (B2.6) and (B2.7) we can estimate the coupling constant for the weak interactions of electrons

$$\alpha_{w(e)} = \alpha_{w(p)} [\alpha_{w(p)} m_e / (n - p)]^2 = \alpha_{w(p)}^3 [m_e / (n - p)]^2 \approx 1 \cdot 10^{-6} . \quad (\text{B2.8})$$

Number density of quasiparticles normalized by the Cooper-pairs density

Number density, n_i , is inversely proportional to energy of field components E_i (heavier particles are fewer)

$$n_i \sim 1 / E_i \quad (\text{B2.9})$$

We assume that energies of phonons are the electroweak masses of the oscillation masses, radiation masses, and masses of the electron-positron pairs – the three different masses in the electron-positron pair are denoted by M_1 (when interactions occur one after the other, the total coupling constant is the product of the coupling constants)

$$E_{\text{Phonon}} = M_1 \alpha_{w(p)} \alpha_{em} \alpha_{w(e)} \quad (\text{B2.10})$$

so for the number density of the Cooper-pairs, n_{CPs} , we have

$$n_{\text{CPs}} \sim 1 / (M_1 \alpha_{w(p)} \alpha_{em} \alpha_{w(e)}) . \quad (\text{B2.11})$$

We assume that for quasiparticles (QPs) is (emphasize that energy of quasiparticle must be much higher than energy of the composite phonons)

$$n_{\text{QPs}} \sim 1 / (M_2 \alpha_{\text{w(p)}}), \quad (\text{B2.12})$$

i.e. we assume that they are created due to the nuclear weak interactions.

Our definition for number density of quasiparticles normalized by the Cooper-pairs density looks as follows

$$x_{\text{QPs}} = n_{\text{QPs}} / n_{\text{CPs}} = M_1 \alpha_{\text{em}} \alpha_{\text{w(e)}} / M_2. \quad (\text{B2.13})$$

Normalized number density of quasiparticles from the ionizing radiation background (IRB)

Due to the ionizing radiation background, for $M_2 = M_1$, we have

$$x_{\text{QPs,IRB}} = \alpha_{\text{em}} \alpha_{\text{w(e)}} \approx 7 \cdot 10^{-9}. \quad (\text{B2.14})$$

It is consistent with experimental data [1]. It suggests that the Cooper-pair breaking are indeed due to the creations of quasiparticles in the nuclear weak interactions – their energy is $M_2 \alpha_{\text{w(p)}}$.

Most important transitions in superconductors

Assume that following transitions are most important in nucleons ($Y \approx 4\mu^\pm$)

$$m_{\text{FGL}} \rightarrow 2\pi m_{\text{FGL}} \rightarrow Y \rightarrow 4 \mu^\pm \rightarrow k m_{\text{e,bare}} (k \approx 828), \quad (\text{B2.15})$$

and there is involved at least one electron-positron pair $2m_e$.

Relaxation times of bursts

From formula $E_i \tau_i = \text{const.}$, where τ_i is a lifetime of a virtual energy E_i , we have

$$f_{\text{minimum}} = \tau_{\text{Cooper,mean}} / \tau_{\text{burst,1}} = Y / (2 m_e) \approx 415. \quad (\text{B2.16})$$

where $\tau_{\text{Cooper,mean}}$ is the mean period free from quasiparticles, and $\tau_{\text{burst,1}}$ is the lifetime for 1-quasiparticle burst. For $\tau_{\text{Cooper,mean}} \approx 0.4 \text{ s}$ [2], from (B2.16) the relaxation time for 1-quasiparticle burst is $\tau_{\text{burst,1}} \approx 960 \mu\text{s}$.

For two quasiparticles we have $Y \rightarrow 2 Y$ so from (B2.16) we have $\tau_{\text{burst,2}} \approx 480 \mu\text{s}$.

For three quasiparticles we have $Y \rightarrow 3 Y$ so from (B2.16) we have $\tau_{\text{burst,3}} \approx 320 \mu\text{s}$.

For four quasiparticles we have $Y \rightarrow 4 Y$ so from (B2.16) we have $\tau_{\text{burst,4}} \approx 240 \mu\text{s}$.

Our theoretical results are close to experimental data (see Fig.3a in [2]). It validates the transitions presented in (B2.15).

Our formula for relaxation times of bursts created by quasiparticles looks as follows

$$\tau_{\text{burst,i}} \approx 0.4 \text{ [s]} / (f_{\text{minimum}} N_{\text{QP}}), \quad (\text{B2.17})$$

where N_{QP} denotes number of quasiparticles in a burst. For $N_{\text{QP}} = 0$ we obtain $\tau_{\text{burst,i}} \rightarrow \infty$ – it is consistent with [2] (see Fig.3a in [2]). For $4 \leq N_{\text{QP}} \leq 9$, we obtain $\tau_{\text{burst,4-9}} \approx 210 \mu\text{s}$ (see formula (B2.25)).

Lower limit for normalized number density of quasiparticles

The transitions from the circular vibrations to radial vibrations (i.e. $M_1 / M_2 = 1 / (2\pi)$) cause that the lower limit for number density of quasiparticles normalized by the Cooper-pair density is

$$x_{\text{QPs,lower}} = \alpha_{\text{em}} \alpha_{\text{w(e)}} / (2\pi) \approx 1 \cdot 10^{-9}. \quad (\text{B2.18})$$

It is consistent with experimental data [3]. Equality of the experimental result and theoretical result obtained in (B2.18) validates the $m_{\text{FGL}} \rightarrow 2\pi m_{\text{FGL}}$ transitions in the core of baryons.

But for two interacting FGLs, the transition $\pi^0 \rightarrow Y$ gives

$$x_{\text{QPs,pion-Y}} = \pi^0 \alpha_{\text{em}} \alpha_{\text{w(e)}} / Y \approx 2 \cdot 10^{-9}. \quad (\text{B2.19})$$

It is consistent with [2]. It suggests that instead the transitions $m_{\text{FGL}} \rightarrow 2\pi m_{\text{FGL}}$, there dominated the transitions $\pi^0 \rightarrow Y$.

Function for statistical distribution of the broken Cooper pairs

The statistical distribution of the broken Cooper pairs, n^* , is very well described by following our function (it is not the exponential function in [2])

$$N_{\text{events},n^*} = \delta (2^{10-n^*})^\beta, \quad (\text{B2.20})$$

where δ and $\beta = 3/2$ are some factors. Fortunately, for data in [2], there is $\delta = 1!$ So we have

$$\begin{aligned} n^* = 1 & \text{ gives } N_{\text{events},n^*=1} \approx 1.159 \cdot 10^4, \\ n^* = 2 & \text{ gives } N_{\text{events},n^*=2} = 4096, \\ n^* = 3 & \text{ gives } N_{\text{events},n^*=3} \approx 1448, \\ n^* = 4 & \text{ gives } N_{\text{events},n^*=4} = 512, \\ n^* = 5 & \text{ gives } N_{\text{events},n^*=5} \approx 181, \\ n^* = 6 & \text{ gives } N_{\text{events},n^*=6} = 64, \\ n^* = 7 & \text{ gives } N_{\text{events},n^*=7} \approx 22.6, \\ n^* = 8 & \text{ gives } N_{\text{events},n^*=8} = 8, \\ n^* = 9 & \text{ gives } N_{\text{events},n^*=9} \approx 2.82, \\ n^* = 10 & \text{ gives } N_{\text{events},n^*=10} = 1. \end{aligned} \quad (\text{B2.21})$$

The SST results that follow from (B2.20) are in perfect agreement with experimental data (see Fig.2b in [2]). It suggests that the Titius-Bode (TB) numbers are very important

$$2^{10-n^*} = 512, 256, 128, 64, 32, 16, 8, 4, 2, 1 \text{ (the 10 TB numbers)}. \quad (\text{B2.22})$$

The TB numbers very frequently appear in SST.

The origin of the function for statistical distribution of the broken Cooper pairs

Formula (B2.20) requires further research. What is the origin of the parameter $\beta = 3/2$?

We can assume that the decays of the Y spacetime condensate into the entangled electron-positron pairs (see (B2.15)) can be realized via two phenomena, i.e. by creating a string or a loop both composed of the electron-positron pairs. The jet-like expansion of the string has one degree of freedom while the disc-like expansion of the loop has two degrees of freedom.

For a short time, the virtual spacetime condensates Y look like a mini black hole with a jet and an accretion disc.

For the same mass of the jet and disc, their abundances should be the same, i.e. 50% - it leads to conclusion that the decaying and expanding Y or other spacetime condensates have $\beta = 3/2$ degrees of freedom and such is the origin of the parameter β in formula (B2.20).

What is the origin of the TB numbers?

The TB numbers, 2^{10-n^*} , follow from the successive symmetrical decays of the Y – the last decay leads to $512 = 2^{10-1}$ entangled electrons and positrons (**so also electrons in Cooper pairs**; notice that there is one quasiparticle per each electron from the broken Cooper pairs) because their number cannot be bigger than 828 that follows from (B2.15). The ratio $512/828 = 0.618$ is very close to the golden ratio. Jets and discs with fewer pairs are more numerous.

We can normalize the parameter δ to have opportunity to compare different experimental results. If in an experiment, there appear $N_{\text{events},n^*=1}^*$ bursts with one broken Cooper pair then we have

$$\delta = 2^{9\beta} / N_{\text{events},n^*=1}^* . \quad (\text{B2.23})$$

We can see that in [2] is $N_{\text{events},n^*=1}^* \approx 2^{9\beta}$ so $\delta = 1$.

Our normalized function for the statistical distribution of the broken Cooper pairs looks as follows

$$N_{\text{Norma},\text{events},n^*} = 2^{13.5} (2^{10-n^*})^{3/2} / N_{\text{events},n^*=1}^* . \quad (\text{B2.24})$$

Now by applying (B2.21) and (B2.17), we can calculate the mean relaxation time of bursts for $4 \leq N_{\text{QP}} \leq 9$

$$\begin{aligned} \tau_{\text{burst},4-9,\text{mean}} &\approx \\ &\approx 0.4 \text{ [s]} / [415 (4 \cdot 512 + 5 \cdot 181 + 6 \cdot 64 + 7 \cdot 22.6 + 8 \cdot 8 + 9 \cdot 2.82) / (512 + 181 + 64 + 22.6 + 8 + 2.82)] = \\ &= 0.4 \text{ [s]} / [415 (3584.58 / 790.42)] \approx \mathbf{210 \mu\text{s}} . \end{aligned} \quad (\text{B2.25})$$

This SST theoretical result is consistent with the experimental result presented in [2] (see Fig.3a in [2]).

Notice also that there is valid following relationship

$$N_{\text{events},n^*=1} / N_{\text{events},n^*=10} \approx \mathbf{1.16 \cdot 10^4} . \quad (\text{B2.26})$$

Summary

Here we showed that it is impossible to dampen to zero the real and virtual processes in the core of baryons so we cannot eliminate the Cooper-pair breaking in superconductors. There is the lower limit for the number density of quasiparticles which are responsible for the pair-breaking.

The theoretical results obtained in this section, i.e. the normalized number density of quasiparticles, relaxation times of bursts, and statistical distribution of the broken Cooper pairs per burst, are consistent with experimental results presented in [2].

Emphasize that presented here model is very simple.

References

- [1] A. Vepsäläinen, *et al.* (2020). “Impact of ionizing radiation on superconducting qubit coherence”
Nature **584**, 551 (2020)
- [2] E. T. Mannila, *et al.* (20 December 2021). “A superconductor free of quasiparticles for seconds”
Nat. Phys. (2021)
<http://doi.org/10.1038/s41567-021-01433-7>
arXiv:2102.00484v1 [cond-mat.supr-con] (31 Jan 2021)
- [3] K. Serniak, *et al.* (2019). “Direct dispersive monitoring of charge parity in offset-charge-sensitive transmons”
arXiv:1903.00113v2 [cond-mat.mes-hall] (30 July 2019)

C. Nuclear physics

C1. The four-shell model of atomic nucleus

The nucleons that an alpha particle is composed of, occupies the vertices of the square with the diagonal of the square equal to $A + 4B$. The side of the square and side of a cube occupied by each nucleon is

$$a_c = (A + 4B) / 2^{1/2} = 1.9125731 \cdot 10^{-15} \text{ m}. \quad (\text{C1.1})$$

We can assume that the nucleons inside a nucleus are placed on the concentric spheres where the distances between them equal a_c . This means that the radius of the first sphere is equal to $a_c/2$. This, therefore, leads to the following formula for the radii of the spheres (they are not the radii of the nuclei because the spheres have a thickness)

$$r_{sn} = (s - 0.5) a_c, \quad (\text{C1.2})$$

where $s = 1, 2, 3, 4$.

The maximum number of nucleons placed on a sphere is (one nucleon occupies a square with the area equal to a_c^2)

$$A_n = 4 \pi r_{sn}^2 / a_c^2 = 4 \pi (s - 0.5)^2 \quad (\text{C1.3})$$

i.e. $A_1 = 3.14$, $A_2 = 28.27$, $A_3 = 78.54$ and $A_4 = 153.94$.

If we round these numbers to the nearest even number (nuclei containing an even number of nucleons are more stable), we obtain the following series: 4, 28, 78, and 154. This means that on the first four wholly filled spheres there are 264 nucleons. As we see by the first two numbers, the sum of the first and third and the result of subtracting the third and second, and the fourth and second numbers, we can see that the result is the well-known magic numbers of 4, 28, 82, 50, 126. This cannot be a coincidence which confirms that we are on the right path in order to build the correct theory of an atomic nucleus. When the number of neutrons becomes equal to one of the magic numbers then transitions of the protons between lower and higher spheres occurs. This increases the binding energy of a nucleus.

C2. Coupling constants and binding energy

According to SST, the spacetime as a whole is flat. According to Newton's second law, in the regular 3-dimensional Euclidean space is

$$F_i = d p_i / d t . \quad (C2.1)$$

According to SST, constants of interactions G_i are directly proportional to the inertial mass densities of fields carrying the interactions. The following formula defines the coupling constants (or running couplings), α_i , of all interactions (notice that m_i can be both mass or massless energy responsible for interactions)

$$\alpha_i = G_i M_i m_i / (c \hbar) , \quad (C2.2)$$

where M_i defines the sum of the mass of the sources of interaction plus the mass of the component of the field, whereas m_i defines the mass/energy of the carrier of interactions.

The strong coupling constant for pions exchanging the fundamental gluon loop (its mass is a little higher than a half of the mass of neutral pion, $m_{FGL} = 67.544413 \text{ MeV}$) is $\alpha_s = \alpha_s^{\pi\pi, FGL} = 1$. Coupling constant for strongly interacting protons, at low energies (as it is in the atomic nuclei), is $\alpha_s^{pp, \pi} = 14.391187$ whereas for strongly interacting neutrons is $\alpha_s^{nn, \pi} = 14.410335$. To the alpha particle, we can apply the mean value $\alpha_s^{NN, \pi} = 14.400761$. When we accelerate a baryon, then there decreases the spin speed of the FGL so mass of it decreases as well – it leads to the running coupling for the nuclear strong interactions.

Assume that a carrier of interactions interacts simultaneously, for example, strongly and electromagnetically. Then, strong mass is $\alpha_s m$ whereas electromagnetic mass of the strong mass is $\alpha_{em} \alpha_s m$. It leads to conclusion that resultant coupling constant α is the product, Π , of coupling constants involved in the interactions

$$\alpha = \Pi \alpha_i . \quad (C2.3)$$

When a carrier is a binary system then there appears the factor 2 i.e.

$$\alpha = 2 \Pi \alpha_i . \quad (C2.4)$$

Due to the radial emissions of carriers of interactions or radial polarization of virtual pairs, there is the inverse square law

$$F_i = G_i M_i m_i / r^2 . \quad (\text{C2.5})$$

Applying formulae (C2.1) – (C2.5), we obtain

$$\int dp_i = \Pi \alpha_i c \hbar \int (1 / r^2) dt . \quad (\text{C2.6})$$

$$p v = \Pi \alpha_i c \hbar \int (1 / r^2) dr . \quad (\text{C2.7})$$

The radial kinetic energy, E_{kin} , transforms into radiation energy, $E_{\text{radiation}}$, so into binding energy, E_{binding} , as well i.e. $E_{\text{kin}} = p v / 2 = E_{\text{radiation}} = - E_{\text{binding}}$. We can rewrite formula (C2.7) as follows

$$E_{\text{binding}} = - \Pi \alpha_i c \hbar / (2 r) . \quad (\text{C2.8})$$

When we express this energy in MeV then there appears the factor F

$$E_{\text{binding}} [\text{MeV}] = m_{\text{binding}} c^2 = - \Pi \alpha_i c \hbar / (2 r F) , \quad (\text{C2.9})$$

where $F = 1.78266192162742 \cdot 10^{-30} \text{ kg/MeV}$.

Introduce symbol k

$$k = \hbar / (2 c F) = 9.8663490 \cdot 10^{-14} [\text{MeV m}] . \quad (\text{C2.10})$$

Formulae (C2.9) and (C2.10) lead to

$$m_{\text{binding}} [\text{MeV}] = - k \Pi \alpha_i / r . \quad (\text{C2.11})$$

It is the main formula.

Calculate the binding energy of electron in the ground state in hydrogen atom. We have $\Pi \alpha_i = \alpha_{\text{em}} = 1/137.035999085012$ and $r_B = 0.529177211 \cdot 10^{-10} \text{ m}$. Applying formula (C2.11), we obtain the Rydberg energy

$$m_{\text{binding}} [\text{MeV}] = - 13.6056936 \cdot 10^{-6} \text{ MeV} . \quad (\text{C2.12})$$

This value is correct so we can assume that also is correct our derived formula (C2.11).

Calculate the binding energy of the deuteron.

The muon radius of the proton is $R_{p(\mu)} = 0.840391 \text{ fm}$ (see (2.19.7)). When nucleons are in such distance then their spins must lie on the same direction. Such nucleons can interact due to the nuclear weak interactions so from (C2.11) we have (notice that there is only one direction of interactions)

$$m_{\text{binding,deuteron}} [\text{MeV}] = - k \alpha_{w(p)} / R_{p(\mu)} \approx - 2.198 \text{ MeV} . \quad (\text{C2.13})$$

When in (C2.13) we apply the value obtained by Bezginov, *et al.* (2019), i.e. $R_p = 0.833(10) \text{ fm}$ (see Section 2.19), then we obtain $2.218(27) \text{ MeV}$. The best value we obtain for 0.83057 fm , i.e. 2.224 MeV .

Calculate the mean binding energy per nucleon in the alpha particle.

According to the SST, the two protons and two neutrons are placed in vertices of square which diagonal is $D = A + 4B = 2.7047843 \text{ fm}$, where $A = 0.6974425 \text{ fm}$ is the equatorial radius of the core of baryons, whereas $B = 0.50183544 \text{ fm}$. There are 6 directions of strong interactions i.e. the 4 sides of the square and its two diagonal directions. It leads to conclusion that mean distance of strong interactions is

$$R = [2 D + 4 D / 2^{1/2}] / 6 = 2.1766423 \text{ fm} . \quad (\text{C2.14})$$

The strong interactions of the four nucleons follow from the exchanges of the pions. It means that they interact strongly, $\alpha_s^{\text{NN},\pi} = 14.400761$, and electromagnetically α_{em} , i.e.

$$\prod \alpha_i = \alpha_{\text{em}} \alpha_s^{\text{NN},\pi} = 0.10508743 . \quad (\text{C2.15})$$

From formulae (C2.11), (C2.14) and (C2.15) we obtain the total strong binding energy for the alpha particle

$$m_{\text{binding,total}} [\text{MeV}] = -6 k \alpha_{\text{em}} \alpha_s^{\text{NN},\pi} / R = -28.5806056 \text{ MeV} . \quad (\text{C2.16})$$

From the obtained absolute value 28.5806056 MeV , we must subtract the energy E_{em} which follows from the electrostatic repulsion of the protons. The maximum distance between the positively charged $W_{(+),d=1}$ relativistic pions in the alpha particle is $R_{\text{ee}} = (A+4B) + 2(A+B)$. We assume that the two protons in the alpha particle behave in such a way that the two $W_{(+),d=1}$ are always in the distance R_{ee} . Then from the Coulomb's law we obtain

$$E_{\text{em}} = e^2 / (4 \pi \epsilon_0 R_{\text{ee}} c^2 F) = 0.2821611876 \text{ MeV} . \quad (\text{C2.17})$$

The mean binding energy per nucleon, ΔE , in the alpha particle is

$$\Delta E = (m_{\text{binding,total}} + E_{\text{em}}) / 4 = -7.0746111 \text{ MeV} . \quad (\text{C2.18})$$

C3. Model of dynamic supersymmetry for nuclei

From [1] results that the nucleons in a nuclei are grouped in following way

$\Theta \equiv 2$ protons and 2 neutrons,

$\Phi \equiv 3$ protons and 5 neutrons,

$\Gamma \equiv 3$ protons and 4 neutrons,

$\Psi \equiv 1$ proton and 1 neutron.

The SST explains the above as follows

** A proton exists in two states with the probabilities:

$y = 0.50839$ and $1 - y = 0.49161$.

If we multiply these probabilities by two (for a deuteron) or by four (for an alpha particle), we obtain the integers (approximately) because the probabilities are that y and $1 - y$ have almost the same values.

** A neutron exists in two states with the probabilities:

$x = 0.62554$ and $1 - x = 0.37446$.

If we multiply these probabilities by eight, we obtain in the integers approximately 5 (5.004) and 3 (2.996). The 8 is the smallest integer which leads to integers (in approximation). Such structures are the rectangular-prisms.

Table C3 *Main path of stability of nuclei*

ZXA	Θ	Φ	Γ	Ψ	ZXA	Θ	Φ	Γ	Ψ	ZXA	Θ	Φ	Γ	Ψ
1H1					36Kr84	9	6			71Lu175	10	16	1	
2He4 m	1				37Rb85	9	5	1	1	72Hf180	9	18		
3Li7			1		38Sr88 m	10	6			73Ta181	9	17	1	1
4Be9			1	1	39Y89	10	5	1	1	74W184	10	18		
5B11	1		1		40Zr90 m	12	5		1	75Re187	9	18	1	
6C12	3				41Nb93	11	5	1	1	76Os192	8	20		
7N14	3			1	42Mo98	10	7		1	77Ir193	8	19	1	1
8O16 m	4				43Tc97	12	5	1	1	78Pt194 ?	10	19		1
9F19	3		1		44Ru102	11	7		1	79Au197	9	19	1	1
10Ne20	5				45Rh103	12	6	1		80Hg202	8	21		1
11Na23	4		1		46Pd106	12	7		1	81Tl205	7	21	1	1
12Mg24	6				47Ag107	13	6	1		82Pb208 m	8	22		
13Al27	5		1		48Cd114	10	9		1	83Bi209	8	21	1	1
14Si28	7				49In115	11	8	1		84Po209	10	20	1	1
15P31	6		1		50Sn120 m	10	10			85At210	12	20		1
16S32	8				51Sb121	10	9	1	1	86Rn222	5	25		1
17Cl35	7		1		52Te130	6	13		1	87Fr223	6	24	1	
18Ar40	6	2			53I127	10	10	1		88Ra226	6	25		1
19K39	8		1		54Xe132	9	12			89Ac227	7	24	1	
20Ca40 m	10				55Cs133	9	11	1	1	90 th 232	6	26		
21Sc45	7	1	1	1	56Ba138	8	13		1	91Pa231	8	24	1	
22Ti48	8	2			57La139	9	12	1		92U238	5	27		1
23V51 m	7	2	1		58Ce140	11	12			93Np237	7	25	1	1
24Cr52 m	9	2			59Pr141	11	11	1	1	94Pu244	5	28		
25Mn55	8	2	1		60Nd142	13	11		1	95Am243	7	26	1	
26Fe56	10	2			61Pm147	11	12	1		96Cm247	6	27	1	
27Co59	9	2	1		62Sm152	10	14			97Bk247	8	26	1	
28Ni58 m	12	1		1	63Eu153	10	13	1	1	98Cf251	7	27	1	
29Cu63	10	2	1		64Gd158	9	15		1	99Es254	7	28		1
30Zn64	10	2	1	1	65Tb159	10	14	1		100Fm253	9	26	1	1
31Ga69	9	3	1	1	66Dy164	9	16			101Md258	8	28		1
32Ge74	8	5		1	67Ho165	9	15	1	1	102No256	12	26		
33As75	9	4	1		68Er166	11	15		1	103Lr256	14	25		
34Se80	8	6			69Tm169	10	15	1	1	104Ku260	13	26		
35Br79	10	4	1		70Yb174	9	17		1					

ZXA – denotes the atomic-number/symbol-of-element/mass-number
Θ = 2p + 2n = 2He4; **Φ** = 3p + 5n; **Γ** = 3p + 4n = 3Li7; **Ψ** = p + n = 1D2
? - denotes the discrepancy with the results in the periodic table of elements
m – denotes magic-number nucleus

** For a system containing 50% of the proton-type structures and 50% of the neutron-type structures, we obtain the following probabilities

$$(x + y) / 2 = 0.56696 \text{ and } (1 - x + 1 - y) / 2 = 0.43304.$$

This factor is equal to 7 – then we obtain 3.969 i.e. approximately 4, and 3.031 i.e. approximately 3.

A nucleus chooses a mixture of the states Θ , Φ , Γ and Ψ in such a manner the binding energy was the greatest. The Θ groups appear when the interactions of protons dominate whereas the Φ groups appear when the interactions of neutrons dominate.

Applying the model of dynamic supersymmetry for nuclei, we showed the abundances of the structures Θ , Φ , Γ and Ψ in most stable nuclei – the path of stability is presented in Table C3.

The consistency with the experimental data is very high – only one result is inconsistent with experimental data. SST shows that the abundance of the $^{78}\text{Pt}194$ should be slightly higher than the $^{78}\text{Pt}195$.

It should be noted that the relativistic mass of the pions $W_{(+\rightarrow),d=1}$ decreases with the distance from the core of the nucleon, so during their exchanges between nucleons at distances greater than ~ 2.4 fm and less than ~ 6 fm, the volumetric binding energy per nucleon is higher and increases with a decrease in the density of the atomic nucleus (there is an lower limit for such density) – we can say that it is some analogy to the confinement of quarks in the Standard Model.

Let us emphasize that the interactions in the states Θ , Φ , Γ and Ψ are practically saturated, i.e. the structures interact weakly.

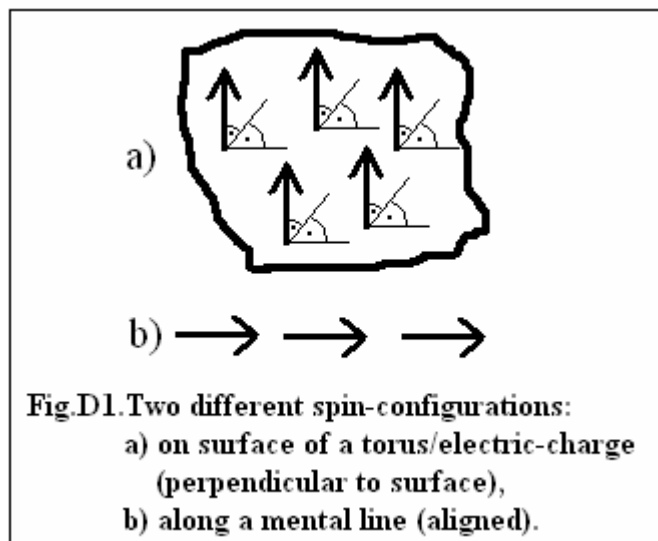
To obtain the correct binding energies per nucleon in heavier nuclei (more than 56 nucleons) the average distances between nucleons in the structures $2p2n$ (~ 9.5 MeV/nucleon) must be greater than those in $3p5n$ (~ 7 MeV/nucleon).

References

- [1] P. Van Isacker, J. Jolie, K. Heyde and A. Frank; *Extension of supersymmetry in nuclear structure*; Phys. Rev. Lett. **54** (1985) 653

D. Brain-mind interactions

D1. The brain-mind interactions



It is very important to unify the particle physics with the mental world via a single field. Consider arrangements of spins of the neutrino-antineutrino pairs in the SST-As.

There are two different spin-configurations of entangled non-rotating-spin neutrino-antineutrino pairs. One configuration leads to the tori/electric-charges whereas the second one leads to the mental lines that can be closed (Fig.D1).

A mental soliton consists of crossing sets composed of concentric circles/loops built of the non-rotating-spin neutrino-antineutrino pairs with aligned spins. Such tangled solitons are the 3-dimensional dark-matter structures. They are the flexible but stable structures and baryonic matter is transparent for them.

Tangled circular electric currents, so those inside brains as well, create the mental solitons. Our minds consist of such DM solitons. Due to the current decays and circuit breakers (for example, neurons can do this), entangled smaller and smaller self-similar mental solitons are produced.

Identical parts in different mental solitons attract each other, so there is a struggle for dominance in the minds. Such processes are the origin of the mind-brain interactions.

Our memory is in the form of mental solitons in the mind.

By neglecting the dark-matter structures, we cannot fully understand Nature.

E. Chaos theory

E1. Feigenbaum constants

Chaotic behaviour arises in simple non-linear dynamical systems [1].

The Logistic Map is written as follows

$$x_{n+1} = r x_n (1 - x_n), \quad (\text{E1.1})$$

where x_n is a number between zero and one (the interval $[0, 1]$) that represents the ratio of existing population to the maximum possible population, whereas r is a parameter. It leads to conclusion that r is defined by the interval $[0, 4]$. There are many different logistic maps that in the limit behave the same – it is the Feigenbaum universality. Such maps describe many physical phenomena. Such maps have a similar shape i.e. have a single quadratic maximum. The parameter r defines steepness of the maximum.

A single bifurcation is a splitting of one value into two values. Such bifurcations appear in the Logistic Map for different values of the parameter r . We let r_n be the value of r at which a stable 2^n cycle first appears. At $r = r_1 = 3$ there is a splitting of one a branch into two i.e. there appears an orbit of period $2^1 = 2$, at $r = r_2 \approx 3.4494897\dots$ there is a splitting of two branches into four (each branch splits into two) i.e. there appears an orbit of period $2^2 = 4$, at $r = r_3 \approx 3.54409\dots$ there is a splitting of four branches into eight (each branch splits into two) i.e. there appears an orbit of period $2^3 = 8$, at $r = r_4 \approx 3.5644\dots$ there is a splitting of eight branches into sixteen i.e. there appears an orbit of period $2^4 = 16$, and so on. At the end of the period-doubling cascade, i.e. at $r \approx 3.569946\dots$, there is the onset of chaos i.e. there appears an orbit of infinite period (solution does not contain a periodic orbit) but there sometimes appear islands of stability i.e. the period-doubling windows.

The bifurcation diagram for the Logistic Map is a function $x = f(r)$.

The first Feigenbaum constant results from a numerical work. It is given by the limit

$$\delta = \lim_{n \rightarrow \infty} (r_{n-1} - r_{n-2}) / (r_n - r_{n-1}) = 4.669201609\dots, \quad (\text{E1.2})$$

or

$$\delta = \lim_{n \rightarrow \infty} (r_{n-2} - r_{n-1}) / (r_{n-1} - r_n) = 4.669201609\dots, \quad (\text{E1.3})$$

where r_n are discrete values of r at the n th period-doubling. We can see that the successive bifurcations are separated by a distance that asymptotically decreases geometrically by the factor δ .

In the Chaos Theory there is defined an operator that performs the iteration and rescaling. Such operator has a fixed point solution for a particular value of α (it is the second Feigenbaum constant)

$$\alpha \approx 2.50281\dots \quad (\text{E1.4})$$

For the strong field in baryons we obtain (see formula (A2.3))

$$\alpha \approx e_{\text{eff, strong}} = 1 / 0! + 1 / 1! + 1 / 2! = 2.500. \quad (\text{E1.5})$$

It is very close to the second Feigenbaum constant. The gluon loops outside the strong fields of baryons behave as the photon loops, so the structure of proton leaks outside the nuclear strong field and can have an influence on behaviour of physical systems.

The successive symmetrical decays of the boson $r_{n-2} = M_{\text{TB}} = 750.29577 \text{ MeV}$ (the bifurcation) lead to the TB orbits. The boson which reaches the last orbit for the strong interactions has mass $r_{n-1} = M_{\text{TB}}/4$. On the other hand, the fundamental gluon loops ($r_n = m_{\text{FGL}} = 67.54441 \text{ MeV}$) that outside the nuclear strong fields behave as the photon loops, leak outside the strong fields of baryons. So in SST, the first Feigenbaum constant can be defined as follows (it is an analog to formula (E1.3))

$$\delta \approx (M_{\text{TB}} - M_{\text{TB}} / 4) / (M_{\text{TB}} / 4 - m_{\text{FGL}}) = 4.688. \quad (\text{E1.6})$$

Such phenomena should be characteristic also for the SST gravitational black holes.

Emphasize that the origin of the Chaos Theory is related to the leakage of the nuclear strong part of the atom-like structure of protons – there are the emissions of the virtual gluon loops that outside the nuclear strong fields behave as the photon loops that interact with the electrically charged particles/structures such as protons, ions, atomic nuclei and electrons.

References

- [1] Steven Strogatz (1994). “Nonlinear Dynamics and Chaos”
Addison-Wesley (1994)

F. Quantum physics

F1. Quantum physics in SST

Here within the SST we derived the fundamental equation of the Matrix Quantum Mechanics i.e. the commutator. The fundamental equation results from the quantum entanglement that leads to the infinitesimal transformations. In reality, the Matrix Quantum

Mechanics that describes excited states of fields (i.e. the quantum particles) is timeless and non-local i.e. non-deterministic. But the Matrix Quantum Mechanics leads to the time-dependent, so deterministic, wave functions that are characteristic for the Statistical Quantum Mechanics. It is the reason why the wave functions appear in the equations of motion. The Statistical Quantum Mechanics or the Quantum Theory of Fields, are the semiclassical/semi-quantum theories.

The presented here extended Matrix Quantum Mechanics leads to the methods applied in the Quantum Theory of Fields but there appear some limitations.

The idea of existence of many separated parallel worlds is incorrect.

In SST, in descriptions of interactions, most important are tori/charges and loops, especially the gluon loops and photon loops, so as it is in the Matrix Quantum Mechanics, we can start from the definition of commutator applied in the ring theory

$$[I, B] = IU - UI, \quad (\text{F1.1})$$

where I and U are some quantities associated with a ring.

For a spin-1 loop is

$$E_{\text{loop}} T_{\text{lifetime}} = \hbar, \quad (\text{F1.2})$$

where $E_{\text{loop}} = m_{\text{loop}} c^2$ defines the mass/energy of a loop, and T_{lifetime} is its lifetime (lifetime of a loop is equal to its period of spinning). Lifetime of a virtual loop is inversely proportional to its mass/energy.

There can be a virtual loop/system composed of n entangled spin-1 loops. Denote the energy/mass of a virtual loop, labeled by n , by iE_n ($i^2 = -1$ because virtual objects produce in field holes with negative mass) whereas its lifetime by T_n . Then we obtain

$$(i E_n) T_n = \hbar. \quad (\text{F1.3})$$

Emission or absorption of one etanglon (its mass is infinitesimal in relation to mass/energy of the loops) by a system changes its spin by $\pm 1\hbar$. Define a change (an amplitude) in mass under the infinitesimal transition from loop labeled by n to loop labeled by k by $E_{n,k}$ whereas a change (an amplitude) in lifetime due to the same transition by $T_{n,k}$. The set of the all $E_{n,k}$ elements is the matrix. The same concerns the $T_{n,k}$. Formula (F1.3) for such a system looks as follows

$$(i E_{n,k}) T_{n,k} = n \hbar, \quad (\text{F1.4})$$

where n denotes the number of entangled loops whereas the pairs n,k label the amplitudes concerning masses and lifetimes. Such is the correct interpretation of the Heisenberg matrices. There can be matrices for other physical quantities such as energy, position, velocity, square of velocity, and so on. But for interactions described within the time-independent Matrix Quantum Mechanics most important is formula (F1.4).

A measurement of, for example, lifetime of a system changes its configuration of mass/energy so the matrices for mass/energy and lifetime does not concern the same configuration. This means that these two physical quantities do not commute.

The generality of the derivation of the commutator will not be limited when we will start from the simpler formula (F1.3). Calculate value of the commutator defined by formula (F1.1) for $I = E_n$ and $U = T_n$. Assume that some observed/interacting system consists of n entangled spin-1 loops that spins are parallel (but there can be more loops that we can group in pairs and the spins of the constituents of the pairs are antiparallel). Then for the whole system labeled by n we obtain

$$(i E_n) T_n = n \hbar . \quad (\text{F1.5})$$

Assume that a component of the system emits the superluminal spin-1 entanglon so the change in spin is $m = n \pm 1$. Mass of the system decreases i.e. $E_m = E_n - E$ whereas lifetime is longer $T_m = T_n + T$. Due to the entanglement, the changes are infinitesimal so $T \rightarrow 0$ and $E \rightarrow 0$. Due to the emission is

$$(i E_m) T_m = m \hbar . \quad (\text{F1.6})$$

Calculate the value of the commutator

$$[E_n , T_m] = E_n T_m - T_n E_m = \hbar \{ n (T_n + T) / T_n - (n \pm 1) T_n / ((T_n + T)) \} / i. \quad (\text{F1.7})$$

For $T \rightarrow 0$ and $E \rightarrow 0$, i.e. under infinitesimal transformation of the lifetime and energy of the system, we obtain

$$[E_n , T_m] = - (\pm \hbar / i) = \pm i \hbar . \quad (\text{F1.8})$$

It is easy to notice that equation (F1.8) is valid for all quantum particles, i.e. for all values of n , when the changes in lifetime and mass are infinitesimal.

On the basis of equation (F1.4), we can rewrite equation (F1.8) as follows

$$[E_{n,k} , T_{m,l}] = \pm i \hbar . \quad (\text{F1.9})$$

The equation (F1.9) is the fundamental equation in the Matrix Quantum Mechanics. We showed that this equation follows from the superluminal quantum entanglements with infinitesimal changes in energy and lifetime.

Denote the matrix $E_{n,k}$ by t_α , the matrix $T_{m,l}$ by t_β whereas ± 1 by $\varepsilon_{\gamma\alpha\beta}$, where $\varepsilon_{\gamma\alpha\beta}$ is $+1$ if γ, α, β is an even permutation or -1 if γ, α, β is an odd permutation. Then, for matrices that are the spin 1 (i.e. $1\hbar$) representation of the Lie algebra of the rotation group, we can rewrite equation (F1.9) as follows

$$[t_\alpha , t_\beta] = i \varepsilon_{\gamma\alpha\beta} t_\gamma . \quad (\text{F1.10})$$

It is the fundamental equation applied in the non-Abelian gauge theories [1]. The gauge invariance we obtain assuming that the Lagrangian is invariant under a set of infinitesimal transformations on the matter fields. It is some analogy to the infinitesimal transformations on the masses of the loops in a set of entangled loops.

We can see that presented here the Matrix Quantum Mechanics based on the entanglement and constancy of spin of the loops in a set of entangled loops leads to the methods applied in

the Quantum Theory of Fields (QTFs). Why we must apply the infinitesimal transformations in the Quantum Physics? It follows from the very small inertial mass of the carriers of the entanglement i.e. of the superluminal binary systems of closed strings. What is the physical meaning of the elements of the matrix $E_{n,k}$? The n and k numbers number the entangled loops in a system so the $E_{n,k}$ are the amplitudes of transitions between different or the same loops in the system. Their squares define the rates of the transitions. But the QTFs is the incomplete theory because of one weak point. Within this theory we neglect internal structure of the bare fermions. This causes that there appear the singularities and infinite energies of fields. The infinities are eliminated due to the procedure that we refer to as the renormalization. This procedure follows from the incorrect formula which can be written symbolically as follows: $\infty - \infty = C = \mathbf{constant} \neq 0$. The C can denote, for example, the bare mass of electron. It leads to conclusion that in reality the bare electron is not a sizeless point. The renormalization partially corrects the wrong initial condition but we still neglect the internal structure of the bare particles, for example, the shapes and dynamics (that leads, for example, to the internal helicity) that are very important in the theory of the nuclear strong and weak interactions. This causes that the QTFs is the messy theory.

What is the correct interpretation of the wave function? Due to the superluminal entanglement of the SST-As components in their excited states, in this spacetime can appear the quantum particles. The initial configuration/distribution of the entangled constituents of a quantum system changes with time. We can say that some configuration disappears and there appears the next one, and so on. There are not continuous trajectories of the components of the quantum system between the succeeding configurations. The succeeding configurations depend stepwise on time. But in an approximation we can say about a time-dependent statistically averaged distribution that is coded by the wave function of the quantum system. In reality, due to the superluminal entanglement, for a defined time, the positions of the components of the quantum state are well-defined. Due to the superluminal quantum entanglement, we find a particle in a place of measurement – the measurement and entanglement cause that a set of entangled states collapses to one of allowed quantum states. Due to the stepwise dependence on time, the equations of motion for a wave function are only some approximation of the quantum reality, i.e. it is some statistical approximation.

Emphasize that according to SST, even pure energy, as for example the rotational energy, have to be carried by physical volumes and the smallest volumes/pieces-of-space (i.e. the SST tachyons) the other particles consist of cannot be simultaneously in two or more different states so the superposition is the wrong idea. But different parts of the same bigger particle can be simultaneously in different states – notice that it is not the superposition.

References

- [1] Steven Weinberg (1996). “The Quantum Theory of Fields”
Volume II, Modern Applications
The Press Syndicate of the University of Cambridge

G. Extraterrestrial communication

G1. Wow! signal

Here we show that in the Wow! signal, an extraterrestrial civilization coded the phase transitions of the initial inflation field and many other fundamental ideas.

The Wow! signal was a radio signal received on August 15, 1977, by Ohio State University's Big Ear radio telescope [1]. Most of its operation was in the 21-cm radio band. The receiver covered an 8-MHz bandwidth from 1411 to 1419 MHz.

The string of numbers and characters "6EQUJ5" we see in channel 2 of the printout [1].

The signal-strength sequence "6EQUJ5" in channel 2 of the computer printout represents the following sequence of signal-to-noise ratios [1]:

6: 6 (up to 7)
 E: 14 (up to 15)
 Q: 26 (up to 27)
 U: 30 (up to 31)
 J: 19 (up to 20)
 5: 5 (up to 6)

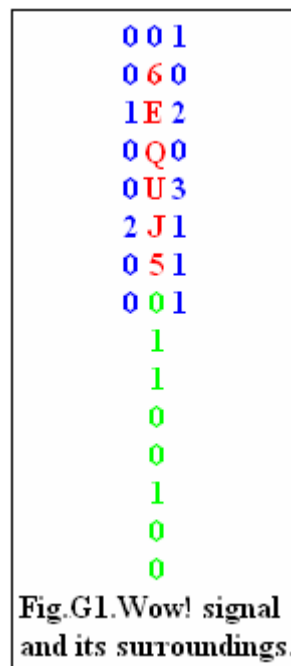
The intensity received (for example, "E") means that the signal was 14.5 ± 0.5 times stronger than the background noise.

Notice that each element in the signal is defined by two numbers (the lower and upper limit) differing by one.

In the printout, the noise is defined by empty place: we can assume that there is zero.

Notice that the two first numbers in the Wow! signal are 6 and 14 (E). Let's check if they can define the true length of the Wow! signal.

The first number 6 defines number of elements in the main part of the Wow! signal. On the other hand, we have $14 = 6 + 8$. This suggests that the signal sender indicates that he also uses eight numbers after the main part of the signal. A sequence of numbers immediately after it is 01100100 (see Fig.G1 and [1]). The second part consists of the low-value signal-to-noise ratios.



How we can interpret it? We can assume that the second part of the string, i.e. the part composed of the zeros and ones, i.e. the part composed of the low-value signal-to-noise ratios:

“01100100”, shows whether we correctly measured the signal-to-noise ratios for the main part “6EQUJ5”. We know that in the binary system, the sequence 01100100 represents the number 100. On the other hand, the sum of all numbers in the main part also is 100

$$6 + E + Q + U + J + 5 = 6 + 14 + 26 + 30 + 19 + 5 = 100.$$

It leads to conclusion that measured by the Ohio-State-University team the signal-to-noise ratios for “6EQUJ5” are correct.

The main part consists of 6 elements. Let’s create two groups each containing three elements and calculate the sum of numbers.

For “6EU” is

$$6 + E + U = 6 + 14 + 30 = 50,$$

and for “QJ5” is

$$Q + J + 5 = 26 + 19 + 5 = 50.$$

The sums are the same so such a division is justified.

We can use as well the English alphabet for our numerology analysis:

1 (A), 2 (B), 3 (C), 4 (D), 5 (E), 6 (F), 7 (G), 8 (H), 9 (I), 10 (J), 11 (K), 12 (L), 13 (M), 14 (N), 15 (O), 16 (P), 17 (Q), 18 (R), 19 (S), 20 (T), 21 (U), 22 (V), 23 (W), 24 (X), 25 (Y), 26 (Z).

Calculate the sums:

$$\text{“6EU”} = 6 + 5 (E) + 21 (U) = 32,$$

$$\text{“QJ5”} = 17 (Q) + 10 (J) + 5 = 32.$$

Such an incredible double coincidence must lead to important information.

In Section 2.14, we described the degrees of freedom of the fundamental objects that appeared in our Cosmos due to the phase transitions of the SST initial inflation field. To simplify the description we rewrite the main equation and Table 4 (see (G1.1) and Table G1).

If N denotes the degrees of freedom then for the rotating-spin loops/closed-strings and the SST cores is

$$N = | 8 (2d - 1) + 2 |, \quad (\text{G1.1})$$

where $d = 0, 1, 2, 4, 8$.

From (G1.1) we obtain respectively 6, 10, 26, 58 and 122. Notice that rotational energy has 2 degrees of freedom.

The Wow! signal is a sequence of the signal-to-noise ratios – each element changes its value from n to $(n + 1)$, for example, for 6 is 6 up to 7. It suggests that following formula is very important in deciphering the Wow! signal

$$N = 2 \cdot [n + (n + 1)]. \quad (\text{G1.2})$$

We can use this formula for the transition from n to N or transformation from N to n .

For the all elements in the complete Wow! signal (i.e. the $14 = 6 + 8$ elements), i.e. for 6, E, Q, U, J, 5, 0 and 1, and the elements in the closest surrounding of the signal we obtain

$$6 \text{ i.e. } n = 6 \text{ so } N = 2 \cdot (6 + 7) = 26$$

$$E \text{ i.e. } n = 14 \text{ so } N = 2 \cdot (14 + 15) = 58$$

$$Q \text{ i.e. } n = 26 \text{ so } N = 2 \cdot (26 + 27) = 106 \text{ i.e. } 10 \text{ and } 6$$

$$U \text{ i.e. } n = 30 \text{ so } N = 2 \cdot (30 + 31) = 122$$

$$J \text{ i.e. } n = 19 \text{ so } N = 2 \cdot (19 + 20) = 78$$

$$5 \text{ i.e. } n = 5 \text{ so } N = 2 \cdot (5 + 6) = 22$$

$$0 \text{ i.e. } n = 0 \text{ so } N = 2 \cdot (0 + 1) = 2$$

$$1 \text{ i.e. } n = 1 \text{ so } N = 2 \cdot (1 + 2) = 6$$

$$2 \text{ i.e. } n = 2 \text{ so } N = 2 \cdot (2 + 3) = 10$$

$$3 \text{ i.e. } n = 3 \text{ so } N = 2 \cdot (3 + 4) = 14 \text{ (it is the E that leads to } 58)$$

We can see that the SST degrees of freedom are indeed encoded in the Wow! signal.

Table G1 *Degrees of freedom of fundamental objects*

Stable object	Co-ordinates and quantities needed to describe position, shape and motions
Tachyon	6 (they always are spinning)
Closed string Entanglon	10 for rotating spin or 8 for non-rotating spin
Neutrino Neutrino-antineutrino (NA) pair	26 or 24 : 8 for entanglons on torus 8 for entanglons in condensate 8 (or 10) for the core as a whole
Core of baryons Electron	58 or 56 : 24 for NA pairs on torus 24 for NA pairs in condensate 8 (or 10) for the core as a whole
An abstract core of Protoworld composed of the baryonic core-anticore (CA) pairs	122 or 120 : 56 for CA on torus 56 for CA in condensate 8 (or 10) for the core as a whole

We can see that the numbers 106, 78 and 22 do not result from formula (G1.1).

But notice that we have

$$N_{22} = \{[6 + 0] + [6 + 0] + 10\} = 22. \quad (\text{G1.3})$$

It is a “gaseous” torus with central ball/scalar both composed of the SST tachyons. The tachyons interact due to the dynamic viscosity which leads to the most fundamental force.

There also is

$$N_{78} = \{[24 + 10] + [24 + 10] + 10\} = 78. \quad (\text{G1.4})$$

It is a torus with central ball/scalar both composed of the non-rotating-spin SST-As components which exchange the rotating-spin entanglons (they are responsible for the quantum entanglement).

There also is

$$N_{106} = \{[24 + 24] + [24 + 24] + 10\} = 106. \quad (\text{G1.5})$$

It is a torus with central ball/scalar both composed of the non-rotating-spin SST-As components which exchange the SST-As components.

When we neglect the stable superluminal objects that cannot be observed directly (i.e. 6 and 10) then the SST leads to following sequence for stable objects

Stable: 26, 58, 122 (it relates to $6\text{EU} = 32$),

and to following sequence for meta-stable objects

Meta: 22, 78, 106 (it relates to $\text{QJ5} = 32$).

Notice that sum of the numbers in each sequence is 206 i.e. is the same. The probability of such a strong coincidence (i.e. 32 and 32, and 206 and 206) as a result of the case is practically equal to zero. It suggests that the Wow! signal was emitted by an Extra-Terrestrial Intelligence (ETI).

Notice that two elements in Wow! signal with highest signal-to-noise ratios, i.e. Q(26) and U(30), are the numbers of protons and neutrons in iron ${}_{26}\text{Fe}^{(26+30)}$ whereas the two lowest ratios, i.e. 5 and 6, are the numbers of protons and neutrons in boron ${}_{5}\text{B}^{(5+6)}$. It forces the division of the Wow! signal into three pairs: QU, EJ and 65. On the other hand, according to SST, the ratios of the angles in the PMNS neutrino-mixing matrix are 4 : 5 : 1 (see Section 2.24). We showed that an ETI suggests following pairing of the Wow! signal elements: QU, EJ and 65. Differences in the signal-to-noise ratios for the components of the pairs are as follows:

$$\begin{aligned} \text{U} - \text{Q} &= 30 - 26 = 4 \\ \text{J} - \text{E} &= 19 - 14 = 5 \\ 6 - 5 &= 1 \end{aligned}$$

The ratios of obtained differences are $(\text{U} - \text{Q}) : (\text{J} - \text{E}) : (6 - 5) = 4 : 5 : 1$ as it is in the PMNS matrix.

We can show that also the fine-structure constant is encoded in the Wow! signal. The inverse of the fine-structure constant leads to a sequence: 1, 3, 7, 0, 3, 6. Using formula (G1.2) two times to each cipher in this sequence, we obtain:

$$1 \text{ so } 2 \cdot (1 + 2) = 6 \text{ (Wow and Stable) so } 2 \cdot (6 + 7) = 26 \text{ (Wow and Stable)}$$

$$3 \text{ so } 2 \cdot (3 + 4) = 14 \text{ (Wow) so } 2 \cdot (14 + 15) = 58 \text{ (Stable)}$$

$$7 \text{ so } 2 \cdot (7 + 8) = 30 \text{ (Wow) so } 2 \cdot (30 + 31) = 122 \text{ (Stable)}$$

0 so $2 \cdot (0 + 1) = 2$ (rotation) so $2 \cdot (2 + 3) = 10$ (**Stable**)

3 so $2 \cdot (3 + 4) = 14$ (**Wow**) so $2 \cdot (14 + 15) = 58$ (**Stable**)

6 so $2 \cdot (6 + 7) = 26$ (**Wow and Stable**) so $2 \cdot (26 + 27) = 106$ (**Meta**)

The probability of such a strong coincidence as a result of the case is very low. It suggests that the Wow! signal was emitted by an Extra-Terrestrial Intelligence (ETI).

Emphasize also that the Wow! signal leads to two isotopes i.e. ${}^6\text{C}^{14}$ and ${}^{14}\text{Si}^{30}$ which select the numbers 6, 14 (E) and 30 (U) in the order recorded here. Such order leads to the number 137.

The Wow! signal leads to discoverer of the Planck constant.

In SST, we showed that the reduced Planck constant is the most fundamental physical constant because it was set first at the start of inflation.

Rank the signal-to-noise ratios from the largest to the smallest

U, Q, J, E, 6, 5 = 30, 26, 19, 14, 6, 5 .

Let's consider the differences between the signal-to-noise ratios (for ratios arranged from the largest to the smallest): 4, 7, 5, 8, 1 or (for ratios arranged from the smallest to the largest): 1, 8, 5, 7, 4

The ciphers 4 and 7 lead to ${}_{19}47$ (date of M. Planck's death).

The ciphers 5 and 8 lead to ${}_{18}58$ (date of Planck's birth).

The ciphers 1 and 8 lead to ${}_{19}18$ (date in which the Nobel Prize for quantifying the radiation of a black body was awarded (received in 1919) to Max Karl Ernst Ludwig Planck).

Notice that the first ciphers 4, 5, 1, are the same as the ratios of the neutrino-mixing angles.

Many other coincidences suggest that the Earth is monitored by an ETI.

References

- [1] Dr. Jerry R. Ehman (Original Draft Completed: July 9, 2007; Last Revision: 28 May 2010). "The Big Ear Wow! Signal"
<http://www.bigear.org/Wow30th/wow30th.htm>

H. Cosmology and astrophysics

H1. Rotation curves of disc galaxies outside their bulges

The DM loops can interact weakly with baryonic matter. But in baryonic plasma can be created also the photon loops and gluon loops so in spinning galaxies, the other interactions can be realized as well.

Internal energy of a loop is defined as follows

$$\mathbf{E} = m_{\text{loop}} v_{\text{spin}}^2 . \quad (\text{H1.1})$$

Virtual mass m^* that is the mediator of the interactions of the DM loops with the actual baryonic mass, m_{BM} , of a vortex, is defined by the product of the baryonic mass m_{BM} and the coupling constant that defines a type of weak interactions. The DM loops interact via the

virtual electron-positron pairs ($\alpha_{w(e)} = 0.951118188679747 \cdot 10^{-6}$) and spin speed of loops and virtual pairs is equal to c so for the mediator we have

$$E = 2 \alpha_{w(e)} m_{BM} c^2, \quad (H1.2)$$

where the factor 2 follows from the fact that there are virtual pairs, not single particles.

The energy defined by (H1.2) was adopted by the spinning initial baryonic matter $m_{o,BM}$ so we have

$$E = m_{o,BM} v_{spin}^2, \quad (H1.3)$$

where v_{spin} is the observed orbital speed of stars outside the bulge of spinning galaxies.

From (H1.2) and (H1.3) is

$$v_{spin} = c (2 \alpha_{w(e)} m_{BM} / m_{o,BM})^{1/2}. \quad (H1.4)$$

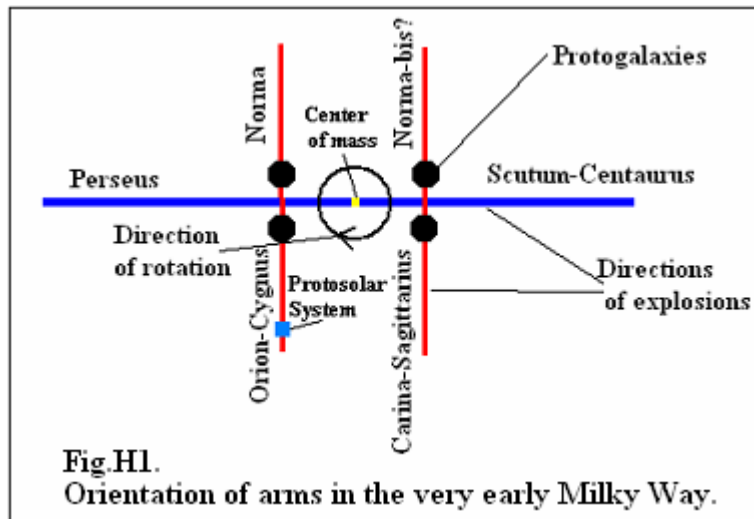
Single protogalaxy was composed of 4^{16} NBHs so its baryonic mass was

$$M_{Proto,BM} = 4^{16} \cdot 24.81 M_{Sun} = 1.066 \cdot 10^{11} M_{Sun}, \quad (H1.5)$$

where M_{Sun} is the mass of the Sun.

From (2.26.1) and (2.26.2) results that singlets, doublets, quadrupoles, and octopoles of protogalaxies were most numerous. From the structure of Milky Way (MW) Galaxy follows that initially there were 4 protogalaxies (Fig.H1).

The MW initially was a quadrupole so it was a binary system of binary systems. It means that we should observe 2 major arms and 4 minor arms. The initial distance between the 2-protogalaxy systems was bigger than the distance between the protogalaxies in the single binary systems. It caused that initially the temperature along the direction defined by Scutum-Centaurus arm and Perseus arm was lower than for the two other directions – it leads to conclusion that the two major arms should contain old stars while the four minor ones should contain younger stars and gas.



The observational data show that there are the two major arms (the Scutum-Centaurus and Perseus) containing old stars, and three or four minor ones (the Norma, Carina-Sagittarius, Orion-Cygnus, and ?) containing gas and young stars. Probably the Norma arm is composed today of two very close arms which practically overlap (Norma and Norma-bis?).

The spiral galaxies that evolved from binary systems of protogalaxies should have only two main arms. The M31 galaxy (Andromeda) evolved from 8 protogalaxies so the arrangement of the major and minor arms should be more complicated.

For MW from (H1.4) we have

$$v_{\text{spin,MW}} = c \{ 2 \alpha_{w(e)} m_{\text{BM}} / (4 M_{\text{Proto,BM}}) \}^{1/2}. \quad (\text{H1.6})$$

Today the mean rotation velocity of the Milky Way for the approximately flat part of the rotation curve is [1]

$$v_{\text{spin,MW}} = 238 \pm 14 \text{ km/s}, \quad (\text{H1.7})$$

so from (H1.6) we can calculate the present-day baryonic mass of MW

$$m_{\text{BM,MW}} = 1.41(17) \cdot 10^{11} M_{\text{Sun}}. \quad (\text{H1.8})$$

The rest of the initial baryonic mass is outside the MW halo – it is the mass of the dwarf galaxies and the intergalactic gas.

The mass of DM is about $N_{\text{DM/BM}} = 5.38979$ times higher than the baryonic mass (see (3.1.4)) so the total mass of MW should be close to

$$M_{\text{MW}} = m_{\text{BM,MW}} (1 + N_{\text{DM/BM}}) = 0.90(11) \cdot 10^{12} M_{\text{Sun}}. \quad (\text{H1.9})$$

Consider the initial stage of the baryonic part of the Universe. There were the two cosmological baryonic loops that created the gluon loops overlapping with the baryonic loops. Such plasma was cold because the NBHs are the cold objects. It means that the interactions between the gluon loops and baryonic loops were via the *single* FGLs at low energy so the coupling constant is $\alpha_s = 1$. From (H1.6) we have

$$v_{\text{spin}} = c (\alpha_s)^{1/2} = c. \quad (\text{H1.10})$$

Radius of the two cosmological loops was $R_{\text{Cosmological}} = 0.1911 \text{ Gly}$ so the period of rotation, $T_{\text{cosmological}}$, was

$$T_{\text{cosmological}} = 2 \pi R_{\text{Cosmological}} = 1.201 \text{ Gyr}. \quad (\text{H1.11})$$

The tidal locking (or a mutual spin-orbit resonance) of the Moon and the Earth caused that the rotation and revolution periods of the Moon are the same. Similar processes caused that the period of rotation of protogalaxies (so of the present-day galaxies as well) was (and still is) equal to the period of spinning of the two cosmological loops composed of the protogalaxies.

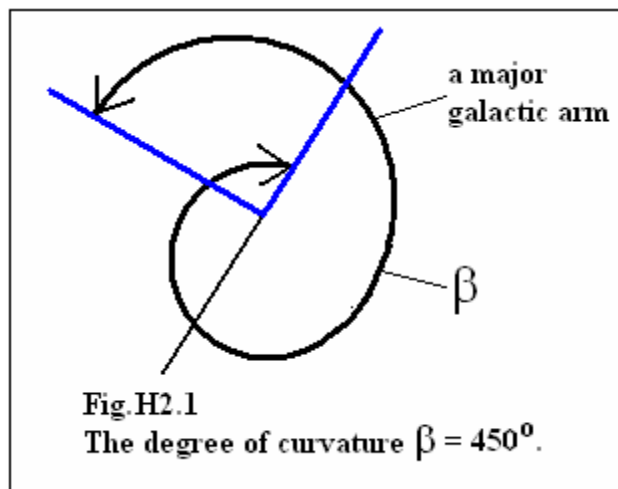
References

- [1] Mareki Honma, et al. (25 December 2012). “Fundamental Parameters of the Milky Way Galaxy Based on VLBI Astronomy”
 Publ. Astron. Soc. Japan (25 December 2012), Volume 64, Issue 6, 136
<https://doi.org/10.1093/pasj/64.6.136>

H2. Age of the Universe from the degree of curvature of the major arms of the massive spiral galaxies

We already proved that the correct age of the Universe is 21.32(1) Gyr.

Ludwig et al. (2009) derived solar ages from 1.7 to 22.3 Gyr [1] – we can read it in some recapitulation concerning the ages of stars [2]. The upper limit is very close to the age of the Universe obtained within SST – we claim that we cannot see the initial period 7.53 Gyr of evolution of galaxies.



Here we show that the degree of curvature of the major arms of the massive spiral galaxies leads to the SST age of the Universe.

Here the degree of curvature β [°] is the central angle defined by a major arm of a spiral galaxy (Fig.H2.1).

The mutual spin-orbit resonance caused that the period of rotation of protogalaxies (so of the present-day galaxies as well) was (and still is) equal to the period of spinning of the baryonic part in the very early Universe (see (3.7.1))

$$T_{\text{cosmological}} = 1.201 \text{ Gyr} . \quad (\text{H2.1})$$

For a constant mass of a loop with increasing radius, from the conservation of spin, we have $r \sim 1/v_{\text{spin}}$. From definition of period of spinning is $T = 2\pi r/v_{\text{spin}}$ so we have $T \sim 1/v_{\text{spin}}^2$. From formula (2.4.23) is $\alpha \sim v_{\text{spin}}$ so we have

$$T \sim 1 / \alpha^2 . \quad (\text{H2.2})$$

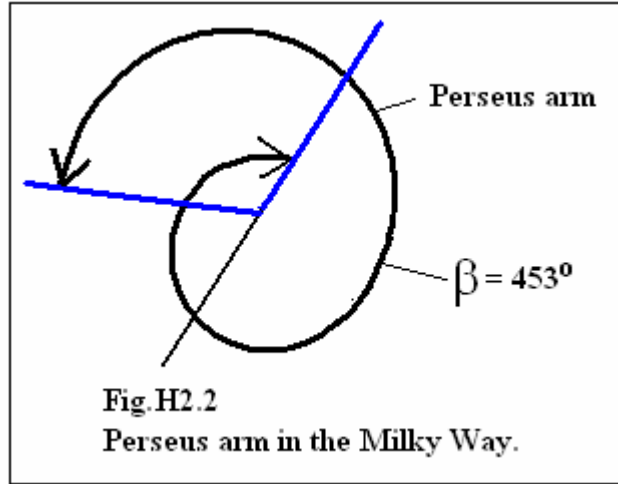
The period of rotation $T_{\text{cosmological}} = 1.201 \text{ Gyr}$ should be characteristic for the edge of the galactic bulge or edge of the central bar where the galactic arms begin. On such edge, the nuclear strong ($\alpha_s = 1$) and nuclear weak interactions ($\alpha_{w(p)} = 0.0187229$) dominated. On

the other hand, on the edge of the baryonic disc dominated the nuclear strong interactions so from (H2.2) we have

$$f = T_{\text{end}} / T_{\text{cosmological}} = [(\alpha_s + 2 \alpha_{w(p)}) / \alpha_s]^2 = 1.0763, \quad (\text{H2.3})$$

where T_{end} is the period of spinning of the end of the major arm, i.e. rotation on the end was a little slower than rotation near the central part. The delay is

$$\Delta\beta = 360^\circ - 360^\circ / f = 25.52 \text{ degrees per } 1.20 \text{ Gyr}. \quad (\text{H2.4})$$

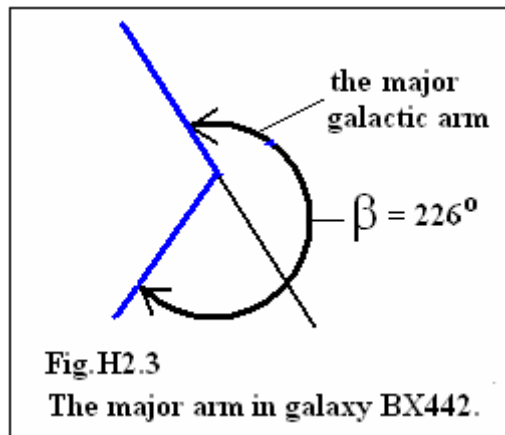


We can see that the Milky Way has already turned $N \approx 17.8$ times ($21.32 \text{ Gyr} / 1.20 \text{ Gyr} \approx 17.8$) so the degree of curvature for the major arm (Perseus arm) should be

$$\beta_{\text{MW}} = \Delta\beta N = 453^\circ \text{ or so}. \quad (\text{H2.5})$$

And it is (Fig.H2.2 and [3]).

For the spiral galaxy BX442 at the time distance 10.7 Gyr we obtain $\beta_{\text{BX442}} = 226^\circ$ or so – and it is (Fig.H2.3 and [4]).



For the spiral galaxy ISOHDFS 27 at the distance 6 Gyr from the Earth we obtain $\beta_{\text{ISOHDFS27}} = 326^\circ$ or so.

And it is (Fig.H2.4 and [5]).

We showed that both the energy density of CMB and the curvatures of the major arms in massive spiral galaxies lead to the age of the Universe about 21.3 Gyr. Moreover, curvature of arms of such galaxies in most distant observed Universe, because we cannot see the initial period 7.53 Gyr of evolution of the protogalaxies, should be about 160 degrees.

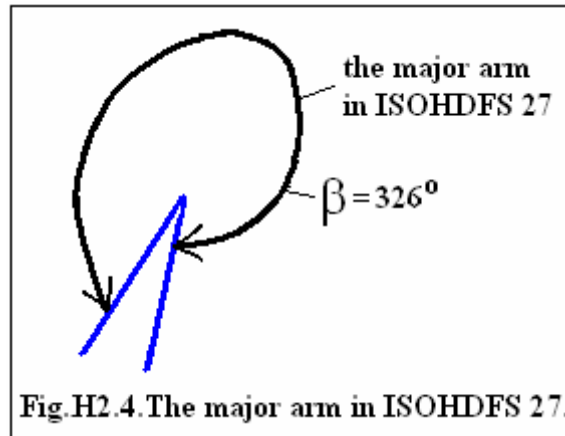


Fig.H2.4.The major arm in ISOHDFS 27.

References

- [1] Ludwig H-G, Caffau E, Steffen M, Bonifacio P, Sbordone L. (2009)
Astron. Astro-phys., in press
- [2] David R. Soderblom (31 March 2010). "The Ages of Stars"
arXiv:1003.6074v1 [astro-ph.SR]
- [3] en.wikipedia.org/wiki/Milky_Way
- [4] <http://astronoo.com/en/articles/galaxies-oldest.html>
- [5] European Southern Observatory (8 December 2000)
www.eso.org/public/poland/images/eso0041a/?lang

H3. Conditions for intensive evaporation of black holes

The SST black holes (BHs) are the NBHs or are the associations of NBHs and neutron stars. It follows from the fact that the very strong short-distance quantum entanglement between the SST-As components on the torus in the core of baryons causes that the cores are indestructible in conditions that can happen in the today inner Cosmos. Moreover, the strong interactions in the neutron stars between the neutrons fix the effective distance between them in such a way that the cores of neutrons do not overlap even partially.

In spinning nuclear plasma are conditions to create the dark-matter loops and the gluon loops that outside the nuclear strong fields behave as the photon loops. They all are composed of the SST-As components so their resultant speed must be equal to c . It leads to conclusion that when spin speed of the loops cannot be equal to c (due to their interactions with matter which is spinning with speeds lower than c) then there are forced their motions in direction perpendicular to the plane on which they lie.

Accretion discs of BHs lie on planes parallel to planes of the equators of BHs so the created loops are concentric and their centres overlap with the BH axis of rotation. It leads to conclusion that the created loops and matter interacting with them move along the rotation axis of BH. Mass of NBHs must be invariant and due to the tremendous dynamic pressure in

the SST-As, such spacetime should be flat. This means that the accreting baryonic matter can create new NBHs or/and such matter is intensively emitted along the BH rotation axis.

The collapse of the Protoworld forced the inflows of the DM loops into the SST BHs – this caused their collisions so some BHs were eaten by others, which converted neutron matter into nuclear plasma. The mass of the black holes decreased rapidly. Only their central parts have survived.

The Universe swelled at the expense of the zero-energy field thickening by incoming dark energy and partly due to the pressure exerted by the CMB created.

H4. The main equation in theory of gamma-ray bursts (GRB)

Here, using the SST, we derived the main equation in theory of GRBs and used it to describe the GRB 080916C. Such theory is closely related to the theory of NBHs which is related to the theory of baryons.

From formula (1.4.25) we have

$$t_{\text{Burst}} = \tau_{\text{Lifetime}} \sim 1 / m^4, \quad . \quad (\text{H4.1})$$

where m is the mass of a condensate or loop composed of the SST-As components or of a star, and t_{Burst} is the duration of a burst.

Emission during creation of a ball/condensate is due to the weak interactions.

The weak mass of NBH is

$$M_{\text{Weak}} = \alpha_{w(p)} M_{\text{NBH}}, \quad (\text{H4.2})$$

where $\alpha_{w(p)} = 0.0187229$, and $M_{\text{NBH}} = 24.81$ **solar masses**.

The strong mass of NBH at low energy (the NBHs are the cold objects) is

$$M_{\text{Strong}} = \alpha_s M_{\text{NBH}}, \quad (\text{H4.3})$$

where $\alpha_s = 1$.

The period of transition of a mass from the $A_{i(\text{NBH})} + B_{i(\text{NBH})}$ state to $A_{i(\text{NBH})} = 36.64$ **km** state, where $A_{i(\text{NBH})} / B_{i(\text{NBH})} = 1.3898$, due to the strong interactions, is

$$t_{\text{strong}} = B_i / c. \quad (\text{H4.4})$$

For the weak interaction, which is weaker, the speed of transition is lower.

From formulae (H4.1)-(H4.4) we have

$$t_{\text{Burst,NBH}} / t_{\text{strong}} = (M_{\text{NBH}} / M_{\text{Weak}})^4. \quad (\text{H4.5})$$

It leads to

$$t_{\text{Burst,NBH}} = (B_{i(\text{NBH})} / c) / \alpha_{w(p)}^4 = 716 \text{ s}. \quad (\text{H4.6})$$

From (H4.1) and (H4.6) we have

$$t_{\text{Burst}} = 716 (m / M_{\text{NBH}})^4 [\text{seconds}], \quad (\text{H4.7})$$

where m [solar masses] is mass of captured star by NBH.

Equation (H4.7) is the main equation in the theory of GRBs.

Some baryonic analog to stars captured by NBH looks as follows

$$m / M_{\text{NBH}} = m_{\text{Particle}} / M_{\text{Neutron}} . \quad (\text{H4.8})$$

Number density of GRBs should be higher for stars that masses relate to the uncharged scalars (they are the Y central condensate in baryons and the $\mu_{\text{bare}}^{\pm}/2$ central condensate in muons) and uncharged pseudoscalars (they are the neutral pions) – from formulae (H4.7) and (H4.8) we obtain that durations of such GRBs are **30 seconds, 0.007 second, and 0.3 second respectively** which is consistent with observational data. Higher number density of GRBs follows from the fact that the nuclear energy produced in center of stars is easier transferred to their surface by uncharged and spin-0 objects so such stars are less stable – it leads to higher abundances of such GRBs.

Consider a star or binary system of stars with total mass which relates to mass of the hyperon $\Lambda = 1115.3 \text{ MeV}$. From formulae (H4.7) and (H4.8) we obtain that some stellar analog to the hyperon Λ has mass equal to $M_{\Lambda} = 24.81 \cdot 1115.3 / 939.57 = 29.45 \text{ solar masses}$, i.e. such star is more massive than NBH. From (H4.8) we obtain that the burst should last

$$t_{\text{Burst,GRB080916C}} = 716 (M_{\Lambda} / M_{\text{NBH}})^4 = 1422 \text{ s} = 23.7 \text{ min} . \quad (\text{H4.9})$$

In the final stage there should appear new NBH while the mass equal to $29.45 - 24.81 = 4.64$ [solar masses] should be emitted as the gamma rays. Since total energy of the Sun is about $1.8 \cdot 10^{54} \text{ erg}$ so emitted isotropic energy should be about $4.64 \cdot 1.8 \cdot 10^{54} = 8.4 \cdot 10^{54} \text{ erg}$.

We can compare these results with data obtained by the Fermi LAT and Fermi GBM Collaborations [1]. They obtained $\sim 1400 \text{ s}$ and $\sim 8.8 \cdot 10^{54} \text{ erg}$ respectively.

References

- [1] The Fermi LAT and Fermi GBM Collaborations (27 March 2009). “Fermi Observations of High-Energy Gamma-Ray Emission from GRB 080916C”
Science VOL 323, pp: 1688-1693
https://www.openu.ac.il/personal_sites/yoni-granot/papers/GRB080916C_Science.pdf

H5. New theory of the Solar System

Here we show that the Titius-Bode (TB) law is a characteristic feature of the surroundings of various types of black holes. Only a star that is a remnant of a black hole may be surrounded by rings (or planets) whose radii (or semi-major axes) are defined by TB law. We explained the origin of Neptune and other massive planets, Kuiper belt and Oort cloud.

The structure of protons, because of the virtual processes in the SST-As and due to the adoption symmetry, leaks outside them – it concerns all the SST types of black holes and it is valid for all size scales. Such is also the origin of the Titius-Bode law for the gravitational black holes – the successive symmetrical decays of the nuclei containing 256 nucleons additionally enforce the adoption symmetry. The initial rings around a black hole were produced in accretion disc.

In the TB law for the Solar System, we have

$$A^* / B^* = 1.3898 , \quad (\text{H5.1})$$

$$A^* + 2B^* = 1 \text{ au} , \quad (\text{H5.2})$$

so we obtain $A^* = 0.41 \text{ au}$ and $B^* = 0.295 \text{ au}$.

Ranges of objects are inversely proportional to their masses so we have:

A^* relates to atomic mass number equal to 256 – it is the semi-major axis of Mercury,

$A^* + B^*$ relates to atomic mass number 256 ~~too~~ but it decays to two parts (for Venus),

$A^* + 2B^*$ relates to 128 (for Earth),

$A^* + 4B^*$ relates to 64 (for Mars),

$A^* + 8B^*$ relates to 32 (for the asteroid/dwarf-planet Ceres),

$A^* + 16B^*$ relates to 16 (for Jupiter),

$A^* + 32B^*$ relates to 8 (for Saturn),

$A^* + 64B^*$ relates to 4 (for Uranus),

$A^* + 96B^*$ relates to 3 (for Neptune): it is not the TB orbit,

$A^* + 128B^*$ relates to 2 (for Pluto),

$A^* + 256B^*$ relates to 1: it is outside the Kuiper cliff so such orbit can be empty. (H5.3)

Assume that a progenitor of the Solar System was a black hole composed of $4^4 = 256$ NBHs so the mass of the progenitor was

$$M_{\text{Progenitor}} = 4^4 m_{\text{NBH}} = 1.263 \cdot 10^{34} \text{ kg} , \quad (\text{H5.4})$$

where $m_{\text{NBH}} = 24.81 \text{ solar masses}$.

Now the central mass is

$$M_{\text{Sun}} = 1.9885 \cdot 10^{30} \text{ kg} . \quad (\text{H5.5})$$

Range is inversely proportional to mass so the semi-major axes of the rings increased following number of times

$$F = M_{\text{Progenitor}} / M_{\text{Sun}} = 6352 . \quad (\text{H5.6})$$

At the beginning, the radius of the Mercury ring, $A_{\text{Beginning}}$, was equal to

$$A_{\text{Beginning}} = G M_{\text{Progenitor}} / c^2 = 9.379 \cdot 10^6 \text{ m} . \quad (\text{H5.7})$$

Now the semi-major axis of Mercury should be

$$A_{\text{Now}} = F A_{\text{Beginning}} = 5.958 \cdot 10^{10} \text{ m} = 0.398 \text{ au} . \quad (\text{H5.8})$$

This value is very close to the actual semi-major axis of Mercury $A_{\text{Mercury,actual}} = 0.387 \text{ au}$. The difference is ~3%.

Can we show that the relationships between the gravitational black holes and the strong black holes in baryons are not only related to the TB law?

Mass of the charged core of baryons is $H^\pm = 727.4387 \text{ MeV}$. It interacts electromagnetically via the bare electron-positron pair which mass is $2m_{e,\text{bare}} = 1.0208 \text{ MeV}$. Assume that mass of the Sun, M_{Sun} , relates to H^\pm while the sum of the masses H^\pm and $2m_{e,\text{bare}}$ relates to the total mass of the Solar System $M_{\text{Solar-System}}$ – then we obtain

$$M_{\text{Sun}} / M_{\text{Solar-System}} = H^{\pm} / (H^{\pm} + 2m_{e,\text{bare}}) = 0.9986 . \quad (\text{H5.9})$$

This value is in perfect agreement with the observational data (see page 10 in [1]).

The Oort cloud contains the long period comets and extends from between $\sim 2,000$ and $\sim 5,000$ au to $\sim 200,000$ au from the Sun [2]. The models based on the observations of the comets suggest that the Oort cloud is divided into two regions: a spherical outer cloud and a scattered disc [3]. As the distance from the Sun increases, the scattered disc expands more and more in the directions transverse to the disc.

With time, the initial black hole was replaced by the Type-Ia supernova. Here we show that the Oort cloud was formed due to the scattering of matter on the Mercury orbit during the Type-Ia supernova (SN) explosion.

In SST, the key role in fermions plays torus. The strong interactions in baryons are associated with the radial motions of gluons emitted by a torus – such interactions, because of the internal structure of the torus, are possible only in hadrons. The electromagnetic interactions relate to the toroidal motions in the plane of the equator of the torus, while the weak interactions relate to the poloidal motions. We can see that the three motions are orthogonal! The poloidal motions are perpendicular to the equatorial plane of the torus so they scatter the radial and toroidal motions.

Most of matter on the Mercury orbit, because of the conservation of the angular momentum, was scattered in the plane of the Mercury orbit. The scattered disc-like region in the Oort cloud is a result of the increasing spin speed of the thin matter torus that overlapped with the Mercury orbit so it was due to the electromagnetic interactions at high energy. On the other hand, the spherical region in the Oort cloud is a result of a volumetric expansion of the thin torus – there appeared the radial motions so it was due to the nuclear strong interactions.

The radius of the Mercury orbit, $A_{\text{SN-Ia}}$, just before the supernova explosion, was

$$A_{\text{SN-Ia}} = A_{\text{Now}} M_{\text{Sun}} / M_{\text{SN-Ia}} = 0.2856 \text{ au} , \quad (\text{H5.10})$$

where $M_{\text{SN-Ia}} = 1.3934$ **solar masses** (see formula (H4.8) for $\mu_{\text{bare}}^{\pm}/2$).

The inner radius, $R_{\text{Oort,inner}}$, of the inner edge of the scattered disc in the Oort cloud follows from the transition from the electromagnetic interactions at high energy on the Mercury orbit to the weak interactions of electrons on the inner edge of the scattered disc. Radius is inversely proportional to coupling constant so we have

$$R_{\text{Oort,inner}} = A_{\text{SN-Ia}} \alpha_{\text{em,high}} / \alpha_{w(e)} \approx 2,350 \text{ au} , \quad (\text{H5.11})$$

where $\alpha_{w(e)} = 0.95111818868 \cdot 10^{-6}$ is the coupling constant of the weak interactions of electrons, and $\alpha_{\text{em,high}} = 1 / 127.5425$ (see (2.3.15)). The “mixture” of the toroidal electromagnetic motions and the radial strong motions caused that with increasing distance from the Sun, the scattered disc expands more and more in the directions transverse to the disc.

The intermediate semi-major axes for the objects in the scattered disc we obtain for the mixed interactions in the Mercury orbit – here they are the strong and electromagnetic interactions.

The inner radius, $R_{\text{Oort,inner-sphere}}$, and outer radius, $R_{\text{Oort,outer-sphere}}$, of the spherical region in the Oort cloud result from the transition from the nuclear strong interactions on the Mercury orbit to the weak interactions of electrons on the most distant sphere. But during the supernova explosion, on the Mercury orbit appeared the turbulent motions so baryons had the relativistic masses. In such nuclear plasma, the coupling constant of the nuclear strong interactions is the

running coupling – inside baryons it changes from $\alpha_{\text{sw,asymptote}} = 0.1138$ (see c_u in (2.4.40)) to $\alpha_s = 1$. Such values define the inner radius and outer radius of the spherical region in the Oort cloud

$$R_{\text{Oort,inner-sphere}} = A_{\text{SN-Ia}} \alpha_{\text{sw,asymptote}} / \alpha_{\text{w(e)}} \approx 34,000 \text{ au} , \quad (\text{H5.12})$$

$$R_{\text{Oort,outer-sphere}} = A_{\text{SN-Ia}} \alpha_s / \alpha_{\text{w(e)}} \approx 300,000 \text{ au} = 4.75 \text{ ly} . \quad (\text{H5.13})$$

The weak interactions of the electrons are very weak in relation to the strong and electromagnetic interactions of baryons so we neglect a deformation of the Oort cloud resulting from the poloidal motions.

We can see also that the mass of the Oort cloud should be close to the mass of the thin torus which overlapped with the Mercury orbit so it should be close to masses of planets.

Notice also that for the weak interactions of nucleons we obtain

$$R^*_{\text{Oort}} = A_{\text{SN-Ia}} \alpha_{\text{w(p)}} / \alpha_{\text{w(e)}} \approx 5,600 \text{ au} , \quad (\text{H5.14})$$

so for such and bigger distances, the number density of comets should be higher. Moreover, such a region should be deformed due to the poloidal motions.

We showed that SST leads to a spherical outer Oort cloud that should extend from $\sim 34,000 \text{ au}$ to $\sim 300,000 \text{ au}$, while a scattered-disc inner Oort cloud should extend from $\sim 2,350 \text{ au}$ to $\sim 34,000 \text{ au}$.

Why, unlike the radii of the planetary rings, did not the semi-major axes of the long-period comets in the Oort cloud increase in size following the SN-Ia explosion?

The thin torus of the nuclear plasma with its internal nuclear strong interactions, which overlapped with the orbit of Mercury, shielded the planetary ring system from destruction and mass changes during the supernova explosion.

Moreover, such a thin torus caused the disc part of the Oort cloud to be scattered.

Over time, as part of the ejected mass by the supernova (about 0.4 solar mass) flowed through the just formed Oort cloud, the masses of the components of this cloud increased, but on the other hand, the decreasing central mass decreased the orbital speeds of the comets. Since the orbital angular momentums of comets must be conserved, which is the product of mass, orbital velocity, and orbital radius, the semi-major axes of comets, contrary to the radii of the planetary rings, should not change significantly – they could decrease as well.

The mechanism of the formation and evolution of the Oort cloud described in this section differs significantly from that proposed in mainstream astrophysics. Under the mainstream mechanism, unlike the one presented here, we cannot accurately predict the properties of the Oort cloud. We can see, however, that the appearing free parameters in the mainstream mechanism allow us to obtain values of some physical quantities consistent with the observations, but such additional parameters strongly distort the physical picture. Therefore, I warn against theories, models and simulations in which there are free parameters.

From the observations results that a mean mass of the long-period comets is about $5 \cdot 10^{12} \text{ kg}$ – the estimated masses of a set of long-period comets are $[0.5, 10] \cdot 10^{12} \text{ kg}$ [4]. The number of long-period comets is $\sim 10^{12}$ [5].

From observational data results that the more massive black holes (as, for example, in quasars) are surrounded by an opaque torus. Assume that our black hole composed of the 256 NBHs also was surrounded by such a torus. Assume also that the characteristic sizes of the black hole and its torus were directly proportional to the sizes in the core of baryons.

On the assumption that the radius of the central condensate in baryons relates to the present-day semi-major axis of Mercury, $A_{\text{Mercury,actual}} = 0.387 \text{ au}$, we obtain that the today mean distance of the initial opaque torus from the Sun, $R_{\text{Torus,mean}}$, should be

$$R_{\text{Torus,mean}} = A_{\text{Mercury,actual}} / \alpha_{w(p)} \approx 20.7 \text{ au} , \quad (\text{H5.15})$$

while its today equatorial radius, $R_{\text{Torus,equator}}$, should be

$$R_{\text{Torus,equator}} = R_{\text{Torus,mean}}^{3/2} \approx 31.0 \text{ au} . \quad (\text{H5.16})$$

We can see that the calculated distances are close to the present-day semi-major axes of the Uranus (19.2 au) and Neptune (30.1 au), respectively, so there should be formed the Neptune even when the symmetry describing the symmetrical decays is not broken.

Today, the inner radius of the opaque torus, $R_{\text{Torus,inner}}$, should be equal to 1/3 of its equatorial radius

$$R_{\text{Torus,inner}} = R_{\text{Torus,equator}} / 3 \approx 10.3 \text{ au} . \quad (\text{H5.17})$$

Table H5 *Comparison of semi-major axes in [au]*

	$R_{\text{SM-O}}$ from observations	$R_{\text{SM-T}}$ from opaque torus	$R_{\text{SM-TB}}$ from TB
Saturn	9.6	10.3	9.9
Uranus	19.2	20.7	19.3
Neptune	30.1	31.0	28.7

The value in (H5.17) is close to the semi-major axis of the Saturn (9.6 au).

In Table H5, we compared the observed semi-major axes, $R_{\text{SM-O}}$, of the Saturn, Uranus and Neptune with semi-major axes calculated from the sizes of the opaque torus, $R_{\text{SM-T}}$, and from the TB law that follows from the symmetrical decays of the atomic nuclei ($R_{\text{SM-TB}} [\text{au}] = 0.41 + d \cdot 0.295$, where $d = 32, 64$ and 96).

Initially, the orbits of Saturn, Uranus and Neptune were additionally fed with matter from the opaque torus so the three planets are today the massive planets. But why is the Jupiter the most massive planet? Initially, the inner accretion disc (i.e. from the black hole to the opaque torus) also was fed with matter from the opaque torus. On the other hand, the Jupiter orbit was the closest orbit to the inner boundary of the opaque torus – it is the reason that today Jupiter is the most massive planet.

A short recapitulation

It is impossible to understand the cosmogony of the Solar System without two new symmetries described in SST, i.e. the adoption symmetry and symmetrical decays of atomic nuclei in nuclear plasma.

The large-scale structure of the Universe we are seeing today was formed before it began to expand.

The cosmogony of the Solar System begins with a black hole containing 256 NBHs, which captures the extra NBH and converts it into an accretion disc.

Notice that there was a quantum resonance between the 256 NBHs in the black hole and the 256 nucleons in the atomic nuclei created in the nuclear plasma near the equator of the black hole.

The inflows of dark energy and dark-matter loops cause that the black hole evaporates, ejecting matter mainly along its axis of rotation. This mechanism causes protoplanet orbital radii to increase.

When the central star's mass decreased to about 1.4 solar masses, it exploded as a supernova, a key moment for the survival of the Solar System. Our Sun was formed about 4.6 Gyr ago from the remnants of such an explosion.

The question is: where are the remaining fragments of the original black hole? New stars were formed from the nuclear plasma ejected along the axis of rotation, and these are stars scattered around the Solar System inside a sphere with a radius of about 100 light-years.

The only planet whose semi-major axis does not obey the TB law is Neptune, but note that the symmetry of symmetrical decays relates to hot nuclear plasma. Thus, this symmetry at the periphery of the accretion disc can be broken. Helium-4 is for Uranus and deuterium is for Pluto, so the orbit for the stable He-3 should have a semi-major axis which is the arithmetic mean of the semi-major axes of Uranus and Pluto – this is consistent with the observational data for Neptune. Notice that the broken symmetry for Neptune was forced by the fact that the Neptune orbit had overlapped with the equatorial radius of the opaque torus.

The Kuiper belt is the remnant of the outer edge of the initial accretion disc, while the Oort cloud is the remnant of the type Ia supernova explosion.

The Solar System is unique because its history goes back to the origins of our Universe and its structure could have been damaged many times.

References

- [1] M M Woolfson (2000). "The Origin and Evolution of the Solar System"
Institute of Physics Publishing, Bristol and Philadelphia
ISBN 0 7503 0457 X (hbk)
ISBN 0 7503 0458 8 (pbk)
- [2] www.phys.org/news/2015-08-oort-cloud.html
- [3] The European Space Agency
www.esa.int/ESA_Multimedia/Images/2014/12/Kuiper_Belt_and_Oort_Cloud_in_context
- [4] Julio A. Fernández, Andrea Sosa (October 2011). "Mass estimates of long-period comets coming close to the Sun"
EPSC Abstracts, Vol. 6, EPSC-DPS2011-152-1, 2011, EPSC-OPS Joint Meeting 2011
- [5] The European Space Agency
www.esa.int/Science_Exploration/Space_Science/Rosetta/How_many_comets_are_there

H6. Magnetars versus pulsars

Calculate the radius of the spin-1 dark-matter loops (see formula (2.1.20))

$$R_{\text{DM-loop,spin=1}} = \hbar / (M_{\text{DM-loop}} c) = 16.915 \text{ km} . \quad (\text{H6.1})$$

Such a radius of neutron star leads to its mass equal to the TOV limit, i.e. 2.441 **solar masses** (see formulae (3.3.3) and (3.3.4)). The spin speed of the resting DM loops is equal to c .

We claim that magnetars are the neutron stars interacting weakly with the spin-1 DM loops i.e. the initial mass of magnetars should be close to the TOV limit: $M_{\text{Magnetar}} = 4.854 \cdot 10^{30}$ **kg**. Due to the weak interactions of the spin-1 DM loops with the nuclear-plasma vortex on surface of a magnetar, angular momentum of the vortex increases. We define the nuclear plasma as the plasma composed of 50% of protons and 50% of neutrons. Initially the weak interaction increases the spin speed of the nuclear-plasma vortex so there is created the very strong magnetic field, but as time goes on, the star's rotation slows down so the strong

magnetic field weakens. Slowing the magnetar's rotation causes the radii of the DM loops to increase, separating them from the magnetar. Such increases in the radii of the DM loops combined with the weak interactions cause that the baryon matter is scattered, so with time mass of the magnetar decreases.

Magnetic axis of magnetar has the same direction as the angular momentum of the DM loops. In neutron-stars, there can be an angle different from zero between the magnetic axis and the axis of rotation.

Rotation of the free NSs is slowing down because of the friction between the rotating part of the SST absolute spacetime inside the NSs and the non-rotating part outside them.

The friction in the SST-As together with strong magnetic field causes the emission of the polarized electromagnetic radiation.

The observed pulse periods of the so-called "normal pulsars" are between 0.3 s and 3 s. Assume that a pulsar with a mass of the TOV limit (so its radius is $R_{\text{Magnetar}} = 1.6915 \cdot 10^4 \text{ m}$) has the pulse period equal to $t = 1 \text{ s}$. Then the spin speed of the nuclear-plasma vortex, v_{Vortex} , is

$$v_{\text{Vortex}} = 2 \pi R_{\text{Magnetar}} / t = 1.0628 \cdot 10^5 \text{ m/s} . \quad (\text{H6.2})$$

On the other hand, from (H1.10) follows (there instead the α_s is $2\alpha_{w(p)}$) that the DM loops, due to their weak interactions with the condensates in centres of baryons, increase the spin speed of the nuclear-plasma vortex to $v_{\text{Vortex-with-loops}}$

$$v_{\text{Vortex-with-loops}} = c (2\alpha_{w(p)})^{1/2} = 5.8013 \cdot 10^7 \text{ m/s} . \quad (\text{H6.3})$$

It means that the DM loops increase the spin speed and decrease the vortex period, t^* , N times

$$N = v_{\text{Vortex-with-loops}} / v_{\text{Vortex}} = 546 , \quad (\text{H6.4})$$

$$t^* = t / N = 1.83 \cdot 10^{-3} \text{ s} . \quad (\text{H6.5})$$

The Biot-Savart law relates magnetic fields to the currents. The magnetic field (magnetic flux density), B , at centre of a current loop (of the nuclear-plasma vortex) with a radius R is

$$B = \mu_o Q / (2 R t) , \quad (\text{H6.6})$$

where t is the period (in magnetars it is the vortex period t^*), $\mu_o \approx 1.26 \cdot 10^{-6} \text{ H/m}$ is the magnetic constant (the vacuum permeability), and Q is the total charge of the loop/vortex.

From (H6.6) results that magnetic field is inversely proportional to pulse period. Since the DM loops decrease the pulse period N times so magnetic field of a magnetar with such a mass is N times higher than the pulsar in the absence of the DM loops. We can see that magnetic fields of magnetars are indeed very strong.

The mass of the nuclear-plasma vortex, M_{Plasma} , should be as many times lower than the mass of the magnetar as the mass of the DM loop, $M_{\text{DM-loop}} = 2.07958 \cdot 10^{-47} \text{ kg}$, is lower than the mass n of the neutron

$$M_{\text{Plasma}} = M_{\text{Magnetar}} M_{\text{DM-loop}} / n = 6.027 \cdot 10^{10} \text{ kg} . \quad (\text{H6.7})$$

It leads to the total electric charge, Q , of the nuclear-plasma vortex

$$Q = e M_{\text{Plasma}} / (2 M_{\text{Nucleon}}) = 2.885 \cdot 10^{18} \text{ C} , \quad (\text{H6.8})$$

where e is the electric charge of proton, and M_{Nucleon} is the mean mass of proton and neutron.

From the Biot-Savart law with the vortex period t^* , we have

$$B_{\text{Magnetar}} = \mu_0 Q / (2 R_{\text{Magnetar}} t^*) = 5.87 \cdot 10^{10} \text{ T} . \quad (\text{H6.9})$$

This result is consistent with observational data because the magnetic field of magnetars is from 10^{10} to 10^{11} T.

The initial period of the nuclear-plasma vortex t^* in magnetar with the TOV-limit mass does not depend on initial period of pulsar

$$t^* = 2 \pi R_{\text{Magnetar}} / v_{\text{Vortex-with-loops}} = 1.83 \cdot 10^{-3} \text{ s} . \quad (\text{H6.10})$$

For such a magnetar, Q and R_{Magnetar} are the initially invariant values so the magnetic field equal to $\sim 6 \cdot 10^{10}$ T is the upper limit **unless there appears an accretion disc** (it strengthens magnetic field).

From formulae (H6.9) and (H6.3) follows that the ratio of the magnetic field of the nuclear-plasma vortex, B_{Nuclear} , to the magnetic field of the vortex of electrons, B_{Electron} , is

$$B_{\text{Nuclear}} / B_{\text{Electron}} = t^*_{\text{Electron}} / t^*_{\text{Nuclear}} = (\alpha_{w(p)} / \alpha_{w(e)})^{1/2} = 140.3 , \quad (\text{H6.11})$$

so we can neglect the B_{Electron} in comparison with the B_{Nuclear} .

The composition of the nuclear-plasma vortex suggests that there dominates ionized helium-4. Radius of the ground-state orbit/shell in helium, $R_{\text{Helium-4}}$, has the radius 4 times smaller than the Bohr first orbit in hydrogen

$$R_{\text{Helium-4}} = 0.52918 \cdot 10^{-10} \text{ m} / 4 = 0.1323 \cdot 10^{-10} \text{ m} . \quad (\text{H6.12})$$

From (H6.10) results that the $P \sim r_{\text{Pulsar}}$ is a relationship between the period, P , of a pulsar and its radius r_{Pulsar} . Assume that the first-time derivative of the period for pulsars, dP/dt (it defines the changes over time in period of the pulsars) is defined by the ratio of the radius of the DM loops overlapping with the ground-state orbit in helium-4, $R_{\text{Helium-4}}$, to radius of the DM loops overlapping with the magnetic equator of the pulsar. For $r_{\text{Pulsar}} = R_{\text{Magnetar}}$, we obtain

$$(dP/dt)_{\text{Pulsar}} = R_{\text{Helium-4}} / R_{\text{Magnetar}} = 0.7821 \cdot 10^{-15} \text{ s/s} . \quad (\text{H6.13})$$

From (H6.13) follows that pulsars with smaller the equatorial radii have the first-time derivative of the period higher. Such values for pulsars are consistent with the observational data – see Figure 1 in [1].

In the pulsars, there is the friction between the rotating and non-rotating parts of the Einstein spacetime. But the friction in magnetars is much stronger because there appears also the very strong friction between the neutron star and the nuclear-plasma vortex. We can assume that the friction in pulsars leads to the electroweak interactions so there are produced the electron-neutrino pairs with energy equal to the mass distance between the charged and neutral pions: it is $\Delta\pi \approx 4.6 \text{ MeV}$. On the other hand, the friction in magnetars leads to the nuclear strong interactions represented by the fundamental gluon loops with energy equal to $m_{\text{FGL}} = 67.544 \text{ MeV}$. We can assume that the thermodynamic temperature T in the Stefan-Boltzmann law (see formula (1.4.20)) is directly proportional to involved energy while the total emitted energy is directly proportional to the changes in period, so we have

$$(\text{dP}/\text{dt})_{\text{Magnetar}} / (\text{dP}/\text{dt})_{\text{Pulsar}} = (m_{\text{FGL}} / \Delta\pi)^4 = 4.6 \cdot 10^4 . \quad (\text{H6.14})$$

From (H6.13) and (H6.14) we obtain

$$(\text{dP}/\text{dt})_{\text{Magnetar}} = 3.6 \cdot 10^{-11} \text{ s/s} . \quad (\text{H6.15})$$

From (H6.13) and (H6.14) results that magnetars with smaller the equatorial radii have the first-time derivative of the period higher. Such values for magnetars are consistent with the observational data – see [2] and figure 1 in [1].

Due to the strong friction in magnetars between the nuclear-plasma vortex and neutron star, the high temperature of the very thin iron crust below the vortex sometimes damages it almost simultaneously at two or more points, each with a diameter of several dozen metres. Through the damages, high-energy photons and neutrinos from beta decays are emitted. The damages are quickly repaired when the local pressure is reduced – such a mechanism produces millisecond pulses, and their time distance may be a second or so. Such a phenomenon was observed in magnetar SGR 1935+2154 [3].

References

- [1] Australia Telescope National Facility. “Pulsars, magnetars and RRATs”
www.atnf.csiro.au/news/newsletter/jun06/RRATs.htm
- [2] McGill Online Magnetar Catalog (1 September 2020).
www.physics.mcgill.ca/~pulsar/magnetar/main.html
- [3] F. Kirsten, et al. (16 November 2020). “Detection of two bright radio bursts from magnetar SGR 1935+2154”
Nature Astronomy (2020), <https://doi.org/10.1038/s41550-020-01246-3>
arXiv:2007.0501v2 [astro-ph.HE] 9 October 2020

H7. Space roar and the second mass of the bottom quark

The space roar is the unsolved problem in cosmology and particle physics. Here, applying the SST, we showed that the ARCADE 2 [1] and other literature the space roar for frequencies from 22 MHz to 10 GHz follows from the atom-like structure of baryons and from the expansion of the Universe (the wavelengths increased $F_U = 72.16$ times). Here as well we calculated the second mass of the bottom quark: $m_{b,2} = 4167.6 \text{ MeV}$.

The radio background from ARCADE 2 and radio surveys is a factor of ~ 6 brighter than the estimated contribution of radio point sources [1].

According to the SST, the expanding Universe is the result of evolution of the cosmic structure (the Protoworld) that appeared after the SST inflation. Initially, the baryonic part of the Universe was the double loop with a radius of $R_{\text{Cosmological}} = 0.191109 \text{ Gly}$. The today

spatial radius of the sphere filled with baryonic matter is $R_{\text{BM, today}} = 13.79(1) \text{ Gly}$, so size of the baryonic part increased about F_U times

$$F_U = R_{\text{BM, today}} / R_{\text{Cosmological}} = 72.16(5), \quad (\text{H7.1})$$

and the same concerns the wavelengths that appeared at the beginning of the expansion of the Universe i.e. when the CMB was produced.

We showed that the black body spectrum (see Section 3.9) and the CMB anisotropy spectrum (see Section 3.6) are directly associated with the internal structure of baryons. On the other hand, the neutral pion ($\pi^0 = 134.97687 \text{ MeV}$ – see Section 2.4) is created on the circular axis which is the most inner orbit for the strong interactions in baryons while the SST bottom quark-antiquark pairs, $m_b m_{b, \text{anti}}$, are produced on the last TB orbit for the strong interactions (see Section 2.23).

The simplest neutral pion consists of four neutrinos, i.e. $E_{\text{neutrino}} = 33.7442 \text{ MeV}$, so at high energies, due to the four-object symmetry, it can create four the bottom quark-antiquark pairs – it is an octopole of bottom quarks that can decay to a photon pair. Due to the expansion of the Universe, frequency of such photons decreased F_U times. We see that the following transformations in the early Universe and in very hot baryonic plasma can appear

$$E_{\text{neutrino}} \rightarrow m_b m_{b, \text{anti}}. \quad (\text{H7.2})$$

Such transformations lead to following spectral index β

$$E_{\text{neutrino}}^\beta = 2 m_b. \quad (\text{H7.3})$$

In Section 2.23 we already calculated the first mass of the bottom quark

$$m_{b,1} = 4190.33 \text{ MeV} \quad (\text{H7.4})$$

so formula (H7.3) leads to the index β equal to ~ 2.56726 . But the spectral index should result from some interactions. Notice that the spectral index is close to the ratio of the coupling constant of the nuclear weak interactions ($\alpha_{w(p)} = 0.0187229$) to the fine structure constant ($\alpha_{em} = 1/137.035999$)

$$\beta = \alpha_{w(p)} / \alpha_{em} = 2.56571. \quad (\text{H7.5})$$

From (H7.3) and (H7.5) we can calculate the second mass of the bottom quark

$$m_{b,2} = 4167.6 \text{ MeV}. \quad (\text{H7.6})$$

According to PDG [2], applying the minimal subtraction scheme to absorb the infinities that arise in perturbative calculations beyond leading order, introduced independently by Gerard 't Hooft (1973) and Steven Weinberg (1973), the mass of the bottom quark is $m_{b, \text{exp}} = 4.18(3) \text{ GeV}$ so both theoretical results are consistent with the PDG result.

In collisions of baryons at high energies are created strings composed of the $X^+ X^-$ pairs with spins tangent to the strings – they can collapse to the SST-As condensates. Mass of such

string, m_{string} , is directly proportional to its length/wavelength, λ_{string} , and we have that frequency is directly proportional to mass of such string $v_{\text{string}} \sim m_{\text{string}}$

$$v_{\text{string}} \sim m_{\text{string}} \sim \lambda_{\text{string}} \quad (\text{H7.7})$$

so from the Wien's displacement law we have

$$\Delta T \sim 1 / v_{\text{string}} , \quad (\text{H7.8})$$

where ΔT is an excess temperature.

Due to the transition from the nuclear weak interactions to the electromagnetic interactions at low energy and because $m^\beta \sim v^\beta$, we have the transition

$$v_{\text{string}} \rightarrow v^\beta . \quad (\text{H7.9})$$

From the two last formulae we obtain

$$\Delta T v^\beta = T_o v_o^\beta . \quad (\text{H7.10})$$

i.e.

$$\Delta T = T_o (v / v_o)^{-\beta} . \quad (\text{H7.11})$$

Such power law distorts the frequency spectrum of the CMB.

Assume that at some temperature of the early Universe, from the strings were created octopoles of the $Y = 424.12174 \text{ MeV}$ condensates that decayed to photon pairs.

From (2.18.3) and because lifetime of a string is directly proportional to its length and mass we have

$$m_1 = m_2 (\alpha_2 / \alpha_1)^4 . \quad (\text{H7.12})$$

The transition from the nuclear weak interactions of the associations of the Y condensates to the weak interactions of the charged fermion-antifermion pairs in presence of dark matter ($\alpha'_{w(e),DM} = 1.1194462 \cdot 10^{-5}$) caused that the initial energy of the emitted photons was (see (H7.12))

$$E_{\gamma,\text{initial}} = 4 Y (\alpha_{w(p)} / \alpha'_{w(e),DM})^4 = 2.1681 \cdot 10^{-10} \text{ MeV} , \quad (\text{H7.13})$$

i.e.

$$m_{\gamma,\text{initial}} = F E_{\gamma,\text{initial}} = 3.8649 \cdot 10^{-40} \text{ kg} . \quad (\text{H7.14})$$

The initial frequency was

$$v_{\gamma,\text{initial}} = m_{\gamma,\text{initial}} c^2 / (2 \pi \hbar) = 52.423 \text{ GHz} . \quad (\text{H7.15})$$

From (H7.15) and (H7.1) we obtain the today frequency

$$\nu_o = \nu_{\gamma, \text{initial}} / F_U = 726.5 \text{ MHz} \quad (\text{H7.16})$$

so it relates to the today CMB temperature [2]

$$T_o = 2.7255 \text{ K} . \quad (\text{H7.17})$$

Our power law looks as follows

$$\Delta T = 2.7255 \text{ [K]} (\nu / 726.5 \text{ [MHz]})^{-\beta} . \quad (\text{H7.18})$$

From it follows that when ν increases then the excess ΔT decreases.

Our results are collected in Table H7.

Table H7 *Today frequency and excess temperature*

Octopole of ...	Today frequency ν	Excess temperature ΔT (formula (H7.18))
ΔE_{core}	$\sim 26 \text{ MHz}$	14,000 K
-----	310 MHz	24.2 K ARCADE 2 plus others: $24.1 \pm 2.1 \text{ K}$ [1]
Y	$\nu_o = 726.5 \text{ MHz}$	$T_o = 2.7255 \text{ K}$
-----	3.3 GHz	56 mK ARCADE 2: $54 \pm 6 \text{ mK}$ [1]
$m_{b,2}$	$\sim 7.1 \text{ GHz}$	7.9 mK

$$\beta = \alpha_{w(p)} / \alpha_{\text{em}} = 2.56571$$

References

- [1] D. J. Fixen, A. Kogut, *et al.* (17 May 2011). “ARCADE 2 Measurement of the Absolute Sky Brightness at 3–90 GHz”
The Astrophysical Journal, 734:5 (11pp)
- [2] P.A. Zyla, *et al.* (Particle Data Group)
Prog. Theor. Exp. Phys. **2020**, 083C01 (2020)

H8. Absorption profile from the primordial cold hydrogen field

Within the SST we calculated the baryonic-matter (BM) density (see formula (3.5.17)) that is a little lower than the observed density. It suggests that outside the hot baryonic field of the Protoworld that relates to the nuclear strong field in baryons (radius of such cosmological field was $R_U = 2\pi R_{\text{Cosmological}} = 1.201 \text{ Gly}$, where $R_{\text{Cosmological}} = 0.191109 \text{ Gly}$ (see Section 3.7 and formula (2.1.25)), there already before the expansion of the Universe was the primordial field of cold hydrogen. When the photons from the expanding Universe reached such field, there was created the absorption profile centred at $\nu_{\text{flip,initial}} = 1420.406 \text{ MHz}$ – it was due to the spin flip in the ground state of hydrogen atoms. There were absorbed photons with wavelength equal to $\lambda_{\text{flip}} = 0.21106 \text{ m}$. Since the today radius of the CMB is $R_{\text{CMB}} = 21.32(1) \text{ Gly}$ (see formula (3.5.4)) so the central frequency decreased to

$$\nu_{\text{flip,today}} = \nu_{\text{flip,initial}} R_U / R_{\text{CMB}} = 80.1 \text{ MHz} . \quad (\text{H8.1})$$

It is close to observational data [1].

The primordial hydrogen field outside the hot baryonic field of the Protoworld was very cold so the amplitude of the absorption profile must be today significantly high.

Notice also that described here phenomena did not lead to the mainstream Dark Ages in cosmology. When the Universe started to expand there was no a period called the Dark Ages.

References

- [1] Judd D. Bowman, *et al.* (13 October 2018). “An absorption profile centered at 78 megahertz in the sky-averaged spectrum”, arXiv:1810.05912 [astro-ph.CO]

H9. The SST large numbers law, Gravity versus the Standard Model, and the gravitational black holes

In SST, the ratio of the constant of the electron-positron electromagnetic interactions, G_{em} , to the gravitational constant, G , is exactly equal to the ratio of the gravitational-mass density of the SST absolute spacetime, ρ_{As} , to the inertial-mass density of the SST Higgs field, ρ_{Hf}

$$N_{em/gr} = G_{em} / G = \rho_{As} / \rho_{Hf} = 4.165798 \cdot 10^{42}. \quad (H9.1)$$

It is the SST large numbers law that follows from constancy of the SST initial parameters because there is the stable boundary of the inner Cosmos and very high dynamic pressure in the SST two-component spacetime.

We see that in the SST-As are created the electron-positron pairs i.e. this part of the SST spacetime relates to the electromagnetic interactions. On the other hand, in the SST superluminal Higgs field are created the gravitational fields i.e. this part of the SST spacetime relates to the gravitational interactions. Properties of the SST-As and SST-Hf are very different so unification of the electromagnetic interactions (also the weak and strong) with gravitational interactions (i.e. the Standard Model with Gravity) within the same methods is impossible.

The wrong assumption in the mainstream theories that the observed flows in the SST absolute spacetime (for example, by LIGO) are the gravitational waves suggests incorrectly that unification of the Standard Model and Gravity is possible.

Gravity appears because the neutrinos composed of the entanglons are placed in the SST Higgs field. On the other hand, the binary systems of neutrinos are the components of the SST absolute spacetime so SST shows that the internal structure of neutrinos marks the boundary between the gravitational fields and those described in the Standard Model.

The Schwarzschild surface is an abstract surface. Near the black holes (BHs) composed of the neutron black holes, the SST-As components, which have gravitational mass, spiral towards the centre of BH – it is because below equators of BHs ($R_{equator,BH} = GM/c^2$), orbital speed of the SST-As components should be higher than c . But due to the very high dynamic pressure ($\sim 10^{45}$ Pa) and constant speed of the neutrino-antineutrino pairs, these components are pulled along the BH's axis of rotation despite having a non-zero gravitational mass. The weak interactions between the SST-As jets and particles are the cause of the removal of gravitating matter from inside the black hole.

H10. Creation of dark energy (DE) and dark matter (DM)

Structure of the DM loops and DM tori we described in Section 2.1 – they were produced at the end of the SST inflation.

The increase in the relativistic mass of protons is a result of the formation of successive layers above the surface of the torus/electric-charge which is inside of the core of baryons. Such an increase does not cause a change in electric charge when the spins of the entangled

neutrino-antineutrino pairs are polarized along electric-field lines (they are the DE segments) which converge on the circular axis (see Fig.2) of the torus/electric-charge.

To form DM loops, the relativistic mass of the proton torus must be about 81.3% of the Planck's mass, $m_{\text{Planck}} = 2.1765 \cdot 10^{-8} \text{ kg}$, because then the DE segments contain K^2 of entangled stable neutrinos with spins polarized tangentially to the loop. The X^\pm torus has one layer built of the neutrino-antineutrino pairs so there must be created $K^2/2$ such layers. Then mass of such relativistic torus is

$$M_{\text{rel}} = X^\pm K^2 / 2 = 0.813 m_{\text{Planck}} . \quad (\text{H10.1})$$

The DE segments composed of K^2 stable neutrinos curl up into the DM loops while the DM loops were building blocks of the DM tori. To create the DM tori we need vortices excited in the SST absolute spacetime i.e. we need circular/poloidal flows on the torus/electric-charge in the cores of baryons because such flows force transformation of the DE segments into DM loops with sufficiently high linear density. **The DE segments wound around the proton torus.**

Due to the collapse of the outer shell of the expanding SST absolute spacetime at the end of the SST inflation, there was created the thickened SST-As near the front of the SST-As – it also had led to production of the DM tori by even resting baryons so probability of such phenomena was very high. But from (H10.1) results that production of the DM tori in Earth laboratories is impossible. We would have to be very lucky to detect the cosmological DM tori with a mass of $\sim 727.44 \text{ MeV}$.

The Protoworld was destroyed because the DM tori decayed to the DM loops with a mass of $\sim 2.0796 \cdot 10^{-47} \text{ kg}$. The cosmological DM loops took the angular momentum of the baryon plasma, so their radii increased significantly. Today we can learn the origin of dark matter mainly by studying the rotation curves of galaxies.

From (1.4.26) follows that G_i (so field density, ρ , as well) is directly proportional to coupling constant. The DE segments were produced due to the nuclear weak interactions while the DM loops and the DM tori due to the electromagnetic interactions (there are the closed lines of electric field). We see that the ratio of abundances/densities of DE, ρ_{DE} , and DM, ρ_{DM} , should be close to

$$\rho_{\text{DE}} / \rho_{\text{DM}} = \alpha_{\text{w(p)}} / \alpha_{\text{em}} = 2.5657 . \quad (\text{H10.2})$$

It is consistent with observational data: $(\rho_{\text{DE}} / \rho_{\text{DM}})_{\text{obs}} = 68.63\% / 26.46\% \approx 2.59$.

DE segments have much larger surface area than the SST-As components, so virtual photons moving divergently effectively pushed the DE segments out of the interior and immediate surroundings of the Protoworld. **Initially, the Protoworld was free from DE composed of the DE segments.**

There, at low energies, due to the electroweak interactions of electrons, can be created low-density DM loops (LDDMLs). We need short-lived circular electric currents to produce LDDMLs with different masses and radii. The tangle of LDDMLs creates a DM soliton. Such solitons are produced by circular currents excited in the brain and they are components of the mind. But the linear densities are too low to create low-density DM tori.

I. Particle physics

II. The origin of the transverse radii of hyperons at the LHC

Here we show that the effective Gaussian source radii for the proton-hyperon pairs obtained at the LHC follow from the atom-like structure of baryons.

The ALICE team at the LHC has shown that the source radii for the proton-hyperon pairs can be determined in proton-proton collisions via a function of the transverse mass m_T [GeV/c] [1]. They obtained an effective Gaussian source radius (we will call it the transverse radius) equal to 1.02(5) fm for $p-\Xi^-$ pairs and equal to 0.95(6) fm for $p-\Omega^-$ pairs. The average m_T of such pairs are 1.9 GeV/c and 2.2 GeV/c respectively.

In the relativistic proton-proton collisions, spins of protons are parallel or antiparallel to the direction of the collisions. On the other hand, the created gluon loops are in planes perpendicular to the direction of collisions. Thus, the breakdown of the gluon loops (or annihilation of the X^+X^- pairs) causes their masses to appear as transverse masses.

In interacting strongly hyperons, the gluon loops appear on the first four orbits with the radii equal to $R_{\text{FGL}} = 2A/3$, $R_{d=0} \approx A$, $R_{d=1} = A + B$, and $R_{d=2} = A + 2B$, so the mean transverse radius of all hyperons, $R_{\text{T,hyperons,SST}}$, should be

$$R_{\text{T,hyperons,SST}} = (R_{\text{FGL}} + R_{d=0} + R_{d=1} + R_{d=2}) / 4 = 1.0157 \text{ fm} \approx 1.02 \text{ fm} . \quad (\text{II.1})$$

We can see that our result is equal to the central value for the LHC $p-\Xi^-$ pairs.

The SST transverse mass for all proton-hyperon pairs, $m_{\text{T,hyperons,SST}}$, should be – the hyperon interacts strongly with proton via π_{bound}^0

$$\begin{aligned} m_{\text{T,hyperons,SST}} &= X^\pm + \pi_{\text{bound}}^0 + S_{(+),d=0} + S_{(+),d=1} + S_{(+),d=2} = \\ &= 1902 \text{ MeV} \approx 1.9 \text{ GeV} . \end{aligned} \quad (\text{II.2})$$

Why did the LHC experiment get different results for the $p-\Omega^-$ pairs?

Mass of the hyperon Ω^- is [2]

$$\Omega^- = 1672.45(29) \text{ MeV} . \quad (\text{II.3})$$

It means that a $p-S_{(+),d=0}$ pair can mimic the mass of the hyperon Ω^- because the mass distance is very low

$$p + S_{(+),d=0} = 1665.71 \text{ MeV} . \quad (\text{II.4})$$

In the $p-pS_{(+),d=0}$ pair, there are occupied only the states $d = 0$ and $d = 1$ (there does not appear an additional pion π_{bound}^0 but there are two the $S_{(+),d=0}$ gluon loops) so we have

$$R_{\text{T,p-pS}(+),\text{SST}} = (R_{d=0} + R_{d=1}) / 2 = 0.948 \text{ fm} \approx 0.95 \text{ fm} . \quad (\text{II.5})$$

We can see that our result is equal to the central value for the LHC $p-\Omega^-$ pairs.

The SST transverse mass for the $p-pS_{(+),d=0}$ pairs, $m_{\text{T,p-pS}(+),\text{SST}}$, should be

$$m_{\text{T,p-pS}(+),\text{SST}} = X^+ + 2S_{(+),d=0} + S_{(+),d=1} = 2196 \text{ MeV} \approx 2.2 \text{ GeV} . \quad (\text{II.6})$$

It also is consistent with the LHC result.

References

- [1] ALICE Collaboration (9 December 2020). “Unveiling the strong interaction among hadrons at the LHC”
Nature **588**, 232-238 (9 December 2020)
- [2] P.A. Zyla, *et al.* (Particle Data Group)
 Prog. Theor. Exp. Phys. **2020**, 083C01 (2020)

I2. Masses of Upsilon and chi_b mesons

Here we described composition and calculated masses of the Upsilon (Y) and chi_b (χ_b) mesons.

According to SST, the Upsilon mesons are the mesonic nuclei (see Section 2.20) defined by the $I^G(J^{PC}) = 0^-(1^{--})$, where I is the isospin, G is the isoparity (G-parity), J is the spin, P is the parity, and C is the charge conjugation, while the chi_b mesons contain the bottom quark-antiquark pair and are denoted by $\chi_{bJ}([J + 1]P)$ and defined by the $I^G(J^{PC}) = 0^+(J^{++})$, where $J = 0, 1$ and 2 .

We already calculated the mass of the ground state of the Upsilon mesons: $Y(1S) = 9464.92 \text{ MeV}$ (see Section 2.20) and the two masses of the bottom quark: $m_{b,1} = 4190.33 \text{ MeV}$ and $m_{b,2} = 4167.6 \text{ MeV}$ (see Section 2.23 and (H7.6) respectively).

To explain the mass spectrum of the Upsilon mesons we need some objects S_i defined by the $I^G(J^{PC}) = 0^+(0^{++})$ which can be entangled with the ground state i.e. with $Y(1S)$ for which is $I^G(J^{PC}) = 0^-(1^{--})$. Such objects must satisfy the four-object symmetry so from Section 2.26 results that number of particles in the S_i objects should be 4, 8 or 16. Moreover, the total electric charge, Q , and total spin, J , of S_i both must be equal to zero.

Table I2.1 *Upsilon mesons*

Upsilon meson	S_i 4, 8 or 16 particles, $Q = J = 0$	Composition	Theoretical mass [MeV]	Experimental mass [MeV] [1]
Y(1S)	----	Y(1S)	9464.92*	9460.30(26)
Y(2S)	$4 \pi^\pm$	Y(1S) + S_i	10023.20	10023.26(31)
Y(3S)	$6 \pi^\pm + 2 m_B$	Y(1S) + S_i	10352.77	10355.2(5)
Y(?)	$6 \pi^\pm + 2 m_{FGL}$	Y(1S) + S_i	10437.43	?
Y(4S)	$8 \pi^\pm$	Y(1S) + S_i	10581.48	10579.4(1.2)
Y(10860)	$8 \pi^\pm + 2 m_{FGL} + 6 m_B$	Y(1S) + S_i	10867.85	$10885.2^{+2.6}_{-1.6}$ $\Gamma = 37(4)$
Y(11020)	$8 \pi^\pm + 6 m_{FGL} + 2 m_B$	Y(1S) + S_i	11037.17	11000(4) $\Gamma = 24^{+8}_{-6}$
Y(11700)	$16 \pi^\pm$	Y(1S) + S_i	11698.05	?

*Notice that mass distance between our result and the experimental mass

is equal to $\pi^\pm - \pi^0$ so we can assume that our mass is the mass of the bound Y(1S).

To solve the problem we need following masses: mass of the charged pion: $\pi^\pm = 139.5703 \text{ MeV}$, mass of the fundamental gluon loop: $m_{FGL} = 67.5444 \text{ MeV}$, and mass/energy of the

gluons created due to the transitions between the baryonic shells: $m_B = 25.213 \text{ MeV}$ (see formula (2.21.2)).

In Table I2.1 we present our results concerning the Upsilon mesons.

We claim that the ground state of the χ_b mesons consists of the bottom quark-antiquark pair and the pair of the bosons responsible for creation of the TB orbits for the nuclear strong interactions: $M_{TB} = 750.29577 \text{ MeV}$ (see formula (2.7.16)). The mean mass of the bottom quark is $m_{b,\text{mean}} = 4178.97 \text{ MeV}$ so we have

$$\chi_{b0}(1P) = 2 (m_{b,\text{mean}} + M_{TB}) = 9858.53 \text{ MeV} . \quad (I2.1)$$

The quarks have antiparallel spins. The parity of $\chi_{b0}(1P)$ is positive while total spin and total charge are equal to zero.

We need some objects U_i defined by the $I^G(J^{PC}) = 0^+(1^{++})$ to explain the spin distances between χ_{b1} and χ_{b0} and between χ_{b2} and χ_{b1} . We need also some objects W_i defined by the $I^G(J^{PC}) = 0^+(0^{++})$ to explain the mass distance between $\chi_b(2P)$ and $\chi_b(1P)$ and between $\chi_b(3P)$ and $\chi_b(2P)$.

We claim that composition of the W_i objects is as follows (see Table 2)

$$W_{2P-1P} = 2 S_{(+),d=4} = 375.15 \text{ MeV} , \quad (I2.2)$$

$$W_{3P-2P} = S_{(o),d=4} + m_{FGL} = 254.43 \text{ MeV} , \quad (I2.3)$$

while composition of the U_i objects is as follows

$$U_{b1-b0} = m_B = 25.213 \text{ MeV} , \quad (I2.4)$$

$$U_{b2-b1} = m_B \alpha_{em} / \alpha_{w(p)} = 9.827 \text{ MeV} . \quad (I2.5)$$

Our results are collected in Table I2.2.

Table I2.2 *Chi_b mesons*

	χ_{b0} Theory [MeV]	χ_{b0} Exper. [1] [MeV]	χ_{b1} Theory [MeV]	χ_{b1} Exper. [1] [MeV]	χ_{b2} Theory [MeV]	χ_{b2} Exper. [1] [MeV]
1P	9858.53	9859.44(73)	9883.74	9892.7(57)	9893.57	9912.21(57)
2P	10233.68	10232.5(9)	10258.89	10255.46(72)	10268.72	10268.65(72)
3P	10488.11	-----	10513.32	10513.4(7)	10523.15	10524.0(8)

References

- [1] P.A. Zyla, *et al.* (Particle Data Group)
Prog. Theor. Exp. Phys. **2020**, 083C01 (2020)

I3. The neutron mean square charge radius and the origin of the Standard Model

New measurements of the charge radius of the neutron show that the neutron has a mean square charge radius of [1]

$$\langle r_n^2 \rangle = -0.1101 \pm 0.0089 \text{ fm}^2. \quad (\text{I3.1})$$

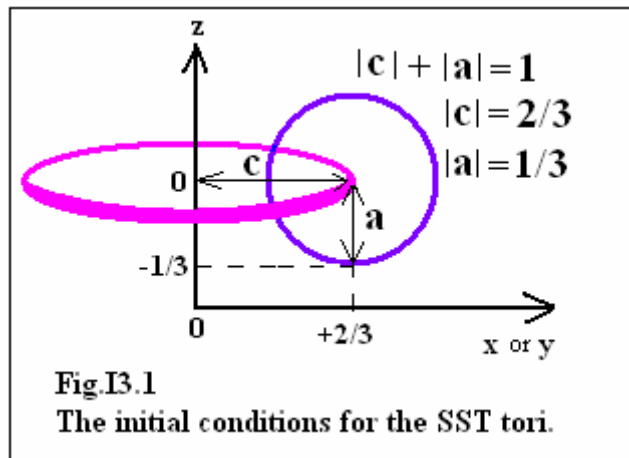
The negative sign in (I3.1) refers to the negatively charged cloud created by the relativistic negative pion located in the outer part of the neutron [2]. In SST, such pion is in orbit with radius $A + B$, where $A = 0.6974425 \text{ fm}$ and $B = 0.5018354 \text{ fm}$.

Quantum chromodynamics (QCD) leads to a positive core and a negative outer region in the neutron [3] – the same we have in SST for one state of the two states of neutron (frequency of occurrence of this state is $\sim 62.6\%$: see Section 2.7). In the second state of the neutron ($\sim 37.4\%$), all main components of the neutron are neutral (see Section 2.7).

The origin of the Standard Model

In SST, the electron charge consists of both the electron-loop that carries mass of the charge and the zero-mass ring-torus/electric-charge. The electron-loop and the equator of the torus practically overlap. The same concerns the quark charge – there is the gluon-loop and torus/quark-charge. The ring torus is most stable when for $|c| + |a| = 1$ is $|c| = 2/3$ and $|a| = 1/3$ (see Fig.I3.1). Such values lead from the elementary electric charge, e , ($|e| = 1$) to the electric charges of quarks ($q_{u,c,t} = +2/3$ and $q_{d,s,b} = -1/3$) in the Standard Model (SM).

The Kasner metric is an exact solution to theory of general relativity (GR) for an anisotropic universe without matter so it is a spacetime solution. For the dimensions $D = 3 + 1$ and the Kasner conditions we have $(2/3, 2/3, -1/3)$ [4]. Notice that the three number fractions as well represent the electric charges of quarks in the proton and in particles built of two quarks carrying the charge $+2/3$ and one carrying the charge $-1/3$. So there is a link between GR (a spacetime solution) and the quarks in some particles in SM.



The mean square charge radius of the neutron

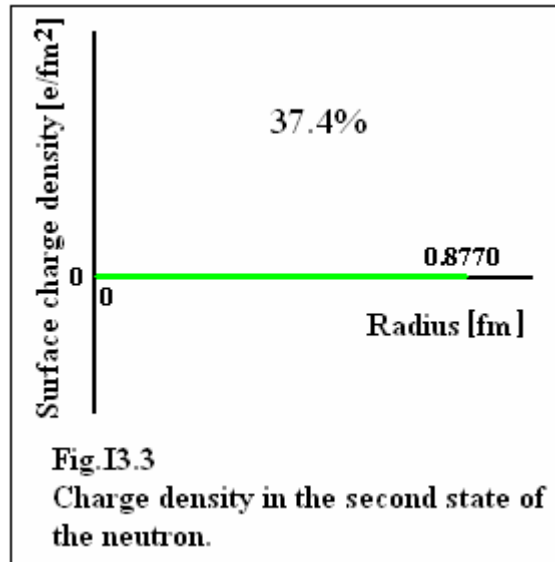
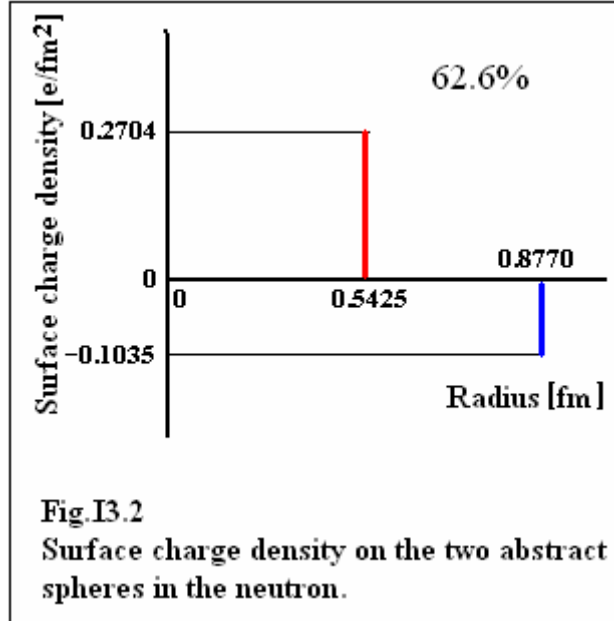
With time, a photon loop in a thermal neutron changes orientation of its plane so it leads to an abstract charged sphere. The negative pion in the $A + B$ state creates the negatively charged cloud – it is a cylinder with the orthogonal radii equal to $R_x^- = R_y^- = A + B$ and $R_z^- = A/3$.

The arithmetic mean of the above orthogonal radii, which is the radius of the abstract negatively charged sphere, which is the mean negative charge radius of the neutron, R_{o,n^-} , is

$$R_{o,n^-} = (R_x^- + R_y^- + R_z^-) / 3 = [2(A + B) + A / 3] / 3 = 0.877012 \text{ fm}. \quad (\text{I3.2})$$

Similar considerations for a positively charged photon loop (then the poloidal motion is left-handed) with a radius of $R_x^+ = R_y^+ = A$ (we assume that $R_z^+ = R_z^-$), which transforms into the torus/electric-charge in the core of baryons, lead to the mean positive charge radius of the neutron, $R_{o,n+}$

$$R_{o,n+} = (R_x^+ + R_y^+ + R_z^-) / 3 = (2A + A/3) / 3 = 0.542455 \text{ fm} . \quad (13.3)$$



The neutron mean charge radius, r_n , is defined as the distance between the two abstract charged spheres

$$r_n = R_{o,n-} - R_{o,n+} = 0.334557 \text{ fm} \quad (13.4)$$

so, in SST, the mean square charge radius of the neutron is

$$\langle r_n^2 \rangle = -0.11193 \text{ fm}^2 . \quad (13.5)$$

It is consistent with experimental data [1].

In Fig.I3.2, we present the surface density of electric charges on the abstract spheres in the first state of the neutron.

In Fig.I3.3, we present the surface density of electric charges in the second state of the neutron.

The ratio of the radii of the two abstract electrically charged spheres is close to the golden ratio (~ 1.618)

$$R_{o,n-} / R_{o,n+} \approx 1.617 . \quad (I3.6)$$

References

- [1] Benjamin Heacock, *et al.* (10 September 2021). “Pendellösung interferometry probes the neutron charge radius, lattice dynamics, and fifth forces”
Science, 10 Sep 2021, Vol 373, Issue 6560, pp. 1239-1243,
DOI: 10.1126/science.abc2794
- [2] S. Kopecky, *et al.* (1995)
Phys. Rev. Lett. **74**, 2427 (1995)
- [3] Jo van den Brand, *et al.* (1996)
Physics World, February 35, 1996
- [4] Edward Kasner (1921). “Geometrical theorems on Einstein’s cosmological equations”
Am. J. Math. **43**, 217-221 (1921)

I4. Lepton universality

According to SST, both the electron and muon have similar structures with different sizes of the components (a loop, torus and central condensate) but there is a difference: contrary to the electron, inside the muon central condensate, there are two energetic neutrinos (see Section 2.10). It causes that interactions of the two different leptons are not the same so the magnetic moment of the muon is higher than it should be (see Section 2.10).

Lepton universality is defined as follows: All three types of charged lepton particles interact in the same way with other particles.

SST shows that the **B** bosons are produced inside baryons.

We will show that the different branching ratios, **BR**, for the decays $B^0 \rightarrow K_S^0 \mu^+ \mu^-$ and $B^0 \rightarrow K_S^0 e^+ e^-$ follow from the structure and dynamics of baryons.

According to SST, the $\mu^+ \mu^-$ pairs in B^0 are produced near the condensate **Y** in centre of the baryons so for production of the $B_{\mu^+ \mu^-}^0$ bosons (i.e. $K_S^0 \mu^+ \mu^- \rightarrow B_{\mu^+ \mu^-}^0$) are responsible the nuclear weak interactions ($\alpha_{w(p)} = 0.0187229$: see (2.4.15)). **Notice that particles “remember” which coupling constants were responsible for their production so in the decays of such $B_{\mu^+ \mu^-}^0$ bosons appear the $\mu^+ \mu^-$ pairs.**

On the other hand, the $e^+ e^-$ pairs are produced outside the electrically charged core of baryons so for the production of the $B_{e^+ e^-}^0$ bosons (i.e. $K_S^0 e^+ e^- \rightarrow B_{e^+ e^-}^0$) are responsible the nuclear electroweak interactions (i.e. $\alpha_{w(p)} + \alpha_{em}$, where α_{em} is the fine structure constant).

We define the branching ratio as inversely proportional to lifetime so by applying formula (1.4.29) we have

$$BR \sim \alpha_i , \quad (I4.1)$$

where α_i is the coupling constant responsible for production/decay of a particle.

Such remarks lead to the SST ratio, $R_{\text{SST,low-energy}}$, of the considered here two different branching ratios for decays of the B bosons at low energy

$$\begin{aligned} R_{\text{SST,low-energy}} (K_S^0 \text{ or } K^{*+}) &= \text{BR}(B^0_{\mu^+\mu^-} \rightarrow K_S^0 \mu^+ \mu^-) / \text{BR}(B^0_{e^+e^-} \rightarrow K_S^0 e^+ e^-) = \\ &= \alpha_{w(p)} / (\alpha_{w(p)} + \alpha_{em}) = 0.71955 . \end{aligned} \quad (\text{I4.2})$$

Emphasize that the result $R_{\text{SST,low-energy}} = 0.71955$ follow from the fact that inside baryons the electron-positron pairs are created more frequently than the $\mu^+ \mu^-$ pairs.

Value of the fine structure constant increases at high energies because there increases the local effective electric charge. For value about $\alpha_{em,\text{high-energy}} = 1 / 127.54$ (see (2.3.15)) we obtain

$$R_{\text{SST,high-energy}} (K_S^0 \text{ or } K^{*+}) = \alpha_{w(p)} / (\alpha_{w(p)} + \alpha_{em,\text{high-energy}}) = 0.7048 . \quad (\text{I4.3})$$

Our results, i.e. $R_{\text{SST,low-energy}} \approx 0.720$ and $R_{\text{SST,high-energy}} = 0.705$, are consistent with the last experimental data for $B^0 \rightarrow K_S^0 l^+ l^-$ decays and $B^+ \rightarrow K^{*+} l^+ l^-$ decays [1]

$$R(K_S^0) = 0.66^{+0.20}_{-0.14} (\text{stat.})^{+0.02}_{-0.04} (\text{syst.}) . \quad (\text{I4.4})$$

$$R(K^{*+}) = 0.70^{+0.18}_{-0.13} (\text{stat.})^{+0.03}_{-0.04} (\text{syst.}) . \quad (\text{I4.5})$$

More precise experimental data will show whether our atom-like structure and dynamics of baryons are correct.

References

[1] LHCb collaboration (19 October 2021).

“Tests of lepton universality using $B^0 \rightarrow K_S^0 l^+ l^-$ and $B^+ \rightarrow K^{*+} l^+ l^-$ decays”
arXiv:2110.09501v2 [hep-ex]

I5. The structure of Type-X particles

Here, using the Scale-Symmetric Theory, we have described all Type-X particles that are defined by the following quantum quantities: $I^G(J^{PC}) = 0^+(1^{++})$.

The $X(3872)$ particle (also known as $\chi_{c1}(3872)$) is an exotic meson candidate with a mass of $3871.65(6)$ MeV [1]. The origin of this particle is still not fully understood.

The last data concerning its prompt production at $(s_{\text{NN}})^{1/2} = 5.02$ TeV are presented in [2].

The quantum numbers of the Type-X particles (today they are called $f_1(\dots)$, $\chi_{c1}(\dots)$ and $\chi_{b1}(\dots)$) are defined as follows: $I^G(J^{PC}) = 0^+(1^{++})$ [1], [3]. There are nine such particles [1].

Here we will show that the internal structure of the Type-X mesons applies to all three types of interactions described in the Standard Model (SM), i.e. strong and weak and electromagnetic interactions, which allows for their better understanding. It is therefore a very important problem.

In SST, in the nuclear plasma at very high energy, the Titius-Bode (TB) orbits for the nuclear strong and electroweak interactions are destroyed so the intrinsic dynamics of the

cores of baryons dominates. Recently, the Type-X particles scientists detected in very hot nuclear plasma [2] so their creation must follow from structure of the core.

According to SST, in very hot nuclear plasma, the cores of baryons, for a short time, are packed to the maximum so they are moving slowly – then are created the Type-X and other particles so the coupling constant for the nuclear strong interactions inside baryons is not running and is $\alpha_s = 1$. On the other hand, the running coupling constant for nuclear strong interactions concerns relativistic baryons. Such a scenario greatly simplifies the dynamics of collisions at high energies.

The core consists of the torus/electric-charge, $X^\pm = 318.2955481 \text{ MeV}$, which produces the bare electron-positron pairs – they are responsible for the electromagnetic interactions defined by the fine-structure constant $\alpha_{em} = 1 / 137.035999085012$.

Inside the torus/electric-charge are produced the fundamental gluon loops (FGLs), $m_{FGL} = 67.544413 \text{ MeV}$, which are responsible for the nuclear strong interactions. Between nucleons in atomic nuclei or colliding nucleons are exchanged pions, so we can say that the neutral pion, $\pi^0 = 134.976874 \text{ MeV}$ (it is a pair of FGLs), is the ground state of the nuclear strong interactions. The coupling constant for the nuclear strong interactions depends on energy so it is the running coupling.

In centre of the torus/electric-charge, there is the spin-0 spacetime condensate $Y = 424.12176 \text{ MeV} \approx 4\mu^\pm$, where $\mu^\pm = 105.65838 \text{ MeV}$ denotes the muon. The spacetime condensates are built of the carriers of photons which are the rotational energies of the carriers. Photons and the bare electron-positrons pairs carry the electromagnetic interactions so the spacetime condensates can interact due to the electroweak interactions. When spins of the carriers of photons in a spacetime condensate do not rotate then the condensate interacts only due to the nuclear weak interactions defined by the coupling constant $\alpha_{w(p)} = 0.0187229$. At higher energies of colliding protons or atomic nuclei, there are created spacetime condensates with masses higher than Y .

Here we use also the following quantities.

*Mass of electron: $m_e \equiv e^\pm = 0.510998946 \text{ MeV}$.

*Bare mass of electron: $m_{e,bare} \equiv e_{bare}^\pm = 0.51040705135 \text{ MeV}$.

*Lifetime of the muon: $\tau_{muon} = 2.194935 \cdot 10^{-6} \text{ s}$.

*Mass of the condensate in muon: $M_{Con,Muon} \approx 52.768 \text{ MeV}$.

*Mass of the charged core of baryons: $H^\pm = 727.43922 \text{ MeV}$.

Notice that our theoretical results are very close to the central values of the experimental data [1].

In the core of baryons, most important are following transitions

$$m_{FGL} \rightarrow 2\pi m_{FGL} \text{ (or } 3.14159\dots \cdot \pi^0) \rightarrow Y \rightarrow 4 \mu^\pm \rightarrow k m_{e,bare} \text{ (} k \approx 828) \quad (15.1)$$

and there is involved at least one electron-positron pair $2m_{e,bare}$.

Our model of the Type-X particles is as follows.

A) SST shows that the FGLs in nuclear strong fields, despite the fact that they are the bosons (not fermions), behave as electrons in atoms so we can use the Pauli Exclusion Principle and the Hund's rule – it follows from the fact that both the nuclear strong fields and gluons have internal helicity. In reality, gluons have two internal helicities and one external helicity, i.e. they have three “colours” so there are 8 different gluons. In atoms, the first shell (K) can hold up to two electrons, the second one (L) can hold up to eight electrons ($2 + 6$), and so on. The K shell has one subshell called $1s$ – when it is fully filled there are **two** electrons ($1s^2$). The next L shell has two subshells called $2s$ and $2p$ – when it is fully filled there are eight electrons ($2s^2 2p^6$). The fully filled two first shells contain **ten** electrons ($1s^2 2s^2 2p^6$).

Most stable should be particles with fully filled nuclear shells, i.e. a ground state should contain two FGLs, while the first excited state should contain ten FGLs.

Masses of the central spacetime condensate in the Type-X different particles must be different. It follows from the fact that all particles are created simultaneously so mass of central condensate in the ground state also must be unique.

The spacetime condensates interact weakly and electromagnetically so the product $\alpha_{w(p)}\alpha_{em}$ relates to the ground state (when interactions occur one after the other, the total coupling constant is the product of the coupling constants).

B) Assume that the X(3872) is the most ground state of the $I^G(J^{PC}) = 0^+(1^{++})$ particles. There should be a spacetime condensate, $M_{Con,EW}$ ($M_{Con,EW}: J^{PC} = 0^{++}$), two separated FGLs ($2m_{FGL}: J^{PC} = 0^{++}$), and a pair of one real and one virtual spin-1 e^+e^- pairs, Q ($Q = e^+e^- + [e^+e^-]_{virtual} = 1.022 \text{ MeV}$). On the other hand, in decays of X(3872) we sometimes observe only one electron-positron pair or only one particle-antiparticle pair composed of charged particles – it leads to conclusion that the observed J of Q is 1. The observed parity and charge parity of the Q both should be +1. So we have for Q : $(J^{PC})_{Observed} = 1^{++}$. The Q is exchanged between the spacetime condensate and the FGLs.

The Q is a quadrupole of fermions – the four-fermion symmetry dominates in the core of baryons.

C) Quantization of the mass $M_{Con,EW}$ follows from the condition that its electroweak mass is equal to mass of the bare electron.

Mass of the spacetime condensate $M_{Con,EW}$

In SST, when interactions of a particle with a mass M are defined by a coupling constant α_i then there are created objects with masses equal to M_i

$$M_i = \alpha_i M . \quad (15.2)$$

When interactions occur one after the other, the total coupling constant is the product of the coupling constants

$$M_{Total} = \prod_i \alpha_i M . \quad (15.3)$$

From point C) and from (15.3) we have

$$M_{Con,EW} \alpha_{em} \alpha_{w(p)} = m_{e,bare} \quad (15.4)$$

so we obtain

$$M_{\text{Con,EW}} = 3735.75 \text{ MeV} . \quad (15.5)$$

Structure and quantum numbers of X(3872)

From the point B) we have

$$M_{\text{Con,EW}}(3735.75 \text{ MeV}) + 2 m_{\text{FGL}} + Q = 3871.86 \text{ MeV} \text{ and } (J^{\text{PC}})_{\text{Observed}} = 1^{++} . \quad (15.6)$$

It is the X(3872) = 3871.65(6) MeV [1].

Lifetime of X(3872)

In SST, there is obligatory following formula for lifetime

$$\tau_{\text{Lifetime}} \sim 1 / \alpha . \quad (15.7)$$

Range of the nuclear strong interactions in baryons is $\sim 3.0 \text{ fm}$ so a typical lifetime for such interactions is $\tau_s \approx 3.0 \text{ [fm]} / c \approx 10^{-23} \text{ s}$.

The X(3872) decays due to the transition from the strong interactions of FGLs to the weak interactions of the spacetime condensate $M_{\text{Con,EW}}$, so we have

$$\tau_{\text{X(3872)}} = \tau_s \alpha_s / \alpha_{\text{w(p)}} \approx 5.3 \cdot 10^{-22} \text{ s} . \quad (15.8)$$

This lifetime relates to the full width $\Gamma \approx 1.2 \text{ MeV}$ ($\Gamma = \hbar / \tau_{\text{Lifetime}}$) – it is consistent with experimental data [1].

Masses of particles defined by $I^G (J^{\text{PC}}) = 0^+ (1^{++})$

We have 9 such particles: four χ_{c1} and three χ_{b1} (see Table I5) and two f_1 .

We claim that their basic states/particles (they are not the ground states with lowest energy/mass) are as follows: $\chi_{c1}(3872)$, $\chi_{b1}(2P)$ with a mass of 10255.46(72) MeV and $f_1(1285) = 1281.9(5) \text{ MeV}$ [1] – we prove it below.

To conserve the quantum numbers of the basic states, there can be realized following scenarios.

*The basic particles can absorb a pair of pions. When the pions are charged then there is produced a virtual spin-0 electron-positron pair. For such objects is $J^{\text{PC}} = 0^{++}$. Then mass of the basic particles increases by 269.95 MeV for two neutral pions and by 279.14 MeV for $\pi^+\pi^-$ pair with virtual spin-0 electron-positron pair. The mean value is $F_{\pi,\text{mean}} = 274.55 \text{ MeV}$.

*Next they can both absorb two separated FGLs with a total mass of $F_{\text{FGL}} = 2m_{\text{FGL}} = 135.09 \text{ MeV}$, or emit the X^+X^- pair with virtual spin-0 electron-positron pair – then the mass decreases by $F_{X(\pm)} = 636.59 \text{ MeV}$. For such objects is $J^{\text{PC}} = 0^{++}$.

The basic state of χ_{c1} is (it is the $1s^2$ state for the FGLs – the K shell)

$$\chi_{c1,\text{basic}} = M_{\text{Con,EW}} + 2 m_{\text{FGL}} + Q = 3871.86 \text{ MeV} . \quad (15.9)$$

Calculate mass of a spacetime condensate when two electromagnetic interactions occur one after the other – from (I5.3) we have

$$M_{\text{Con,EE}} \alpha_{\text{em}}^2 = m_{\text{e,bare}} \quad (I5.10)$$

so we obtain

$$M_{\text{Con,EE}} = 9584.86 \text{ MeV} . \quad (I5.11)$$

The basic state of χ_{b1} is (it is the $1s^2 2s^2 2p^6$ state for the FGLs – the K plus L shells)

$$\chi_{b1,\text{basic}} = M_{\text{Con,EE}} + 10 m_{\text{FGL}} + Q = 10261.32 \text{ MeV} . \quad (I5.12)$$

Assume that electromagnetic mass of a spacetime condensate $M_{\text{Con,E}}$ is equal to the mass of bare electron

$$M_{\text{Con,E}} \alpha_{\text{em}} = m_{\text{e,bare}} \quad (I5.13)$$

so $M_{\text{Con,E}} = 69.944 \text{ MeV}$.

Table I5 *The particles χ_c and χ_b with $I^G(J^{PC}) = 0^+(1^{++})$*

Structure	χ_{c1} Theory [MeV]	χ_{c1} Exper. [1] [MeV]	χ_{b1} Theory [MeV]	χ_{b1} Exper. [1] [MeV]
Basic	3871.86	3871.65(6)	10261.32	10255.46(72)
Basic+F $_{\pi,\text{mean}}$	4146.41	4146.8(2.4)	10535.87	10513.4(7)
Basic+F $_{\pi,\text{mean}}+F_{\text{FGL}}$	4281.50	4274 $^{+8}_{-4}$	10670.96	~10648 ?
Basic+F $_{\pi,\text{mean}}-F_{X(\pm)}$	3509.82	3510.67(5)	9899.28	9892.76(57)

Assume also that in the basic state of f_1 , there is fully filled the M shell (it is the $3s^2 3p^6 3d^{10}$ state, i.e. there are 18 the FGLs)

$$f_{1,\text{basic}} = f_1(1285) = M_{\text{Con,E}} + 18 m_{\text{FGL}} + Q = 1286.77 \text{ MeV} . \quad (I5.14)$$

The $f_1(1285)$ cannot emit the $F_{X(\pm)}$ as it is doing by the χ_c and χ_b particles because $M_{\text{Con,E}} \ll F_{X(\pm)}$. But the $f_1(1285)$ meson can fully fill the K shell for the FGLs ($1s^2$) so we have

$$f_1(1420) = f_1(1285) + 2 m_{\text{FGL}} = 1421.85 \text{ MeV} . \quad (I5.15)$$

Probably the $f_1(1420)$ meson can fully fill the L shell for the FGLs ($2s^2 2p^6$) so we have

$$f_1(1959) = f_1(1420) + 8 m_{\text{FGL}} = 1962.21 \text{ MeV} . \quad (I5.16)$$

We predict also a new $I^G(J^{PC}) = 0^+(1^{++})$ χ_b particle with a mass of (see Table I5)

$$\chi_{b1}(10659) \approx 10648 \div 10671 \text{ MeV} . \quad (I5.17)$$

The second proposal for the χ_{b1} mesons, that leads to similar a little lower masses, we present in Section **I2** – masses of them are closer to experimental data because they are created at lower energies nearly the edge of the strong fields, not in the cores of baryons.

To conserve the quantum numbers of the basic χ_c and χ_b mesons presented here, there must be absorbed or emitted the pairs composed of uncharged particles, i.e. $2m_{\text{FGL}}$ or $2\pi^0$, or the quadrupoles of charged particles, i.e. $2(\pi^\pm + m_{e,\text{virtual}})$ or $2(X^\pm + m_{e,\text{virtual}})$. Probability of absorption and emission of heavier pairs by the basic X particles is higher – it follows from the fact that lifetime of heavier pair is shorter so coupling constant is bigger and vice versa.

There are absorbed associations of gluons and there are emitted quadrupoles of fermions – it follows from the fact that there are the shells for FGLs while quadrupoles of fermions are emitted by spacetime condensates when they are excited by the absorbed FGLs. Probably the first absorption (of $2\pi^0$ or $2(\pi^\pm + m_{e,\text{virtual}})$) forces the emission of the X^+X^- pair of fermions by the spacetime condensate.

By the way, notice that coupling constants for electroweak interactions of condensates are weaker than the strong interactions of FGLs so the electroweak interactions are slower. When we neglect the hyperon Σ^0 , the hyperons are created quickly due to the strong interactions and decay slowly due to the weak interactions.

We can see that the stronger/faster interactions of the particles are, generally, realized first.

The other possibilities

Assume that nuclear weak mass of a spacetime condensate $M_{\text{Con,W}}$ is equal to the mass of bare electron

$$M_{\text{Con,W}} \alpha_{w(p)} = m_{e,\text{bare}} \quad (15.18)$$

so $M_{\text{Con,W}} = 27.261 \text{ MeV}$.

But SST shows that to create a metastable spacetime condensate, it should have mass equal or higher than the mass of the spacetime condensate in muon $M_{\text{Con,Muon}} \approx 52.768 \text{ MeV}$. It leads to conclusion that we should not observe some X particles containing $M_{\text{Con,W}}$.

Calculate mass of a spacetime condensate when two nuclear weak interactions occur one after the other – from (I5.3) we have

$$M_{\text{Con,WW}} \alpha_{w(p)}^2 = m_{e,\text{bare}} \quad (15.19)$$

so we obtain

$$M_{\text{Con,WW}} = 1456.03 \text{ MeV} . \quad (15.20)$$

But this mass is very close to mass of the $H^+H^- = 1454.88 \text{ MeV}$ pair so the condensate $M_{\text{Con,WW}}$ very quickly decays into such pair so some X particles containing such a condensate are not created.

Probability of creation of spacetime condensates due to three or more interactions occurring one after the other is very low so here we do not investigate them.

Summary

The strength of our model is simplicity and consistency of theoretical results with experimental data.

Very important is the fact that mass of the spacetime condensate in **X(3872)** is due to a *resonance* between its electroweak mass and mass of the bare electron! Therefore, there are no accidental coincidences in the presented model.

Emphasize that our theoretical masses for particles defined by the $I^G(J^{PC}) = 0^+(1^{++})$ quantum numbers are very close to experimental data – it validates our model of the core of baryons described within the Scale-Symmetric Theory. In the Standard Model, the calculate masses of particles are *much worse* than in SST, and in SM, we must apply much more parameters.

We showed that we can apply the Pauli Exclusion Principle and the Hund’s rule to the FGL shells around the spacetime condensates.

We predict two new Type-X particles.

The SM is incomplete and it partially incorrectly describes Nature. We are not only unable to define the structure and dynamics of dark matter and dark energy within SM, find the cause of the matter-antimatter asymmetry or explain why gravity and the SM interactions cannot be described within the same methods, but we are also unable to calculate the exact masses, spin and magnetic moments of the proton and neutron, so of the basic building blocks of ordinary matter. The origin of masses of neutrinos also cannot be explained within SM, also origin of physical constants and we cannot solve tens of fundamental problems. Contrary to the mainstream scientific community, we can safely say that in practice basic physics is in its infancy. Some physicists say we know almost everything, and the truth is, we know almost nothing. It really is time to come to your senses. Time for radical changes and the SST is an effective solution.

References

- [1] P.A. Zyla, *et al.* (Particle Data Group)
Prog. Theor. Exp. Phys. **2020**, 083C01 (2020) and 2021 update
- [2] CMS Collaboration (19 January 2022). “Evidence for X(3872) in Pb-Pb Collisions and Studies of its Prompt Production at $\sqrt{s_{NN}} = 5.02$ TeV”
Phys. Rev. Lett. **128**, 032001
arXiv:2102.13048
- [3] LHCb Collaboration (2013). “Determination of the X(3872) meson quantum numbers”
Phys. Rev. Lett. **110** (22): 222001
arXiv:1302.6269

I6. Internal structure of all particles

We already described internal structure of gauge bosons, Higgs bosons, leptons, masses of quarks, lightest mesons, kaons, $\Delta(1232)$ resonance, all Upsilon, nucleons, hyperons, all chi-b and the Type-X particles. Here we described all other baryons with 4- or 3-star status (144 baryons) and all other mesons marked with a dot on the list of mesons (116 mesons). We described also the pseudoscalar axion and solved the strong CP problem not via an axion field.

All masses are in MeV so for simplicity we omit units.

In baryons is a core and relativistic pions (we call them the W pions) in the $d = 1, 2$ and 4 states. At higher energies, there can appear relativistic pion or kaon in the $d = 0$ state that transform into the spacetime condensates, **C**, that are scalars. There can be created also neutral or charged gluon loops overlapping with the d states (we call them the S particles). The approximate masses of the W pions and S loops are listed in Table I6.1. The $XX = X^+X^- = 2 \cdot 318.2955 \text{ MeV} \approx 637 \text{ MeV}$ is mass of the pair composed of the torus/electric-charge in the

core of baryons and its antiparticle – mass of it in $d = 0$ state is 5732 MeV and such pseudoscalar, \mathbf{Ps}_{xx} , appears in the bottom charmed mesons.

For properties of hyperons are responsible the relativistic pions in the $d = 2$ state which is the ground state above the Schwarzschild surface for the nuclear strong interactions.

The experimental central masses of baryons and their resonances are from [1], [2] and [3].

The symbol $\Delta(1232 | 1233)$ means that it concerns the $\Delta(1232)$ resonance and that our theoretical mass is 1233 MeV and it is marked in red.

The symbol $\{3/2^+u\}$ means that $J = 3/2$, the sense of J is “up”, and the parity is $P = +1$. Our results are marked in red. The “d” in $\{3/2^+d\}$ means that the sense of J is “down”.

Table I6.1 *Masses of W pions and S loops [MeV]*

States d	$S_{(+),d}$	$S_{(o),d}$	$W_{(+),d}$	$W_{(o),d}$
0	727	725	$C_{\pi^\pm} = 1257$ $C_{K^\pm} = 4445$	$C_\pi = 1215$ $C_K = 4480$ $\mathbf{Ps}_{xx} = 5732$
1	423	421	216	209
2	298	297	182	176
4	188	187	162	157

The $I^G(J^{PC})$ quantum numbers in SST

The basic objects presented in Table I6.2 are created inside the nucleons, hyperons, and are the parts of mesons.

Table I6.2 *Basic objects created in baryons*

Object	Mass [MeV]	$I^G(J^{PC})$
π^0 (the single neutral pion)	135	$1^-(0^+)$
$\pi^{0,\pm}$	Mean 138	(0^-)
m_{FGL} (spin-1 fundamental gluon loop) $W_{(o)}$ gluons or $S_{(o)}$ open gluon loops ΔW_{2-4} (a gluon [1])	67.5 19.4	$0^-(1^-)$
$2m_{FGL}$ $2W_{(o)}$ or $2S_{(o)}$ $2\Delta W_{2-4}$ The single gluons in the pairs interact one with other	135 39	$0^+(0^+)$ or $0^+(2^-)$ *
$2m_{FGL}$ $2W_{(o)}$ or $2S_{(o)}$ or $2\Delta W_{2-4}$ The single gluons in the pairs do not interact with each other	135	$0^+(0^+)$ or $0^+(2^+)$
$3m_{FGL}$ The single gluons in the triplet do not interact with each other	203	$0^-(1^-)$
Spacetime condensates C		$0^+(0^+)$
Pseudoscalar \mathbf{Ps}_{xx}	5732	$0(0^-)$
$\mathbf{X^+X^-}$	637	(0^-) or (1^-)

*When spins are antiparallel then it behaves as neutral pion. When we change the sense of a vector boson in a particle then parity is conserved.

The transitions of the relativistic pions from the $d = 2$ state to the $d = 4$ state, cause that there appear the vector bosons with a mean mass $\Delta W_{2,4} = 19.367 \text{ MeV} \approx 19 \text{ MeV}$ $\{I^G(J^{PC}) = 0^-(1^-)\}$.

Notice that neutral pions are the binary systems of the FGLs.

We know that the baryon resonances decay due to the nuclear strong interactions. On the other hand, parity, P , is conserved in nuclear strong interactions and electromagnetic ones.

Below we present some examples concerning the SST.

The SST Higgs boson is the non-rotating spacetime condensate composed of the confined SST-absolute-spacetime (SST-As) components so it is a *scalar* $I^G(J^{PC}) = 0^+(0^{++})$. Such scalars decay, generally, to two photons. The same concerns the condensate in centre of baryons or the predicted in SST scalar with a mass of $\sim 17.1 \div 17.2 \text{ TeV}$.

The SST neutral pion is the *pseudoscalar* $J^{PC} = 0^{-+}$ (two spin-1 loops with antiparallel spins and the same internal helicity) – it decays to two photons. In such a way was organized the neutron matter in the Protoworld – there were the thin-disc massive protogalaxies composed of neutron stars so we observe too many massive thin-disc galaxies in comparison to the predicted number of them in the mainstream Lambda cold dark matter (Λ CDM) model in the standard model of cosmology.

Photon and gluon are the rotational energies of the SST-As components so they are the *vectors* $J^{PC} = 1^{--}$. The same concerns the spin-1 gluon loops and the open gluon loops created in the nuclear strong interactions. For the single vectors is $C = -1$ (photons in strong fields behave as gluons).

We define isospin as a number of members in a multiplet, N , minus one and then we divide it by two.

We already described the isospin selection rules for nucleons and hyperons.

Isospins, I , of the baryon resonances, because of the attached only neutral objects, are the same as the basic particles: $I = 1/2$ for N , $I = 3/2$ for Δ , $I = 0$ for Λ , $I = 1$ for Σ , $I = 1/2$ for Ξ and $I = 0$ for Ω . Isospin of baryons follows from number of charge states, N_Q

$$N_Q = 2 I + 1 . \quad (\text{I6.1})$$

The G-parity is defined as follows

$$G = (-1)^{I+S+L} . \quad (\text{I6.2})$$

SST shows that for the gluon loops (due to their behaviour) is $L = 0$, so we have

$$G = (-1)^{I+S} . \quad (\text{I6.3})$$

For the neutral pion is $I = 1$ and there are two gluon loops so we have $G = -1$.

For a single gluon we have $I + S = 1$ so $G = -1$.

But there are 17 mesons (about 12% of all mesons with defined $I^G(J^{PC})$) that do not fit to the above SST model: the 10 Type-X particles and 7 other particles, i.e. two a_1 mesons, two π_1 mesons, $\psi_2(3823)$, $R_{c0}(4240)$ and $Y_2(1D)$. We claim that such discrepancy follows from the fact that such particles contain the spin-0 quadrupole composed of one real spin-1 electron-positron pair and one virtual spin-1 electron-positron pair – for such an object is $I^G(J^{PC}) = 0^+(0^{++})$ but the unobserved spin-1 of the virtual pair causes that the observed quantum numbers are as follows: $\{I^G(J^{PC})\}_{\text{Observed}} = 0^+(1^{++})$ – its mass is $Q \approx 1 \text{ MeV}$.

Part 1: Baryons

$\Delta(1232)$

We already described the origin of the $\Delta(1232)$ resonance:

$\Delta(1232 | 1233) \{3/2^+\} = 1232.83 \text{ MeV}$ (see Section 2.22).

The basic objects in $\Delta(1232)$ are created in the $d = 2$ state, i.e. in the ground state above the Schwarzschild surface for the nuclear strong interactions. Radius of the $d = 2$ state is $R_{d=2} = 1.7011 \text{ fm}$. It means that the FGL produced in the core of baryons reaches the $d = 2$ orbit after $\tau = R_{d=2} / c = 5.67 \cdot 10^{-24} \text{ s}$. From formula $\Gamma = \hbar / \tau$ we can calculate the full width that relates to τ : **116 MeV**. On the other hand, the Breit-Wigner full width for mixed charges of the $\Delta(1232)$ is $114 < \Gamma < 120 \text{ MeV}$ [1] so our result (116 MeV) overlaps with the experimental data – it validates our assumption that the basic objects listed in Table I6.2 indeed are created in the $d = 2$ state.

J^P for $S_{(o),d=2}$ can be 1^- for open gluon loop and $\sim 2^-$ for gluon loop (it follows from the fact that when it behaves as the $S_{(o),d}$ object then there is $J \approx 2.6 \hbar$ while when it behaves as the $W_{(o),d}$ object there is $J \approx 1.6 \hbar$ so the mean value is $\sim 2.1 \hbar$). The mean value $\sim 2.1 \hbar$ is not equal to $J = 2$ so the correct structure of $\Delta(1232)$ is defined by formulae in Section 2.22. Moreover, the sum $N(939) + S_{(o),d=2} > \Delta(1232 | 1233)$ so the second state is the ground state.

From formula $\Gamma = \hbar c / R$ we know that width is inversely proportional to distance covered by gluons and that for $R \approx 1.7 \text{ fm}$ is about $\Gamma \approx 116 \text{ MeV}$ – it is for the Λ and Σ resonances. It means that when most of gluons are created in $d = 0$ state (then $\Delta R \approx 1 \text{ fm}$) then $\Gamma \approx 200 \text{ MeV}$, when most are created in $d = 1$ ($\Delta R \approx 0.5 \text{ fm}$) then $\Gamma \approx 400 \text{ MeV}$ – it is for the N and Δ resonances. When most are created on the $d = 2$ (then maximum distance is equal to diameter: $\Delta R \approx 3.4 \text{ fm}$) then $\Gamma \approx 60 \text{ MeV}$ – it is for the Ξ and Ω resonances. But different intrinsic interactions can change value of the mean full width. Generally, in more massive resonances gluons cover bigger distances.

There are the four charge states so isospin of $\Delta(1232)^{+++,0,-}$ is $I = 3/2$.

Nucleon resonances

$$N(939 | 939) \{1/2^+u\} + 4 \pi^0 \{0^+\} + m_{\text{FGL}} \{1^-d\} = N(1535 | 1547) \{1/2^-\}$$

$$N(939 | 939) \{1/2^+u\} + 2 S_{(o),d=2} \{2^-d\} = N(1520 | 1533) \{3/2^-\}$$

$$N(1520 | 1533) \{3/2^-u\} \rightarrow m_{\text{FGL}} \{1^-u\} + N(1440 | 1465) \{1/2^+u\}$$

$$N(1440 | 1465) \{1/2^+u\} + 3 m_{\text{FGL}} \{1^-d\} = N(1650 | 1668) \{1/2^-\}$$

$$N(1650 | 1668) \{1/2^-u\} + m_{\text{FGL}} \{1^-u\} = N(1720 | 1736) \{3/2^+\}$$

$$N(939 | 939) \{1/2^+u\} + S_{(o),d=2} \{1^-u\} + S_{(o),d=2} \{1^-d\} + 2 m_{\text{FGL}} \{2^-u\} = N(1675 | 1668) \{5/2^-\}$$

$$N(1535 | 1547) \{1/2^-u\} + 2 m_{\text{FGL}} \{2^-u\} = N(1680 | 1682) \{5/2^+\}$$

$$N(1680 | 1682) \{5/2^+u\} + \Delta W_{2-4} \{1^-d\} = N(1700 | 1701) \{3/2^-\}$$

$$N(1700 | 1701) \{3/2^-u\} + \Delta W_{2-4} \{1^-d\} = N(1710 | 1720) \{1/2^+\}$$

$$N(1720 | 1736) \{3/2^+u\} + 2 \pi^0 \{0^+\} + m_{\text{FGL}} \{1^-u\} = N(2060 | 2074) \{5/2^-\}$$

$$N(2060 | 2074) \{5/2^-u\} + 4 \pi^0 \{0^+\} = N(2570 | 2614) \{5/2^-\}$$

$$N(2060 | 2074) \{5/2^-u\} \rightarrow \Delta W_{2-4} \{1^-u\} + N(2040 | 2055) \{3/2^+u\}$$

$$N(1710 | 1720) \{1/2^+u\} + S_{(o),d=2} \{1^-d\} + m_{FGL} \{1^-u\} = N(2100 | 2085) \{1/2^+\}$$

$$N(2100 | 2085) \{1/2^+u\} \rightarrow 3 m_{FGL} \{1^-d\} + N(1875 | 1882) \{3/2^-u\}$$

$$N(1875 | 1882) \{3/2^-u\} \rightarrow \Delta W_{2-4} \{1^-d\} + N(1860 | 1863) \{5/2^+u\}$$

$$N(1875 | 1882) \{3/2^-u\} + \Delta W_{2-4} \{1^-d\} = N(1880 | 1901) \{1/2^+\}$$

$$N(1880 | 1901) \{1/2^+u\} + \Delta W_{2-4} \{1^-d\} = N(1895 | 1920) \{1/2^-\}$$

$$N(1895 | 1920) \{1/2^-u\} + \Delta W_{2-4} \{1^-u\} = N(1900 | 1939) \{3/2^+\}$$

$$N(1710 | 1720) \{1/2^+u\} + 2 \pi^0 \{0^+\} + 4 m_{FGL} \{4^+u\} = N(2220 | 2260) \{9/2^+\}$$

$$N(2220 | 2260) \{9/2^+u\} + 2 \pi^0 \{0^+\} + m_{FGL} \{1^-u\} = N(2600 | 2598) \{11/2^+\}$$

$$N(2220 | 2260) \{9/2^+u\} \rightarrow m_{FGL} \{1^-u\} + N(2190 | 2192) \{7/2^-u\}$$

$$N(2600 | 2598) \{11/2^+u\} + m_{FGL} \{1^-u\} + 2 \Delta W_{2-4} \{0^-\} = N(2700 | 2705) \{13/2^+\}$$

$$N(1700 | 1701) \{3/2^-u\} + S_{(o),d=2} \{1^-u\} = N(2000 | 1998) \{5/2^+\}$$

$$N(1720 | 1736) \{3/2^+u\} + \pi^0 \{0^-\} + 2 m_{FGL} \{2^-u\} = N(1990 | 2006) \{7/2^+\}$$

$$N(1680 | 1682) \{5/2^+u\} + 4 \pi^0 \{0^+\} + 2 \Delta W_{2-4} \{2^-u\} = N(2250 | 2261) \{9/2^-\}$$

$$N(1990 | 2006) \{7/2^+u\} + 2 m_{FGL} \{2^-d\} = N(2120 | 2141) \{3/2^-\}$$

$$N(2100 | 2085) \{1/2^+u\} + \pi^0 \{0^-\} + m_{FGL} \{1^-d\} = N(2300 | 2288) \{1/2^+\}$$

Delta resonances

$$\Delta(1232 | 1232.8) \{3/2^+u\} = N(938.92) \{1/2^+u\} + \pi^+_{rel}(274.55) \{0^-\} + \Delta W_{2-4}(19.37) \{1^-u\}$$

$$\Delta(1232 | 1233) \{3/2^+u\} + S_{(o),d=2} \{1^-u\} + m_{FGL} \{1^-d\} = \Delta(1600 | 1598) \{3/2^+\}$$

$$\Delta(1600 | 1598) \{3/2^+u\} + \Delta W_{2-4} \{1^-d\} = \Delta(1620 | 1617) \{1/2^-\}$$

$$\Delta(1620 | 1617) \{1/2^-u\} + \pi^0 \{0^-\} = \Delta(1750 | 1752) \{1/2^+\}$$

$$\Delta(1750 | 1752) \{1/2^+u\} \rightarrow m_{FGL} \{1^-d\} + \Delta(1700 | 1684) \{3/2^-u\}$$

$$\Delta(1620 | 1617) \{1/2^-u\} + 2 \pi^0 \{0^+\} = \Delta(1900 | 1887) \{1/2^-\}$$

$$\Delta(1900 | 1887) \{1/2^-u\} + 2 \Delta W_{2-4} \{2^-u\} = \Delta(1905 | 1926) \{5/2^+\}$$

$$\Delta(1900 | 1887) \{1/2^-u\} + \Delta W_{2-4} \{1^-d\} = \Delta(1910 | 1906) \{1/2^+\}$$

$$\begin{aligned}
\Delta(1900 | 1887) \{1/2^-u\} + \Delta W_{2-4} \{1^-u\} &= \Delta(1920 | 1906) \{3/2^+\} \\
\Delta(1920 | 1906) \{3/2^+u\} + \Delta W_{2-4} \{1^-u\} &= \Delta(1930 | 1925) \{5/2^-\} \\
\Delta(1910 | 1906) \{1/2^+u\} + \Delta W_{2-4} \{1^-u\} &= \Delta(1940 | 1925) \{3/2^-\} \\
\Delta(1930 | 1925) \{5/2^-u\} + \Delta W_{2-4} \{1^-u\} &= \Delta(1950 | 1944) \{7/2^+\} \\
\Delta(1700 | 1684) \{3/2^-u\} + S_{(o),d=2} \{1^-u\} &= \Delta(2000 | 1981) \{5/2^+\} \\
\Delta(1940 | 1925) \{3/2^-u\} + \pi^0 \{0^-\} + m_{\text{FGL}} \{1^-d\} &= \Delta(2150 | 2128) \{1/2^-\} \\
\Delta(1905 | 1926) \{5/2^+u\} + S_{(o),d=2} \{1^-u\} &= \Delta(2200 | 2223) \{7/2^-\} \\
\Delta(2200 | 2223) \{7/2^-u\} + m_{\text{FGL}} \{1^-u\} &= \Delta(2300 | 2291) \{9/2^+\} \\
\Delta(2300 | 2291) \{9/2^+u\} + \pi^0 \{0^-\} &= \Delta(2400 | 2426) \{9/2^-\} \\
\Delta(2400 | 2426) \{9/2^-u\} \rightarrow \Delta W_{2-4} \{1^-d\} + \Delta(2390 | 2407) \{7/2^+u\} \\
\Delta(2400 | 2426) \{9/2^-u\} + \Delta W_{2-4} \{1^-u\} &= \Delta(2420 | 2445) \{11/2^+\} \\
\Delta(2400 | 2426) \{9/2^-u\} + S_{(o),d=2} \{1^-u\} + \Delta W_{2-4} \{1^-u\} &= \Delta(2750 | 2742) \{13/2^-\} \\
\Delta(2750 | 2742) \{13/2^-u\} + 3 m_{\text{FGL}} \{1^-u\} &= \Delta(2950 | 2945) \{15/2^+\} \\
\Delta(2390 | 2407) \{7/2^+u\} \rightarrow m_{\text{FGL}} \{1^-d\} + \Delta(2350 | 2339) \{5/2^-u\}
\end{aligned}$$

Lambda resonances

$$\begin{aligned}
\Lambda(1116) \{1/2^+u\} + S_{(o),d=2} \{1^-d\} &= \Lambda(1405 | 1413) \{1/2^-\} \\
\Lambda(1116) \{1/2^+u\} + 2 \pi^0 \{0^+\} + 2 m_{\text{FGL}} \{2^-d\} &= \Lambda(1520 | 1521) \{3/2^-\} \\
\Lambda(1520 | 1521) \{3/2^-u\} \rightarrow m_{\text{FGL}} \{1^-u\} + m_{\text{FGL}} \{1^-u\} + \Lambda(1385 | 1386) \{1/2^-d\} \\
\Lambda(1405 | 1413) \{1/2^-u\} + 2 \pi^0 \{0^+\} &= \Lambda(1670 | 1683) \{1/2^-\} \\
\Lambda(1670 | 1683) \{1/2^-u\} \rightarrow m_{\text{FGL}} \{1^-u\} + \Lambda(1600 | 1615) \{1/2^+d\} \\
\Lambda(1405 | 1413) \{1/2^-u\} + S_{(o),d=2} \{1^-d\} &= \Lambda(1710 | 1710) \{1/2^+\} \\
\Lambda(1710 | 1710) \{1/2^+u\} \rightarrow \Delta W_{2-4} \{1^-d\} + \Lambda(1690 | 1691) \{3/2^-u\} \\
\Lambda(1520 | 1521) \{3/2^-u\} + S_{(o),d=2} \{1^-u\} &= \Lambda(1820 | 1818) \{5/2^+\} \\
\Lambda(1670 | 1683) \{1/2^-u\} + \pi^0 \{0^-\} &= \Lambda(1810 | 1818) \{1/2^+\} \\
\Lambda(1810 | 1818) \{1/2^+u\} \rightarrow \Delta W_{2-4} \{1^-u\} + \Lambda(1800 | 1799) \{1/2^-d\} \\
\Lambda(1820 | 1818) \{5/2^+u\} + 2 \Delta W_{2-4} \{0^-\} &= \Lambda(1830 | 1857) \{5/2^-\}
\end{aligned}$$

$$\Lambda(1830 | 1857) \{5/2^- u\} + m_{\text{FGL}} \{1^- d\} = \Lambda(1890 | 1925) \{3/2^+\}$$

$$\Lambda(1800 | 1799) \{1/2^- u\} + \pi^0 \{0^-\} + 2 m_{\text{FGL}} \{2^- u\} = \Lambda(2080 | 2069) \{5/2^-\}$$

$$\Lambda(2080 | 2069) \{5/2^- u\} \rightarrow \Delta W_{2-4} \{1^- u\} + \Lambda(2070 | 2050) \{3/2^+ u\}$$

$$\Lambda(2070 | 2050) \{3/2^+ u\} \rightarrow 2 \Delta W_{2-4} \{0^-\} + \Lambda(2050 | 2011) \{3/2^- u\}$$

$$\Lambda(2080 | 2069) \{5/2^- u\} + \Delta W_{2-4} \{1^- u\} = \Lambda(2085 | 2088) \{7/2^+\}$$

$$\Lambda(1710 | 1710) \{1/2^+ u\} + S_{(o),d=2} \{1^- d\} = \Lambda(2000 | 2007) \{1/2^-\}$$

$$\Lambda(1820 | 1818) \{5/2^+ u\} + S_{(o),d=2} \{1^- u\} = \Lambda(2100 | 2115) \{7/2^-\}$$

$$\Lambda(2100 | 2115) \{7/2^- u\} \rightarrow \Delta W_{2-4} \{1^- u\} + \Lambda(2110 | 2096) \{5/2^+ u\}$$

$$\Lambda(2050 | 2011) \{3/2^- u\} + 2 \pi^0 \{0^+\} = \Lambda(2325 | 2281) \{3/2^-\}$$

$$\Lambda(2050 | 2011) \{3/2^- u\} + 4 \pi^0 \{0^+\} = \Lambda(2585 | 2551) \{3/2^-\}$$

$$\Lambda(1810 | 1818) \{1/2^+ u\} + 2 \pi^0 \{0^+\} + 4 m_{\text{FGL}} \{4^+ u\} = \Lambda(2350 | 2358) \{9/2^+\}$$

Sigma resonances

$$\Sigma(1193) \{1/2^+ u\} + \pi^0 \{0^-\} + m_{\text{FGL}} \{1^- u\} = \Sigma(1385 | 1396) \{3/2^+\}$$

$$\Sigma(1385 | 1396) \{3/2^+ u\} + \pi^0 \{0^-\} + 2 m_{\text{FGL}} \{2^- d\} = \Sigma(1660 | 1666) \{1/2^+\}$$

$$\Sigma(1660 | 1666) \{1/2^+ u\} + \Delta W_{2-4} \{1^- u\} = \Sigma(1670 | 1685) \{3/2^-\}$$

$$\Sigma(1385 | 1396) \{3/2^+ u\} + 4 \pi^0 \{0^+\} = \Sigma(1940 | 1936) \{3/2^+\}$$

$$\Sigma(1940 | 1936) \{3/2^+ u\} \rightarrow S_{(o),d=2} \{1^- u\} + \Sigma(1620 | 1639) \{1/2^- u\}$$

$$\Sigma(1620 | 1639) \{1/2^- u\} + 2 \pi^0 \{0^+\} = \Sigma(1900 | 1909) \{1/2^-\}$$

$$\Sigma(1900 | 1909) \{1/2^- u\} + 2 \Delta W_{2-4} \{2^- u\} = \Sigma(1915 | 1948) \{5/2^+\}$$

$$\Sigma(1620 | 1639) \{1/2^- u\} + \pi^0 \{0^-\} + 2 m_{\text{FGL}} \{2^- d\} = \Sigma(1910 | 1909) \{3/2^-\}$$

$$\Sigma(1910 | 1909) \{3/2^- u\} \rightarrow \pi^0 \{0^-\} + \Sigma(1780 | 1774) \{3/2^+ u\}$$

$$\Sigma(1780 | 1774) \{3/2^+ u\} \rightarrow \Delta W_{2-4} \{1^- d\} + \Sigma(1775 | 1755) \{5/2^- u\}$$

$$\Sigma(1780 | 1774) \{3/2^+ u\} \rightarrow \Delta W_{2-4} \{1^- u\} + \Sigma(1750 | 1755) \{1/2^- u\}$$

$$\Sigma(1750 | 1755) \{1/2^- u\} + \pi^0 \{0^-\} = \Sigma(1880 | 1890) \{1/2^+\}$$

$$\Sigma(1880 | 1890) \{1/2^+ u\} \rightarrow S_{(o),d=2} \{1^- d\} + \Sigma(1580 | 1593) \{3/2^- u\}$$

$$\Sigma(1780 | 1774) \{3/2^+u\} + 2 \pi^0 \{0^+\} = \Sigma(2080 | 2044) \{3/2^+\}$$

$$\Sigma(2080 | 2044) \{3/2^+u\} + m_{\text{FGL}} \{1^-d\} = \Sigma(2110 | 2112) \{1/2^-\}$$

$$\Sigma(2110 | 2112) \{1/2^-u\} + 2 m_{\text{FGL}} \{2^-d\} = \Sigma(2230 | 2247) \{3/2^+\}$$

$$\Sigma(2230 | 2247) \{3/2^+u\} \rightarrow 2 m_{\text{FGL}} \{2^-d\} + \Sigma(2110 | 2112) \{7/2^-u\}$$

$$\Sigma(1880 | 1890) \{1/2^+u\} + 2 m_{\text{FGL}} \{2^-d\} = \Sigma(2010 | 2025) \{3/2^-\}$$

$$\Sigma(2010 | 2025) \{3/2^-u\} + 2 \Delta W_{2,4} \{2^-u\} = \Sigma(2030 | 2064) \{7/2^+\}$$

Notice also that mass distances between some resonances with the highest masses are close to mass of four pions, for example

$$\Sigma(3170) - \Sigma(2620) = 550 \text{ MeV} \approx 4 \pi^0$$

$$\Sigma(3000) - \Sigma(2455) = 545 \text{ MeV} \approx 4 \pi^0.$$

On the other hand, SST shows that one of a few new symmetries is the four-particle symmetry. Moreover, SST shows that range of an association of four neutral pions is equal to the equatorial radius of the core of baryons.

Xi resonances

$$\Xi(1315) \{1/2^+u\} + \pi^0 \{0^-\} + m_{\text{FGL}} \{1^-u\} = \Xi(1530 | 1518) \{3/2^+\}$$

$$\Xi(1315) \{1/2^+u\} + S_{(o),d=2} \{1^-d\} = \Xi(1620 | 1612) \{1/2^-\}$$

$$\Xi(1620 | 1612) \{1/2^-u\} + m_{\text{FGL}} \{1^-u\} = \Xi(1690 | 1680) \{3/2^+\}$$

$$\Xi(1690 | 1680) \{3/2^+\} + \pi^0 \{0^-\} = \Xi(1820 | 1815) \{3/2^-\}$$

$$\Xi(1820 | 1815) \{3/2^-u\} + \pi^0 \{0^-\} = \Xi(1950 | 1950) \{3/2^+\}$$

$$\Xi(1950 | 1950) \{3/2^+u\} + m_{\text{FGL}} \{1^-u\} = \Xi(2030 | 2018) \{5/2^-\}$$

$$\Xi(1820 | 1815) \{3/2^-u\} + S_{(o),d=2} \{1^-d\} = \Xi(2120 | 2112) \{1/2^+\}$$

$$\Xi(2120 | 2112) \{1/2^+u\} + \pi^0 \{0^-\} = \Xi(2250 | 2247) \{1/2^-\}$$

$$\Xi(2250 | 2247) \{1/2^-u\} + \pi^0 \{0^-\} = \Xi(2370 | 2382) \{1/2^+\}$$

$$\Xi(2370 | 2382) \{1/2^+u\} + \pi^0 \{0^-\} = \Xi(2500 | 2517) \{1/2^-\}$$

Omega resonances

$$\Omega(1672) \{1/2^+u\} + 2 \pi^0 \{0^+\} + m_{\text{FGL}} \{1^-u\} = \Xi(2012 | 2010) \{3/2^-\}$$

$$\Omega(1672) \{1/2^+u\} + 2 S_{(o),d=2} \{2^-d\} = \Xi(2250 | 2266) \{3/2^-\}$$

Masses of the charmed and bottom baryons

In decays of the charmed and bottom baryons, very frequently appear pions and kaons. On the other hand, such baryons live relatively long so it suggests that there appears a spacetime condensate which interacts due to the slow weak interactions. We claim that there is a transition of relativistic neutral pion or relativistic neutral kaon in the $d = 0$ state (their mass increases about 9.0036 times – see (2.4.8)) into spacetime condensate. Masses of the condensates are as follows

$$C_\pi = 1215 \text{ MeV} \quad \text{and} \quad C_K = 4480 \text{ MeV} . \quad (\text{I6.4})$$

Notice that these masses are close to masses of the charm and bottom quarks [1]

$$m_c = 1270(20) \text{ MeV} \quad \text{and} \quad m_b = 4180^{+30}_{-20} \text{ MeV} . \quad (\text{I6.5})$$

Within SST we calculated masses of gluon loops that relate to the masses of quarks. Such gluon loops can transform into spacetime condensate. Here we need mass of spacetime condensate which is equal to mass of the SST charm quark (see Paragraph 2.23)

$$C_{c,SST} = 1267 \text{ MeV} . \quad (\text{I6.6})$$

The gluon-condensate ambiguity causes that it is difficult to determine clearly parity and spin of the charmed and bottom baryons so here we concentrate, first of all, on the masses.

We already calculated the mean lifetime of hyperons ($\tau_{H,lifetime} \approx 1.1 \cdot 10^{-10}$ s) that decay due to the nuclear weak interactions – the coupling constant is $\alpha_{w(p)} = 0.0187229$. On the other hand, due to the additional pions, FGLs, and transitions from relativistic pions to condensates in the c-baryons and b-baryons, we have a transition from the nuclear weak interactions into the nuclear strong interactions (inside slowly moving baryons, the coupling constant for the nuclear strong interactions is $\alpha_s = 1$) so, because $\tau_{lifetime} \sim 1/\alpha$ (see (1.4.29)), lifetime of the b-baryons and the c-baryons should be close to

$$\tau_{lifetime,Bb,Bc} = \tau_{H,lifetime} \alpha_{w(p)} / \alpha_s \approx 2 \cdot 10^{-12} \text{ s} . \quad (\text{I6.7})$$

Notice also that the additional condensate in c-baryons has lower mass so it should have an influence on lifetime.

Masses of the charmed baryons are as follows.

$$\Lambda_c(2286 | 2288)^+ \{1/2^+u\} = p(938) \{1/2^+u\} + C_\pi \{0^+\} + m_{FGL} \{1^-u\} + m_{FGL} \{1^-d\}$$

$$\Lambda_c(2595 | 2597)^+ \{1/2^-u\} = \Lambda_c(2286 | 2288)^+ \{1/2^+u\} + 2 \pi^0 \{0^+\} + 2 \Delta W_{2,4} \{0^-\}$$

$$\Lambda_c(2625 | 2626)^+ \{3/2^-u\} = \Lambda_c(2286 | 2288)^+ \{1/2^+u\} + 2 \pi^0 \{0^+\} + m_{FGL} \{1^-u\}$$

$$\Lambda_c(2860 | 2867)^+ \{3/2^+u\} = \Lambda_c(2595 | 2597)^+ \{1/2^-d\} + \pi^0 \{0^-\} + m_{FGL} \{1^-u\} + m_{FGL} \{1^-u\}$$

$$\Lambda_c(2880 | 2867)^+ \{5/2^+u\} = \Lambda_c(2595 | 2597)^+ \{1/2^-u\} + \pi^0 \{0^-\} + m_{FGL} \{1^-u\} + m_{FGL} \{1^-u\}$$

$$\Lambda_c(2940 | 2935)^+ \{3/2^-u\} = \Lambda_c(2880 | 2867)^+ \{5/2^+u\} + m_{FGL} \{1^-d\}$$

$$\Sigma_c(2455 | 2460) \{1/2^+u\} = \Sigma(1193) \{1/2^+u\} + C_{c,SST} \{0^+\}$$

$\Sigma_c(2520 | 2528) \{3/2^+ u\} = \Sigma_c(2455 | 2460) \{1/2^+ u\} + m_{\text{FGL}} \{1^- u\}$
 J^P has not been measured, $3/2^+$ is the quark-model prediction [1]. Our value is $3/2^-$.

$$\Sigma_c(2800 | 2798) = \Sigma_c(2520 | 2528) \{3/2^- u\} + 2 \pi^0 \{0^+\}$$

$\Xi_c(2468 | 2461)^+ + \pi^- = \Xi(1315 | 1315)^0 + C_{c,\text{SST}} + \Delta W_{2-4}$
 J^P has not been measured, $1/2^+$ is the quark-model prediction [1].

$\Xi_c(2470 | 2466)^0 + \pi^0 = \Xi(1315 | 1315)^0 + C_{c,\text{SST}} + \Delta W_{2-4}$
 J^P has not been measured [1].

$$\Xi'_c(2578 | 2596) = \Xi_c(2468 | 2461) + \pi^0$$

$$\Xi_c(2645 | 2635) = \Xi'_c(2578 | 2596) + 2 \Delta W_{2-4}$$

$$\Xi_c(2790 | 2770) = \Xi_c(2645 | 2635) + \pi^0$$

$$\Xi_c(2815 | 2809) = \Xi_c(2790 | 2770) + 2 \Delta W_{2-4}$$

$$\Xi_c(2970 | 2944) = \Xi_c(2815 | 2809) + \pi^0$$

Notice also that $\pi^0 + 2 \Delta W_{2-4} = 174 \text{ MeV} \approx W_{(o),d=2} = 175.7 \text{ MeV}$ so there is an additional resonance.

$$\Xi_c(3055 | 3040) = \Xi_c(2790 | 2770) + 2 \pi^0$$

$$\Xi_c(3080 | 3079) = \Xi_c(2815 | 2809) + 2 \pi^0$$

$$\Omega_c(2695 | 2666)^0 + \pi^- + \pi^0 = \Omega(1672 | 1674)^- + C_{c,\text{SST}}$$

$$\Omega_c(2770 | 2734)^0 = \Omega_c(2695 | 2666)^0 + m_{\text{FGL}}$$

$$\Omega_c(3000 | 3004)^0 = \Omega_c(2770 | 2734)^0 + 2 \pi^0$$

$$\Omega_c(3065 | 3072)^0 = \Omega_c(3000 | 3004)^0 + m_{\text{FGL}}$$

$$\Omega_c(3050 | 3053)^0 + \Delta W_{2-4} = \Omega_c(3065 | 3072)^0$$

$$\Omega_c(3090 | 3092)^0 = \Omega_c(3050 | 3053)^0 + 2 \Delta W_{2-4}$$

$$\Omega_c(3120 | 3111)^0 = \Omega_c(3090 | 3092)^0 + \Delta W_{2-4}$$

Mass of the doubly charmed baryon is as follows.

$$\Xi_{cc}(3622 | 3638)^{++} + 2 \pi^- = \Xi(1315 | 1315)^0 + 2 C_{c,\text{SST}} + m_{\text{FGL}}$$

Masses of the bottom baryons are as follows.

$$\Lambda_b(5620 | 5595)^0 \{1/2^+ u\} = \Lambda(1116 | 1115)^0 \{1/2^+ u\} + C_K \{0^+\}$$

$$\Lambda_b(5912 \text{ and } 5920 \mid 5933)^0 \{1/2^- \bar{u} \text{ or } 3/2^- \bar{u}\} = \\ = \Lambda_b(5620 \mid 5595)^0 \{1/2^+ \bar{u}\} + 2 \pi^0 \{0^+\} + m_{\text{FGL}} \{1^- \bar{d} \text{ or } 1^- \bar{u}\}$$

$$\Lambda_b(6070 \mid 6068)^0 = \Lambda_b(5912 \text{ and } 5920 \mid 5933)^0 + \pi^0$$

$$\Lambda_b(6146 \text{ and } 6152 \mid 6136)^0 = \Lambda_b(6070 \mid 6068)^0 + m_{\text{FGL}}$$

$$\Sigma_b(\sim 5813 \mid 5808) = \Sigma(1193)^0 + C_K + \pi^0$$

$$\Sigma_b^*(\sim 5833 \mid 5827) = \Sigma_b(\sim 5813 \mid 5808) + \Delta W_{2-4}$$

$$\Sigma_b(6097 \mid 6097) = \Sigma_b^*(\sim 5833 \mid 5827) + 2 \pi^0$$

$$\Xi_b(\sim 5795 \mid 5795) = \Xi(1315 \mid 1315) + C_K$$

$$\Xi_b'(\sim 5945 \mid 5930) = \Xi_b(\sim 5795 \mid 5795) + \pi^0$$

$$\Xi_b(6227 \mid 6200) = \Xi_b'(\sim 5945 \mid 5930) + 2 \pi^0$$

$$\Omega_b(6046 \mid 6019) + \pi^0 = \Omega(1672 \mid 1674) + C_K$$

$$\Omega_b(6316 \mid 6311) = \Omega(1672 \mid 1674) + C_K + W_{(o),d=4}$$

Masses of the P_c^+ baryons

In the Type-X mesons, there is the spacetime condensate with a mass of $C_X = 3736 \text{ MeV}$ (see Section I5). We claim that such a condensate is in $P_c^+(4312)^+$

$$P_c(4312 \mid 4310)^+ + 2W_{(+),d=2} = p(938 \mid 938) + C_X$$

$$P_c(4380 \mid 4378)^+ = P_c(4312 \mid 4310)^+ + m_{\text{FGL}}$$

$$P_c(4440 \mid 4445)^+ = P_c(4312 \mid 4310)^+ + \pi^0$$

$$P_c(4457 \mid 4464)^+ = P_c(4440 \mid 4445)^+ + \Delta W_{2-4}$$

Notice that the six objects, i.e. m_{FGL} , π^0 , ΔW_{2-4} , W and S vectors in the $d = 2$ state, and spacetime condensates C , are the typical objects inside baryons.

Part 2: Mesons

Light unflavored mesons

We already described the internal structure of pions.

$$\eta(548 \mid 549) \ 0^+(0^{++}) = C_Y \ 0^+(0^{++}) + m_{\text{FGL}} \ 0^-(1^- \bar{u}) + 2 \Delta W_{2-4} \ 0^+(0^{++}) + \Delta W_{2-4} \ 0^-(1^- \bar{d})$$

In centre of all baryons, there is the spacetime condensate $C_Y \approx 424$ MeV so it also appears in the mesonic nuclei.

$$\eta'(958 | 964) 0^+(0^+) = \eta(548 | 540) 0^+(0^+) + C_Y 0^+(0^{++})$$

$$\eta(1295 | 1292) 0^+(0^+) = f_2(1270 | 1253) 0^+(2u^{++}) + 2 \Delta W_{2-4} 0^+(2d^{++})$$

$$\eta(1405 | 1379) 0^+(0^+) = \eta(1295 | 1292) 0^+(0^+) + (m_{FGL} + \Delta W_{2-4}) 0^+(0^{++})$$

$$\eta(1475 | 1494) 0^+(0^+) = \eta(548 | 549) 0^+(0^+) 0^+(0^+) + 14 m_{FGL} 0^+(0^{++})$$

$$\eta_2(1645 | 1610) 0^+(2u^{++}) + 2 \Delta W_{2-4} 0^+(2d^{++}) = \eta(1405 | 1379) 0^+(0^+) + 4 m_{FGL} 0^+(0^{++})$$

$$\eta_2(1870 | 1846) 0^+(2^+) = \eta(1475 | 1494) 0^+(0^+) + 2 W_{(o),d=2} 0^+(2^{++})$$

$$f_0(500 | 510) 0^+(0^{++}) + 2\Delta W_{2-4} 0^+(0^+) = \eta(548 | 549) 0^+(0^+)$$

$$f_0(980 | 983) 0^+(0^{++}) = 2 C_Y 0^+(0^{++}) + 2 m_{FGL} 0^+(0^{++})$$

$$f_0(1370 | 1350) 0^+(0^{++}) = C_\pi 0^+(0^{++}) + 2 m_{FGL} 0^+(0^{++})$$

$$f_0(1500 | 1485) 0^+(0^{++}) = f_0(1370 | 1350) 0^+(0^{++}) + m_{FGL} 0^-(1u^-) + m_{FGL} 0^-(1d^-)$$

$$f_0(1710 | 1702) 0^+(0^{++}) = f_0(1370 | 1350) 0^+(0^{++}) + 2 W_{(o),d=2} 0^+(0^{++})$$

$$f_2(1270 | 1253) 0^+(2^{++}) = 2 C_Y 0^+(0^{++}) + 4 m_{FGL} 0^+(0^{++}) + 2 m_{FGL} 0^+(2^{++})$$

$$f_2'(1525 | 1523) 0^+(2^{++}) = f_2(1270 | 1253) 0^+(2^{++}) + 4 m_{FGL} 0^+(0^{++})$$

$$f_2(1950 | 1966) 0^+(2^{++}) = 4 C_Y 0^+(0^{++}) + 2 m_{FGL} 0^+(0^{++}) + 2 m_{FGL} 0^+(2^{++})$$

$$f_2(2010 | 2016) 0^+(2^{++}) = f_0(1710 | 1702) 0^+(0^{++}) + 2 W_{(o),d=4} 0^+(2^{++})$$

$$f_4(2050 | 2055) 0^+(4^{++}) = f_2(2010 | 2016) 0^+(2u^{++}) + 2 \Delta W_{2-4} 0^+(2u^{++})$$

$$f_2(2300 | 2296) 0^+(2^{++}) = f_0(1710 | 1702) 0^+(0^{++}) + 2 S_{(o),d=2} 0^+(2^{++})$$

$$f_2(2340 | 2335) 0^+(2^{++}) = f_2(2300 | 2296) 0^+(2^{++}) + 2 \Delta W_{2-4} 0^+(0^{++})$$

$$\rho(770 | 782) 1^+(1^-) = \eta(548 | 540) 0^+(0^+) + \pi^0 1^-(0^+) + m_{FGL} 0^-(1^-) + 2 \Delta W_{2-4} 0^+(0^{++})$$

$$\rho(1450 | 1457) 1^+(1^-) = \rho(770 | 782) 1^+(1^-) + 10 m_{FGL} 0^+(0^{++})$$

$$\rho(1700 | 1690) 1^+(1^-) = \rho(770 | 782) 1^+(1^-) + 4 m_{FGL} 0^+(0^{++}) + Q_{XXee} 0^+(0^{++})$$

Here the $Q_{XXee} = X^+X^-e^+e^- \approx 638$ MeV is the real spin-0 quadrupole that transforms into spacetime condensate.

$$\rho_3(1690 | 1690) 1^+(3^-) = \rho(770 | 782) 1^+(1u^-) + 3 m_{\text{FGL}} 0^-(3u^-) + m_{\text{FGL}} 0^-(1d^-) + Q_{\text{XXcc}} 0^+(0^{++})$$

$$\omega(782 | 782) 0^-(1^-) = 11 m_{\text{FGL}} 0^-(1^-) + 2 \Delta W_{2-4} 0^+(0^{++})$$

$$\omega(1420 | 1418) 0^-(1^-) = C_\pi 0^+(0^{++}) + 3 m_{\text{FGL}} 0^-(1^-)$$

$$\omega(1650 | 1688) 0^-(1^-) = \omega(1420 | 1418) 0^-(1^-) + 4 m_{\text{FGL}} 0^+(0^{++})$$

$$\omega(1670 | 1688) 0^-(3^-) = \omega(1420 | 1418) 0^-(1u^-) + 3 m_{\text{FGL}} 0^-(3u^-) + m_{\text{FGL}} 0^-(1d^-)$$

$$a_0(980 | 983) 1^-(0^{++}) = 2 C_Y 0^+(0^{++}) + \pi^0 1^-(0^-) + 2 \Delta W_{2-4, \text{virtual}} 0^+(0^{++})$$

$$a_1(1260 | 1254) 1^-(1^{++}) = a_0(980 | 983) 1^-(0^{++}) + Q 0^+(1^{++}) + 4 m_{\text{FGL}} 0^+(0^{++})$$

$$a_1(1640 | 1678) 1^-(1^{++}) = a_1(1260 | 1254) 1^-(1^{++}) + C_Y 0^+(0^{++})$$

It contains $Q 0^+(1^{++})$.

$$a_2(1320 | 1335) 1^-(2^{++}) = a_0(980 | 983) 1^-(0^{++}) + 2 W_{(o),d=2} 0^+(2^{++})$$

$$a_0(1450 | 1470) 1^-(0^{++}) = a_2(1320 | 1335) 1^-(2u^{++}) + 2 m_{\text{FGL}} 0^+(2d^{++})$$

$$a_2(1700 | 1701) 1^-(2u^{++}) + 2 \Delta W_{2-4} 0^+(2d^{++}) = a_0(1450 | 1470) 1^-(0^{++}) + 4 m_{\text{FGL}} 0^+(0^{++})$$

$$a_4(1970 | 1971) 1^-(4^{++}) = a_2(1700 | 1701) 1^-(2u^{++}) + 3 m_{\text{FGL}} 0^-(3u^-) + m_{\text{FGL}} 0^-(1d^-)$$

$$\Phi(1020 | 1013) 0^-(1^-) = 15 m_{\text{FGL}} 0^-(1^-)$$

$$\Phi(1680 | 1651) 0^-(1^-) = \Phi(1020 | 1013) 0^-(1^-) + Q_{\text{XXcc}} 0^+(0^{++})$$

$$\Phi_3(1850 | 1855) 0^-(3^-) = \Phi(1020 | 1013) 0^-(1u^-) + 2 S_{(o),d=1} 0^+(2u^{++})$$

$$\Phi(2170 | 2169) 0^-(1^-) = \Phi_3(1850 | 1855) 0^-(3u^-) + 2 W_{(o),d=4} 0^+(2d^{++})$$

$$h_1(1170 | 1148) 0^-(1^+) = 17 m_{\text{FGL}} 0^-(1^-) + 2 \Delta W_{2-4, \text{virtual}} 0^+(0^-)$$

$$h_1(1415 | 1418) 0^-(1^+) = h_1(1170 | 1148) 0^-(1^-) + 4 m_{\text{FGL}} 0^+(0^{++})$$

$$b_1(1235 | 1234) 1^+(1^+) = 16 m_{\text{FGL}} 0^+(0^{++}) + \pi^0 1^-(0^-) + \Delta W_{2-4} 0^-(1^-)$$

$$\pi(1300 | 1350) 1^-(0^+) = C_\pi 0^+(0^{++}) + \pi^0 1^-(0^-)$$

$$\pi_1(1400 | 1351) 1^-(1^+) = \pi(1300 | 1350) 1^-(0^+) + Q 0^+(1^{++})$$

$$\pi_1(1600 | 1621) 1^-(1^{++}) = \pi_1(1400 | 1351) 1^-(1^{++}) + 4 m_{\text{FGL}} 0^+(0^{++})$$

It contains $Q 0^+(1^{++})$.

$$\pi_2(1670 | 1663) 1^-(2^{++}) + 2 \Delta W_{2-4} 0^+(0^{++}) = \pi(1300 | 1350) 1^-(0^{++}) + 2 W_{(o),d=2} 0^+(2^{++})$$

$$\pi(1800 | 1798) 1^-(0^{++}) = \pi_2(1670 | 1663) 1^-(2u^{++}) + 2 m_{\text{FGL}} 0^+(2d^{++})$$

$$\pi_2(1880 | 1890) 1^-(2^{++}) = \pi(1300 | 1350) 1^-(0^{++}) + 6 m_{\text{FGL}} 0^+(0^{++}) + 2 m_{\text{FGL}} 0^+(2^{++})$$

K strange mesons

For all kaons is $I = 1/2$ so we define only J^P .

One of the two FGLs in a charged pion (it is a pseudoscalar), due to the transition from its circumference to its radius, transforms into the spacetime condensate Y – it means that the $[Y + m_{\text{FGL}} + (e^\pm v)_{\text{virtual}}]$ is a pseudoscalar. The $4m_{e,\text{bare}}$ is a scalar, so K^\pm is a pseudoscalar $J^P = 0^-$. The $(e^\pm v)_{\text{virtual}}$ stabilizes the $[Y + m_{\text{FGL}}]$ pair. We have

$$K(493.677(16) [3] | 493.708)^\pm = K(493.7 | 493.7)^\pm = [Y + m_{\text{FGL}} + (e^\pm v)_{\text{virtual}}] + 4 e^\pm_{\text{bare}}$$

The spin-0 neutral kaon K^0 is created because the neutral pion, after the transition described above, attaches the electromagnetic mass of the quadrupole of neutral pions ($M_{\text{em}} = 4\pi^0 \alpha_{\text{em}} = 3.940 \text{ MeV}$) to stabilize the $[Y + m_{\text{FGL}}]$ pair – SST shows that range of the quadrupole $4\pi^0$ is equal to the equatorial radius of the core of baryons so it is distinguished.

$$K(497.611(13) [3] | 497.648)^0 = K(497.6 | 497.6)^0 = [Y + m_{\text{FGL}} + M_{\text{em}}] + 4 e^\pm_{\text{bare}}$$

The spacetime condensate $C_Y \equiv Y$ in $K(497.6 | 497.6)^0$ can decay to maximum 6 FGLs. On the other hand, the FGLs occupy the nuclear shells for FGLs (see Section **I5**) and there is the four-particle symmetry. We have $1s^2 2s^2 2p^6$ so there are two possibilities, i.e. $1s^2 2s^2$ (there appear 2 pions) or $2p^6$ (there appear 3 pions) – it solves the Tau-Theta problem.

The composition of $K_o^*(700)$ is as follows

$$K_o^*(700)_{\text{mass}} = 2 C_Y 0^+ \text{ so mass is } 848 \text{ MeV.}$$

But one of the two C_Y condensates can decay to two neutral pions so the mean mass is

$$K_o^*(700)_{\text{mean}} = C_Y 0^+ + 2 \pi^0 0^+ = 694 \text{ MeV} \approx 700 \text{ MeV.}$$

We will denote this kaon as $K_o^*(700 | 848) 0^+$.

$$K^*(892 | 897) 1^- = C_Y 0^+ + 3 m_{\text{FGL}} 1^- + 2 \pi^0 0^+$$

$$K_1(1270 | 1249) 1^+ = K^*(892 | 897) 1^- + 2 W_{(o),d=2} 0^-$$

$$K_1(1400 | 1384) 1^+ = K_1(1270 | 1249) 1^+ + 2 m_{\text{FGL}} 0^+$$

$$K^*(1410 | 1437) 1^- = K^*(892 | 897) 1^- + 4 \pi^0 0^+$$

$K_o^*(1430 | 1422) 0^+$: there are two possibilities

$$K_o^*(700 | 848) 0^+ + 4 \pi^0 0^+ = 1388 \text{ MeV}$$

$$K^*(1410 | 1437) 1u^- + \Delta W_{2-4} 1d^- = 1456 \text{ MeV,}$$

so the mean mass is 1422 MeV.

$K_2^*(1430 | 1422) 2^+$: there are two possibilities

$$\begin{aligned} K_0^*(700 | 848) 0^+ + 3 \pi^0 0^- + 2 m_{\text{FGL}} 2^- &= 1388 \text{ MeV} \\ K^*(1410 | 1437) 1u^- + \Delta W_{2-4} 1u^- &= 1456 \text{ MeV,} \\ \text{so the mean mass is } 1422 \text{ MeV.} \end{aligned}$$

$$K(1460 | 1461) 0^- = K_0^*(1430 | 1422) 0^+ + 2 \Delta W_{2-4} 0^-$$

$$K_1(1650 | 1664) 1^+ = K(1460 | 1461) 0^- + 3 m_{\text{FGL}} 1^-$$

$$K^*(1680 | 1703) 1^- = K_1(1650 | 1664) 1^+ + 2 \Delta W_{2-4} 0^-$$

$$K_2(1770 | 1775) 2^- = K^*(1460 | 1461) 0^- + 2 W_{(o),d=4} 2^+$$

$$K_3(1780 | 1789) 3^- = K^*(1410 | 1437) 1u^- + 2 W_{(o),d=2} 2u^+$$

$$K_2(1820 | 1805) 2^- = K_1(1400 | 1384) 1u^+ + S_{(o),d=1} 1u^-$$

$$K_2^*(1980 | 2001) 2^+ = K(1460 | 1461) 0^- + 3 \pi^0 0^- + 2 m_{\text{FGL}} 2^+$$

$$K_4(2045 | 2040) 4^+ = K_2^*(1980 | 2001) 2u^+ + 2 \Delta W_{2-4} 2u^+$$

D charmed mesons

For all D charmed mesons is $I = 1$ so we define only J^P .

$$D(1865 | 1864)^0 0^- = C_{c,\text{SST}} 0^+ + 2 S_{(+),d=2} 0^-$$

$$D(1870 | 1869)^\pm 0^- = D(1865 | 1864)^0 0^- + \Delta\pi^\pm = 4.6 \text{ MeV } 0^+$$

$$D^*(2007 | 2010)^0 1^- = C_{c,\text{SST}} 0^+ + 11 m_{\text{FGL}} 1^-$$

$$D^*(2010 | 2015)^\pm 1^- = D^*(2007 | 2010)^0 1^- + \Delta\pi^\pm 0^+$$

$$D_0^*(2300 | 2348) 0^+ = D^*(2007 | 2010)^0 1u^- + 2 \pi^0 0^+ + m_{\text{FGL}} 1d^-$$

$$D_1(2420 | 2415) 1^+ = D^*(2007 | 2010)^0 1^- + 3 \pi^0 0^-$$

$$D_1(2430 | 2424) 1^+ = D^*(2007 | 2010)^0 1^- + \pi^0 \pi^+ \pi^- 0^-$$

$$D_2^*(2460 | 2458) 2^+ = D^*(2010 | 2015)^\pm 1u^- + C_Y 0^+ + \Delta W_{2-4} 1u^-$$

$$D_3^*(2750 | 2755) 3^- = D_2^*(2460 | 2458) 2u^+ + S_{(o),d=2} 1u^-$$

D charmed, strange mesons

For all D charmed, strange mesons is $I = 0$ so we define only J^P .

$$D_s(1968 | 1966)^\pm 0^- = C_{c,\text{SST}} 0^+ + C_Y 0^+ + \pi^\pm 0^- + 2 m_{\text{FGL}} 0^+$$

$$D_s^*(2112 | 2101)^\pm ?^? = D_s(1968 | 1966)^\pm 0^- + m_{\text{FGL}} 1d^- \text{ (or } 2 m_{\text{FGL}})$$

$$D_{s0}^*(2317 | 2317)^\pm 0^+ = D_s(1968 | 1966)^\pm 0^- + 2 W_{(o),d=2} 0^-$$

$$D_{s1}(2460 | 2471)^\pm 1^+ = D_{s0}^*(2317 | 2317)^\pm 0^+ + \pi^0 0^- + \Delta W_{2-4} 1^-$$

$$D_{s1}(2536 | 2520)^\pm 1^+ = D_{s0}^*(2317 | 2317)^\pm 0^+ + \pi^0 0^- + m_{\text{FGL}} 1^-$$

$$D_{s2}(2573 | 2587) 2^+ = D_{s0}^*(2317 | 2317)^\pm 0^+ + \pi^0 0^- + 2 m_{\text{FGL}} 2^-$$

$$D_{s1}(2700 | 2741)^\pm 1^- = D_{s0}^*(2317 | 2317)^\pm 0^+ + 2 \pi^0 0^+ + 2 m_{\text{FGL}} 0^+ + \Delta W_{2-4} 1^-$$

B bottom mesons

For all B bottom mesons is $I = 1/2$ so we define only J^P .

SST shows that there can be a spacetime condensate with a mass equal to the mass of the charged kaon in the $d = 0$ state $C_{K^\pm} = 4445 \text{ MeV}$ (see Table I6.1).

$$B(5279 | 5279)^\pm 0^- = C_{K^\pm} 0^+ + C_Y 0^+ + \pi^0 \pi^0 \pi^\pm 0^-$$

We can see that there are two states because of the π^\pm .

$$B(5279 | 5279)^0 0^- = C_{K^\pm} 0^+ + C_Y 0^+ + 3 \pi^0 0^- \text{ (or } \pi^0 \pi^+ \pi^- 0^-)$$

So there are also two states because of $3\pi^0$ and $\pi^0 \pi^+ \pi^-$.

There can be a loop ($J^P = 1^-$) with a mass equal to the mass of the SST bottom quark: $L_{b,\text{SST}} = 4190 \text{ MeV}$ (see Section 2.23).

$$B^*(5325 | 5325) 1^- = L_{b,\text{SST}} 1^- + 4 \pi^0 0^+ + 2 S_{(o),d=2} 0^+ \text{ (or } 2 S_{(+,-),d=2} 0^+)$$

So there are also two states because of $2S_{(o),d=2}$ and $2S_{(+,-),d=2}$.

$$B_1(5721 | 5730) 1^+ = B^*(5325 | 5325) 1^- + 3 \pi^0 0^-$$

$$B_2^*(5747 | 5742) 2^+ = B(5279 | 5279)^\pm 0^- + C_Y 0^+ + 2 \Delta W_{2-4} 2^-$$

$$B_1(5970 | 5964) 0^- \text{ or } 2^- \text{ or } 4^- = B_2^*(5747 | 5742) 2^+ + \pi^0 0^- + m_{\text{FGL}} 1^- + \Delta W_{2-4} 1^-$$

B bottom, strange mesons

For all B bottom, strange mesons is $I = 0$ so we define only J^P .

There can be a spacetime condensate ($J^P = 0^+$) with a mass equal to the mass of the SST bottom quark: $C_{b,\text{SST}} = 4190 \text{ MeV}$.

$$B_s(5367 | 5367)^0 0^- = C_{b,\text{SST}} 0^+ + 4 \pi^0 0^+ + X^+ X^- 0^-$$

$$B_s^*(5415 | 5405) 1^- = L_{b,\text{SST}} 1^- + C_\pi 0^+$$

$$B_{s1}(5830 | 5810)^0 1^+ = B_s^*(5415 | 5405) 1^- + 3 \pi^0 0^-$$

$$B_{s2}^*(5840 | 5826)^0 2^+ = B_s^*(5415 | 5405) 1u^- + S_{(o),d=1} 1u^-$$

B bottom, charmed mesons

For all B bottom, charmed mesons is $I = 0$ so we define only J^P .

$$B_c(6274 | 6277)^+ 0^- = P_{S_{XX}} 0^- + \pi^0 \pi^0 \pi^0 \pi^+ 0^+$$

$$B_c(2S: 6871 | 6871)^\pm 0^- = P_{S_{XX}} 0^- + \pi^0 \pi^0 \pi^0 \pi^\pm 0^+ + 2 S_{(o),d=2} 0^+$$

The CC_{anti} mesons

$$J/\psi(1S: 3097 | 3096) 0^-(1u^{--}) + X^+X^- 0^-(1d^{--}) = 2 D(1870 | 1869)^\pm 0^+(0^{++}) \\ \text{or} = 2 D(1865 | 1864)^0 0^+(0^{++})$$

$$\psi(3770 | 3771) 0^-(1^{--}) = J/\psi(1S: 3097 | 3096) 0^-(1u^{--}) + 10 m_{\text{FGL}} 0^+(0^{++})$$

$$\psi(2S: 3686 | 3684) 0^-(1^{--}) + m_{\text{FGL}} 0^-(1u^{--}) + \Delta W_{2-4} 0^-(1d^{--}) = \psi(3770 | 3771) 0^-(1^{--})$$

$$\psi(4040 | 4041) 0^-(1^{--}) = \psi(3770 | 3771) 0^-(1^{--}) + 2 \pi^0 0^+(0^{++})$$

$$\psi(4160 | 4176) 0^-(1^{--}) = \psi(4040 | 4041) 0^-(1^{--}) + 2 m_{\text{FGL}} 0^+(0^{++})$$

$$\psi(4230 | 4215) 0^-(1^{--}) = \psi(4160 | 4176) 0^-(1^{--}) + 2 \Delta W_{2-4} 0^+(0^{++})$$

$$\psi(4360 | 4350) 0^-(1^{--}) = \psi(4230 | 4215) 0^-(1^{--}) + 2 m_{\text{FGL}} 0^+(0^{++})$$

$$\psi(4415 | 4446) 0^-(1^{--}) = \psi(4160 | 4176) 0^-(1^{--}) + 2 \pi^0 0^+(0^{++})$$

$$\psi(4660 | 4620) 0^-(1^{--}) = \psi(4360 | 4350) 0^-(1^{--}) + 2 \pi^0 0^+(0^{++})$$

$$\eta_c(1S: 2984 | 2978) 0^+(0^{+-}) = 2 C_{c,\text{SST}} 0^+(0^{++}) + 3 \pi^0 0^+(0^{+-}) + 2 \Delta W_{2-4} 0^+(0^{++})$$

$$\eta_c(2S: 3638 | 3653) 0^+(0^{+-}) = \eta_c(1S: 2984 | 2978) 0^+(0^{+-}) + 10 m_{\text{FGL}} 0^+(0^{++})$$

$$\chi_{c0}(1P: 3415 | 3420) 0^+(0^{++}) = 2 (C_{c,\text{SST}} + C_Y + \Delta W_{2-4}) 0^+(0^{++})$$

$$\chi_{c2}(1P: 3556 | 3555) 0^+(2^{++}) = \chi_{c0}(1P: 3415 | 3420) 0^+(0^{++}) + 2 m_{\text{FGL}} 0^+(2^{++})$$

$$\chi_{c2}(3930 | 3929) 0^+(2^{++}) = \chi_{c2}(1P: 3556 | 3555) 0^+(2^{++}) + 2 S_{(0),d=4} 0^+(0^{++})$$

$$\psi_2(3823 | 3820) 0^-(2^{--}) = Q 0^+(1d^{++}) + \psi(2S: 3686 | 3684) 0^-(1u^{--}) + 2 m_{\text{FGL}} 0^+(2u^{++})$$

$$\psi_3(3842 | 3858) 0^-(3^{--}) = \psi(2S: 3686 | 3684) 0^-(1u^{--}) + 2 m_{\text{FGL}} 0^+(2u^{++}) + 2 \Delta W_{2-4} 0^+(0^{++})$$

$$h_c(1P: 3525 | 3549) 0^-(1^{+-}) + 2 m_{\text{FGL}} 0^+(0^{+-}) = \psi(2S: 3686 | 3684) 0^-(1^{--})$$

$$Z_c(3900 | 3896) 1^+(1^{+-}) = \chi_{c0}(1P: 3415 | 3420) 0^+(0^{++}) + m_{\text{FGL}} 0^-(1^{--}) + \pi^0 \pi^0 \pi^{0\pm} 1^-(0^{+-})$$

$$Z_c(4430 | 4436) 1^+(1^{+-}) = Z_c(3900 | 3896) 1^+(1^{+-}) + 4 \pi^0 0^+(0^{++})$$

$$X(3915 | 3915) 1^-(0^{+-}) = Z_c(3900 | 3896) 1^+(1u^{+-}) + \Delta W_{2-4} 0^-(1d^{--})$$

$$X(4020 | 4055)^\pm ? (0^+) = X(3915 | 3915) 1^-(0^{+-}) + \pi^\pm (0^-)$$

Note the following:

$$\chi_{c1}(3872) - \chi_{c1}(3511) = 361 \text{ MeV} \approx 2 W_{(+),d=2} = 363.4 \text{ MeV}$$

$$\chi_{c2}(\text{mass} = 3923) - \chi_{c2}(1P: 3556) = 367 \text{ MeV} \approx 2 W_{(+,-),d=2}$$

The bb_{anti} mesons

Notice that in all such mesons there are two the $C_{K\pm}$ spacetime condensates.

$$Y(1S: 9460 | 9471) 0^-(1^{--}) = 2 C_{K\pm} 0^+(0^{++}) + C_Y 0^+(0^{++}) + W_{(o),d=4} 0^-(1^{--})$$

The second proposal is presented in [1] – it leads to 9465 MeV.

$$Y_2(1D: 10164 | 10158) 0^-(2^{--}) = 2 C_{K\pm} 0^+(0^{++}) + 8 \pi^0 0^+(0^{++}) + S_{(o),d=4} 0^-(1u^{--}) + Q 0^+(1u^{++})$$

$$h_b(2P: 10260 | 10262) 0^-(1^{+-}) = 2 C_{K\pm} 0^+(0^{++}) + \pi_{d=0}^0 1215 \text{ MeV } 0^+(0^{+-}) + W_{(o),d=4} 0^-(1^{--})$$

$$Z_b(2P: 10610 | 10619) 1^+(1^{+-}) = 2 (C_{K\pm} + C_Y + 5 m_{\text{FGL}}) 0^+(0^{++}) + \pi^{0,\pm} 1^-(0^{+-}) + m_{\text{FGL}} 0^-(1^{--})$$

$$Z_b(10650 | 10658) 1^+(1^{+-}) = Z_b(2P: 10610 | 10619) 1^+(1^{+-}) + 2 \Delta W_{2-4} 0^+(0^{++})$$

$$\eta_b(1S: 9399 | 9424) 0^+(0^{+-}) + 2 W_{(o),d=4} 0^+(0^{+-}) = 2 (C_{K\pm} + C_Y) 0^+(0^{++})$$

The pseudoscalar axion and the strong CP problem

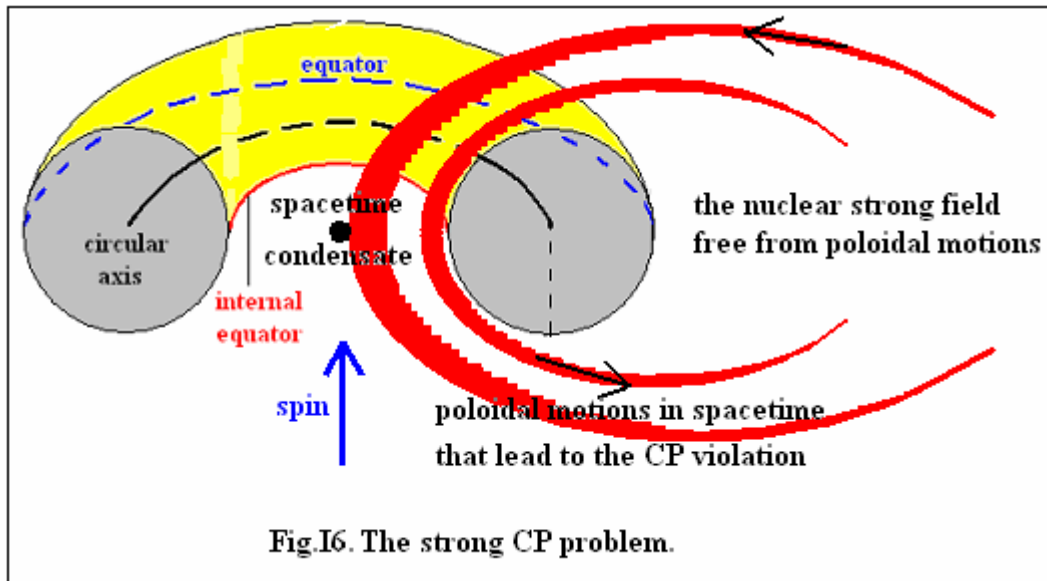
We must pay special attention to dark-matter (DM) particles (see Section 2.1). But we must add a few remarks. SST shows that there should be in existence the stable DM loops with different angular momentums and sizes (their size can be from 0.465 fm up to sizes of the halos of the massive spiral galaxies) but their mass is invariant $\sim 1.17 \cdot 10^{-11}$ eV. Such stable loops with the spin speed equal to the speed of light c , can interact with the “ordinary” matter via the weak interactions of the virtual electron-positron pairs so the coupling constant is $\sim 10^{-6}$ – such interactions are via the spacetime condensates that also appear in this paper. But emphasize that such stable DM loops, due to their internal structure, cannot interact electromagnetically! **Assume that such stable DM loops can create an unstable pion-like pairs which we can call the SST pseudoscalar axions.** Their spin is zero and CP is odd. Their invariant mass is $\sim 2.3 \cdot 10^{-11}$ eV. But emphasize also that similar to the pseudoscalar pions, the SST pseudoscalar axions should be unstable so we rather should try to detect the stable DM loops.

The mainstream axions are described in [5]. In paper [6], it is suggested that an axion field “is the most popular solution to the strong CP problem”, i.e. the CP violation has not been observed in the strong interactions – it leads to a conclusion that the neutron has not an electric dipole moment. Here we show that Nature does not realize such popular solution.

SST shows that the CP violation in the weak interactions of the spacetime condensate in the centre of baryons is due to the poloidal motions of the torus/electric-charge in the core of baryons. Very small changes in the mean distance between the SST absolute-spacetime (As) components cause that there appears the confinement of them and confinement between them and the torus which also consists of the SST-As components. The poloidal motions of the torus and the confinement cause poloidal motions to be transferred to spacetime in baryons. But the toroidal speed on the equator of the torus is equal to c so on it, the poloidal speed is equal to zero – it causes that outside the core of baryons, on the plane of the equator (there take place the nuclear strong interactions), the poloidal motions vanish so the CP is not violated in the strong interactions.

We see that the poloidal speed is maximal in direction of the spin of the torus, i.e. in the surroundings of the central spacetime condensate which is responsible for the weak interactions – it is the reason that the CP violation is characteristic for the weak interactions. In

Fig.I6, the thickness of the red curves represents the momentum density of the poloidal motion.



Emphasize that to stabilize the torus with different poloidal and toroidal speeds, there are exchanged the SST-As components the torus consists of. Moreover, there appear the radial motions which are responsible for creation of the central spacetime condensate.

In the pseudoscalar axions are two parallel loops with opposite spin speed so an axion field could shield the poloidal motions of the torus on the assumption that the confinement does not apply to the axion field (SST shows that it is untrue). **But then also we should not observe the CP violation in the weak interactions.** We know from experimental data that Nature does not implement such a scenario, so it is not possible to solve the strong CP problem by using an axion field.

Summary

Exactly 64 years ago (March 1, 1958), in a letter from Pauli to Gamow, the former commented on Heisenberg's radio interview that they had decoded the structure of all particles known at that time. Pauli drew a blank square and found it depicted the world but lacking technical details [7].

Resonances, due to their interactions and charge states, have experimental widths of about one to even five hundred mega-electron-volts or so. Deciphering their internal structure is not an easy task. Here, using the atom-like structure of baryons and very simple model, our theoretical masses are very close to the experimental central values. Our quantum numbers I, G, J, P and C, are fully in line with the experimental data. It validates the SST.

The charmed and bottom baryons are more stable than the baryon resonances because there is the additional spacetime condensate that interacts due to the nuclear weak interactions (such interactions are much slower than the nuclear strong interactions). Masses of the condensates are close to masses of the charm and bottom quarks.

Very important is the $d = 0$ state which is in contact with the equator of the core of baryons. Mass of particles in such state increases 9.0036 times. But to conserve the half-integral spin of the core of baryons, such relativistic particles quickly transform into the scalar spacetime condensates, C , which are responsible for the additional nuclear weak interactions. In resonances, most important is the natural spacetime condensate in the centre of baryons, $C_Y = Y$, and the spacetime condensates created from the relativistic pions and kaons which are

produced in the core of baryons – it causes that some of the baryonic and mesonic resonances can be created in the nuclear plasma composed of the cores of baryons packed to maximum (i.e. the $d = 1, 2$ and 4 states are destroyed).

The root-mean-square deviation in mass (RMSDM), i.e. for the mass distances between the SST masses and the mean central values observed, is defined as follows

$$\text{RMSDM} = \pm (\sum_i \Delta m_i^2 / N_i)^{1/2}, \quad (\text{I6.8})$$

where N_i is the number of particles of higher mass, i.e. $\Delta m_i > 0$, (or lower mass, i.e. $\Delta m_i < 0$) plus a half of number of particles with the same mass, i.e. $\Delta m_i = 0$.

Our global result is

$$M_{\text{central}}^{+\text{RMSDM}}_{-\text{RMSDM}} \approx 2800^{+17}_{-15} \text{ MeV}, \quad (\text{I6.9})$$

where M_{central} is a mean central-mass observed for all 260 particles described in this paper.

We can see that the mean RMSDM (in plus or in minus) is only about 0.6%.

Generally, the gluons and their associations interact with one or more spacetime condensates because of the nuclear weak interactions. The additional spacetime condensates are produced in collisions of the nucleons.

In this book we described a total of about 310 particles – they include all major and all high-status particles. Here we described also the SST pseudoscalar axion and we solved the strong CP problem.

References

- [1] P.A. Zyla, *et al.* (Particle Data Group)
Prog. Theor. Exp. Phys. **2020**, 083C01 (2020) and 2021 update
- [2] P.A. Zyla, *et al.* (Particle Data Group) (1 June 2020)
Prog. Theor. Exp. Phys. **2020**, 083C01 (2020)
V. Burkert, *et al.* (July 2019). “N and Δ Resonances”
V. Burkert, *et al.* (December 2019). “ Λ and Σ Resonances”
- [3] P.A. Zyla, *et al.* (Particle Data Group) (1 June 2020)
Prog. Theor. Exp. Phys. **2020**, 083C01 (2020)
C. G. Wohl (LBNL) (Revised 2004). “ Ξ Resonances”
- [4] M. Tanabashi, *et al.* (Particle Data Group)
Prog. Theor. Exp. Phys. Rev. D **98**, 030001 (2018) and 2019 update
- [5] P.A. Zyla, *et al.* (Particle Data Group)
Prog. Theor. Exp. Phys. **2020**, 083C01 (2020) and 2021 update
A. Ringwald, *et al.* (October 2019). “91. Axions and Other Similar Particles”
- [6] Francesca Chadha-Day, John Ellis, David J. E. Marsh, *et al.* (23 February 2022). “Axion dark matter: What is it and why now?”
Science Advances, Vol 8, Issue 8, DOI: 10.1126/sciadv.abj3618
- [7] George Gamow (1985). “Thirty years that shook physics: The Story of Quantum Theory”
Dover Publications, Inc., New York
ISBN 0-486-24895-X

17. Harbinger of a revolution in physics

The foundations of quantum physics and general relativity were formulated at the beginning of the 20th century, i.e. about a hundred years ago. There is a view that theoretical physics is practically complete. But when we ignore the Scale-Symmetric Theory, the truth is quite

different. 95 percent of physics by mass/energy is dark matter and dark energy, and we still do not know the origin of these forms of matter and energy. The remaining 5 percent is mainly baryon matter and we still cannot calculate the exact masses and spins of the proton and neutron from the initial conditions used in the Standard Model. Moreover, these initial conditions cannot be considered fundamental. When we add to this the problems with the rate of formation of supermassive black holes in the early universe and dozens of unsolved fundamental problems such as, for example, the origin of masses of neutrinos or the matter-antimatter asymmetry, we can confidently say that we know very little, which contradicts the statement that theoretical physics is coming to an end.

What main mistakes are repeated by successive generations of physicists that the theory of everything is still beyond the horizon for them? The main mistake is to ignore the internal structure of bare fermions – it is straight path to infinite values in your calculations and the need to use mathematical tricks to match the theoretical results with your experimental data. But even such treatments do not lead to accurate results, as can be seen from the anomalous magnetic moment of the muon and the properties of the nucleons. Other errors are assumptions about the quantum superposition of a mathematical point, the coherence of wavefunctions without superluminal communication, the simultaneous constancy of the speed of light with respect to all inertial systems, or the smooth transformation from inflation (that created spacetime and boundary of the inner Cosmos) to the expansion of the universe, and so on.

Several experimental results lead directly to the Scale-Symmetric Theory.

The baryon-antibaryon strong interaction potential is [1]

$$r_{0,\text{experiment,STAR}} = 2.83 \pm 0.12 \text{ fm} . \quad (\text{I7.1})$$

On the other hand, radius of the SST last orbit for the strong interactions is $R_{d=4} = A + 4B_{\text{mean}} = 2.705 \text{ fm}$ – it is very close to the lower limit in (I7.1), while the SST range of the nuclear strong interactions is $L_{\text{Strong}} = 2.958 \text{ fm}$ – it is very close to the upper limit in (I7.1).

So-called “hard core of nucleons” of an infinite strength was first introduced phenomenologically by Jastrow in 1950 [2]. We assume that it concerns the SST fundamental gluon loop (FGL).

When a beam is flowing in direction of the spin of a target (i.e. the spins of the target components are polarized) then we should obtain the radius of FGL – it is at the zero-temperature limit and it is the upper limit for the radius of the hard core of nucleons in our model

$$R_{\text{Hard-core,upper}} = R_{\text{FGL}} = 2A/3 = 0.465 \text{ fm} . \quad (\text{I7.2})$$

On the other hand, for thermal nucleons (i.e. their spins are not polarized) we obtain the lower limit for radius of the hard core of nucleons. Along the x-axis and y-axis, the radius is R_{FGL} while along the z-axis the radius is zero so an approximate mean value that is the lower limit is

$$R_{\text{Hard-core,lower}} = (2 R_{\text{FGL}} + 0) / 3 = 0.31 \text{ fm} . \quad (\text{I7.3})$$

In paper [3], there are calculated the properties of a neutron star (NS) at zero-temperature limit (so spins of neutrons are polarized). They found the hard core radius for the baryons

$$0.425 \text{ fm} < R_{\text{Hard-core,NS,[3]}} < 0.476 \text{ fm} . \quad (\text{I7.4})$$

This result is consistent with our result (I7.2).

In paper [4], authors claim that a comparison with the phenomenology of neutron stars implies that the hard-core radius of nucleons has to be temperature and density dependent. Their result for the hard-core radius of nucleons is

$$0.3 \text{ fm} < R_{\text{Hard-core,NS,[4]}} < 0.36 \text{ fm} . \quad (\text{I7.5})$$

This result is consistent with our result (I7.3).

Consider the ATOMKI anomalies. In measurements of the angular correlation of electron-positron pairs in the isoscalar and isovector decays of atomic nuclei, a large deviation was found from quantum electrodynamics (QED) prediction for internal pair conversion (IPC). Applying the Scale-Symmetric Theory we show that such correlations are not associated with a fifth force but with creation of very unstable condensates from the SST-As components because of the nuclear weak interactions (the coupling constant is $\alpha_{w(p)} = 0.0187229$). They found a neutral boson with a mass around **9 MeV** [5], neutral bosons with the dominant peaks at **12.42 MeV** and **14.55 MeV** [6], and around **17 MeV** (the X17 particle) [7], and few others.

Our model is as follows. A weak mass, $\alpha_{w(p)}M$, of a characteristic mass, M , in the core of baryons attaches the electron-positron pair, $2m_e$, so the neutral resultant mass, M_{boson} , is

$$M_{\text{boson}} = \alpha_{w(p)}M + 2 m_e . \quad (\text{I7.6})$$

For the central condensate $M = Y = 424.17 \text{ MeV}$ we obtain $M_{\text{boson}} = 8.96 \text{ MeV}$.

For the pair of the tori/electric-charges $M = X^+X^- = 2X^\pm = 636.59 \text{ MeV}$ we obtain $M_{\text{boson}} = 12.94 \text{ MeV}$.

For the core of baryons $M = H^\pm = 727.44 \text{ MeV}$ we obtain $M_{\text{boson}} = 14.64 \text{ MeV}$.

For the pair of the central condensates $M = 2Y = 848.34 \text{ MeV}$ we obtain $M_{\text{boson}} = 16.91 \text{ MeV} \equiv \text{X17}$.

But there are created also pions, muons and other objects so we should observe also the insignificant peaks.

We can see that the ATOMKI anomalies lead to the structure of the core of baryons.

When quarks are probed with low energy $Q = 0.143 \text{ GeV}$, the experimental value of the QCD effective charge is $\alpha_{g1} = 3.064 \pm 0.043 \text{ (stat.)} \pm 0.018 \text{ (syst.)}$ [8]. On the other hand, SST shows that at low $Q < X^\pm = 318.29555 \text{ MeV}$, the virtual bound pion π^0_{bound} is exchanged between the relativistic boson $W_{(+),d=1} = 215.76069 \text{ MeV}$ (see Table 2) in one proton and the relativistic boson $W_{(o),d=1} = 208.64305 \text{ MeV}$ (see Table 2) in the second one. In SST, by applying formula (2.4.31), we obtain that the strong coupling constant at low Q for such a process is invariant and is

$$\alpha_{S,\text{low-Q}} = \alpha_S^{\text{pp},\pi} (W_{(+),d=1} + W_{(o),d=1}) / (2 p + m_{\text{FGL}}) = 3.14166 \approx \pi , \quad (\text{I7.7})$$

where $\alpha_S^{\text{pp},\pi} = 14.391187$ (see (2.4.31)). For energies: **318 MeV** $< Q <$ **a few GeV**, we have a mixture of two phenomena, i.e. one described above and the second one described by formula (2.4.40).

Moreover, from [8] results that when quarks are probed with lower energy, their effective mass grows to $\sim 300 \text{ MeV}$, i.e. it is close to mass of the SST spin-1/2 charge X^\pm .

But emphasize that our model differs radically from the QCD.

Notice also that new images from James Webb Space Telescope show that even at redshift $z \approx 14$ we still observe galaxies [9], not a smooth field of first stars – it is consistent with the SST cosmology.

In the future, we should observe the two following anomalies:

* Due to the different weak interactions of muons and electrons and the decays of the $\mu^+\mu^-$ pairs into the electron-positron pairs, we should observe an excess in quanta with energy equal to 2.76 keV (see Sections **3.9**).

** Within the Scale-Symmetric Theory we predict existence of new scalar boson and/or vector boson with a mass of $17.12 - 17.17 \text{ TeV}$ that results from structure of the core of baryons and density of the SST absolute spacetime (see Section **2.16**) – there are four different formulae leading to such anomaly.

References

- [1] Adam Kisiel, *et al.* (3 March 2014). “Extracting baryon-antibaryon strong interaction potentials from $p\Lambda_{\text{anti}}$ femtoscopic correlation function”
arXiv:1403.0433v1 [nucl-th]
J. Adams, *et al.* (STAR Collaboration)
Phys. Rev. **C74**, 064906 (2006), nucl-ex/0511003
- [2] R. Jastrow, Phys. Rev., **81**, 165 (1951).
- [3] Violetta V. Sagun and Ilidio Lopes (20 November 2017). “Neutron Stars: A Novel Equation of State with Induced Surface Tension”
The Astrophysical Journal, 850:75 (6pp), 2017 November 20
- [4] K. A. Bugaev, *et al.* (6 November 2018). “Hard-core Radius of Nucleons within the Induced Surface Tension Approach”
arXiv:1810.00486v2 [hep-ph]
- [5] F. W. N. de Boer, *et al.* (2001). “Further search for a neutral boson with a mass around $9 \text{ MeV}/c^2$ ”
J. Phys. G: Nucl. Part. Phys. **27** L29
- [6] Fokke de Boer (6 January 2006). “Anomalous Internal Pair Conversion Signaling Elusive Light Neutral Particles”
arXiv:hep-ph/0511049v2
- [7] A. J. Krasznahorkay, *et al.* (29 January 2016). “Observation of Anomalous Internal Pair Creation in ^8Be : A Possible Indication of a Light, Neutral Boson”
Phys. Rev. Lett., **116**, 042501 (2016)
- [8] A. Deur, *et al.* (31 May 2022). “Experimental Determination of the QCD Effective Charge $\alpha_{g1}(Q)$ ”
Particles 2022, 5(2), 171-179
<https://doi.org/10.3390/particles5020015>
- [9] Steven L. Finkelstein, *et al.* (25 July 2022). “A Long Time Ago in a Galaxy Far, Far Away: A Candidate $z \sim 14$ Galaxy in Early JWST CEERS Imaging”
arXiv:2207.12474 [astro-ph.GA]

J. A very short recapitulation

*The viscid interactions between the tachyons and between the tachyons and entanglons are the fundamental interactions and they follow from smoothness of surfaces of the tachyons – they lead to the gravitational fields. On the other hand, the quantum entanglement and the confinement of the SST-As components lead to the electromagnetic, weak, and strong interactions. Unification of Gravity and Quantum Mechanics is impossible.

*The structure of neutrinos and the atom-like structure of baryons are the fundamental structures in particle physics. Oscillations of neutrinos are an illusion.

*Due to the cosmological collision, the SST inflation was the explosion of space (of the initial inflation field).

*At the end of the SST inflation, the external left-handedness of the initial inflation field led to the emergence of the matter-antimatter asymmetry – just the baryons are internally left-handed.

*The expansion of the Universe was separated in time from the SST inflation – such expansion is the result of the evolution of the Protoworld composed of the SST-absolute-spacetime components.

*The Universe is anisotropic because of the initial anisotropies and protuberances. But mass density of the isotropic SST-As dominates so the Universe is practically flat.

*Dark matter and dark energy differ from matter in the arrangement of the spins of the components of the SST absolute spacetime.

*Quantum Mechanics wrongly describes structure and dynamics of the zero-energy field.

*Excited states of the SST two-component spacetime (i.e. the SST-Hf plus SST-As) have $6+26=32$ degrees of freedom. On the other hand, among the first 32 natural numbers there are 11 prime numbers. **Theory of Everything that contains 11 initial parameters is mathematically simplest one.** But we can reduce the number of initial parameters from eleven to seven.

By applying our theory of electron described in Section 2.6 we can eliminate the mass of electron from our initial parameters.

It is obvious that the binding energy of the core of baryons should be a result of emission of the nuclear weak mass of the three basic objects in the core, i.e. X^\pm , Y and m_{FG} , and that during the creation of the core, there should be an increase in range of the core from the equator of the core with the radius of A to the $d = 1$ state i.e. to $R_{d=1} = A + r_{C(p)}$ so the binding energy slightly decreases

$$\Delta E_{\text{core}} = \alpha_{w(p)} (X^\pm + Y + m_{FGL}) A / (A + r_{C(p)}) \approx 14.978 \text{ MeV}. \quad (\text{J1.1})$$

Notice that in Section 2.9 appears the energy $\Delta E_{\text{volumetric}} = 0.1537996308 \text{ MeV}$ (see formula (2.9.4)) that leads to the volumetric confinement that leads to the density of the spacetime condensates, so we can eliminate the initial parameter ρ_Y from our theory.

SST shows that the elementary electric charge, e^\pm , independently of its masses, creates the $N_{NA} = 8.50713316753319 \cdot 10^{38}$ lines of the electric force, and such an object we define as the $e^\pm = 1.602176634 \cdot 10^{-19} \text{ C}$. It means that the e^\pm is not an initial parameter in the SST because we described its origin. In SST, the electron charge consists of the electron-loop and the zero-mass torus/electric charge. The loop and the equator of the torus overlap. The electron-loop carries the mass of the electric charge and the spins of the SST-As components does not rotate and are perpendicular to the loop. The spins of the SST-As components in an electron-loop all point towards the center of the loop and in the antiparticle outside the loop and lie in its plane. The torus/electric-charge is only the polarized part of the SST-As so spins of the SST-As components behave similarly as in the electron-loop – it leads to conclusion

that the resultant mass of the torus/electric-charge is zero. There is also the central spacetime condensate with a mass equal to the mass of the electron-loop and there is only one virtual electron-positron pair.

In such a way we reduced number of initial parameters from eleven to seven, i.e. the SST is in fact a seven-parameter theory but the math of such a theory is much more complicated because we have to solve systems of equations with a large number of unknowns. In reality, we have the 6 parameters describing the SST Higgs field (it concerns the gravitational fields) and 1 parameter describing the SST absolute spacetime, i.e. the gravitational mass density of the SST-As.

Emphasize also, that the 3 parameters that describe the exact Planck scale (i.e. \hbar , c and G), i.e. it concerns the spin-1 components of the SST-As, are derived from the more fundamental initial conditions. The SST-As components can rotate with the maximum spin-speed equal to the c – then their gravitational mass is close to the Planck mass.

Wow! signal again (an extension of Section G1)

The first number in the Wow! signal is “6” that relates to “f” in English alphabet and “H” or “y” in Polish alphabet. On the other hand, in SST, we have “Hf” (the Higgs field) or “yf” (the ylem field) that has the 6 degrees of freedom. The term “ylem” was used by George Gamow and it is defined as “the first substance from which the elements were supposed to have been formed” (“ylem”, Oxford English Dictionary).

The second symbol/number is E(14). On the other hand, in SST, there are two Elementary objects the all other objects are built of: it is the tachyon which has 6 degrees of freedom and the closed string which in the ground state has 8 degrees of freedom, so the total number of degrees of freedom is $6+8=14$.

The third symbol/number is Q(26). On the other hand, the Quantum Physics concerns the excited states of the SST absolute spacetime and it has 26 degrees of freedom.

The fourth symbol/number is U(30). On the other hand, the ground state of the SST two-component spacetime that fills the SST Universe has $6+24=30$ degrees of freedom.

The Wow! signal suggests that we should separate the first four even numbers (6, 14, 26 and 30) from the last two odd numbers (19 and 5). The even numbers describe the creation of our Cosmos: at first there appeared the tachyons (6), next the closed strings interacting with tachyons ($6+8=14$), next the excited states of the SST absolute spacetime (26), and next the ground state of the two-component spacetime ($6+24=30$) because at the end of the SST inflation there was created the stable boundary of our Cosmos.

Such interpretation of the four even numbers suggests that the two last odd numbers describe a destruction of our Cosmos. We should have two even numbers (notice that different states of spacetime are described by even numbers/degrees-of-freedom) one for the present-day state ($19+5=24$) and one for the state after the destruction ($19-5=14=6+8$). It suggests that due to an event (it will be the damage to the stable boundary of our Cosmos), there will be a decay of the ground state of the SST absolute spacetime (24) into the tachyons (6) and closed strings (8).

The two last symbol/numbers are as follows J(19) and 5. In English alphabet we have $19=S$ and $5=E$. On the other hand, in Polish alphabet we have $5=U$ and $5=G$. It means that we have the letters J, U, G and S and we assume that the English letters dominate. So the J leads to JUDGE and E to End or Eventual, i.e. to the Last/Eventual Judgement in the

Bible, i.e. then the chosen people will be saved. We can assume also that the damage to the boundary of the spacetime will be due to a **JEt-StrinG**.

Coincidence between the numbers appearing in the Wow! signal and the degrees of freedom in SST and the fact that the letters in the Wow! signal (given by humans!) have a physical sense (ylem field, elementary, quantum, Universe, jet-string, and last Judgement) suggest that the ultimate theory has already been discovered in our universe and that quantum telepathy plays a key role in our understanding of the laws that govern Nature.

Notice also that there are following coincidences. In the simplest version of the SST, there are eleven initial parameters that describe the excited states of the SST two-component spacetime (the SST Higgs field plus the SST absolute spacetime) while the mainstream M-theory is eleven-dimensional. When we consider the ground state of the SST two-component spacetime (it has $6+24=30$ degrees of freedom) there among the first 30 natural numbers are 10 prime numbers, so a theory of the ground state should be described by 10 parameters – on the other hand, in the mainstream string theory, spacetime is ten-dimensional. So we have

Number of dimensions = number of initial parameters = number of prime numbers

Index

3+ means “page 3 and beyond”

- absolute spacetime (SST-As) 8
- astrophysics 129+
- atomic nucleus 114+
- atomic physics 93+
- ATOMKI 158
- atom-like structure of baryons 39+
- azimuthal number Fig.9

- baryonic matter 33, 75+, 81+, 129+
- baryons 9, 15+, 25+ to the end of book
- black body 18+, 89+, 145
- black hole 11, 15, 26, 28, 39, 76, 78+, 113, 134, 136+, 148

- chaos theory 120+
- charge conjugation 8, 13, 151
- chi_b mesons 151+
- closed string 8, 13, 15, 24+, 68
- CMB 65, 81 – 89, 147+
- condensates 12, 31+
- confinement 8, 43+
- Cooper pairs 109+
- core of baryons 15, 25+, 33, 40, 44+, 59, 65+
- cosmology 75+, 129+
- Cosmos 10, 75, 77+, 91
- coupling constant 6, 21, 30, 31+, 115+

- dark-matter 10, 15, 33+, 37, 75+, 148+
- dark energy 10, 75+, 148+
- degrees of freedom 12, 49+, 63, 127
- dynamics of core of baryons 28+

- electron 13, 21, 29+, 37+
- entanglement (quantum) 8, 10, 25, 26, 51
- entanglon 7, 8+

- fine-structure constant 29+, 47+, 128+
- fundamental gluon loop 16+, 28, 104

- galaxies 11, 67, 75, 84, 88, 129+, 132+
- gluons 8+, 48+, 75, 84, 89

- gamma-ray bursts 135+
- gravitational constant 27+

- half-jet asymmetry 13+
- helicity 7+
 - external 7+
 - internal 7+
- Higgs boson 52
- Higgs field (SST-Hf) 8
- Hubble constant 81+
- hydrogen atom 37, 52+, 96+, 99+, 116, 147
- hyperons 39, 54, 60+, 66, 68+, 73, 150

- inflation field (initial) 7, 8, 14, 24+, 75, 77+, 91
- initial conditions 11+
- interactions 50+, 119

- Lamb-Retherford shift 52+
- large numbers law 148
- large structures 67, 80+
- leptons (electrically charged) 9, 21+, 33
- lepton universality 155+
- lifetimes 20, 53+, 71, 122

- magnetars 141+
- matrix PMNS 63+
- matrix CKM 65+
- matter-antimatter asymmetry 21+
- mental world 119+
- mesons 58+, 151+
- muon 45+

- neutrinos 7, 9+, 12, 15, 26, 43+, 50+, 63+, 76+, 145
- neutron 41+, 55, 61, 78+, 81
- neutron black holes (NBHs) 11, 15, 28, 33, 76, 78+
- neutron charge radius 152+
- nuclear physics 114+
- number K 15, 24

- parameters (initial) 12+, 185+
 parity Fig.5, 58
 particle physics 24+, 150+
 Pauli Exclusion Principle 93+
 phase transitions 7, 10, 13, 15, 24+
 phonon fields 102+
 photons 8, 10+, 20, 36, 48+
 physical constants 7, 24+
 pion 14, 17, 26, 31+, 39+
 Planck constant 21, 24+, 129
 proton 9, 23, 29+, 34+, 41, 42+, 53, 56+,
 59, 61, 62, 81, 84+, 96+, 100+,
 104+, 110, 115, 117+, 121, 149+
 Protoworld 7, 15, 25+, 33, 76-91, 135,
 147+
 pulsars 141+
- QCD effective charge 186
 quantum gravity 51
 quantum physics 95, 121+, 181
 quarks 11, 21, 62+, 65+, 73, 145, 153,
 183+
- range of strong interactions 16+, Fig.8
 relativistic mass 9, 17+, 31+, 39, Table 2,
 62, 101, 148+
 resonances 61+, 69, 162-180
 Reynolds number 24
 running coupling constant 35+
- Solar System 136+
 space roar 144+
 spacetime (SST-S) 8
 speed c 8, 9, 10+
 spin-flip in hydrogen 99+
 Standard Model 65, 148, 152+
 standard ruler 88+
 Stefan-Boltzmann law 18+, 21, 28, 90,
 144
- superconductivity 102+
 symmetries (new) 6, 13+
 - adoption symmetry 13
 - decay symmetry 13
 - four-object symmetry 13
 - invariant surface-density symmetry 13
 - saturation symmetry 13
- tachyons 6+, 8, 12+, 24+, 50+, 68
 tauon 47+, 54
 thermodynamics 24+
 time reversal 13, Fig.6
 Titius-Bode law 9, 13+, 40+, 61, 69,
 136+
 - strong interactions 13+, Fig.7
 - gravitational interactions 136+
 torus/tori (fundamental) 8+, 12, 13, 15,
 16, Fig.7, 21+, 25+, 38, 51
- ultimate equation 68+
 uncertainty 23
 unification 10, 69, 148, 185
 universes 77+
 Universe 11, 14, 15, 33, 64, 75+, 80+,
 81+, 88, 89-92, 132+, 140+,
 144+, 147+, 182, 186+
 Upsilon mesons 58, 63, 151+
- virtual particles 10, Fig.3, 18, 55, 69
- W boson 49, 55+
 Wien's displacement law 18+, 28, 81,
 86, 89, 104, 146
 Wow! signal 124+, 186+
- X particles 156+
 Z boson 49, 55+
 zero-energy field 10, 12, 16+, 20, 23,
 36, 38, 44, 51, 65, 80, 135, 184